Report to the
Water Research Commission

The long term impact of *Acacia mearnsii* trees on evaporation, streamflow, low flows and ground water resources

Phase II: Understanding the controlling environmental variables and soil water processes over a full crop rotation

Project: K5/2022

by:
Everson CS
Clulow AD
Becker M
Watson A
Ngubo C
Bulcock H
Mengistu M
Lorentz S
Demlie M

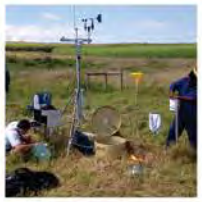

January
2014

UNIVERSITY OF
KWAZULU-NATAL
INYUVESI
YAKWAZULU-NATALI

The long term impact of *Acacia mearnsii* trees on evaporation, streamflow, low flows and ground water resources.
Phase II: Understanding the controlling environmental variables and soil water processes over a full crop rotation.

Report to the

Water Research Commission

by

CS Everson, AD Clulow, M Becker, A Watson, C Ngubo, H Bulcock, M Mengistu, S Lorentz and M Demlie

Centre for Water Resources Research (CWRR),
School of Agricultural, Earth and Environmental Sciences, University of KwaZulu-Natal

WRC Report No. 2022/1/13
ISBN 978-1-4312-0516-5

March 2014

Obtainable from

Water Research Commission
Private Bag X03
Gezina, 0031

orders@wrc.org.za or download from www.wrc.org.za

DISCLAIMER

This report has been reviewed by the Water Research Commission (WRC) and approved for publication. Approval does not signify that the contents necessarily reflect the views and policies of the WRC nor does mention of trade names or commercial products constitute endorsement or recommendation for use.

© Water Research Commission

EXECUTIVE SUMMARY

The Two Steams catchment is one of South Africa's most intensively studied long-term forestry research catchments, with 14 years of detailed hydrological process observations. Used to study the impacts of *Acacia mearnsii* (Wattle) trees on riparian zones, the progress thus far is a complex story of scientific advances in riparian zone management and groundwater/surface water interactions. The project is a direct consequence of the need for high quality scientific research, in response to national needs for application of the National Water Act of 1998 and for future policy and forest management decisions. The main aim of the project has been to answer the important questions 'What processes allow exotic tree plantations use more water than grassland in areas being converted to commercial forestry plantation' and "What are the long-term effects of commercial forestry species on deep soil- water profiles, streamflow and total evaporation'? The Two Streams research catchment is helping to revolutionise our fundamental understanding of catchment hydrology in South Africa and has become a multi-disciplinary 'outdoor laboratory' encompassing, detailed evaporation measurements with large aperture scintillometers, the eddy covariance and surface renewal methods, tree transpiration with the heat pulse velocity technique, soil and ground water studies, isotopes studies and canopy interception. The catchment has been used by many students for both undergraduate and post-graduate studies, providing a crucial training ground for young South African hydrologists. As this long-term research study enters its 15th year, this report of the work undertaken over the past three years, fulfils an important link to the previous work at Two Streams.

Internationally long term catchment studies including actual measurements of all the water balance components are scarce, while locally this represents a unique study on the impact of an exotic tree plantation on catchment hydrological processes. The current study has enabled the data record at Two Streams to be extended to 14 years allowing for a full rotation of the planted wattle.

The current project used a range of technologies to study the hydrological processes in the catchment and these are fully described in the methodology section. Some of these technologies such as the soil water measurement using time domain reflectometry in deep profiles, rainfall sampling (ALCO sampler) and isotope extraction were improved through this research.

The interception studies conducted at Two Streams showed that interception plays a very important role in the forest hydrological cycle in this climatic zone, with only 65.7% of gross precipitation being available water that drains to the soil, after the losses due to canopy and litter interception under various commercial forestry species are taken into account. Stemflow during the winter period from two events of 2.1 and 1.6 mm showed the percentage of stemflow converted to rainfall varied between 1.3% and 28.3%. In summer these values were as high as 39 and 50% of the gross rainfall. These preliminary results have highlighted the importance of taking into account all the interception processes when attempting to account for losses and gains in effective rainfall.

An important result from the evapotranspiration measurements showed that the increasing trend in maximum summer ET rates observed during the first three summers over the wattle stand in 2006 to 2009 in the previous research project had halted, indicating that with maturity, the water-use of the trees has plateaued.

The long-term runoff:rainfall relationship has changed significantly each year from 2001 to 2013 with felling and planting cycles confirming that the commercial forestry at Two Streams has had an impact on streamflow.

The present study has continued to demonstrate the impact of the deep rooted trees on sourcing water from the deep soil profile and groundwater and shown that the average unaccounted losses estimated through the catchment water balance in the catchment are 395 mm over the 7 year period from 2006 to 2013. Roots were found in excess of 8 m below the soil surface and there was a consistent drying out of the soil profile from 2007 to 2013. The link to the groundwater reserves has not been fully investigated (this is a current MSc topic) and is expected to provide answers to the unaccounted losses in the catchment water balance

The results of tree transpiration measurements have shown that the *A. mearnsii* tree water use is highly variable with respect to both aspect and slope position and highlights the importance of accounting for this spatial variability in the catchment water balance and hydrological models.

Over the 2012-2013 hydrological year, a comparison of the total evaporation from the eddy covariance system (ET_{ec}) and tree transpiration at the upper south site, revealed estimates of 1157 mm and 1076 mm respectively. The 81 mm margin in the total evaporation compared to the tree transpiration is attributed to soil and litter evaporation not measured by the heat pulse velocity methodology. Soil and litter evaporation therefore represented about 8% of the total evaporation in the wattle plantation.

The conceptual groundwater hydrological model has shown that the deeper soil represents the deep weathering of the bedrock surface and the fractured basement rock which are dominant factors governing the flow paths of water in the catchment. The water flow is likely horizontal, lateral and upward. Therefore, water ponds on the bedrock surface and leaks through granite fractures to recharge the deep aquifer. There is no evidence of tree roots extracting groundwater from the deep aquifer at this stage.

The time domain reflectometry probes for measuring volumetric water content in the soil profile to depths of up to 4.8 m have been modified and improved. Long cable lengths combined with short waveguides resulted in signal noise from the previous probes. The cable quality has been improved and the wave guides extended to 0.15 m.

Isotope sampling of rainfall, streamflow, groundwater, soil water and tree sap provided information on the water pathways within the catchment. An automatic rainfall sampler was developed, able to differentiate between rainfall events and even separate out samples during extended rainfall events where isotopic signatures can change. In addition, the problem of evaporation from sample bottles in automatic samplers (rainfall and streamflow) was addressed by developing a glass funnel with a U-tube trap inserted into the lids of the bottles to prevent evaporation which normally alters the isotope signature of the field samples through fractionation. Soil water was extracted successfully using water distillation and thoroughly tested as a technique and found to be more suitable than extracting tree sap due to the problems with hydrocarbons and viscosity of the samples. Samples were extracted from soil down to 8 m without showing any contribution from groundwater at this depth.

The research site has been an integral part of the Hydrology courses offered at the University of KwaZulu-Natal. Undergraduate field excursions have offered practical exposure of field techniques to students and a number of postgraduate studies are based in the Two Streams catchment. In addition, it has encouraged collaboration with staff from the University of the Free State who have utilized the research catchment for postgraduate studies.

Extent to which contract objectives have been met

The objectives of the project contract have been met as described below:

a. The first objective was to quantify the long-term effects of *A. mearnsii* on deep soil water profiles, streamflow and evaporation over a full crop rotation. Through detailed water balance studies this objective was achieved and the hydrological record for Two Streams extended by a further three years to 14 years.

b. Objective two was to quantify and understand the controlling environmental and soil water processes (including root distribution) which allow for ET to exceed the annual rainfall. The Two Streams research catchment is helping to revolutionise our fundamental understanding of catchment hydrology in South Africa, and has become a multi-disciplinary 'outdoor laboratory' with a large focus on hydrological process studies, which have all contributed to a better understanding of these processes through a detailed account of the catchment water balance.
c. Objective three was to provide a modelling framework for the catchment water balance to improve stream flow predictions and specifically low flows in afforested catchments. Fourteen years of detailed hydrological data provides an excellent data source for verification and development of hydrological models and to date the SWAT, ACRU, WAVES and HYDRUS models have been tested using the Two Streams data sets for model validation.
d. Objective four was to gain a better understanding of the spatial distribution of transpiration from trees growing on different hillslope positions. This was achieved by transpiration studies on different hillslope positions and aspects.
e. To extend the hydrological record for Two Streams to provide a long-term database of the catchment hydrological variables for future modelling studies. The catchment hydrological record has now been successfully extended to 14 years.

Future research

- The contribution of mist to the Two Streams water-balance has not conclusively been established. The Two Streams catchments falls within a mist-belt and the frequency and contribution of mist to precipitation, interception and stemflow needs to be quantified.
- The isotope sampling brought to light the difficulty in extracting samples from tree sap. A procedure to obtain samples for analysis without organic contamination would be highly beneficial. Hydrocarbons result in analysis errors and low injection volumes due to the high viscosity of the samples.
- Following one particularly large rainfall event (88.3 mm on 19 November 2004), significant erosion and sedimentation was observed during tree harvesting within the catchment in 2004. The management strategies around tree harvesting and burning of residue can influence the soil surface condition which is exposed to potential erosion especially during the post-harvest period. This risk in forestry catchments of high erosion during and after harvesting is exacerbated by the removal of vegetation cover, hydrophobic soil, steep slopes and compacted soils. It is strongly recommended that tree harvesting in wet seasons in areas susceptible to erosion be evaluated with further research.
- Over the past 14 years, the impacts of different tree clearing treatments to the riparian zone and upslope areas have been assessed. The interaction of the hydrological processes between these two areas (i.e. the interface) is still not well understood. In the catchment, the two zones are distinct from vegetation, slope, soils and ground water perspective and yet they interact within the hydrological cycle. For hydrological models to capture this interaction, further research into the transfer functions at the interface are required as well as improved understanding of the groundwater flow dynamics and contribution to streamflow. The latter can be improved by defining the groundwater contributing area, surveying the borehole elevations and determining the storativity after pumping.
- The existing *A. mearnsii* stand will be replaced by *Eucalyptus* trees in the near future. Continued measurement of all the water-balance components of the catchment is required to determine the influence of these fast growing trees on the hydrological processes in the catchment.

- Surface energy balance models using remote sensing data can provide estimates of plant water-use over wide areas but require validation for South African conditions. The state-of-the-art total evaporation measurements recorded at the site provide an excellent opportunity for testing these techniques in afforested catchments. These will, in the future, provide water resource managers with catchment-wide water-use estimates and assist researchers in monitoring the impacts and changes associated with global climate change.

DATA STORAGE

All processed data have been stored at:
Centre for Water Resources Research
School of Agricultural, Earth and Environmental Sciences
Agriculture Faculty
University of KwaZulu-Natal
Carbis Road
Scottsville
Pietermaritzburg
3209
South Africa

ACKNOWLEDGEMENTS

The research project was funded by the Water Research Commission and The Department of Environmental Affairs, Working for Water, for whose assistance we are sincerely grateful. The Department of Water Affairs is thanked for assistance with borehole sensors. Mondi are thanked for allowing access to their catchment and for contributions in kind (labour, management operations and data). We also wish to acknowledge contributions made by members of the reference group:

Mr W Nomquphu	*Water Research Commission (Chairman)*
Prof GPW Jewitt	*University of KwaZulu-Natal, CWRR*
Mrs J Shuttleworth	*Mondi Forests*
Dr MB Gush	*CSIR*
Mr C Ngubo	*Department of Agriculture and Environmental Affairs*
Mr P Gardiner	*Mondi Forests*
Prof. J Annandale	*University of Pretoria*
Mr M Smart	*Department of Water Affairs*
Prof B Kelbe	*University of Zululand*
Dr N Jovanovic	*CSIR*
Dr C Burchmore	*Mondi Forests*
Mr PP Msimongo	*Department of Water Affairs*
Mr V Tshabalala	*Department of Water Affairs*
Dr D Versfeld	*Dirk Versfeld cc*
Dr C Jarmain	*University of KwaZulu-Natal, CWRR*

Siphiwe Mfeka and Bruce Scott-Shaw provided valuable technical assistance to the trial. The Centre for Water Resources Research (UKZN) is acknowledged for their support through assistance from post-graduate students.

CONTENTS

LIST OF FIGURES

LIST OF TABLES

LIST OF ACRONYMS

ACRU	Agricultural Catchments Research Unit
CSIR	Council for Scientific and Industrial Research
DWA	Department of water Affairs
FOA	Food and Agriculture Organisation of United Nations
GMWL	Global Meteoric Water Line
HYDRUS	Modelling software for analysis of water flow, heat and solute transport in soils
IAEA	International Atomic Energy Agency
IRIS	Isotope Ratio Infrared Spectrometer
IRMS	Isotope Ratio Mass Spectrometer
LGR	Los Gatos Research
LMWL	Local Meteoric Water Line
MAP	Mean Annual Precipitation
NBS1	US National Bureau of Standards
OA-ICO	Off-Axis Integrated Cavity Output Spectroscopy
REBS	Radiation Energy Balance Systems
SCI	Spectral Contaminant Identifier
SFRA	Streamflow Reduction Activity
SMOW	Standard Mean Ocean Water
SPAC	Soil Plant Atmospheric Continuum
SWAT	Soil and Water assessment Tool
UKZN	University of KwaZulu-Natal
VSMOW	Vienna Standard Mean Ocean Water
WAVES	Water, Vegetation, Energy, Solute
WRC	Water Research Commission

LIST OF SYMBOLS AND CHEMICAL FORMULAS

$\sqrt{\varepsilon}$	Dielectric permittivity,
ε	The ratio of molecular weights of water vapour and air
(e_s- e_a)	Saturation vapour pressure deficit
K_{sat}	Saturated hydraulic conductivity
S_p	Potential water uptake rate
S_e	Effective water content
θ_r	Residual water content
θ_s	Saturated water content
Δ_t	Output time interval (s).
ΔT_s	Temporal change in temperature over the output interval
‰	Parts per Thousand
^{15}N	Nitrogen-15
^{16}O	Oxygen-16
^{17}O	Oxygen-17
^{18}O	Oxygen-18
^{1}H	Hydrogen-1
^{2}H	Hydrogen-2 (Deuterium)
^{3}H	Hydrogen-3 (Tritium)
a	Amplitude of the air temperature ramps
AWS	Automatic Weather Station
B	Tree basal area (cm^2)
C	Velocity of signal in free space
Ca^{+2}	Calcium
Cl^-	Chloride
CO_2	Carbon dioxide
CO32-	Carbonate
c_p	Specific heat capacity of air
CPA	Crown Projection Area
c_s	The specific heat capacity of soil (J kg^{-1} K^{-1}),
d	Depth of the heat flux plates in the soil (m)
DBH	Diameter at breast height
DO	Dissolved Oxygen
E	Energy
ε	Isotope enrichment factor
$e_{a'}$	The instantaneous departures from the mean horizontal velocity, *T* and *e*
e_a	Actual vapour pressure
EC	The electrical conductivity
Eh	Redox Potential
e_s	Saturation vapour pressure
ET	Total evaporation
ET_0	Reference evapotranspiration

ET_{ec}	Actual total evaporation from eddy covariance
ET_{LAS}	LAS-based total evaporation
ET_{P-T}	Priestley-Taylor-based total evaporation
F.R.	Funnelling ratio
FAO-56	Food and Agriculture Organisation, paper no. 56
F_{plate}	The heat flux at a depth of 80 mm (W m^{-2}),
F_s	Soil heat flux at the surface (W m^{-2}),
F_{stored}	Flux of heat storage in the soil (W m^{-2}),
G	Rainfall depth (cm).
G	Soil heat flux density
Gw	Groundwater
h	Pressure head
HCO_3	Bicarbonate
HCO_3^-	Bicarbonate
HPV	Heat Pulse Velocity technique
H_r	Relative humidity
j	Sample lag between data points corresponding to a time lag $r = j/f$,
K^+	Potassium
Ka	Dielectric constant
Kc	ET/ETo (crop factor)
Kc	Crop co-efficient
Kp	Probe constant
L	Actual length
L	Waveguide length
La	Apparent length
La	Real probe length
LA/L	Start distance and End distance
LAI	Leaf Area Index
m	The number of data points in the time interval measured at frequency f (Hz)
m	Mass
M	Molecular weight of water
Mg^{+2}	Magnesium
n	The power of the function
Na^+	Sodium
OH^-	Hydroxide
ORP	Oxidation Reduction Potential
P	Precipitation
P	The atmospheric pressure.
Q	Streamflow calculated using the water balance equation
Q_a	Actual streamflow
R	Universal gas constant
R^2	Coefficient of determination
REBS	Radiation Energy Balance Systems
R_n	Net radiation at the crop surface
SCF	Soil cover fraction defined as constant b.
SO_4^{-2}	Sulphate
Sw	Soil water
T'	*A*ir temperature
T	Absolute temperature
t	Travel time
TC's	Thermocouples

TDR	Time Domain Reflectometry
TDS	Total Dissolved Solids
T_i	The i^{th} temperature sample.
T	Mean daily air temperature at 2 m height
u'	Mean horizontal velocity
u^2	Wind speed at 2 m height
V	Stemflow volume (ml)
V	Velocity
Vp	Relative propagation velocity
z	Measurement height,
Zc	Cable impendence
A	Weighting factor
Δ	Delta values (deviation from the international standards)
ΔS	Changes in soil water storage
Θ	Volumetric water content
ρ	Reflection coefficient
ρ_a	Density of air,
ρ_s	Bulk density of soil (kg m^{-3}),
σ	Bulk electrical conductivity
τ	Total ramping period.
Ψ_{PLWP}	Predawn Leaf Water Potential
Δ	Slope vapour pressure curve
γ	Psychrometric constant
Es	Potential soil evaporation
Et	Potential plant transpiration
Sc	Storage capacity
k	rExtinct
l	Pore-connectivity parameter
n	Measure of pore-size distribution index
x	Rainfall intensity
z	Gravitational Head
α	The inverse of the air entry suction
$\alpha(h)$	Root-water uptake stress function
$\theta(h)$	Water retention curve
θ	Volumetric water content

1. INTRODUCTION

Commercial afforestation is one of the most important agricultural activities in South Africa as it is estimated that it accounts for approximately 6.3% of the country's gross agricultural production (FAO, Allen *et al.,* 1998). Although commercial afforestation provides numerous benefits to the economy and society, it has negative impacts on the hydrological system (Scott *et al.*, 2000). Presently, commercial afforestation is regarded as a stream flow reduction activity (SFRA) and is the only water-use activity to be given this status, according to the National Water Act of 1998 (DWAF, 2005). Commercial forestry is therefore regulated in South Africa according to the impact it has on water resources. This affects individual citizens, businesses and the economy as a whole. It is for this reason that we need to understand forest hydrology and the impacts of forestry on the hydrological cycle for fair and reasonable policy regarding commercial forestry and its water-use.

This report documents the three year WRC project K5/2022 from inception (April 2011) to January 2014. It describes the installation of new equipment at the Two Streams research catchment and the continued monitoring of precipitation (P), streamflow (Q), evaporation (ET), groundwater (Gw) and soil water (Sw). Individual tree water-use on different hillslope positions was a new focus area of study during this project. The design of time domain reflectometry (TDR) probes for measuring water content in deep soil profiles (>3 m) was completed and the probes calibrated and installed. Isotope studies were implemented to better understand the flow-paths of water through the catchment. In addition, the HYDRUS 1D model (Pc-Progress) was used to estimate the transpiration rate from the *Acacia mearnsii* stand.

This project was being conducted by researchers and students of the University of KwaZulu-Natal. It supports the ongoing, long-term research conducted in forest process hydrology within the Two Streams catchment and has become an integral part of the fieldwork component of the hydrology course offered at UKZN. Undergraduate students have received practical infield training in measurement techniques and been exposed to the critical issues of water-use and water allocation within the forestry sector. Students witness how these issues are best addressed through measurement and hydrological modeling. In-turn, the project has benefitted intellectually by the participation of numerous postgraduate students that have continued their studies in hydrology through their exposure to the Two Streams catchment research at an undergraduate level.

1.1 Background

The Two Streams catchment experiments have been used over the past 14 years to study the impact of trees on hydrological processes (Everson *et al.*, 2007 and Clulow *et al.*, 2010). The experiments have provided a good opportunity to extend our understanding of hydrological processes such as low flows and deeper soil water dynamics. The Two Streams catchment is one of the few remaining small catchment research areas in South Africa. Streamflow gauging started

in 1999 in a mature stand of *A. mearnsii* (Wattle). Following a short calibration period, all the trees in the riparian zone were cleared in July 2000. The trees in the remainder of the catchment were removed in 2004/2005 and the catchment was replanted with wattle in August 2006. With nine years of intense hydrological monitoring, this catchment presented an ideal opportunity to study the impact of a newly planted *A. mearnsii* rotation on the water balance of the catchment and direct research towards previously unanswered questions.

Burger (1999), for example, estimated total evaporation (*ET*) using the Bowen ratio energy balance method and showed that annual total evaporation exceeded annual rainfall when measured over *A. mearnsii* at Two Streams. This suggested that either (i) the instruments used were providing incorrect results, (ii) that tree roots were accessing groundwater and depleting soil water reserves from within the deep soil profile or (iii) that there are unaccounted for additions to the water balance in the Two Streams catchment.

Initial studies at Two Streams (WRC K5/1284, Everson *et al*., 2007), showed that removing riparian wattle trees had a significant impact on increasing streamflow. The relative contribution of the riparian zone compared to the upslope region during the period when both areas were cleared (January 2004 to May 2006) was 16 mm and 78 mm respectively (the riparian zone therefore contributing 21% to annual streamflow). Since the riparian zone represented only 11% of the total catchment area (7.5 ha versus 65 ha), the significance of the riparian zone to streamflow generation was clearly demonstrated. Subsequently (WRC K5/1682), Clulow *et al.* (2012) provided results showing high rates (7 to 10 mm day^{-1}) of ET during the exponential growth phase of the Wattle trees (< 3yrs old). Over a period of approximately 2.5 years the ET exceeded the rainfall by 46%. This raised concern over the long-term impact of afforestation on the water balance, particularly the sustainability of groundwater levels.

This new phase of research has provided an opportunity to extend the valuable datasets such as streamflow and rainfall. In addition the ET measurements have been continued to determine whether the high rates of ET are sustained over a full rotation of the trees. Improvements to existing instrumentation such as recently developed TDR probes has been undertaken as well as isotope research, sapflow studies on different slope positions and HYDRUS 1D modelling.

1.2 Project Objectives

1. To quantify the long-term effects of *A. mearnsii* on deep soil water profiles, streamflow and evaporation over a full crop rotation,
2. To quantify/understand the controlling environmental and soil water processes (including root distribution) which allow for ET to exceed the annual rainfall,
3. To provide a modelling framework for the catchment water balance to improve streamflow prediction and specifically low flows
4. To gain a better understanding of the spatial distribution of transpiration from trees growing on different hillslope positions, and
5. To extend the hydrological record for Two Streams to provide a long-term database of the catchment hydrological variables for future modelling studies.

1.3 History of Research and Funding at Two Streams

The original "Two Streams" project (funded by Working for Water), was planned for three years and was started in 1999 and ended in March 2002 (Everson *et al*., 2007). This project was the focus of intensive research by the CSIR's hydrology group in Pietermaritzburg and the scale of the research expanded greatly in these first three years. The construction of gauging weirs, drilling of boreholes and instrumentation of the catchment took longer than originally anticipated. As a result, it became clear during the 2000 year that additional support would be needed in order gain maximum benefit from the funds already invested. Thus a second proposal to support this research and extend the measurements was submitted to the WRC and approved in April 2001. This funding extended the monitoring into early 2003.

Following a short calibration period, all the *A. mearnsii* trees in the riparian zone were cleared in July 2000. Eighteen months of data were collected to assess the impact of this clear-felling on runoff and hillslope hydrological processes. The plans to remove all the trees from the entire catchment in 2002 were delayed by technical problems experienced by Mondi with stripping bark and the trees were only finally felled from the catchment by December 2004. Although this allowed extended monitoring of the recovery of the riparian zone, it shortened the monitoring period of the cleared catchment. The continuation of the monitoring of the project in 2004 to 2005 and subsequent data analysis and write up in 2006 was therefore requested from Working for Water and the project was awarded an extension until 2006. These funds were transferred to the WRC who continued to manage the project.

By 2006, the Two Streams catchment had become one of the most intensely monitored forestry research catchments in South Africa, providing quantitative measurements of the impact of riparian management on the hydrology of the catchment. During the period from 2006 to 2009 the WRC funded further work to:

- Continue the existing measurements in the catchment to extend the database,
- confirm the high rates of ET from the Wattle trees measured in the past,
- construct a probe to measure soil water that can be installed at depths beyond 2 m
- test the performance of some hydrological models

There was a gap in project funding during 2009 and 2010 but basic monitoring of climatic variables and streamflow were continued until the current project commenced in April 2011. The Water Research Commission and Working for Water are responsible for the current funding allocation and are kindly acknowledged for their contributions. Mondi have contributed in numerous ways over the years providing access to the research catchment but also by fully funding a new 24 m high lattice mast. This has enabled the continued monitoring of ET over the *A. mearnsii* stand which has been essential in determining the long-term ET at the research site, something which until now has not been achieved in South Africa. In summary, the research focus areas of the current work at Two Streams include, (1) the installation of sapflow systems on the south and north-facing slopes in lower and mid-slope positions to determine the possible influence of aspect on sapflow, (2) modification of the TDR probes which can be installed at depths of up to 4.8 m, (3) isotope studies with extraction of soil water and tree sap for isotope

analysis, (4) an investigation into the contribution of stemflow to the water balance of the catchment and (5) the continued monitoring of ET, groundwater, soil water, rainfall and streamflow.

The sections below build on some of the work reported on in the previous Two Streams research project reports. The data record lengths have been extended and the results have been updated and reported on. In some cases, such as rainfall and streamflow, the entire data sets (since 1999) have been included for completeness.

2. THE STUDY AREA

The Two Streams catchment is situated 70 km from Pietermaritzburg near Seven Oaks on the Greytown road (Figure 2.1). The Bioregion is 'midlands mistbelt grassland'. The area is generally hilly with rolling landscapes and a high percentage of arable land. It is dominated by forb-rich, tall, sour *Themeda triandra* grasslands of which only a few patches remain due to invasion of native *Aristida junciformis.* Soil forms are apedal and plinthic and are derived mainly from the Ecca Group with dolerite dykes and sills. Rainfall is primarily in summer with an annual rainfall ranging from 659 to 1139 mm. Rain is most commonly from summer thunderstorms or cold fronts. Mist can be heavy and frequent and might add significantly to precipitation. Moderate frosts, droughts, hail and berg winds are also common to the area (Mucina and Rutherford, 2006).

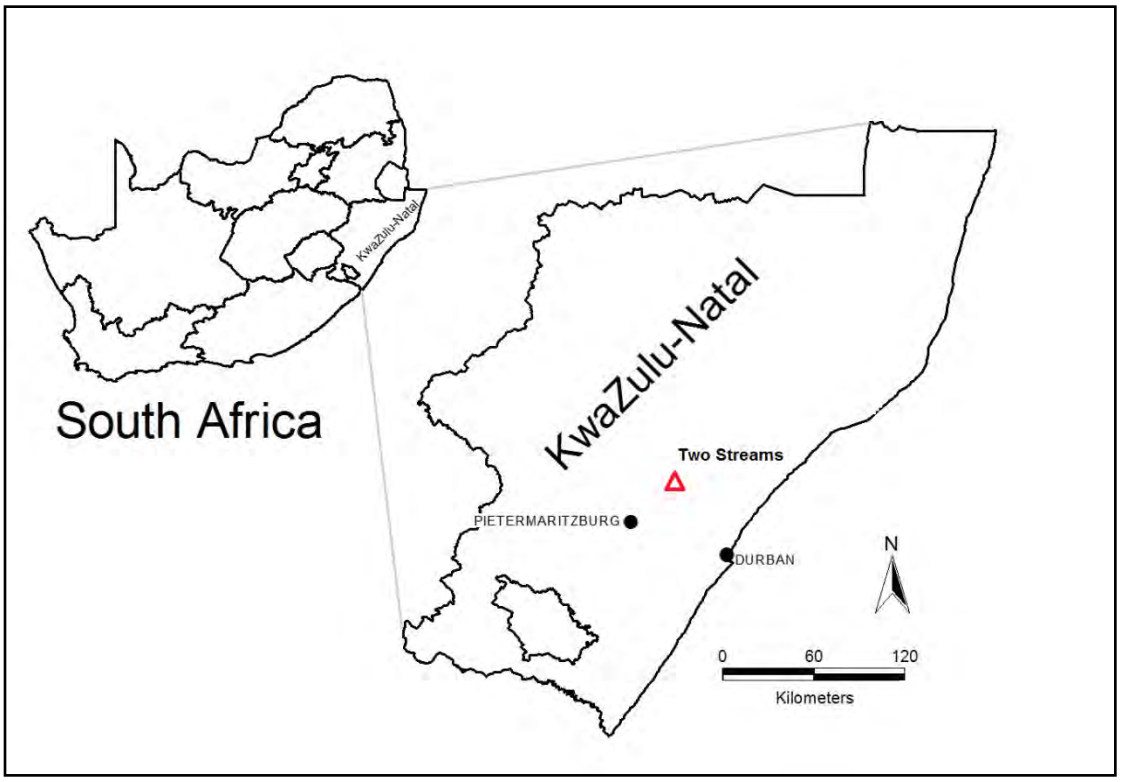

Figure 2.1: Location of the Two Streams Catchment in the Seven Oaks district in the KwaZulu-Natal midlands.

2.1 Study Sites

A number of study sites have been established across the small catchment area known as Two Streams. Some sites have been well established during the course of previous research projects. For example, a weir was constructed in 1999, an Automatic Weather Station (AWS) was setup in

2006 and boreholes were drilled in 2001 and 2007. This current project benefitted significantly from these established sites and they were refurbished and maintained during the course of this project. However, to fulfil the specific objectives of this project (see section 1.2), a number of new sites and monitoring strategies were implemented. A lattice mast was erected (September 2011) close to the centre of the Wattle stand (6 ha). In the vicinity of the mast, total evaporation (ET) and sapflow (upper sapflow site) were measured (Figures 2.2 and 2.3). A full automatic weather station was installed on the top of the mast which recorded the climatic conditions and net radiation above the canopy while soil heat flux was measured below the canopy. The borehole near this tower was monitored with sensors provided by Department of Water Affairs. Newly designed and manufactured TDR probes were installed to measure soil volumetric water content (down to 4.8 m) and watermark sensors were installed to measure water potential (down to 8.8 m). Further down the slope and closer to the riparian area (Figure 2.3), a comparative site was installed at which sapflow (lower sapflow site) was also measured. In addition, sapflow systems were installed on the opposite, north-facing slopes in upper and lower positions to assess the influence of aspect on tree water-use (Figure 2.3). Isotope studies were implemented during 2012 with sampling including the stream water, rainfall, groundwater and tree sap. In 2013 this sampling was continued but with a focus on extracting soil water and improving the rainfall and streamflow sampling with automated systems.

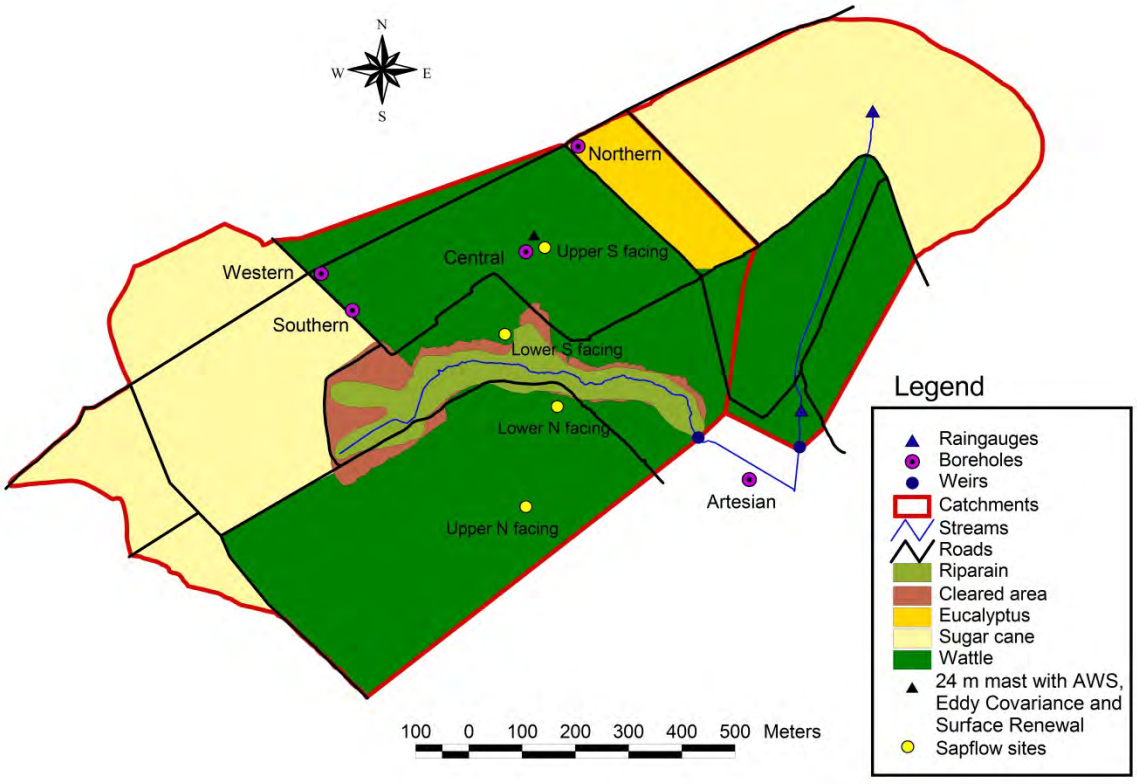

Figure 2.2: The principal research sites within the Two Streams catchment.

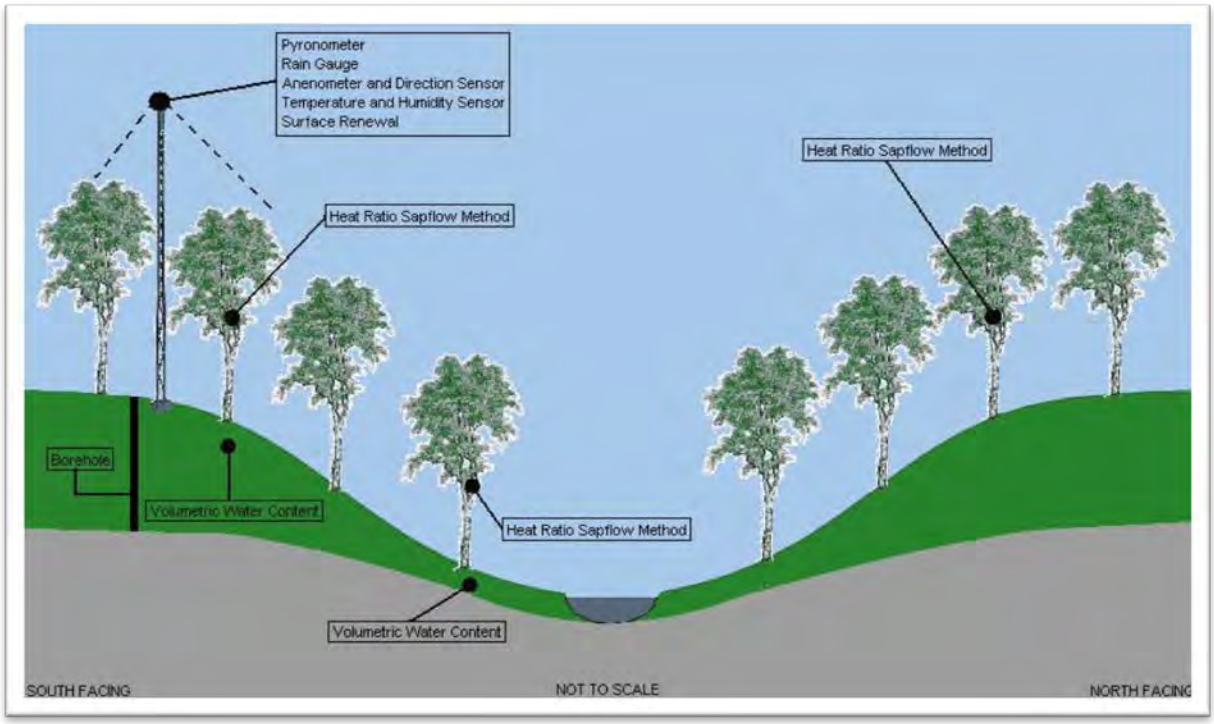

Figure 2.3: The distribution of measurement sites and instrumentation on the north and south facing slopes of the catchment.

3. MATERIALS AND METHODS

3.1 Tree Growth

Tree heights were sampled along the old path length of the scintillometer at monthly intervals (Clulow *et al.*, 2012). Measurements commenced at planting (June 2006) and have been continued up to the present eight year growth stage. Measurements were taken with a tree height rod of the same trees every month at 30 different sites, equally spaced on the previously sited LAS transect (Clulow *et al*., 2012). A hypsometer (Vertex Laser VL402, Haglof, Sweden) was used once the trees reached a height of 10 m.

A LiCor LAI-2000 Plant Canopy Analyser was used to measure Leaf Area Index (LAI) to give an indication of tree canopy growth. LAI is the surface area of leaf material per unit area of ground. Direct measurement of LAI is tedious and labour intensive but LiCor have developed an optical sensor connected to a control unit which enables easy estimation of LAI. Light readings made below the canopy are divided by readings made above the canopy to compute transmittances at five angles. A control unit records these readings and calculates LAI from the transmittances. There are a number of operating principals and limitations to the use of the LAI-2000 that should be noted. Sky conditions, sky brightness non-uniformity, field of view, canopy conditions and foliage size can cause error and need to be within the specification of the instrument (LAI-2000 Plant Canopy Analyser, 1989).

Once the tree height increased beyond 2.0 m, two Plant Canopy Analysers were required. One for below canopy measurements and the other to log above canopy light readings on the scaffolding above the trees. The data files were downloaded to a computer and LiCor software was used to merge the two files and calculate a LAI value at each of the 30 sites used along the transect.

Root samples were collected during the previous project in February 2008 and again in February 2009 by auguring to depths of 4.8 m. This was repeated on October 2011 and October 2012 to determine changes in the rooting distribution. The soil samples were passed through a 2 mm sieve using water and the remaining roots were air-dried and weighed. A representative root weight was calculated by dividing the weight of roots from a certain depth by the weight of the soil sample taken at that depth in order to obtain the mass of the roots (g) per kg of soil.

3.2 Rainfall

Rainfall has been monitored at four sites in the catchment using tipping bucket raingauges since 1999 until present. Two MCS-160 raingauges with a 0.2 mm resolution and two Texas Instruments raingauges with a 0.1 mm resolution were used. MCS raingauge 1 was located in the upper portion of the catchment while the lower raingauge 2 was situated close to the main weir. The third site was located in the plantation where the lattice mast was deployed and the forth at the weather station near the farm office, estimating the FAO-56 short grass reference

evaporation. It was therefore possible to obtain an area weighted average of the rainfall as input into the water balance calculations.

Interception studies at Two Streams have greatly enhanced our understanding of effective rainfall and the importance of considering rainfall interception in afforested areas. The historic rainfall record from September 1998 to March 2011, as well as the rainfall during the study period from April 2008 to March 2011 is illustrated in Figure 3.1. Both periods show a similar rainfall distribution, indicating that the recent study period was typical in terms of rainfall. The high percentage of "small" events is noticeable. Rainfall events less than 1 mm account for 50.8% of the events during the study period. The events below 4.0 mm account for approximately 73.6% of all the rainfall events during the study period. This is significant, because during these "small" events, it is likely that most of the rainfall will be intercepted by the canopy and the litter, depending on the antecedent canopy and litter moisture content.

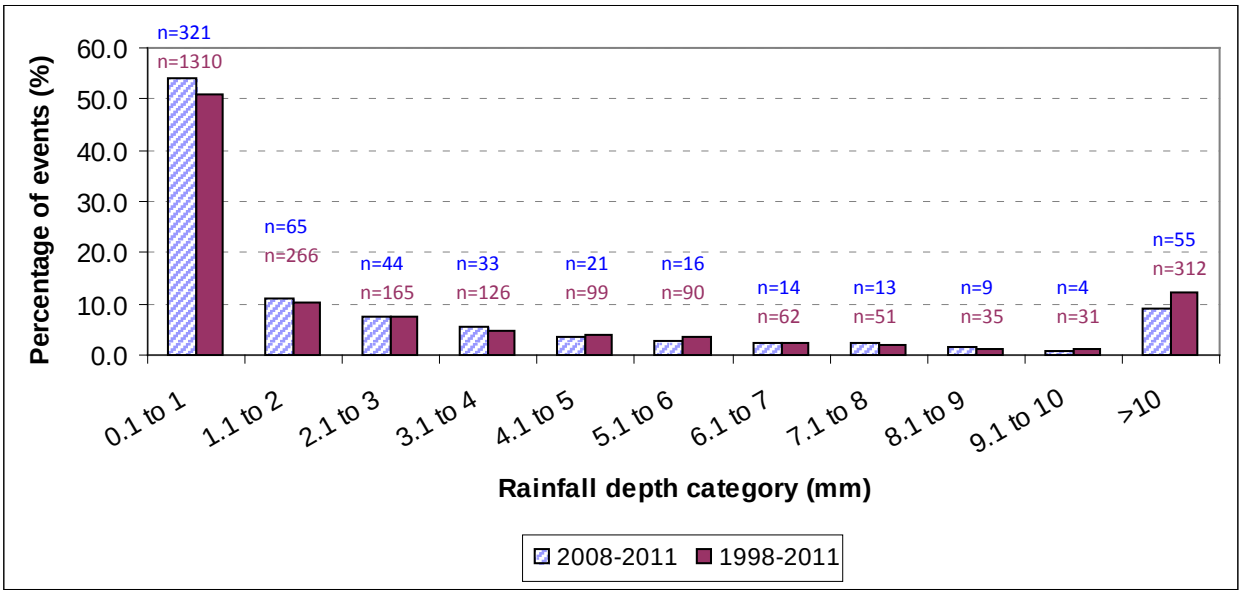

Figure 3.1: Percentage of rainfall events per rainfall depth category (n=595 and n=2577).

3.2.1 Canopy interception measurements

Throughfall measurements were made using a nest of three "V" shaped troughs at the south site tower, constructed from galvanised iron sheeting (Figure 1) based on the design of Cuartus *et al*. (2007). The dimensions of each trough were 0.1 m wide x 2.0 m long. Conventional "U" or "V" shaped troughs are susceptible to blockage by fallen debris and water loss from splash out, however, this system minimizes splash out by using steep "V" shaped sides. The troughs were covered with mosquito netting to minimize the entry of debris, which reduced the demand of cleaning and maintaining the system. A correction factor for each trough was derived from

laboratory measurements to account for the "initial abstraction" from the netting. The three troughs were then connected to a single tipping bucket gauge and an event data logger. Because the trough represents a linear and continuous sampling surface, the linear variation of leaves, branches, and tree crown, its catches were assumed to be a representative integral of throughfall. A shortcoming of the throughfall troughs was that they were still susceptible to occasional blockages (8 out of 595 events, i.e. 1.3%) during large rainfall events, particularly at the *A. mearnsii* site which has very small compound leaves that were still able to fit through the netting. From field observations and analysis of the raw data, such events were patched for further analysis in this study. One nest of three troughs was deemed to be sufficient, due to the uniform spacing of the trees in the plantation. Also, the radial arrangement of the three troughs accounts for the linear variability within the canopy.

Figure 3.2: Throughfall troughs with a covering of mosquito netting (a) and a blockage due to leaves in the trough outlet (b).

3.2.2 Stemflow

Precipitation falling over a forested catchment does not make its way directly to the ground surface, but is instead diverted by leaves, branches and stems (Steinbuck, 2002). The way in which water is captured or impeded by the stems and leaves of trees is referred to as interception (discussed above). The intercepted water may make its way back to the atmosphere as evaporation, or it may pass down the forest canopy (Steinbuck, 2002). Precipitation reaches the forest floor *via* two main methods: throughfall, which is water that drips off leaves and branches or water that falls to the forest floor through gaps within the forest, and stemflow, which is the portion of water that flows down the branches and stems of the tree to the forest floor (Hanchi and Rapp, 1997). Stemflow is usually a thin film of water which clings to the branches and stems of trees (Steinbuck, 2002). As a hydrological process, stemflow is often considered an insignificant contributor to the water budget of a catchment (Steinbuck, 2002). The majority of studies relating to the partitioning of rainfall focus more on the throughfall component, without considering stemflow. This could be due to difficulty in attaining stemflow measurements in terms of a quantitative value (mm).

3.2.2.1 Significance of Stemflow in Plantations

Previous studies have indicated that stemflow in certain areas consists of a small proportion of precipitation; hence it is a small component of the water balance of a catchment. Due to it being perceived as a small percentage, it is often overlooked when forest hydrologic studies are conducted. However, this view is not entirely true as, in some instances; stemflow is large enough to warrant special care (Crockford and Richardson, 2000).

A study conducted by Taniguchi *et al*. (1996) on the significance of stemflow on groundwater recharge showed that, even though stemflow consists of a small portion of precipitation, the effect on groundwater recharge was relatively large. According to research conducted by Taniguchi *et al*. (1996), the ratio of stemflow to precipitation was relatively small, ranging from 0.5 to 1.2%, but the groundwater recharge rate of stemflow compared to the total recharge rate was, considerably higher, ranging from 10.9 to 19.1%. Results from this study illustrate the effects and importance of stemflow on forest hydrology, hence it cannot be overlooked.

Rainfall is an important source of nutrients for a forest ecosystem, more so in areas where rock weathering is very slow (Ling-hao and Peng, 1998). The rainfall over a plantation is altered when it comes into contact with the tree surface, as it washes off nutrients that are stored in the tree canopy or on the branches, resulting in the deposition of nutrients and minerals to the forest floor via stemflow or throughfall (Ling-hao and Peng, 1998). Throughfall and stemflow also form pathways in nutrient cycling, as dry atmospheric nutrient deposits are returned to the forest floor via these processes (Ling-hao and Peng, 1998). Due to the importance of nutrient cycling in a forest ecosystem, the movement of nutrients via stemflow and throughfall are studied in detail, to attain the nutrient balance of the ecosystem (Ling-hao and Peng, 1998). These studies enable us to have some idea with regard to the long-term sustainability of the forest stand.

3.2.2.2 Factors Influencing Stemflow

Stemflow is affected by a variety of factors (Crockford and Richardson, 2000; Williams, 2004), with some having greater influence than others (Williams, 2004). These are the climatic factors as well as, the characteristics of the tree species concerned, in this case *A. mearnsii*. Crockford and Richardson (2000) have identified various tree species characteristics and climatic factors which influence stemflow. These tree characteristics were considered when selecting *A. mearnsii* stems in the forests stand at the Two Streams catchment.

The tree characteristics noted by Crockford and Richardson (2000) include:

- Crown size. The greater the crown size, the greater the potential stemflow yield. The crown of a tree comprises of all the branches, stems and leaves of the tree, i.e. all the above-ground parts. *Acacia mearnsii* does not have a relatively large crown size, hence the potential stemflow yield is lower, compared to trees with a larger crown size.
- Leaf shape and orientation. Leaf orientation and shape play a role in the interception of water, the water-holding capacity of the tree and the leaf area index of the species. If leaves are angled above the horizontal, intercepted precipitation is channeled down the

branch onto the stem of the tree. Larger leaves would intercept more water, hence, depending on their orientation; the potential stemflow yield is increased or decreased. The leaves of the *A. mearnsii* are slightly above the horizontal. The leaves are small, but close together, which results in an increased water-holding capacity. As a result, the potential stemflow yield of *A. mearnsii* is high, due to leaf shape and orientation.

- Branch angle. Steeper branches have a greater potential to contribute to stemflow. The branches of the *A. mearnsii* are very steep and above the horizontal, hence greater potential stemflow yield.
- Flow path obstructions. These include scars on the branches or detaching bark pieces, which can impede the flow of water to the stem. The impeded water then forms part of throughfall. This may not have a great influence on the tips of the branches, but, closer to the stem, obstructions could result in far greater quantities of water being "lost" to throughfall. In the concerned plantation of *A. mearnsii*, the flow path obstructions are limited, as the plantation is well-maintained and there are limited disturbances in the area.
- Bark type. The bark thickness and type differ greatly among species. Smoother thin barks have a higher potential to contribute to stemflow because they are easily wetted and water can flow with ease down the stem, as opposed to rough barks, which offer resistance to flows and may cause channelization. Thicker barks often need to be saturated before any stemflow can occur. It is also easier to install stemflow measuring equipment to smoother barks. *A. mearnsii* has a smooth bark, which could result in greater potential for stemflow.
- Canopy gaps. Gaps in the canopy may also affect stemflow, as precipitation could have direct access to the stems of the trees. These gaps could also result in less stemflow and increased throughfall. With respect to the *A. mearnsii* plantation, there are not many large gaps between stems, hence stemflow resulting directly from rainfall is limited.

Climatic factors as identified by Crockford and Richardson (2000) are as follows:

- Temperature and relative humidity. The greater the air temperature and lower the relative humidity, the greater the amount of evaporation occurring. Greater amounts of evaporation could result in lower stemflow yields.
- Rainfall duration and intensity. Longer duration events result in greater stemflow yields when compared to shorter duration events. Events with a greater intensity may result in increased stemflow quantities, but this is dependent on duration. At the location of the plantation, high intensity summer rainfall is the predominant form of precipitation. As a result, large amounts of precipitation are converted to stemflow in this plantation.
- Wind speed and direction. Rain angle, which is influenced by wind direction, also plays a role in the quantity of stemflow generated.

Another factor, which is unique to the location of the plantation, is that it lies in a mist belt, which would have an effect on stemflow. Mist cannot be measured with a standard rain gauge and it may form an additional component to the catchment's water balance. The mist could however, be intercepted by the stems and branches, resulting in increased stemflow during rainfall events or even stemflow without rainfall if mist is present.

3.2.2.3 Review of methodologies used to calculate stemflow

There is no standard methodology used to determine stemflow and numerous different techniques have been implemented internationally (Levia and Frost, 2002). The lack of a universal methodology to measure stemflow prompted Hanchi and Rapp (1997) to review the procedures used for stemflow measurement internationally and they summarise three methodologies used:

Method 1 (Representative Area)
This method involves the selection of a site within a forest stand which represents the stand in terms of tree diameter, canopy density and spatial distribution. The stemflow measurements for each rainfall event are divided by the area of the study site to give an average percentage of rainfall that is converted to stemflow over the entire site. Results of this method seem fairly representative; however it is critical that the site area is representative of the forest stand and that the forest is well managed and uniform such as is found at Two Streams. This method was therefore applied during the course of this study to obtain stemflow depth for comparison against rainfall.

Method 2 (Rainfall/Stemflow Correlation)
This method involves establishing correlations between the volume of stemflow for representative trees of a certain class (p) and the rainfall outside the forest stand. The stemflow volume is then multiplied by the number of representative trees of that class (p) in a hectare. This is done for all the different classes and summed up. This method has a tendency to overestimate stemflow as it is essentially based on the correlation between stemflow volume and precipitation which can vary between storms.

Method 3 (Tree/Stemflow Correlation)
This method takes into account all trees in the stand classified according to their diameters at breast height (DBH). Using data attained from all representative trees, regressions are calculated for each storm. To determine the stemflow of the stand for each storm, the mean stemflow volume for each class is multiplied by the number of trees in the class per hectare. The main advantage of this method is that it directly accounts for the entire stand. This method does not require a fully representative site.

3.2.2.4 Equipment installation

Stemflow systems were installed at two sites in different locations within the catchment (Figure 3.3 and Table 3.1). Two trees at the middle of the plantation and two at the edge of the stand were instrumented. At each location, the stems are situated close to each other to account for the non-uniformity of rainfall. The two different sites were chosen to determine if the “edge effect” has any influence on stemflow. The effect of tree diameter on stemflow measurements was also analysed.

A silicone tube (10 mm inside diameter, 25 mm outside diameter) was sliced open part of the way down its length. This sliced section of silicon tube was nailed into position and glued with silicone

to seal the edges of the tube with the bark in a spiral pattern around the stem (Figures 3.4 and 3.5). The closed section of tube carried the water collected from the stem into a tipping bucket raingauge that was covered to exclude direct rainfall or throughfall.

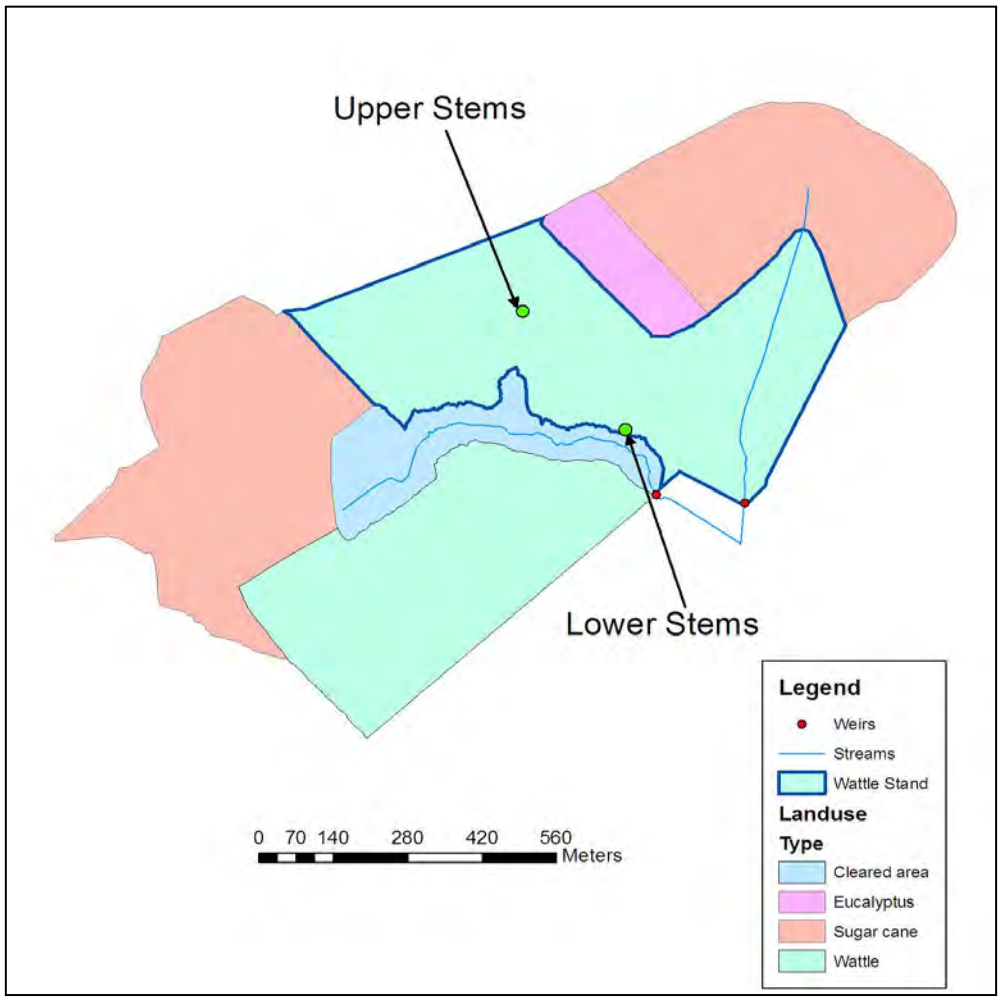

Figure 3.3: The location of the two stemflow sites indicated by green circles (upper and lower) in the *A. mearnsii* stand at Two Streams.

Table 3.1: Four different trees were instrumented at two separate sites with thick and thin trunks.

	Location	Tree Height (m)	Stem Diameter (cm)	Date Installed
Upper Thicker	Centre of the plantation	17.4	44.5	28/02/13
Upper Thinner	Centre of the plantation	17.0	35.1	28/02/13
Lower Thicker	Edge of the plantation	17.1	49	14/03/13
Lower Thinner	Edge of the plantation	17.0	43.2	14/03/13

Figure 3.4: Silicon tube and tipping bucket raingauge to measure stemflow.

Figure 3.5: A close-up view of the silicone tube glued with silicone sealant to the bark of the stem that collects stemflow.

3.2.3 Litter interception and water that drains into the soil

The experimental layout for measuring litter interception and water that drains to the soil is shown in Figure 3.6. The litter interception and water that drains to the soil were measured using two round galvanized iron basins that fit into each other. Two litter interception basins were placed in each site to account for the spatial variability of the litter thickness. The upper basin which had an inner diameter of 0.5 m was filled with litter and had a geotextile lining on top of a wire mesh base, so that water could percolate into the lower basin, but the fine particles from the litter are retained. A flat spade was used to slide under the litter at the litter-soil interface as carefully as possible so as to limit the disturbance of the sample. This sample was then placed

into the interception basin. The water that was collected in the lower basin drains into a Davis tipping bucket (Davis Instruments, 2001) and the water that would have drained to the soil was recorded with a HOBO® pendant event logger (Onset Computer Corporation, 2005). The litter interception is then calculated as the difference between throughfall measurements obtained and the water that drained to the soil. The experiment was replicated twice at each of the three sites.

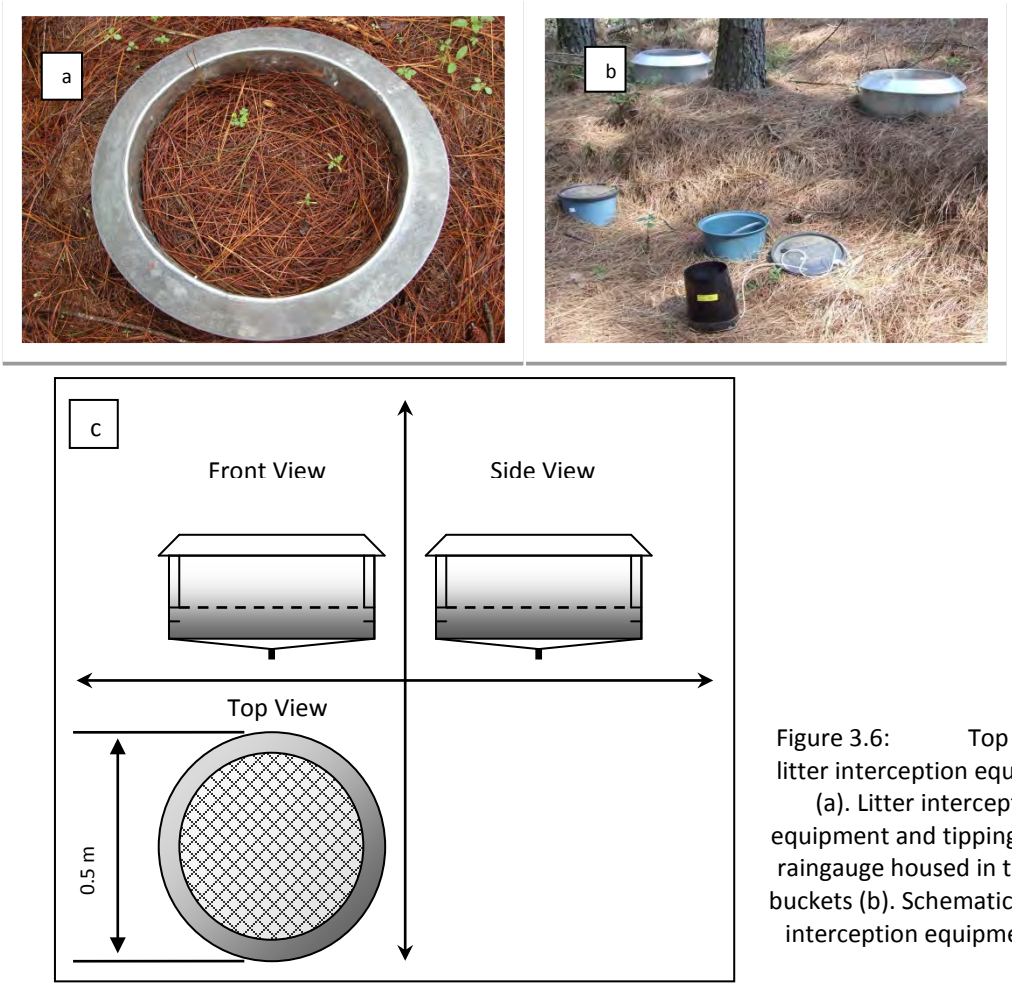

Figure 3.6: Top view of litter interception equipment (a). Litter interception equipment and tipping bucket raingauge housed in the blue buckets (b). Schematic of litter interception equipment (c).

3.3 Lattice Mast Installation

During the previous measurements of ET from 2006 to 2008, a large aperture scintillometer was used (Clulow *et al.*, 2012). A transmitter and receiver were mounted on opposite ends of the *A. mearnsii* stand on towers above the trees. However, in the current project the tree height was beyond 15 m. For scintillometery, beam alignment of the transmitter onto the receiver is critical. On tall towers, sway and vibration can result in misalignment and erroneous readings. For this reason a 24 m lattice mast (Guyed 450, Webb Industries) was installed in the middle of the stand (Figures 3.7 and 3.8) and the eddy covariance and surface renewal methods used to determine

the ET (see section 3.5 below). A hinged base plate was embedded in 1 m^3 of concrete (Figure 3.7). Eight 3 m sections were bolted together on the ground and a crane was used to raise the mast. Steel guys at two heights (12 m and 24 m) were attached to support the mast. They were anchored by steel plates embedded in concrete (Figure 3.9). The tower has provided a firm and stable structure ideal for mounting instruments within and above the canopy.

….. / Figure 3.7

Figure 3.7: Base of the 24 m lattice mast in the centre of the Wattle tree stand. A hinged base-plate was concreted into the ground for stability.

Figure 3.8: The upper sections of the 24 m lattice mast in the centre of the Wattle tree stand. Steel guys were attached at 12 m and 24 m for stability.

Figure 3.9: The steel guys were secured onto custom brackets that were concreted into the ground.

3.4 General Climatic Variables

Two Campbell Scientific automatic weather stations collected standard atmospheric data at Two Streams. The one station was setup in a short grassland area to calculate the short grass reference evaporation according to the American Society of Civil Engineers-Environmental and Water Resources Institute (ASCE-EWRI) method (based on the Penman-Monteith method) (Figure 3.10). For further information on the ASCE method for determining the reference evaporation (ET_{sz}), refer to Allen *et al*. (2005) and Allen *et al*. (2006). The second AWS was attached at the top of the 24 m lattice mast above the canopy to provide additional data for the energy balance calculations to determine ET using the eddy covariance and surface renewal systems (Figure 3.11).

The Penman-Monteith method is internationally recognised and popular for a number of reasons, including the relatively low data requirements and the relationship established between the reference and the ET known as the crop factor (K_c) where $K_c = ET/ET_{sz}$. This relationship allows agronomists and hydrologists to estimate ET from easily acquired standard weather station data.

The results of ET will be compared to the short grass reference standard and a crop factor for *A. mearnsii* calculated relative to the height of the trees.

The weather stations measured standard climatic parameters including solar radiation, ambient air temperature, relative humidity, rainfall, wind speed and wind direction using Campbell Scientific Inc. data loggers (CR23X and CR1000).

Figure 3.10: Automatic weather station near the Two Streams site established over short grass and used to calculate the short grass ASCE reference evaporation.

Figure 3.11: Automatic weather station on the 24 m lattice mast within the Wattle tree stand.

Additional sensors at the weather station measured the net radiation and soil heat flux components of the shortened energy balance. The net irradiance was measured using an NR-LITE (Kipp and Zonen) net radiometer. The soil heat flux was also measured using two soil heat flux plates (REBS) placed at a depth of 80 mm below the soil surface. A system of parallel thermocouples at depths of 20 and 60 mm were used for measuring the soil heat stored above the soil heat flux plates. Volumetric soil water content in the first 60 mm was also measured using a CS616 time domain reflectometer (TDR) (Campbell Scientific) (Figure 3.12). The measurements were sampled every 10 s with a Campbell scientific CR23X and 30-minute averages were computed. The net irradiance was stored directly in the logger memory. Soil heat flux was calculated in an Excel spreadsheet using the thirty-minute data from the soil heat flux plates, the soil temperature averaging probes and the Campbell Scientific CS616 volumetric soil-water reflectometer using Equations 3.1 and 3.2.

$$F_s = F_{plate} + F_{stored} \quad (3.1)$$

$$F_{stored} = \frac{\rho_s \, \Delta T_s \, c_s \, d}{\Delta t} \quad (3.2)$$

where F_s is the soil heat flux at the surface (W m^{-2}), F_{plate} is the heat flux at a depth of 80 mm (W m^{-2}), F_{stored} is the flux of heat storage in the soil (W m^{-2}), ρ_s is the bulk density of soil (kg m^{-3}), ΔT_s is the temporal change in temperature over the output interval (K), c_s is the specific heat capacity of soil (J kg^{-1} K^{-1}), d is the depth of the heat flux plates in the soil (m) and Δ_t is the output time interval (s).

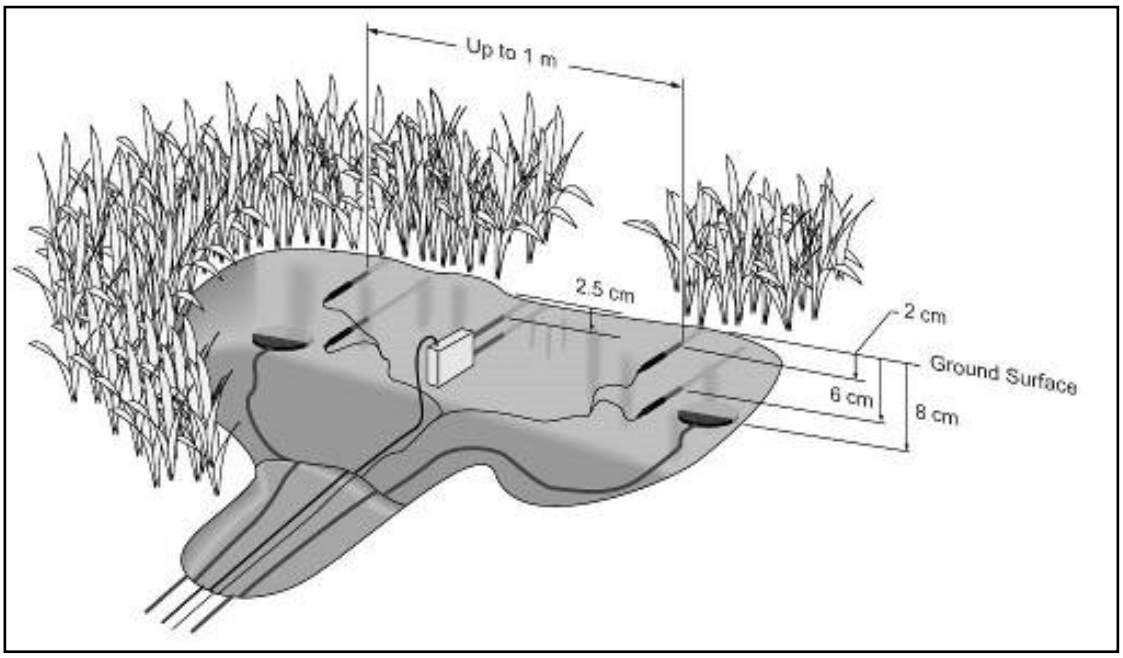

Figure 3.12: Layout of sensors used to estimate soil heat flux (after Campbell, 2003).

The micrometeorological conditions within the canopy were recorded at the lattice mast site. Climatic conditions below the tree canopy are different to those measured above the canopy. Solar radiation and windspeed are likely to be the parameters most affected by below canopy differences, both being important factors in the evaporation process and clearly important in litter interception and soil evaporation estimates.

3.5 Evapotranspiration Measurement Using Eddy Covariance and Surface Renewal

Sensible heat flux was calculated using the surface renewal (SR) technique in the centre of the Wattle stand. Air temperature was measured using two unshielded type-E (chromel/constantan) fine-wire (76 µm diameter) thermocouples (TC's) placed at heights of 19 m and 21 m above the ground surface, raised on 26/11/2012 to 20 m and 22 m. Results were recorded with a datalogger (CR3000, Campbell Scientific Inc., Logan, Utah, USA) powered by two 70 Ah batteries and one 20 W solar panel. Data were saved onto a 2 GB compact flash card able to store up to six weeks of high frequency (10 Hz) data. The SR technique is based on the principle that an air parcel near the surface is renewed by an air parcel from above (Paw U *et al*., 1995). This process involves ramp like structures (rapid increase and decrease of a scalar), which are the result of turbulent coherent structures that are known to exhibit ejections and sweeps under shear conditions (Gao *et al*., 1989; Raupach *et al*., 1996; Paw U *et al*., 1992). The theory of heat exchange between a surface and the atmosphere using the SR method is described in detail by Paw U *et al*. (1995), Snyder *et al*. (1996), Paw U *et al*. (2005) and Mengistu and Savage (2010). The exchange of heat energy between a surface and the atmosphere, also known as sensible heat flux (*H*), is expressed as:

$$H=\alpha\rho_a c_p z\frac{a}{\tau} \qquad (3.3)$$

where, α is a weighting factor, ρ_a is the density of air, c_p is the specific heat capacity of air, z is the measurement height, a is amplitude of the air temperature ramps and τ is the total ramping period. The amplitude and the ramping period were deduced using analytical solutions of Van Atta (1977) for air temperature structure function:

$$S^n(r)=\frac{1}{m-j}\sum_{i=1+j}^{m}(T_i-T_{i-j})^n \qquad (3.4)$$

where, n is the power of the function, m is the number of data points in the time interval measured at frequency f (Hz), and j is the sample lag between data points corresponding to a time lag $r=j/f$, T_i is the I^{th} temperature sample. Time lags of 0.4 and 0.8 s were used in this study. Second, third and fifth orders of the air temperature structure parameter are required to solve for a and τ.

The weighting factor (α) is required to determine H (Eq. 2). It depends on the measurement height, canopy architecture and thermocouple size (Snyder *et al*., 1996; Spano *et al*., 1997; Spano *et al*., 2000). Once determined by calibration, it is fairly stable and does not change regardless of weather conditions unless the surface roughness changes (Snyder *et al*., 1996; Spano *et al*., 2000; Paw U *et al*., 2005). An eddy covariance system was deployed over intermittent periods totaling nine months on the mast at the Wattle stand to determine α.

The Eddy Covariance system is generally based on very high frequency measurements of water vapour and CO_2 above vegetation canopies (10 Hz). In our case we used a single sonic

anemometer and the sonic temperature to derive the sensible heat flux (see equation 3.10), as this is a much cheaper option for determining the evapotranspiration, as it does not require the expensive infra-red gas analyser. Such frequent measurements describe gas concentrations in eddies of air that are particularly important drivers of gas exchange above aerodynamically rough vegetation. The technique is especially valuable in studies where information on both the water and carbon fluxes are significant indicators of water-use efficiency, and which may be compared to similar data obtained over vegetation in other countries.

In fully turbulent flow the mean vertical flux *F* of an entity *s* per unit mass of the fluid is given by

$$F = \overline{\rho_a w s} \qquad (3.5)$$

where ρ_a is the density of air, *w* the vertical wind velocity, and the over bar denotes the average value during a time period of suitable length. In the surface boundary layer all atmospheric entities exhibit short-period fluctuations about their mean value. Therefore, the instantaneous values of *w*, *s*, and ρ_a can be expressed by:

$$w = \overline{w} + w', \qquad s = \overline{s} + s', \qquad \rho_a = \overline{\rho_a} + \rho_a' \qquad (3.6)$$

where the prime symbol denotes an instantaneous departure from the mean. These expressions can be substituted into Equation 3.7 and if we neglect fluctuations in density, the mean vertical flux *F* reduces to:

$$F = \overline{\rho_a w s} + \overline{\rho_a w' s'} \qquad (3.7)$$

or by writing ρ_a for $_a$

$$F = \rho_a \overline{w s} + \rho_a \overline{w' s'} \qquad (3.8)$$

The first term on the right-hand side of Equation (3.8) represents the flux due to the mean vertical flow or mass transfer. The second term represents flux due to eddying motion or eddy flux. The mass transfer term may arise from a convergence or divergence of air due to sloping surface. For a sufficiently long period of time over horizontally uniform terrain the total quantity of ascending air is approximately equal to the quantity descending and the mean value of the vertical velocity will be negligible. Therefore, Equation (3.8) reduces to

$$F \approx \rho_a \overline{w' s'} \qquad (3.9)$$

Based on the above equation, the sensible heat flux (H) and water vapour flux (E) can be expressed as:

$$H = \rho_a C_p \overline{w'T'} \quad (3.10)$$

and

$$E = \frac{\varepsilon}{P} \rho_a \overline{w'e'_a} \quad (3.11)$$

where u', T', and $e_{a'}$ are the instantaneous departures from the mean horizontal velocity, air temperature and vapour pressure; and ε is the ratio of molecular weights of water vapour and air and P is the atmospheric pressure.

Over the course of the measurements, the sensible heat flux was derived from either of the two thermocouples (Tc's) or the eddy covariance system (sonic anemometer) directly. Where data overlapped, the order of priority in which the data was preferably used, was sonic anemometer, Tc2 (upper) and then Tc1 (lower). The Tc1, Tc2 and sonic anemometer were initially installed on the 26 October 2011 at heights of 20 m, 22 m and 21 m respectively. Due to tree growth they were raised on 26 November 2012 to 20 m, 22 m and 23 m respectively. The alpha calibration for each Tc separated based on changes in measurement heights. A compact flash card error resulted in data loss for approximately 4 weeks from the 21 June 2012 over which period the ET was modeled using the Priestley-Taylor model (Priestley and Taylor, 1972).

3.6 Tree Water-use

The techniques described above measure the ET above a stand of trees which includes evaporation from the soil surface, litter layer, intercepted water from the leaves and transpiration from the trees. Where tree water-use is to be compared between sites, these numerous components adds significant complexity to the comparison. Sapflow measurement techniques, therefore, provide an ideal system for comparing the water-use of trees in different slope positions.

Three popular sapflow systems are; the Compensation Heat Pulse (CHPV) (Burgess *et al.,* 2001), Heat Ratio (HR) (Burgess *et al.,* 2001) and Granier Method (Lu *et al.,* 2004). A short-term study was conducted with the assistance of a Hydrology Honours student (UKZN) to evaluate: experimental design, costs, system set-up, installation, post installation, data collection and processing, battery usage and the results obtained, to provide guidelines to potential users. In this study the three different systems were installed in the riparian area of the Two Streams catchment. The result of the evaluation showed the HPV heat ratio method to be most suitable and it has been employed for the sapflow study at Two Streams. Initially, two sites on the south-facing slope were instrumented with HPV equipment. The lower sapflow site is close to the riparian area and the upper sapflow site is near the lattice mast in centre of the wattle stand.

Three trees at each of these sites are referred to as south-facing lower tree 1 to 3 (SF_LT1..3) and south-facing upper trees 1 to 3 (SF_UT1..3) and were instrumented with probes at different depths in the sapwood (Table 3.2). Following some initial results between the sites, a third and fourth (upper and lower), north facing sites were instrumented in order to investigate the influence of aspect on sapflow. In addition, roots were instrumented at the upper south-facing site to investigate hydraulic lift (Figure 3.13).

Table 3.2: The tree measurements and probe insertion depths of the north and south-facing lower and upper sites.

Tree	Circumference (cm)	Probe 1 (mm)	Probe 2 (mm)	Probe 3 (mm)	Probe 4 (mm)
SF_LT1	46.0	5	12	20	30
SF_LT2	35.0	5	10	17	25
SF_LT3	42.0	5	10	17	25
SF_UT1	57.5	5	10	20	40
SF_UT2	60.0	7	10	20	40
SF_UT3	44.1	5	10	20	25
NF_LT1	42.5	7	10	17	25
NF_LT2	63.0	7	15	20	35
NF_LT3	55.0	7	12	20	30
NF_UT1	40.0	5	10	20	25
NF_UT2	59.0	5	15	25	35
NF_UT3	49.0	5	10	20	30

The HPV technique is recognised internationally as an accepted method for the measurement of sap flow in woody plants. It has received much attention by researchers in recent years, and a wide variety of systems have been developed (Smith and Allan, 1996). It has also been extensively applied in South Africa (Dye and Olbrich, 1993; Dye *et al.*, 1996; Gush, 2008).

The heat ratio method (Burgess *et al*., 2001) of the HPV technique requires that a central line heater be implanted into the sapwood portion of the stem. The 60 mm long line-heaters are typically made from 1.8 mm outside-diameter stainless steel tubing, enclosing a constantan filament. Two additional holes are drilled 5 mm above and 5 mm below the heater probe. Thermocouple (TC) probes (consisting of type T copper-constantan thermocouples embedded in 2 mm outside-diameter PTFE tubing), are inserted into the upper and lower holes to a specific depth below the cambium. All drilling is performed with the drill bit projecting through a drill guide strapped to the tree, to ensure that the holes are as close to parallel as possible (Figure 3.13). The thermocouples are wired to a multiplexer (AM16/32) and datalogger (mostly CR10X or CR1000), while the heater probes are connected to a relay control module and 12 V battery (Figure 3.14). Generally, four pairs of probes (each set comprises upper and lower TCs and a heater) are implanted in a tree stem, depending on the size of the tree. The TCs are inserted to different depths below the cambium to sample different regions of the sapwood. Sap flow is generally fastest in the younger xylem closer to the cambium, but slows in the older, deeper xylem. To account for long-term changes in position as a result of stem diameter growth or the

release of gum (Figure 3.15), the TCs are completely removed and repositioned to their correct depths once or twice a year. In addition the heaters are dipped in Vaseline to provide a protective film from the corrosive gum.

Figure 3.13: Installation of an HPV system to measure sap flow in a lateral root.

Figure 3.14: A metal security enclosure on the left housed the HPV data logger, multiplexer, relay control module and battery. On the right the thermocouple and heater probes inserted into an *A. mearnsii* tree.

Figure 3.15: At the location of the wounding where the probes are inserted, the *A. mearnsii* trees produce a gum that is corrosive and can adjust the depth of the probes in the sapwood.

The data loggers are programmed to initiate measurements at pre-determined intervals (generally hourly). The temperatures in the upper and lower TCs are first measured. The temperature of each TC is measured 10 times and an average of those 10 measurements is calculated to determine the current temperature for each TC. These values are stored in the logger for later calculations. Directly thereafter, a short (e.g. 0.4 second) pulse of heat is released through the entire set of heater probes connected to the relay control module. The heater probes are in groups of four (termed a heater cluster) and each cluster is individually wired to the relay control module. The individual clusters are fired sequentially, and the pulse of heat diffuses through the adjacent wood and is taken up by the sap moving upwards through the xylem of the tree. The length of time used for the heat pulse can be varied in the programme but usually ranges from 0.4-0.8 seconds. As the heat pulse is conducted up the tree by the sap, the upper thermocouple begins to warm (generally to a greater extent than the lower thermocouple due to heat transport by the sap, although there is some conduction of heat to the lower thermocouple as well). Logging of the changing heat ratio commences 60 seconds after the initiation of the heat pulse and is measured continuously (approximately every second, depending on the processing speed of the logger) until 100 seconds after the heat pulse (after Burgess *et al.*, 2001). To determine the heat ratio, first the change in temperature (Δtemp) is measured for each TC. This equates to the current (heated) temperature minus the average pre-pulse temperature determined earlier. The heat ratio (Δtemp upper TC / Δtemp lower TC) is then calculated for each probe set consecutively, and this value changes as the heated sap moves through the xylem. These individual heat ratio values are accumulated for each TC pair, and at the end of the measurement window (e.g. after 100s) the average ratio is calculated for each TC set individually. The heat pulse velocity (for each TC pair) is equal to the natural log of the average heat ratio multiplied by a constant that accounts for the thermal diffusivity of wood and the distance between the heater probe and each TC (after Marshall, 1958). The value of the constant is initially 18, but may vary depending upon wood qualities (Burgess *et al.*, 2001). These hourly heat pulse velocities for each TC set are the final outputs from the logger.

All available HPV data for an individual tree are initially screened to identify periods of missing data. The first step in the patching process is to determine if there are good quality data available from any of the other probes for the period in question. The probes with the highest correlation to the probes being patched are identified through a correlation analysis. A simple linear regression equation is then used to patch the missing data according to the functional probe set. High correlations among different probe sets within the same tree are observed in most cases, giving confidence in the patching technique. Where there are simultaneously missing data for all probe sets in a tree, data from adjacent measured trees may be used in a similar manner to correlate and patch. Where there are missing or suspect single hourly values, these may be in-filled using an average of the preceding and following values. Unrealistically high spikes or low negative values in the data are each checked for realism. If they are not evident in other probes, and/or do not follow any logical pattern in relation to preceding and following values, or environmental changes, they are assumed to be faulty and patched. Automatic weather station sensors are used to monitor hourly air temperature, air humidity, wind speed, solar radiation and rainfall. These measurements are very useful in interpreting sap flow patterns and assisting in the patching process.

Once the above patching and analysis procedure is completed, it is necessary to confirm the "zero flux" value (i.e. those times of the day when HPV values / transpiration would be expected to be zero). This is necessary because the lowest values in the diurnal HPV trends (e.g. those values between 22h00 and 04h00) do not always stabilise around zero. This is a result of slight misalignment in the position of the thermocouple probes in the tree and is corrected by applying an offset to the data to align the lowest values with zero. In cases where destructive felling of sample trees is permitted, this correction may be estimated by simply cutting the stem of the tree, while continuing to monitor HPV data. Alternatively, for deciduous trees, the “zero flux” value may be determined when the trees are completely leafless, and there is no longer any discernible daily trend in sapflow. Under these conditions the data will typically stabilise around a particular "zero flux" value, which, if not exactly at 0, will indicate the offset value necessary to be applied to the data to correct the measured zero flux values to actual zero values. However, from published literature it is known that some species of tree may show reverse sap flow at night (negative night-time HPV values) or actual night-time sap flow (positive night-time HPV values) (Benyon, 1999; Burgess *et al*., 2001). In order to resolve this, it is consequently necessary to determine the ambient conditions under which zero sap flow (zero HPV values) are most likely to occur, and assume that at these times there is zero sap flow. The HPV values at these times may subsequently be adjusted to zero, and the average of these adjustments provides the offset value to be applied to the whole data set (provided the probes were not re-inserted at any point). This procedure therefore does not exclude periods of reverse flow, or night-time sap flow. The methodology used to determine this zero flux value is the satisfaction of a number of pre-determined criteria (e.g. pre-dawn, low soil moisture, high relative humidity) at which sap flux would be expected to be zero (Burgess *et al*., 2001). These particular occurrences may be filtered and an average "zero flux" value calculated, so as to determine the offset value to be applied.

Once the offset has been applied to the HPV data, the final analysis involves the conversion of the hourly HPV values to total daily sap flow (in litres and millimetres). Measurements of sapwood area, moisture content and density, as well as the width of wounded (non-functional) xylem around the thermocouples, are required to convert heat pulse velocities to sap velocities and ultimately sap flow volumes. These sapwood measurements are usually taken at the conclusion of the experiment due to the destructive sampling required (although wood cores are a non-destructive alternative). Firstly the patched and corrected hourly HPV values are corrected for the effects of wound width using wound correction coefficients described by Swanson and Whitfield (1981). These are then converted to sap velocities by accounting for wood density and sapwood moisture content (Marshall, 1958). Finally, the sap velocities are converted to whole-tree total sap flow (litres per hour) by calculating the sum of the products of sap velocity and cross-sectional area for individual tree stem annuli (determined by below-bark individual probe insertion depths and sapwood depth). In this way, point estimates of sap velocity are weighted according to the amount of conducting sapwood in the annulus they represent. Hourly sap flow values are aggregated into daily values.

3.7 Streamflow

Catchment streamflow (*Q*) has been monitored continuously since 1999 using a 457.2 mm; 90° V-notch weir. A Belfort Streamflow recorder, modified with an MCS 250-01 streamflow encoder, was originally used and later replaced with an Ott Streamflow recorder and pressure transducer supplied by Department of Water Affairs (DWA). The calibration of the weir was carried out by DWAF staff and appropriate rating tables provided. During the course of the current project the recording equipment was replaced with a new logger (CR200X, Campbell Scientific) and pressure transducer (CS451, Campbell Scientific).

A sieve was installed in 2004 to avoid twigs and leaves getting trapped in the V-notch and affecting the level of the water in the weir (Figure 3.16). This sieve became rusted and was replaced during 2011 by a new design (Figure 3.17).

Figure 3.16: The old sieve in the main weir at Two Streams in 2006 kept leaves and branches from getting trapped in the V-notch.

Figure 3.17: The new sieve in the main weir at Two Streams in 2011 prevents blocking of the V-notch which affects water level results.

3.8 Groundwater Monitoring

3.8.1 Water table depth

During the previous research project at Two Streams, The Department of Water Affairs (DWA) drilled two deep boreholes (60 m+) at the upper and lower reaches of the catchment to monitor the deep aquifer. Depth to the bedrock varied between approximately 6 m near the stream to 14 m at the top of the slope.

Then during September 2007, DWA made a further contribution to the project and drilled three more boreholes in the Two Steams catchment. One borehole was drilled in the middle of the plantation. The other two were drilled in the western and northern corners of the plantation. The central borehole was drilled to 40 m and the other two on the eastern and northern corners to 60 m. DWA contributed further by providing three Orphimedes (Ott, Hydromet, Germany) water level loggers that use the bubble gauge principal to measure the groundwater level during 2011 (Figures 3.18 and 3.19). They were installed in the central, northern and western boreholes and the water level was monitored at hourly intervals.

Unfortunately the Orphimedes sensors proved to be problematic in the northern and centre boreholes and were damaged when water entered the casing and alternative water level loggers (Solinst levelogger 3001, Ontario, Canada) were purchased (February 2013) and installed in June 2013. A barometric sensor (PTB110, Vaisala Oyj, Finland) to measure the atmospheric compensation was installed at the weather station at the lattice mast.

Figure 3.18: The Ott Orphimedes water level logger lies next to the borehole casing while a student collects a groundwater sample.

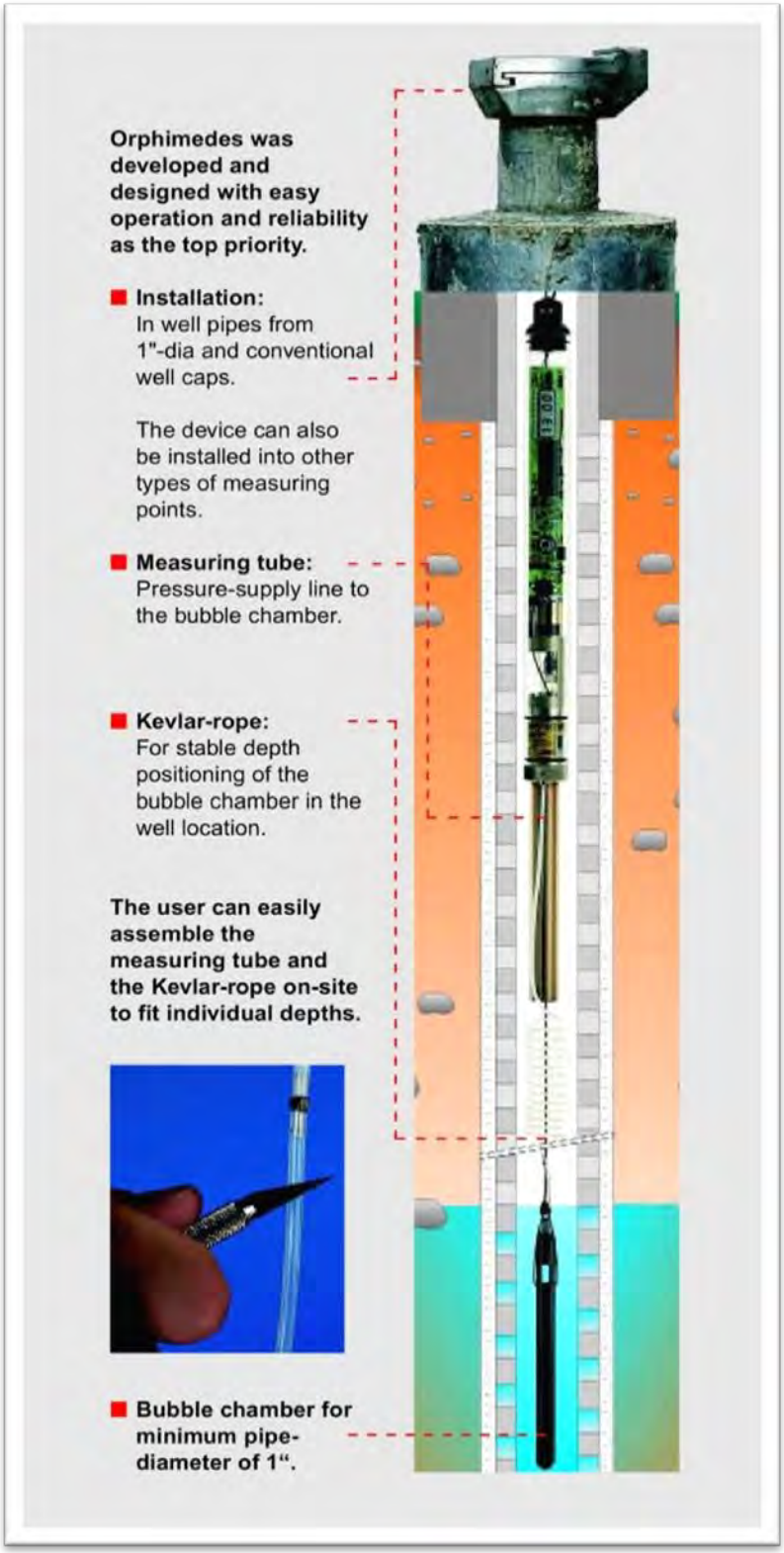

Figure 3.19: The Ott Orphimedes water level sensor is suspended from the cap of the borehole casing. The bubble chamber is lowered on a Kevlar-rope so that it is suspended beneath the water level.

3.8.2 Conceptual Hydrological Modelling of the Catchment

The conceptual model of the Two-Streams catchment was developed based on the information contained in the hydrological reports and borehole logs of the catchment (Figure 3.20). The soil profile is deep, ranging from 13 m at the crest to 7.5 m in the mid-slopes and approximately 5 m near the stream.

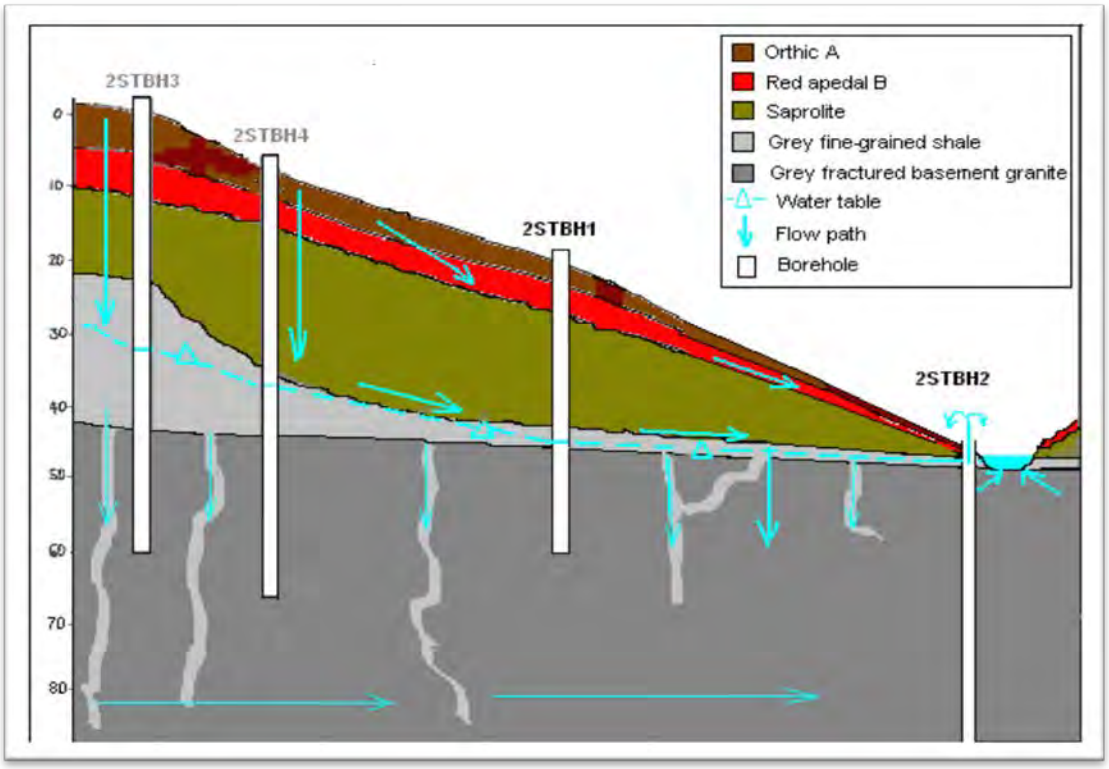

Figure 3.20: Conceptual hydrological behaviour of the Two-Stream Catchment

A hypothesis of the subsurface water flows in the catchment has been developed and explained below. The hypothesis forms part of an MSc (Caiphus Ngubo) and will be further interrogated during the course of 2014. In the hypothesis, the deeper soils (saprolite) represent deep weathering of the bedrock surface and the fractured basement rock and are likely to be a dominant factor in governing flowpaths in the Two Streams catchment. These factors favour bedrock flow, resulting in recharge of the regional water table predominantly in the lower hillslope. The water flow in the catchment is likely to be lateral, horizontal and upward. The tree root systems may affect the groundwater by decreasing recharge through the extraction of water from the unsaturated zone, creating additional storage capacity in the unsaturated zone, without there being a direct abstraction from the groundwater. The lateral flow is minimal due to pathways formed by tree roots which favour lateral flow, except in high intensity and long duration rainfall. The lateral flow is rapid near the surface due to macro-pore conductance, and becomes slower as water infiltrates through the deeper horizons into the bedrock. Two aquifer

systems, namely the shallow aquifer (at the bedrock) and deep aquifer system occur in the catchment.

Flow is restricted within the bedrock (shale) and only occurs in fractures, since the shale is an aquiclude and does not allow water to flow through easily. Therefore, as water ponds on the bedrock surface, some leaks vertically downward to recharge the deeper aquifer system, while some is absorbed by tree roots. In a South African study by Scott and le Maitre (1998), a rooting depth of greater than 53 m was documented for *Acacia* and *Prosopis* plantations. A rooting depth of between 3 m and 20 m within the saprolite is therefore possible at Two Streams depending on hillslope position. The excess water moves laterally to recharge the small stream down-gradient of the catchment.

The borehole 2STBH2 was drilled down-gradient of the catchment near the stream and through an impermeable bedrock layer intercepting the water that is trapped under pressure beneath the impermeable shale confining layer, thus forming an artesian borehole (Figure 3.20).

The vadose zone also known as the unsaturated zone refers to the area between the ground surface and the saturated aquifer. The soil hydraulic properties of the vadose zone have controls on water demand of vegetation, groundwater recharge and movement of pollutants into the groundwater aquifers. The composition and extent of this zone has an important bearing on the rate at which water percolates through the ground surface into the aquifer.

3.8.3 Groundwater Quality Status – Field Measurements

The quality of groundwater primarily refers to the type and concentrations of dissolved substances in water. Many factors can affect groundwater quality. However, the primary factors include; the source and chemical composition of recharge water, lithological and hydrological properties of the geologic unit, various chemical processes occurring within geologic unit and the residence time.

3.8.3.1 Electrical Conductivity Profiles

The electrical conductivity (EC) is a measure of the ability of water to conduct the electric current. It indicates the concentration of dissolved ions in water, which in turn reflects groundwater inputs, catchment geology or diverse human impacts. The EC is directly related to the concentration of salts dissolved in water (TDS). The EC in water is affected by the presence of major positively charged ions such as Sodium (Na^{+}), Calcium (Ca^{+2}), Potassium (K^{+}), Magnesium (Mg^{+2}) and the negatively charged ions such as Chloride (Cl^{-}), Sulfate (SO_4^{-2}), Carbonate (CO_3^{-2}) and Bicarbonate (HCO_3^{-}) (CWT, 2004.)

3.8.3.2 Temperature Profiles

The temperature of groundwater responds to seasonal variations in heat received from the sun and by the conductive and convective movement of heat from the earth's interior. It is generally

equal to the mean air temperature in shallow groundwater systems and usually stays within a narrow range year-round. The determinations of dissolved oxygen concentrations, conductivity, pH, rate and equilibria of chemical reactions, biological activity, and fluid properties rely on accurate temperature measurements.

3.8.3.3 Total Alkalinity, Bicarbonate and pH

Alkalinity is a measure of the capacity of stream/aquifer to neutralise or buffer acids. It is mainly derived from the dissolution of carbonate minerals and carbon dioxide (CO_2) present in the atmosphere and in soil above the water table. The water in areas with limestone deposits tends to have higher alkalinity, whereas areas with granite bedrock tend to have water with lower alkalinity (McDonald, 2006). The most important compounds in water that determine alkalinity include the carbonate (CO_3^{2-}), bicarbonate (HCO_3) and hydroxide (OH^-). The aquifer/stream with relatively high alkalinities has the greater ability to neutralise acidic pollution from the rainfall or wastewater, therefore able to resist major shifts in pH, whereas water with low alkalinity is very susceptible to changes in pH.

3.8.3.4 Electrical Conductivity, Total Dissolved Solids and Temperature

The electrical conductivity (EC) measures the ability of water to conduct an electric current, whereas the Total Dissolved Solids (TDS) defined as the total amount of solids remaining when a water sample is evaporated to dryness, and is directly proportional to the EC of water. The EC in water is affected by the presence of inorganic dissolved solids such as chloride, nitrate, sulfate and phosphate anions or sodium, magnesium, calcium, iron and aluminium cations. It is also affected by temperature (high temperatures result in higher EC) and geology of the area.

3.8.3.5 Redox Potential (Eh), Oxidation Reduction Potential (ORP) and Dissolved Oxygen (DO)

The transfer of electrons from one ion to another in an aqueous solution is called an oxidation-reduction or redox potential reaction (Eh), which is synonymous to ORP (Radu, 2003). The oxidation reaction results in an ion losing or donating its electron(s) to another ion, and the reduction reaction results in an ion gaining or accepting electron(s). The redox potential can be correlated with the amount of dissolved oxygen. As the oxygen content drops, the environment becomes more reducing, meaning redox potential drops (Wilson *et al*., 2002). The positive sign of the redox potential indicates oxidising conditions and is typical of aerobic aquifers. Whereas, negative values indicate that most constituents are in reduced form so that there is a high potential for redox reaction to occur and is typical of anaerobic conditions (Radu, 2003).

The Dissolved Oxygen (DO) is often the principal oxidizing chemical component in groundwater. Its concentration in groundwater is controlled by local inputs of oxygen-rich meteoric water, microbial respiration, biodegradation of organic matter and reaction with reduced mineral phases in the aquifer (Champ *et al*., 1979). It is often assumed that oxygen derived from the atmosphere is rapidly consumed in the soil and the unsaturated zone by microbial respiration and

decomposition of organic matter (Winograd and Robertson, 1982). However, contrary to this prevailing notion, is that appreciable concentrations of D.O. (up to 0.5 mg/l) have been measured in samples representative of relatively deep groundwater in Two-Streams. This probably indicates that the microbial reduction of oxygen is limited in many aquifers or oxygen can be effectively transported to the phreatic zone from the overlying vadose zone. However, there is a risk of intrusion of oxygen during the sampling procedure.

3.9 Soil Water Dynamics

Previous work in the catchment has generated a database of nine years of detailed soil moisture data collected from tensiometers, watermark sensors and a neutron probe. This project required that the soil water measurements be refocused on deep profile water measurements with modification to the previously designed time domain reflectometry (TDR) probe that could be installed at depths in excess of 2 m.

3.9.1 Time domain reflectometry

In TDR methodology the travel time for a pulsed electromagnetic signal is measured. The travel time is dependent on the velocity of the signal and the length of the wave guide. The velocity is dependent on the dielectric constant of the material surrounding the waveguide. The dielectric constant of water relative to other soil constituents is high. Consequently, changes in volumetric water content can be related to changes in the dielectric constant of the soil material (Campbell Scientific TDR100 Instruction Manual, 2004).

In the previous work at Two Streams, TDR_{CSIR} probes were manufactured and installed at depths of up to 4.8 m. Although successfully installed, the results were scattered at times and the interpretation of the waveform was unreliable. During the current project the design was improved by extending the wave guides and improving the quality of the cable to that of a lower impedance.

While the new TDR_{UKZN} probes were being manufactured, instruments from the previous project at Two Streams provided data on soil water content. A pit near the lattice mast was excavated to a depth of 2.5 m (Figure 3.21) on 7 February 2007 and an additional pit near the lower sapflow site on 1 March 2012. Six CS616 probes were installed in each pit to a depth of 2.4 at 0.4 m intervals. They also served as a valuable validation for the data obtained from the previous TDR_{CSIR} probes and the new TDR_{UKZN} probes.

The process of probe design, testing and calibration has been completed and the new TDR_{UKZN} probes with 0.15 m waveguides (Figure 3.22) have been installed near the lattice mast site (Figure 3.23). These probes were installed using a soil auger with 1 m extension bars to a depth of 4.8 m. The probes were lowered down the auger holes (Figures 3.24 to 3.26) and the waveguides pressed firmly into the soil using the auger extensions and handle. In addition watermark sensors for the measurement of soil water potential were installed at 0.4 m intervals to 4.8 m but with a final watermark sensor at 8.8 m.

Figure 3.21: Pit excavated to a depth a 2.5 m near the lattice mast at Two Streams for the installation of CS616 probes at 0.4 m intervals.

Figure 3.22: The TDR_{UKZN} cylindrical probes have 0.15 m long waveguides.

Figure 3.23: Auguring holes for the installation of the TDR_{UKZN} probes at 0.4 m intervals down to 4.8 m.

Figure 3.24: A TDR_{UKZN} probes inserted to a depth of 0.4 m.

Figure 3.25: A TDR_{UKZN} probes inserted to a depth of 1.6 m.

Figure 3.26: A TDR_{UKZN} probes inserted to a depth of 2.4 m

3.10 Water Balance Modelling

A monthly water-balance for the catchment was calculated based on rainfall, streamflow, evaporation and actual change in soil water storage to a depth of 2.4 m. The overall change in soil water storage was calculated as the residual of the water-balance equation.

A catchment water balance using the actual data was calculated at monthly intervals using:

$$P - Q - ET - \Delta S = 0 \qquad (3.12)$$

where, *P* is rainfall (mm), *Q* streamflow out of the catchment (mm), *ET* is total evaporation (mm) and *ΔS* is the change in soil water storage (mm) in the soil profile to a depth of 2.4 m.

3.11 Isotopes

3.11.1 Research Questions

Previous research in a water-balance study by Clulow, 2011 in the Two Streams Research Catchment found that a commercial forestry species (*Acacia mearnsii)* was using more water than was available through precipitation over a 30 month period (i.e. total evaporation was greater than rainfall). Clulow *et al*., 2010 concluded that the trees were drawing the unaccounted water from another source. In this study, field measurements using stable isotopes will be collected to identify the different sources of water used by the trees. Soil water measurements will be used to populate the HYDRUS model to determine the distribution of soil water root uptake. In addition, the estimates of total evaporation from the model will be verified by existing surface renewal and eddy covariance measurements.

The expected questions addressed by this include:

1) Are the trees using groundwater and how does their groundwater usage change between the dry and wet seasons?
2) Is HYDRUS able to accurately model root water uptake and therefore transpiration?
3) Can the HYDRUS model allow for the identification of depth from which the trees are extracting water?

A conceptual representation of the of the parameters to be measured and the interrelationship of the various processes to be analysed is shown in Figure 3.27

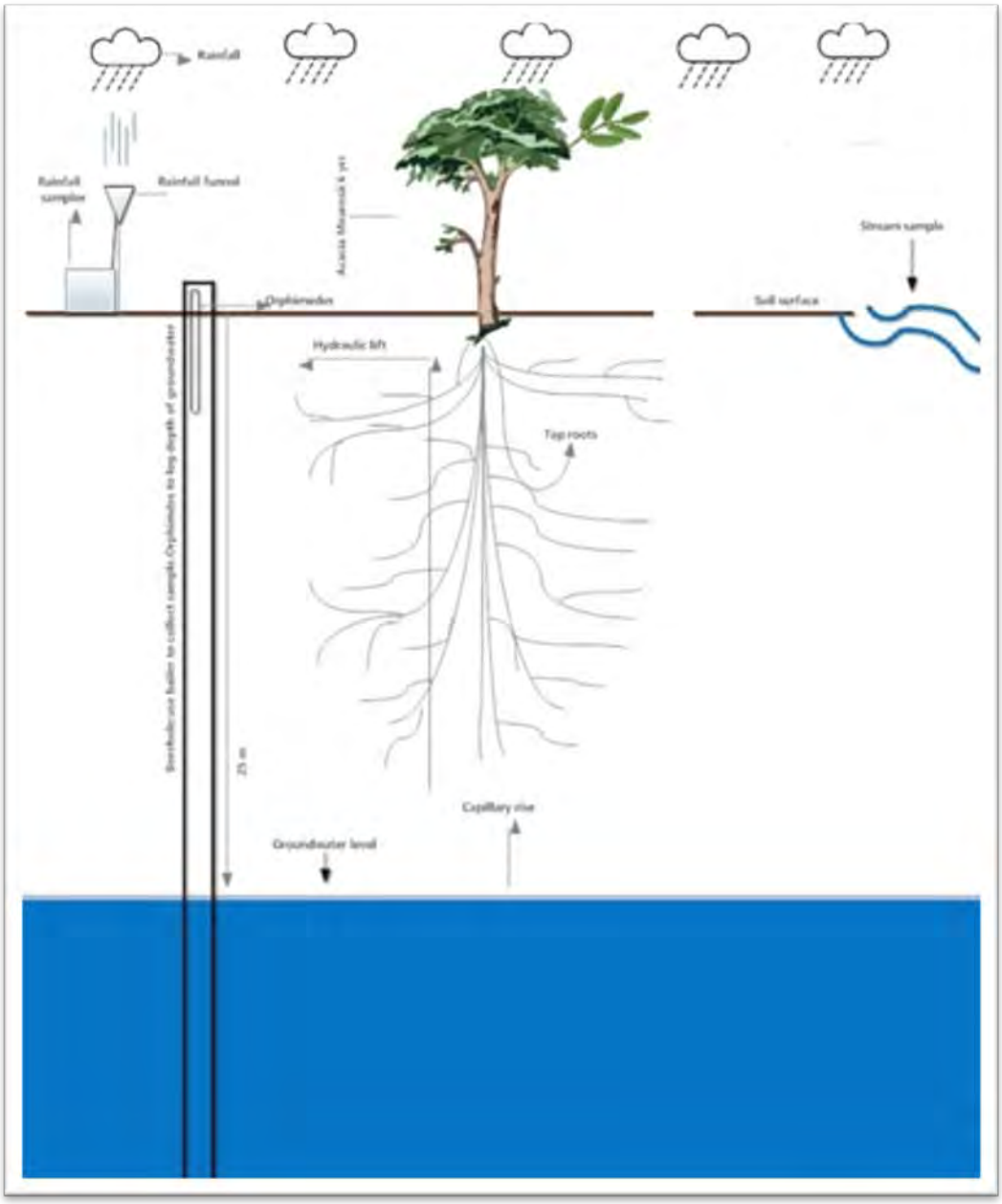

Figure 3.27: Conceptual representation of the processes to be analysed

3.11.2 Gaps in literature

For Southern African conditions literature on *Acacia mearnsii* using groundwater as a source is limited as well the literature on using isotopes to determine in which horizon trees are extracting water from.

3.11.3 Hypothesis

Main Hypothesis:
If total evaporation exceeds net rainfall then either the seven-year-old *Acacia mearnsii* trees are able to extract groundwater or the measurement of total evaporation is flawed. The total evaporation measurement (Surface renewal and Eddy co-variance) takes into account all evaporation coming off a surface even that of mist. Mist interception has not been measured at the catchment, which could mean a source of extra moisture to the catchment.

Sub-Hypothesis 1:
If the isotope signature of soil water for a particular horizon is the same as groundwater and rooting matter has been found in this horizon then the trees are able to access this water due to direct water uptake. If rooting water has not been found in a particular horizon and the isotope signature of soil water is the same as groundwater then trees are using groundwater as a source with the aid of capillary rise.

Sub-Hypothesis 2:
If the isotope signature of groundwater is the same as stream water in winter then the majority of water leaving the catchment comes from baseflow.

Sub-Hypothesis 3:
If the isotope signature of rainfall is the same as stream-water in summer then the rainfall volume and intensity has to be great enough to cause runoff and therefore majority of water leaving the catchment is from recent rainfall.

Sub-Hypothesis 4:
If HYDRUS is able to simulate total evaporation greater than that of rainfall then the trees are able to use summer stored water to transpire freely during winter.

3.12 Isotope Methodology

3.12.1 Isotope analysis

When collecting samples for analysis with the isotope ratio laser spectrometry (9. Los Gatos Research DLT-100 Liquid Water Isotope Analyser), it is important that the sample has not undergone isotope fractionation. If a sample has undergone isotope fractionation due to evaporation or condensation, then the sample will not be representative of the specific water being analysed. Isotope fractionation will alter the ratios between $\delta^{18}O$ and $\delta^{2}H$, which would make the tracing of source water impossible.

Therefore, fractionation was avoided, when collecting samples. Bottles that are used for sample storage were placed away from sunlight, lids were tightly sealed and bottles filled with water, leaving no air spaces. The air space can cause sample phase change within the sample bottle, thus altering the signature. The machine used to analyse the water samples was a laser spectrometer,

which has the capability of measuring $^{1}H/^{2}H(D)$ and $^{18}O/^{16}O$.The samples were collected from the following sources:

3.12.2 Rainfall (rainfall sampler)

Rainfall was collected using an automated sampler, so that rainfall events could be differentiated and the mixing of rainfall prevented. The automated sampler was programmed so that after thirty minutes or more of no rainfall following a rain event, the sampler moved to a new bottle. A funnel was used so that there was a larger collection area to ensure that enough sample was collected in each bottle during low volume events.

3.12.2.1 Development of a method to stop evaporation from occurring within sample bottles

A method was developed to stop evaporation from occurring within the open bottles of the ISCO (stream sampler) and ALCO (rainfall sampler). Weaver and Talma, 2005 used a silicon seal to stop evaporation from occurring within their cumulative rainfall sampler. Concerns were raised, that by adding silicon oil the viscosity of the sample would change thus making the results inaccurate. Silicon oil could also contaminate the sample giving an inaccurate reading.

The results shown below (Figure 3.28) suggests that the addition of silicon oil did not contaminate the sample (although spectral analysis was not done) and that the addition of silicon oil did slow down the evaporation process, although it did not stop the process completely. This could be due to the small quantity of silicon oil added. Figure 3.28 shows the samples and their deviation from standard 1, which was the standard where silicon oil was added. The diagram below shows the isotope signature of standard 1, standard 1 after being evaporated for 1 day at room temperature, standard 1 with silicone seal after 1 day evaporation at room temperature, standard 1 with silicone seal after 4 days evaporation and being placed in an oven for 2 hours at 40 degrees, standard 1 with silicone seal after 4 days evaporation and standard 1 with no silicone seal after 4 days evaporation. As Silicon oil was difficult to source another solution was developed, i.e. a “U” seal. These results clearly showed the importance of preventing evaporation of the samples.

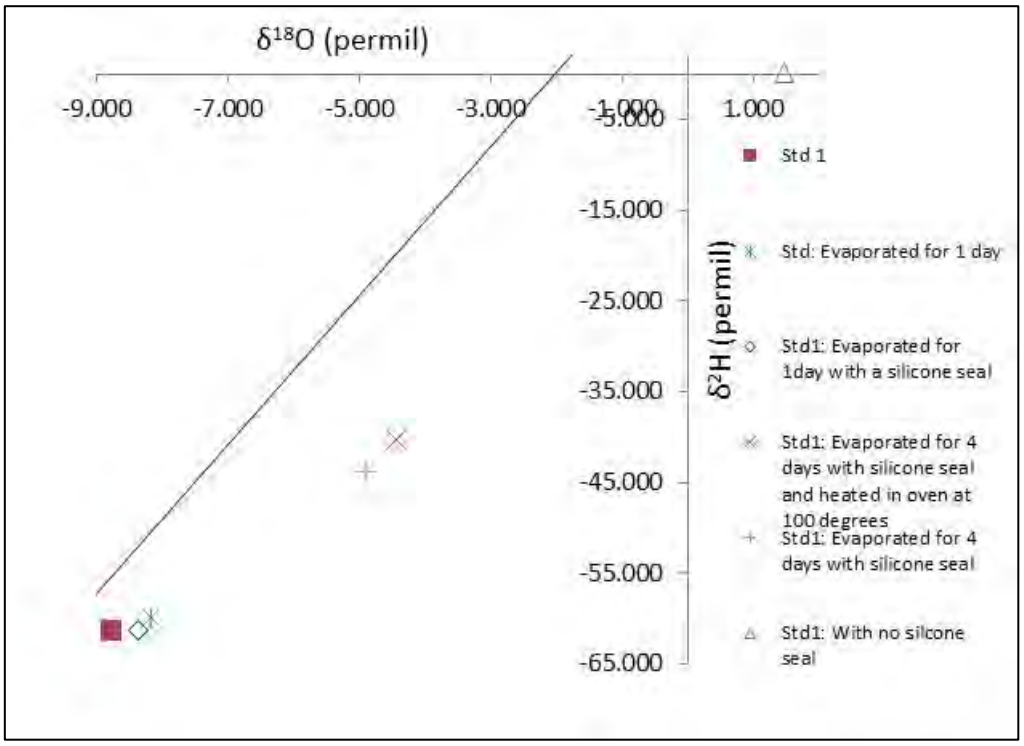

Figure 3.28: Testing of silicone seal to stop evaporation in ISCO and ALCO samplers

A “U” seal was used instead of silicon to stop evaporation within samples bottles (Figures 3.29 to 3.31). The “U” seal made use of a “U” shaped glass tubing that was connected to a small funnel at the top of the U. A small hole in the lid allowed for air to escape from the bottle. The problem with this apparatus was that the peristaltic pump delivered a faster flow rate than could be received by the “U” seal. Overflowing therefore occurred within the sampler but this did not affect the quality of the sample in the bottle. The solution to this would be to install a bypass after the pump to allow for a smaller flow rate to the “U”. Figure 3.22 below shows the isotope results where testing was done using a "U" seal. Testing was done over 4 days at room temperature. From the results below it can be seen that there was little deviation from standard 1 during the time of testing. It was thus deemed a viable solution for stopping evaporation from occurring with the sample bottles.

Figure 3.29: Weather station with automated rainfall sampler and funnel

Figure 3.30: Automated rainfall sampler

Figure 3.31: Rainfall sampler bottles with "U" seal

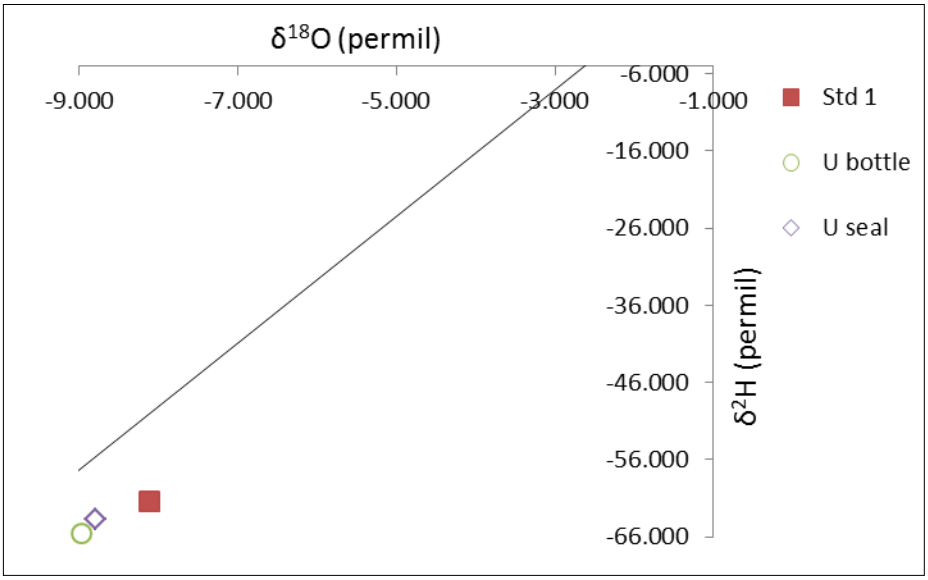

Figure 3.32: Testing of the "U" seal to stop evaporation from occurring within sample bottles

3.12.2.2 *Development of program for sampling of rainfall*

The ALCO was controlled by a CR200X logger and the program altered throughout the year to determine the best way to sample rainfall. The aim of using the ALCO[1] auto sampler was to be able to separate different events from one another while, reducing wasteful sampling and to allow for a longer time period until sampler became full. The criteria of moving to the next bottle were based on separation of isotopic events and interception thresholds. Rainfall of 2.0 mm is intercepted by the tree canopy before rainfall is able to reach the soil surface, thus events that are greater than 2.0 mm need to be separated into different bottles. The ALCO program was developed in CRbasic with a logic structure according to Figure 3.33.

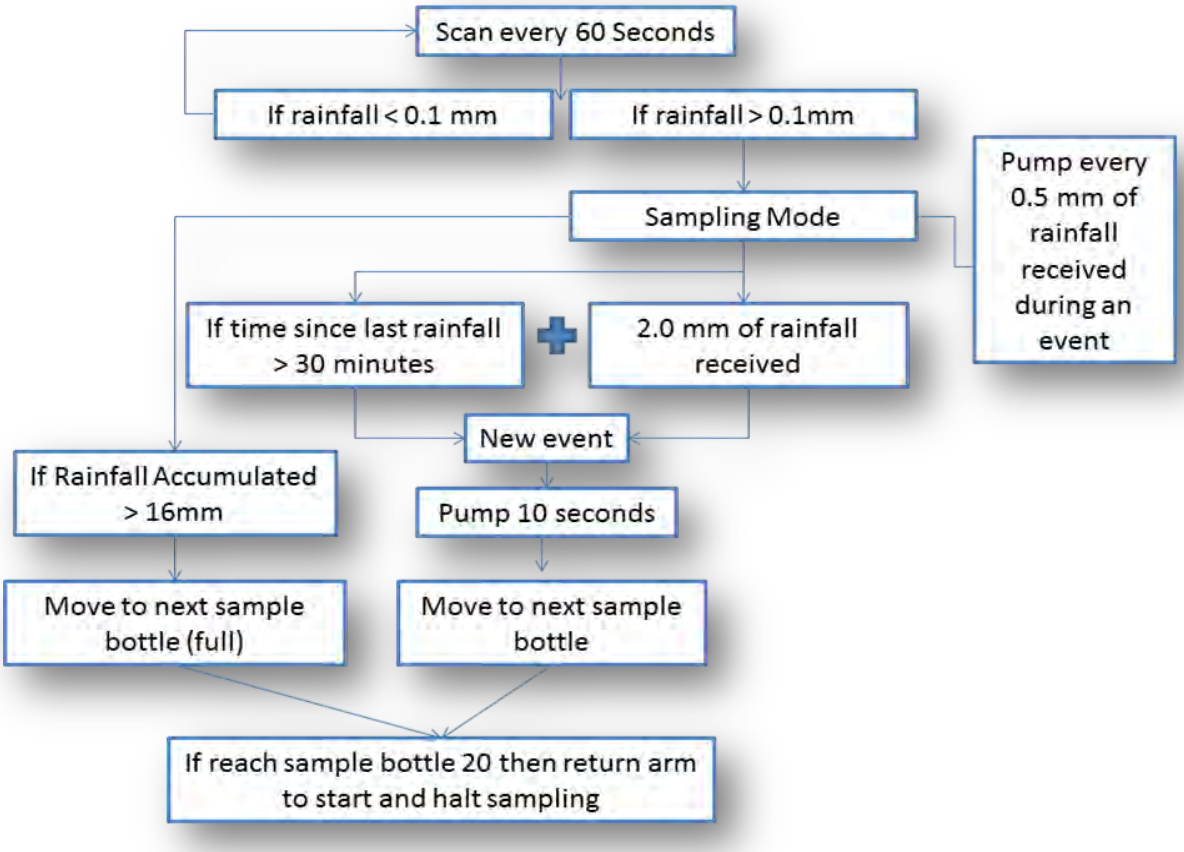

Figure 3.33: Criteria for the ALCO program to sample rainfall

[1] ALCO is a locally manufactured automatic rainfall/stream sampler

3.12.3 Groundwater (boreholes)

Groundwater samples were collected at two locations from a borehole, using a bailer. A bailer is a pipe with a one-way check valve at the top and the bottom. The top check valve allows air to be removed from the bailer, while the bottom one-way check valve stops the water coming out of the bailer (Sundaram *et al*., 2009). When collecting groundwater samples, nine samples were removed from the borehole and the tenth sample was used for analysis. This was done to get a representative groundwater sample and to remove any rainfall that had fallen directly into the borehole. Samples were collected from two boreholes, namely the centre borehole and the northern borehole. The water level in both boreholes was monitored using an Ott Orphimdes level loggers (OTT Hydrometrie, Germany), which recorded the depth of the groundwater at hourly intervals. The centre borehole has been drilled to 40 metres, while the northern borehole had been drilled to 60 metres (Clulow *et al*., 2010).

3.12.4 Stream

Stream samples were collected using, an ISCO automated sampler (Figure 3.34). The samples were collected based on event volume. The ISCO was triggered to sample during times of low flow and times of high flow. A "U" tube seal was used to stop evaporation from occurring within the bottle as previously discussed.

Figure 3.34: ISCO Streamflow sampler positioned at weir

3.12.5 Soil water sampling

The objective of soil water sampling was to identify the horizon in which the rooting system was able to extract groundwater due to hydraulic lift from deep soil layers to drier shallow layers. Hydraulic lift is when there is passive movement of water through roots from wetter, deeper layers in drier shallow layers along a soil water potential gradient. Plant species that are generally able to make use of hydraulic lift are species with dimorphic root systems. Hydraulic lift allows for the redistribution of water to shallow layers where it can be taken up to enhance transpiration (Caldwell *et al*., 1998) Hydraulic lift is an efficient mechanism to enhance transpiration rates and decrease water stress (Dawson, 1993).

In theory the Cryogenic vacuum distillation is a suitable method to extract water from soil (Ehleringer and Osmond, 1989). Cryogenic vacuum distillation (Figure 3.35) is a procedure that uses a cold trap, coupled with heating under a vacuum to vaporise water from a sample and condense the sample into the cold trap. Cryogenic vacuum distillation needs to be run for 24 hours, so that all water in the sample is vaporised and so that both the light and heavy fractions are removed from the soil. Vacuum distillation needs to be air-tight, thus it is essential that no air enters the system.

When using Cryogenic vacuum distillation to extract tree water/soil water, the isotope signature that is collected needs to be representative of the signature of the vegetation and the signature that was in the soil. Thus, when collecting soil water, it is essential that both heavy and light isotopes are removed from the samples and that not only the lighter isotopes (^{16}O and ^{1}H) are evaporated from the sample.

A check was run to determine the length of time that a sample must be run to get a representative sample out of the soil. Standard three (Table 3.4) was added to dry soil and distilled for different time lengths and soil moisture contents.

Figure 3.35: Cryogenic Vacuum Distillation

The cryogenic vacuum distillation method was not used to extract isotopes from soils, due to the poor test results and the lack of availability of equipment. Initially, the problem with the procedure was that the pump was unable to move the vapour from the sampling glass boil into the cold trap. Another problem with the method was that liquid nitrogen sublimed before the entire sample could be collected. The liquid nitrogen also froze the tube where vapour was moving into the cold trap thus halting the collection of the sample (Figure 3.36). Other methods of cooling were tried but were deemed unsuccessful, thus a new apparatus was used to extract samples from soils.

Figure 3.36: Problem with Cryogenic Vacuum distillation

A water distillation unit was however successfully used to extract isotopes from soils (Figure 3.37). The distillation unit uses water to cool down vapour and to collect sample. A water distillation unit makes use of a heating mantle, 5 litre glass bowl, distillation unit and vacuum pump to extract water from the heated media. The vacuum pump was only used to remove initial moisture from the system. A number of checks were run on the distillation procedure to determine if representative samples had been extracted.

Figure 3.37: Water distillation procedure

Silica sand was used to determine how close the isotope signature of standard was to the distilled sample. Initially it was perceived that the % water content was the most important factor that determined how much water was able to be extracted. Later however, further investigation found that soil type had a larger effect on extraction volume.

When samples that were near to ground level where run in the distiller (0.4-1.0 m), the extracted water contained a substance that caused interference in the isotope machine. It was assumed that the distillation procedure therefore extracted hydrocarbons from the rooting matter in this soil. These hydrocarbons caused the isotope machine to give false readings, similar to those of a highly evaporated sample (Figure 3.38). Hydrocarbon contamination was evident in the proceeding samples as the apparatus was not cleaned properly. Subsequently the apparatus was cleaned in the furnace at 600 degrees to burn off contaminants.

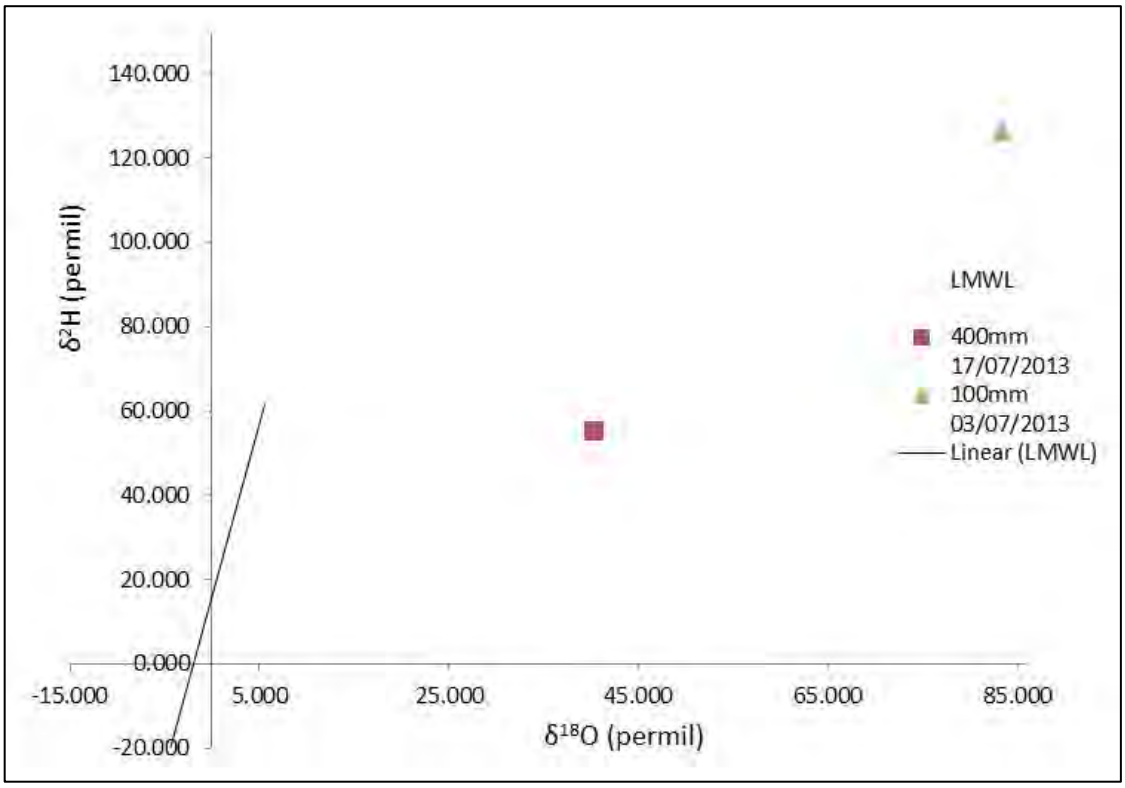

Figure 3.38: Contamination of samples by burning of rooting matter

Phase 1 of system checks involved adding different quantities of Standard 1 to Silica sand to determine how well the extraction process performed (Figure 3.39). The results showed that the extraction process performed poorly as not all the water in the silica sand was extracted. The conclusion being that either heating was not done for long enough or the heating mantle was not hot enough to extract water.

Phase 2 of the system checks involved adding Standard 1 to dry soil from the catchment. This was done to determine the accuracy of the extraction procedure for that horizon of soil. Phase 2 of the system checks also looked at weighing masses of water and soil before and after extraction followed by reheating in the oven to determine the amount of Standard 1 extracted. Results indicated that $\delta^{18}O$ was affected more by extraction percentage than by $\delta^{2}H$ (Figure 3.39). It was decided that results that did not have an extraction percentage higher than 85% would not be displayed.

Phase 3 of system checks involved the making of a new water distillation unit to increase the accuracy of soil isotope extraction. The new distillation unit was made bigger to make extraction quicker. The connection between the 5 litre flask and the water distiller was changed from a "O" ring seal to a hermetic seal to stop the collection of water between the 5 litre flask and the water distillation unit.

3.12.6 Soil water content analysis

Soil moisture content was analysed using the TDR 100 system, which measured volumetric water content. Watermark sensors were used to measure the water potential as electrical resistance (ohm). The watermark sensors gave an indication of the availability of water to the tree roots.

Before the TDR 100 probes were installed, the TDR 100 probes were calibrated. The TDR 100 probes were calibrated to include length from the TDR 100 to the SDMX 50 multiplexers. The PC TDR program was used to determine the LA, LA/L Start distance and End distance, window and temperature of the water (Dielectric). Each probe was calibrated with a different probe offset. When, connecting the TDR probes to the second multiplexer there was a significant difference in probe offset, this was due to the increased length of the cable from the one multiplexer to the other in the calibration. The offsets for each probe were inserted into the CRBasic program.

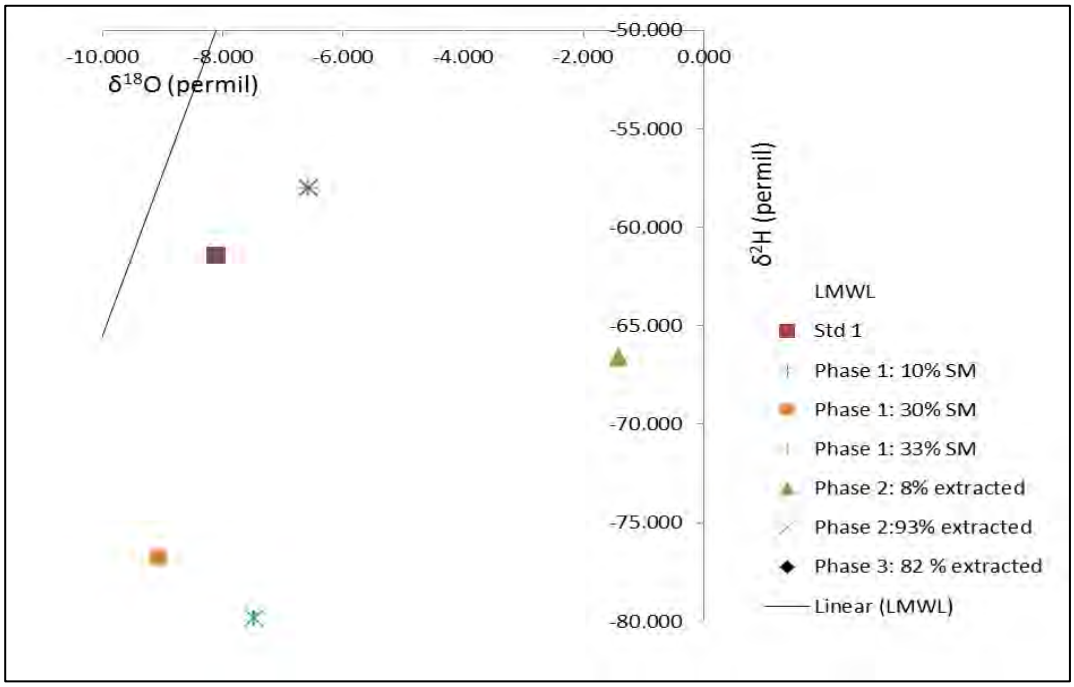

Figure 3.39: Phase 1 and 2 of system checks

The TDR 100 probes were installed at depths of 0.4 m, 0.8 m, 1.2 m, 1.6 m, 2.0 m, 2.4 m, 2.8 m, 3.2 m, 3.6 m, 4.0 m, 4.4 m and 4.8 m (Figure 3.40). The watermark sensors were installed at the same depths as the TDR 100 probes. Watermark sensors were installed in the same augured hole, while the TDR 100 probes were installed into different holes. Diatomatious earth was placed around each of the watermark sensors so that there was no shrinking and swelling of the soil around the sensor due to drying and wetting cycles. The watermark sensors were installed after first being submerged in water for 24 hours.

The results of volumetric water content from the TDR 100 probes were compared to the gravimetric water content to confirm the readings of the TDR 100 probes.

Figure 3.40: Installation of UKZN CS606 probes

3.12.7 Xylem pressure potential

Xylem pressure potential readings were taken once a month over a winter and summer period. Pre-dawn measurements were taken at around 5.30 am while post-dawn measurements were taken at 7.30 am. Pre-dawn leaf water potential readings were used as an indicator of plant stress and possibly to identify when trees are using groundwater as their source water.

3.12.8 HYDRUS Modelling

The HYDRUS model (PC-Progress) was used to determine the root water uptake of a cylindrical column of soil. HYDRUS was run with input data obtained from the measurements in the Catchment. The inputs of potential transpiration/potential evaporation were collected from surface renewal and eddy covariance data.

HYDRUS is a model that is able to simulate Two- and Three-dimensional Movement of Water, Heat and Multiple Solutes in Variably-Saturated Media. The HYDRUS model numerically solves the Richards equation for variable saturated water flow and uses advection-dispersion for both heat and solute transport. Water uptake by plant roots is incorporated using a sink term (Sejna *et al.*, 2011).

The HYDRUS codes are physically based models and thus require little or no calibration when all input parameters have been experimentally determined. The HYDRUS model has been

successfully applied in field and laboratory experiments using parameters that were determined independently of the modelling itself and were not calibrated (Simunek *et al.*, 2011).
HYDRUS was run using input data from the centre tower at Two Streams. Where available Eddy Co-variance data was used otherwise Surface Renewal data were used as total evaporation. In the HYDRUS model total evaporation was separated into transpiration and evaporation.

The HYDRUS 1D model (Pc-Progress) was used to estimate the transpiration rate from the *Acacia mearnsii* stand. The model was set up with data that had been gathered from the Two Streams Research catchment. The HYDRUS model was used to determine if *Acacia mearnsii* trees were using more water than was available through precipitation, or if there was a measurement error within the water balance of the catchment.

Initially it was decided to perform inverse modelling to determine soil hydraulic parameters, but due to there being only two measurements to compare, TDR (soil moisture content) and Watermark (tension at which water is held in the soil in KPa) with simulated soil moisture content it was decided that calibrating the model would lead to equifinality, i.e. that similar results may be achieved with different initial conditions and in many different ways.

The modelling procedure that was followed was based on research done by Hachmann (2011) in the Kruger National Park.

3.12.8.1 Variably saturated flow

Water movement through soils depends not only on pore size distribution but also on antecedent moisture conditions. Water movement through soils is therefore a function of soil properties and volumetric water content. The HYDRUS model numerically solves the Richards' equation for variable saturated conditions:

$$\frac{\partial \theta}{\partial t} = \frac{\partial}{\partial z}\left(K(\theta)\frac{\partial h}{\partial z} + 1\right) \quad (3.13)$$

θ-Volumetric water content (L^3L^{-3}), t is the time (T), h is the pressure head (L) and z is the gravitational head (L).

3.12.8.2 Modelling period and temporal resolution

The modelling time step is broken up into three different periods: December 2012-July 2013 (December included as a warming up period), July 2013-January 2014, January 2014-March 2014 (Closing of catchment and end of measurements). The model was run in a hourly time step (to prevent the model from crashing). When the model was run in a daily time step the model was unable to infiltrate the large rainfall events that were received and thus would crash.

3.12.8.3 Modelling domain

The domain of the simulation was a rectangular column of soil, where the depth of the soil was limited to the depth at which the roots were found in the soil. The node density was set higher at the top of the column and decrease in density towards the bottom. This was done to allow for infiltration of large quality rainfall events. The top boundary condition was set as an atmospheric boundary condition which allowed for the input of time variable boundary conditions. The bottom boundary condition was set as free drainage.

3.12.8.4 Material distribution and Hydraulic properties

Steady state boundary conditions for the HYDRUS run include soil hydraulic properties. Measured data from Two Streams Research catchment was used as input data into soil hydraulic and pore size distribution models. Van Genuchten (1980) soil hydraulic functions for unsaturated water flow and the Mualem (1976) pore size distribution model was used together to determine the unsaturated hydraulic conductivity in terms of soil water retention parameters.

The soil hydraulic parameters were determined by Kuenene *et al.*, 2013 for the Two Stream Research Catchment. These measurements were used as input steady state boundary conditions.

$$\begin{cases} \theta_r + \frac{\theta_s - \theta_r}{1+(\alpha h)^n)^m} & h < 0 \\ \theta_s & h \geq 0 \end{cases} \quad (3.14)$$

$$K(h) = K_{sat} S_e^l \left[1 - \left(1 - S_e^{\frac{1}{m}}\right)^m\right]^2 \quad (3.15)$$

$$S_e = \frac{\theta - \theta_r}{\theta_s - \theta_r} \quad (3.16)$$

$$m = 1 - \frac{n}{1}, \; n > 1 \quad (3.17)$$

$\theta(h)$-water retention curve (L^3L^{-3}), h- matric pressure head (L), θ_r-residual water content ($L^3\ L^{-3}$), θ_s-saturated water content (L^3L^{-3}), α- is related to the inverse of the air entry suction $\alpha > 0$ (L^{-1}), n- is a measure of pore-size distribution index $n > 1$ (dimensionless), K_{sat} -saturated hydraulic conductivity ($L\ T^{-1}$), l-pore-connectivity parameter (dimensionless), S_e-effective water content (dimensionless)

3.12.8.5 Initial conditions

The initial conditions required were soil moisture content and soil water tension. Time Domain Reflectometry probes were developed with a cylindrical head and 150 mm wave-guides for installation in augered holes. These TDR probes and watermarks were installed late in February 2013. The initial conditions that were selected were that of lowest soil moisture content at which

the HYDRUS model would run. Where Residual water content (Qr) is greater than or equal to is initial soil moisture content.

3.12.9 Time dependent variable boundary conditions

3.12.9.1 Rainfall

The input time variable boundary conditions were collected from a FAO 56 weather station that was installed at the Two Streams Research catchment. HYDRUS was run hourly and in cms and conversions were done where necessary. HYDRUS has limited ability to separate runoff from rainfall. When rainfall exceeds the infiltration capacity of the soil, HYDRUS removes water from the soil surface (Rassam *et al*., 2004).

3.12.9.2 Interception

HYDRUS does not account for interception within the model framework. Therefore interception was subtracted from rainfall before it was entered into HYDRUS. In forestry catchment such as Two Streams interception can account of a large portion of rainfall. Bulcock and Jewitt (2012) measured the litter and canopy interception of *Acacia mearnsii* at Two Streams research catchment. The following equation was used to determine the Gross precipitation that was received at Two Streams:

$$Sc = 0.659x^{-0.28} \quad (3.18)$$

Where *Sc* is the storage capacity (mm) and *x* is the rainfall intensity (mm/hour). The storage capacity ranges from 0.77-1.44 mm. Therefore the equation 8.6 was used to determine the storage capacity of an event and if the storage capacity of a consecutive event was greater than 1.44 mm it was assumed the canopy was fully saturated. It was assumed that after two hours of no rainfall, the canopy was dry and storage capacity was at its maximum. The intercepted rainfall amounts are shown in Table 3.3.

Table 3.3: Intercepted rainfall at Two Streams for HYDRUS 1st run

Precipitation (mm)	Gross precipitation (mm)	Total intercepted (mm)
560.6	440.26	120.34

3.12.9.3 Surface runoff

Surface runoff can be separated in two different ways namely Horton-Overland Flow or Saturated Overland Flow. Horton-Overland Flow is when the rainfall intensity exceeds the infiltration rate of the soil, thus water flows horizontally on the surface while infiltrating the soil. Horton-Overland flow is dependent on various soil parameters and antecedent soil moisture content. Dry

soil has a large suction potential and thus can take up water more rapidly, but when the soil is saturated but not waterlogged the rate of infiltration and constant and the infiltration capacity of the soil is equal to the saturated hydraulic conductivity (Hachmann, 2011). Under conditions where water is unable to infiltrate to deeper depth, surface runoff is described as Saturated Overland Flow. For Saturated Overland Flow conditions no water infiltrates the soil profile and the surface runoff that is generated is at full potential (Hachmann, 2011). At Two Streams there is a high litter layer, therefore little surface runoff would occur.

3.12.10 Total Evaporation

The FAO56-Penman Monteith method was used to determine the reference evaporation for a short grass surface. The extension of reference evaporation from daily estimates to hourly estimates were recommended (Allen *et al*., 2006). Reference evaporation was estimated using equations entered by Savage MJ, 2010 (Soil-Plant-Atmosphere Research Unit, School of Environmental Sciences, University of KwaZulu-Natal, Pietermaritzburg, South Africa). The ET_0 equation was used to determine Reference evaporation for hourly intervals.

$$ET_0 = \frac{0.408\Delta(R_n - G) + \gamma \frac{900}{T+273.15} u_2 (e_s - e_a)}{\Delta + \gamma\,(1 + 0.34 u_2)} \quad (3.19)$$

$$\mathrm{Kc} = \mathrm{ETc}/\mathrm{ET}_0 \quad (3.20)$$

ET_0- reference evapotranspiration [mm day^{-1}], R_n- net radiation at the crop surface [MJ $m^{-2}day^{-1}$],G- soil heat flux density [MJ m^{-2} day^{-1}], T-mean daily air temperature at 2 m height [°C], u_2- wind speed at 2 m height [m s^{-1}], e_s- saturation vapour pressure [kPa], e_a- actual vapour pressure [kPa], (e_s- e_a) -saturation vapour pressure deficit [kPa], Δ- slope vapour pressure curve [kPa $°C^{-1}$], γ-psychrometric constant [kPa $°C^{-1}$]

Kc- Crop co-efficient, ET_0- Reference evaporation for short grass crop, ET_c- Crop evapotranspiration.

A Crop factor was determined by plotting Eddy co-variance data against FAO 56 Penman Monteith Reference evaporation and fitting a best fit straight line the data points Figure 3.41). The crop factor was then determined from DAY 335 of 2011 to DAY 335 of 2012 so that the Eddy co-variance data for 2013 could be used as a comparison. An average crop factor for each month was used to determine potential evaporation.

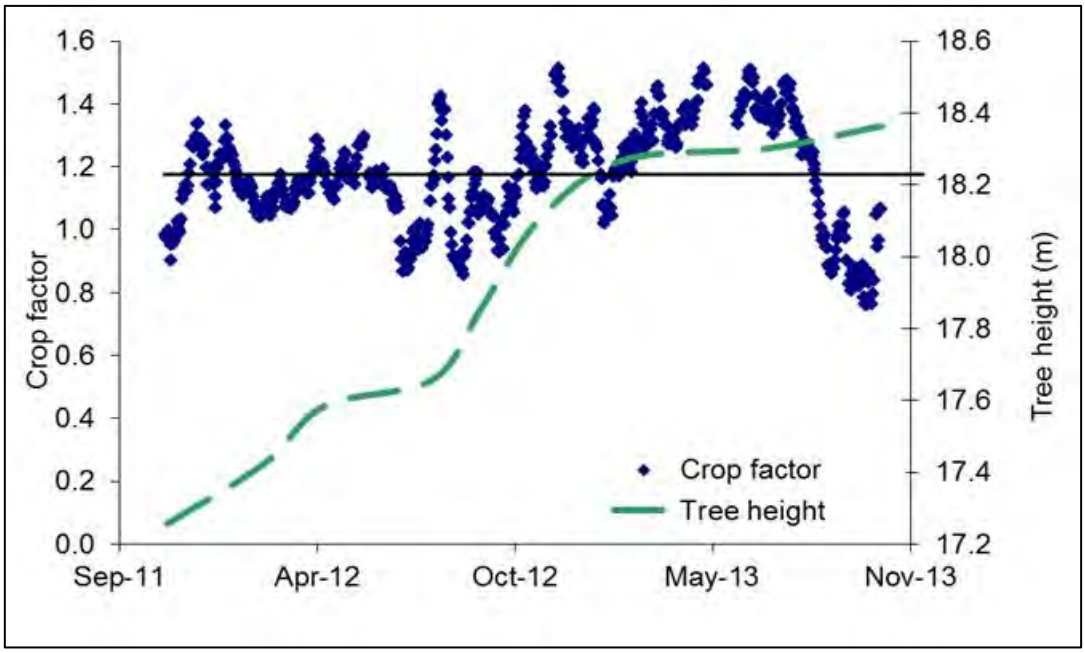

Figure 3.41: Crop factor used to determine potential ET

3.12.10.1 Partitioning root water uptake and soil evaporation

Soil evaporation and transpiration were separated within HYDRUS using Beer's Law:

$$b = 1 - \exp(-k \times LAI) \quad (3.21)$$

$$Et = E \times SCF \quad (3.22)$$

$$Es = E \times (1 - SCF) \quad (3.23)$$

k- rExtinct=0.463, LAI- Leaf area index (L.L^{-1}), Et- Potential plant transpiration, Es- Potential soil evaporation, SCF- soil cover fraction defined as constant b.

The input parameter hCritA is the minimum allowed pressure head at the soil surface. The value can only be activated by evaporation. As long as the pressure head at the soil surface is higher than hCritA the actual evaporation rate will be equal to the potential evaporation rate. Once the pressure head at the soil surface reaches that of hCritA, the actual evaporation rate decreases from the potential evaporation rate because the soil is too dry to deliver this rate (Šimůnek J, 2008). hCritA can be determined using the equation below and, substituting constants values from the HYDRUS manual.

$$Hr=\exp[hMg/R/T] \quad (3.24)$$

where *Hr* is the relative humidity, *h* is the pressure head, *M* is the molecular weight of water [M/mol] (=0.018015 kg/mol), *R* is the universal gas constant [$ML^2/T^2/K/M$] (= 8.314 kg $m^2/s^2/K/mol$, J/mol/K), and *T* is the absolute temperature [K]. It was decided to use a constant from the manual instead of the equation above.

3.12.11 Root water uptake

Root water uptake that is simulated by HYDRUS takes into account two parts: Rooting distribution and root stress function from Feddes *et al*. (1978). The Feddes' model makes use of parameters to determine characteristics of root water uptake. The Feddes *et al.* (1978) model makes the use of S, the sink term, to define the volume of water that is removed from a unit volume of soil per unit time to plant uptake. The S term is defined as:

$$S(h) = \alpha(h)S_p \quad (3.25)$$

where the $\alpha(h)$ is the root-water uptake stress function which is a dimensionless function of the soil water pressure head $0 \leq \alpha \leq 1$) and S_p is the potential water uptake rate (T^{-1}). When soil is at saturation (wetter than h_1) and at wilting point pressure head ($h<h_4$), water uptake is assumed to be close to zero. Water uptake is at its optimal between pressure heads h_2 and h_3 (Figure 3.42). When the pressure head is between h_3 and h_4 water uptake decrease, while pressure head between h_1 and h_2 water uptake increases linearly with h. S_p is a variable that is equal to the water uptake rate during periods of no water stress when $\alpha(h)$=1 (Simunek, 2012).

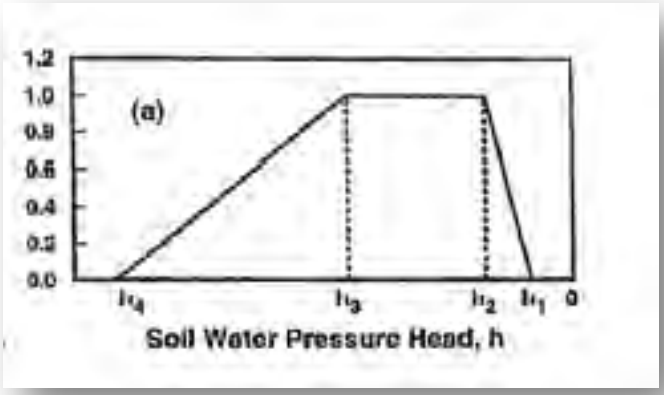

Figure 3.42: Plant water stress response function α(h) (Feddes *et al.,* 1978)

Due to the limited number of studies done by Feddes *et al*. (1978) on the root stress function for different species, the parameter values for *Acacia* mearnsii were estimated. A sensitivity analysis was performed to determine how sensitive the parameters need to be for the determination of transpiration.

The input root distribution function was graphically represented in HYDRUS using root masses that where measured at the Two Streams Research catchment.

3.12.12 Validation

Simulated soil moisture content is validated using TDR 100 and CS616 soil moisture probes (Chapter 4) and simulated Total Evaporation (HYDRUS) is also compared with Actual Total Evaporation (Eddy Covariance).

3.13 Los Gatos Research DLT-100 Liquid Water Isotope Analyser

Samples were analysed using the Los Gatos Research DLT-100 Liquid water Isotope Analyser (Figure 3.43). Los Gatos Research DLT-100 Liquid Water Isotope Analyser uses infrared absorption spectroscopy to quantify the measurement of $^{2}H/^{1}H$ and $^{18}O/^{16}O$ ratios of water samples in an optical cell. The advantages of the laser-based water isotope analyser are; it does not require extensive consumables or sample conversion and that it runs on low power, thus cost per sample is low. The disadvantage of the machine is that samples need to be clean and should not contain dissolved organic matter or alcohols (Berman *et al.*, 2009). Figure 6.1 below shows the configuration of the LGR and how measurements are made by the LGR. (LGR, 2010).

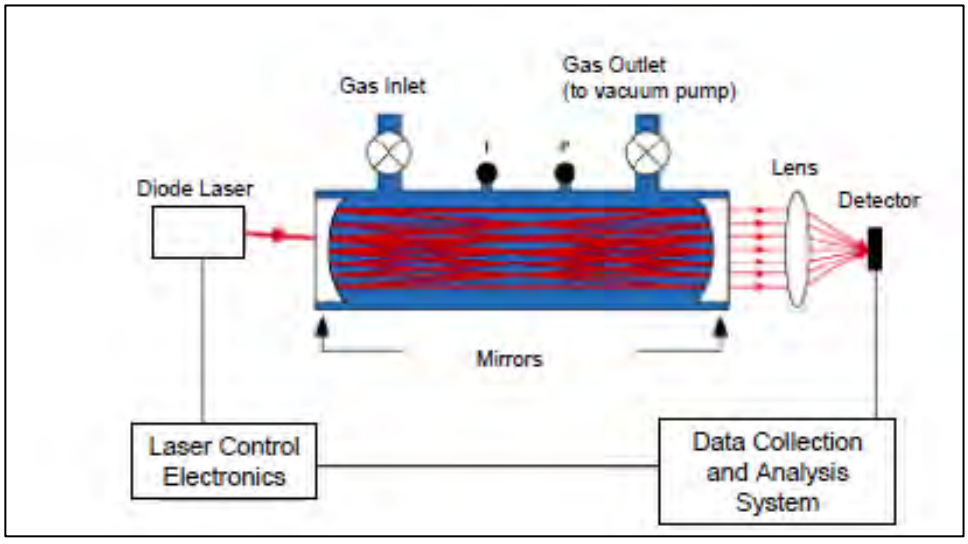

Figure 3.43: Diagram showing LGR configuration (after LGR, 2010)

3.14 Standards and references for isotope analysis

The sample preparation, sample measurement and sample analysis were performed using the following procedure:

3.14.1 Sample Preparation

Samples were shaken to equilibrate before samples were removed from the bottles. A volume of 1.5 ml of each sample was pipetted into marked auto-sampler vials with fresh pipette tips. The samples were then be capped with septa and staked in the auto-sampler trays. Three standards (Table 3.4) were placed in the trays before every five samples and after ever five samples, to allow the machine to calibrate and to clean the needle as samples may contain containments (Pretorius, 2012).

Table 3.4: Standards used for isotope analysis (after Pretorius, 2012)

Standard	Name	δ^2H	$\delta^{18}O$
1	LGR2	-117.00	-15.55
2	VSMOW2 (IAEA)	0.00	0.00
3	IARO53 (IAD)	-61.97	-10.18

3.14.2 Sample Measurement

Each sample was sub-sampled six times, using the Los Gatos Research (LGR) DT-100 Liquid Water Isotope Laser Analyser (Pretorius, 2012).

3.14.3 Sample Analysis

The LGR DT-100 analyser reports $^2H/^1H$ and $^{18}O/^{16}O$ ratios and not δ values on a V-SMOW scale. Post-processing required determining the ratios for the standards and developing a relationship between known V-SMOW δ values and the measured ratios of the different standards. A relationship was applied to determine the ratio to each of the measured sub-sample ratios.

The post-processing checks that were implemented in this research included (after Pretorius 2012):

- Temperature variation of rate of change of less than 0.3°C/hour or a standard deviation for each sample less than 0.004°C.
- Sub-sample density between 2 to 4x 10^{16} molecules/cm^3 and standard deviation between measurement less than 1000 times smaller than the injected density,
- Deviation of $^2H/^1H$ less than 1000x smaller than measured ratio and $^{18}O/^{16}O$ less than 3000x smaller than measured ratio.
- Results of each sub-sample were reported as an average and the standard deviation of the 6 injections. The standard deviation of ^2H results should be less than 2 permil and ^{18}O less than 0.3 permil.

3.15 Sources of Errors

3.15.1 Isotope ratio infrared spectroscopy

The machine that was used to analyse isotope samples was an Off-Axis Integrated Cavity Output Spectroscopy (OA-ICO) Los Gatos Research DLT-100 Liquid Water Isotope Analyser.

Measurements from Isotope Ratio Infrared Spectrometer (IRIS) are comparable with measurements from Isotope Ratio Mass Spectrometer (IRMS). Methods of removing organic contaminants from the samples prior to analysis have not been fully developed or validated, although post-data processing software has been developed to flag samples that contain organic contaminants. Research done by the University of California on sap samples that have been collected by means of cryogenic vacuum distillation, showed samples that should be treated with activated charcoal to remove organics and make samples clear and odourless. This method reduces errors in measurement using the IRIS. The post-data processing software for Off-axis integrated cavity output spectroscopy is a Spectral Contaminant Identifier (SCI) software (West *et al*., 2011). The SCI was used to determine the interference metric that was recorded by the spectra (West *et al*., 2011). The metric was compared with that of known standards and good or bad flags were used to indicate the reliability of the measurement. From the research done at the University of California on sap samples, the results showed that the IRIS gives less error when compared to those from IRMS. Spectral interference can only be used to determine if there are contamination problems and errors in the measurement (West *et al*., 2011).

4. RESULTS

This project has provided the opportunity to collate and document historic results together with recent data. Although the historic data is included in some of the results (such as streamflow and rainfall), it is only discussed where it impacts on the interpretation of recent results. Further information on previous results can be found in Everson *et al*. (2007) and Clulow *et al*. (2012).

4.1 Tree Growth

The management of the plantation and catchment area was facilitated by Mondi Forestry. The wattle stand was planted in June 2006. Blanking was required in August due to an approximate 20% fatality rate. This resulted in trees at two slightly different stages of development. Prior to planting, the stand was sprayed in March with herbicide. During planting, dead plant material and weed re-growth were manually cleared from the rows and left as mulch in the inter-row (Figure 4.1). In October 2007, the inter-rows were sprayed with herbicide to control the weeds and reduce competition using a very effective method which only applied herbicide to the inter-row weeds (Figure 4.2). Since then pruning and thinning has been practiced by Mondi contractors when required.

4.1.1 Tree height

The consistency of the tree height growth curve showed that tree growth was not noticeably affected by seasonal fluctuations (Figure 4.3). This indicated that climatic variables such as rainfall, air temperature and radiation do not appear to limit tree growth significantly at Two Streams. An exponential curve was fitted through the data (R^2=0.997) clearly showing the slowing of the growth in tree height with time.

Figure 4.1: Black Wattle (*Acacia mearnsii*) planted in June 2006 after lying fallow for two years.

Figure 4.2: Spraying herbicide onto the inter-row areas without affecting the trees by using a portable spraying booth connected to backpack sprayers.

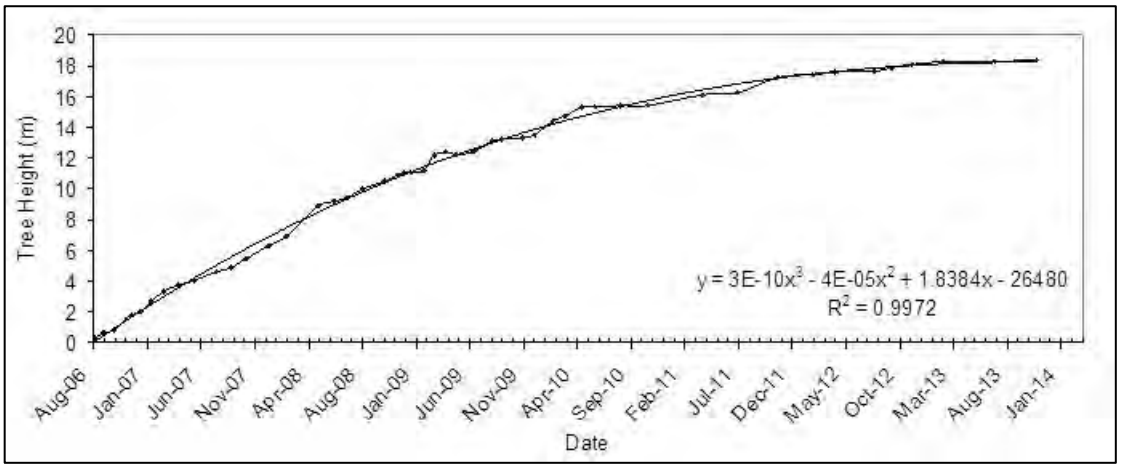

Figure 4.3: Tree heights of *A. mearnsii* measured at Two Streams from August 2006 to November 2013.

4.1.2 Leaf area index (LAI)

The LAI fluctuated initially due to tall, dense weeds during the summer of 2006/2007 when weeds grew vigorously but died off in winter 2007 (Figure 4.4). The influence of weeds was less significant in the following summer of 2007/2008 as the canopy developed and the individual rows became indiscernible and canopy closure was reached. Recent variability in the LAI results is likely to have been due to measurement times and lighting conditions.

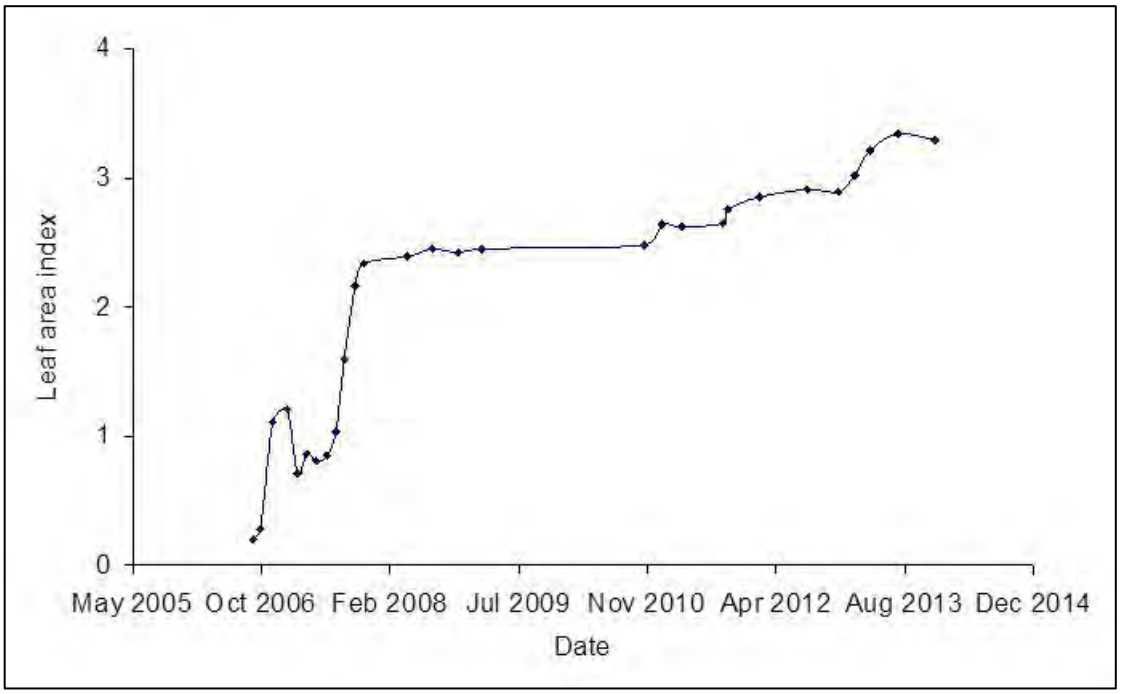

Figure 4.4: LAI measurements at Two Streams from August 2006 to November 2013.

4.1.3 Roots

Excavation of the soil water probe pits provided an ideal opportunity to determine the initial root distribution in the soil profile. Within the open face of the soil pit, a 1 m wide section was cut smooth with a spade and divided into 0.4 m intervals. Individual roots exposed at the cleared face were carefully counted revealing the majority of both large and fine roots were found in the top 0.06 to 0.4 m soil depth (Table 4.1).

The following should be noted:

- for practical reasons the top 60 mm of soil was not included in the data but contains a high density of fine roots and organic matter;
- root diameters < 0.5 mm were classified as fine and those > 0.5 mm as large;
- prior to canopy closure in the summer of 2007/2008 there were a large number of annual weeds in the inter-rows. The data in the upper layers would have contained some of these roots.
- A high proportion of fine roots occurred in the top 1.2 m of the soil profile although some fine roots were still found at 2.4 m. The few large roots were limited to the upper 1.6 m of the soil profile.

Table 4.1: Distribution of root mass on 1 February 2007 in the excavation pit.

Depth (m)	Large roots (> 0.5 mm)	Fine roots (< 0.5 mm)
0.06-0.4	15	189
0.4-0.8	14	135
0.8-1.2	9	120
1.2-1.6	4	51
1.6-2.0	0	16
2.0-2.4	0	2

The distribution of root mass over the profile for the two consecutive years in 2008 and 2009 showed a similar pattern with a high root mass near the surface, a reduction towards a depth of 2 m, followed by a noticeable increase in root mass at 3.2 m (Figure 4.5). There were however significant differences in the 2008 and 2009 data. The root mass at 0.4 m dropped from 0.02 to 0.011 g kg^{-1} as a result of canopy closure and a reduction in the weed root mass in 2009. From a depth of 0.8 m to 4 m the pattern is similar for both samples but the 2009 root mass is greater than the 2008 root mass particularly at depths of 2 m and 3.2 m as a result of the wattle trees extending their roots to deeper depths. The 2011 data shows a five to ten fold increase in root material in the upper 2 m of the soil profile. A decrease in the root density occurred at 2.4 m (almost unchanged from the 2009 data) followed by an increase to about 4 m. Most recently (Oct-2012), the root density at 4 m was higher than in the past and could be characteristic of the specific location where the samples were collected. However, these data show that the root density has increased substantially since planting and that there are roots down to depths of at least 5 m.

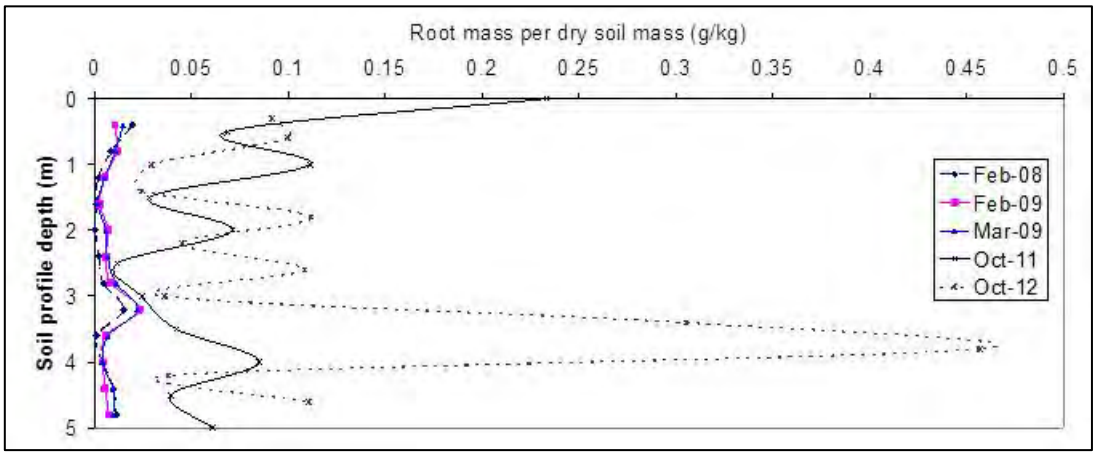

Figure 4.5: The root mass (g kg^{-1} of soil) found at Two Streams on four different occasions.

4.1.4 Stem diameter at breast height

Stem diameters at breast height were measured in previous research at Two Streams and have been continued again during the course of the current project (Figure 4.6). Measurements will be continued as they provide a useful reference for the sapflow results and will be critical for up-scaling the sapflow to stand ET.

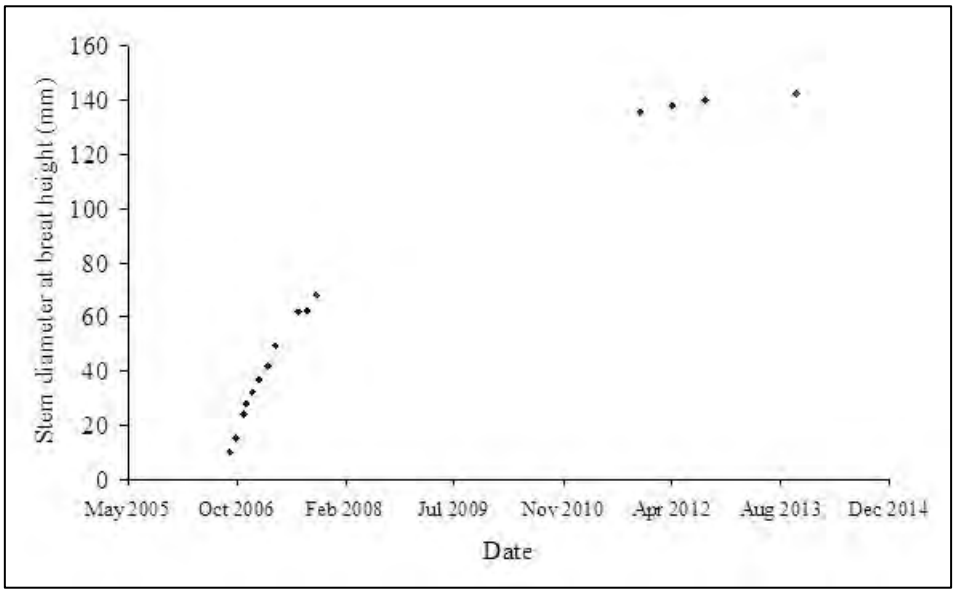

Figure 4.6: Earlier measurements (2006-2007) of stem diameter at breast height were continued during the course of the existing research.

4.2 Rainfall Monitoring

4.2.1 Above Canopy Rainfall

The Two Streams research catchment lies in the summer rainfall zone of South Africa, where summers are wet and humid and the winters are dry and cool. Daily and monthly rainfall totals exhibited typical seasonal trends, with wet summer and dry winter periods (Figures 4.7 and 4.8). The long-term mean annual precipitation for the area is 853 mm (Lynch and Schulze, 2006), however the MAP for the monitoring period using the two long-term rain gauges in the catchment 1999 to 2008 was 876 mm. The annual rainfall for the first hydrological period of study (October 1999 to September 2000) was 1071 mm. This compares with 897, 1170, 659, 727, 1139, 1106, 689, 819, 765, 587, 856 and 846 mm for the 2000/2001 to 2010/2012 seasons respectively. Annual rainfall at the study site was therefore highly variable with a range of 587 mm between the lowest and highest years (minimum = 584 mm and maximum = 1171 mm).

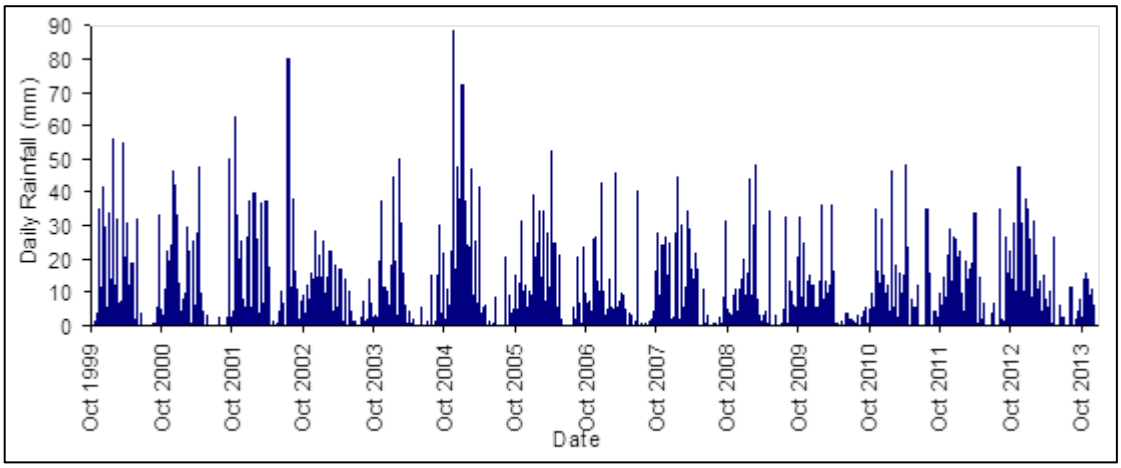

Figure 4.7: Daily rainfall at the Two Streams study site (November 1999 to December 2013).

The thirteen-year study period was characterized by an initial three-year period of normal to wet conditions, while the 2002/2004 period was dry, reflecting the severe drought conditions experienced in KwaZulu-Natal in the 2003/2004 season. The daily distribution of rainfall (Figure 4.7) reflected these dry conditions and only a few rainfall events of over 30 mm were recorded. By contrast the 2004/2005 data showed that the rain events between July and December 2004 were higher than any previously measured rain events for the study period and the highest single rainfall event during this study was measured on 19 November 2004 when over 90 mm of rain fell. The 2006/2007 data once again showed a dry period caused primarily by uncharacteristically dry weather in February and March of 2007. The driest period measured was the 2009/2010 period when the annual precipitation was only 587 mm.

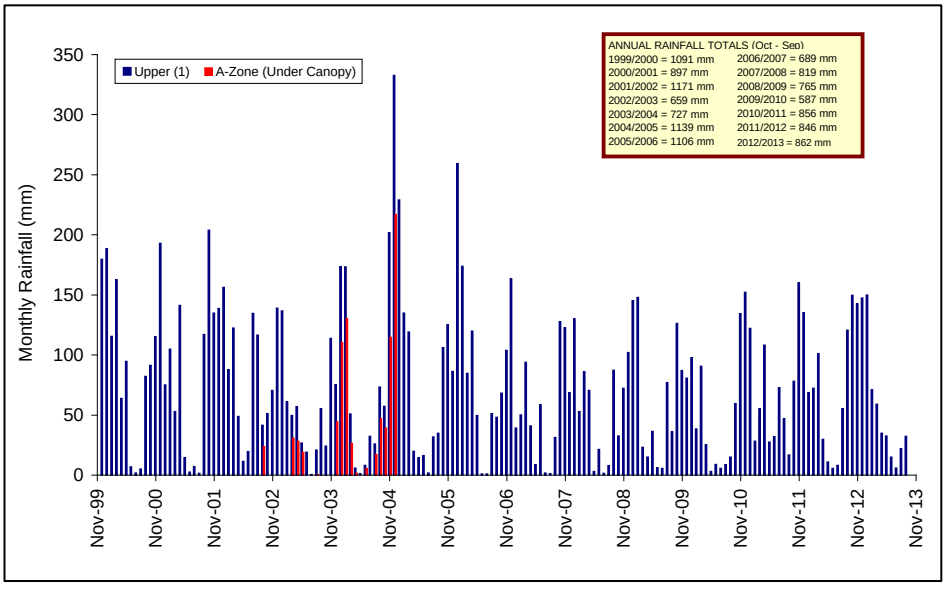

Figure 4.8: Monthly rainfall totals at the Two Streams study site (November 1999 to October 2013) and beneath the wattle canopy at the A-Zone site (August 2002 to November 2004).

4.2.2 Rainfall Interception

This study showed that interception plays a very important role in the forest hydrological cycle, with only 66.5% to 76.2% of gross precipitation being available water that drains to the soil, after the losses due to canopy and litter interception. Canopy interception by *E. grandis*, *A. mearnsii* and *P. patula* accounted for losses of 14.9%, 27.7% and 21.4% of gross precipitation respectively as shown in Table 4.2.

Although litter interception resulted in a smaller portion of the total interception loss, it is none the less important. In this study it was found that litter interception accounted for a loss of 12.1% of gross precipitation by *P. patula*, and 8.5% and 6.6% for *E. grandis* and *A. mearnsii* respectively as shown in Table 4.3.

Table 4.2: Total observed canopy interception from April 2008 to March 2011.

Species	Gross Precipitation (mm)	Observed canopy interception (mm)	Observed canopy interception (%)
E. grandis	1884.7	280.4	14.9
A. mearnsii	1884.7	522.4	27.7
P. patula	1909.7	408.7	21.4

Table 4.3: Observed litter interception by *E. grandis*, *A. mearnsii* and *P. patula*, from April 2008 to March 2011.

Species	Gross Precipitation (mm)	Observed litter interception (mm)	Observed litter interception (%)
E. grandis	1884.7	160.4	8.5
A. mearnsii	1884.7	124.7	6.6
P. patula	1909.7	231.2	12.1

Gerrits (2010) found litter interception to be as high as 22% in a beech forest, and 18% in a needle leaf litter Cedar forest, while Helvey (1964) found litter interception to be 34% in a poplar stand in the USA. Interception not only reduces net precipitation but it is also a threshold process, as a certain amount of water is required before successive processes such as infiltration and runoff can take place. These subsequent processes can only occur once the canopy and litter storage capacities have been reached and it can therefore be said that canopy and litter storage capacity are key factors in the control of canopy and litter interception. Although the storage capacity of the litter is much greater than that of the canopy, canopy interception is greater. This

highlights that the evaporative potential of the canopy is far greater than that of the forest floor litter due to its direct exposure to solar radiation and wind.

One implication of interception being a threshold process is that it causes a delay in the onset of subsequent processes, particularly infiltration (Gerrits, 2010). This delay may be a few seconds to minutes in cases where both the canopy and litter are near saturated or in high intensity storms. Conversely, this delay may be in the order of days to weeks in cases where the next rainfall event is not large enough to exceed the canopy and litter storage capacities, and therefore only after an event large enough to satisfy the combined storage capacities of the canopy and litter will subsequent processes take places. This is evident in Figures 4.9 to 4.11, where there are many events where the throughfall did not exceed the litter storage capacity and therefore no infiltration took place. This delay is also not the same for all species.

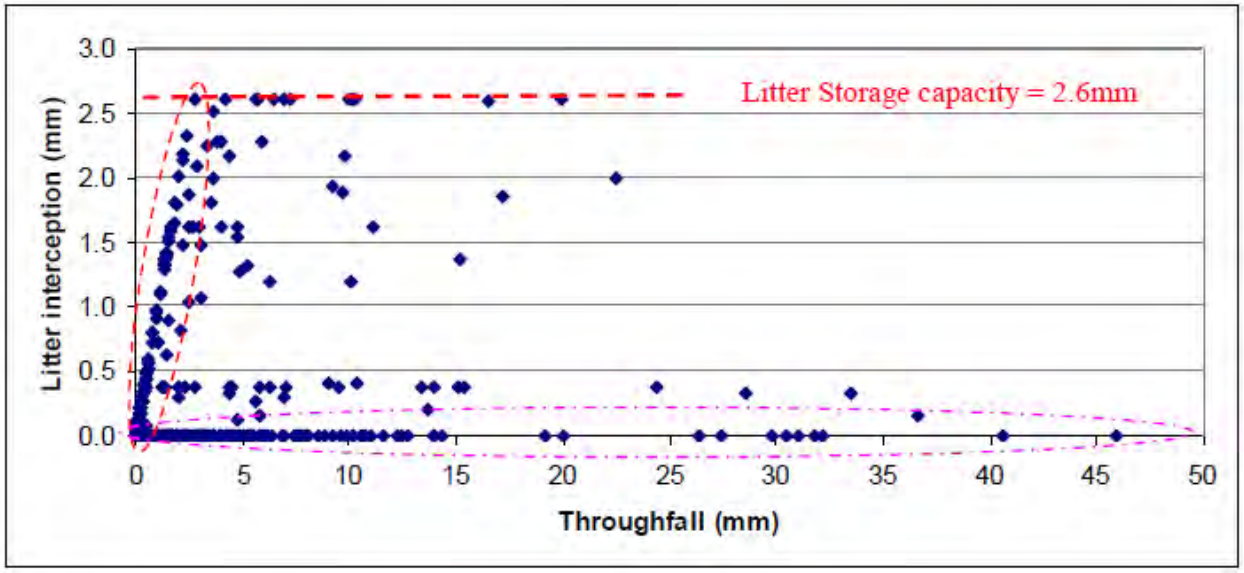

Figure 4.9: Observed litter interception by Eucalyptus grandis at Two Streams. The red circle represents increasing litter interception with increasing throughfall.

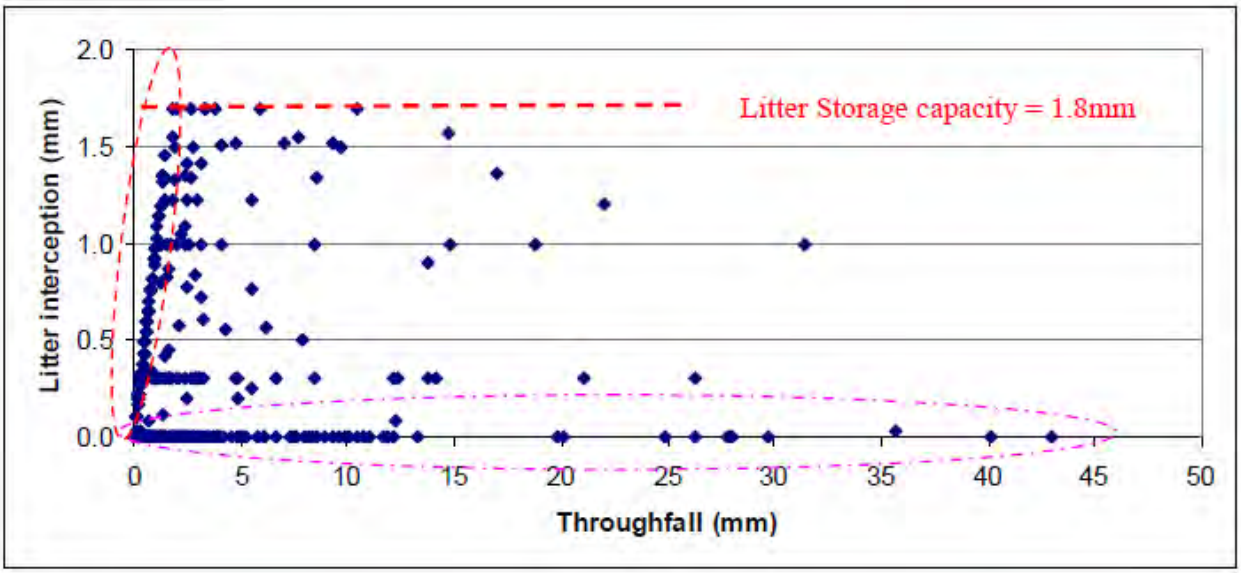

Figure 4.10: Observed litter interception by *Acacia mearnsii* at Two Streams. The red circle represents increasing litter interception with increasing throughfall

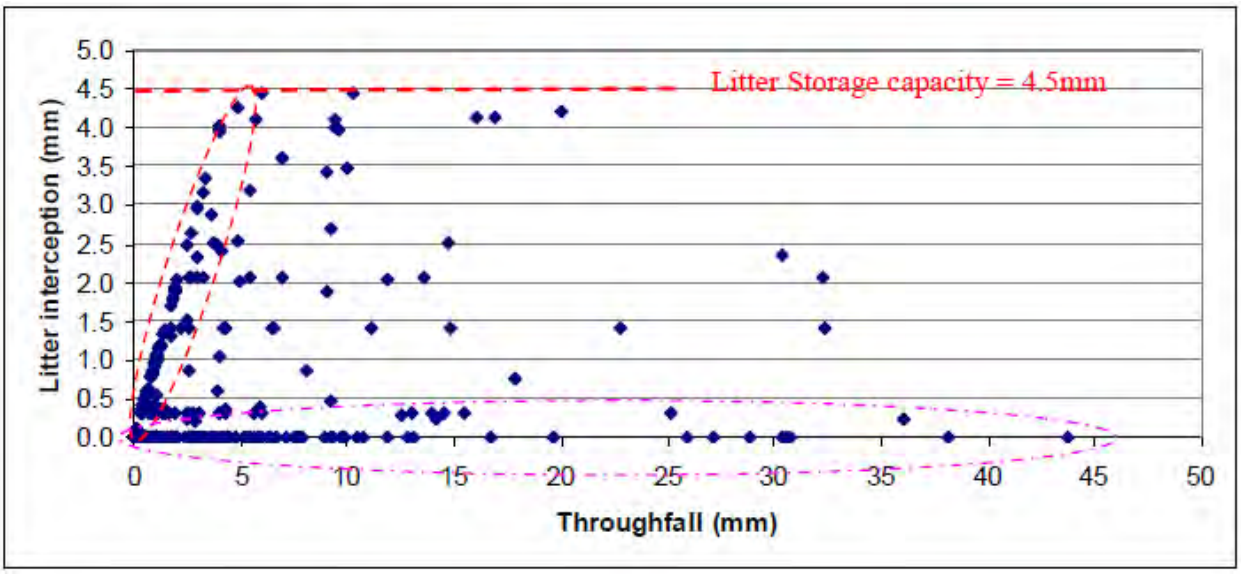

Figure 4.11: Observed litter interception by *Pinus patula* at Two Streams. The red circle represents increasing litter interception with increasing throughfall

As interception reduces and delays subsequent hydrological processes differently for all species, it also determines the spatial distribution of net precipitation. Within a commercially afforested catchment such as the Mistley-Canema estate there are many species and types of vegetation and thus different canopy and litter interception characteristics. The spatial distribution of net precipitation is not only different between stands, but also within the stand. It is for this reason that linear troughs were used to measure throughfall as the throughfall varies from near the

trunk to the edge of the canopy, depending on the structure and water holding characteristics of the canopy. Within a commercial plantation, the spacing and management of the trees will also affect the spatial distribution of throughfall. Therefore, interception plays a far more significant and complex role in a catchment water balance than just as a reducer of rainfall.

As the study site is situated in a mist belt area, where more than 50% of the daily rainfall events are less than 1 mm, it is not surprising that the interception losses are high. As shown in Figure 4.12, the rainfall intensity affects the canopy storage capacity, and should not be considered as a constant.

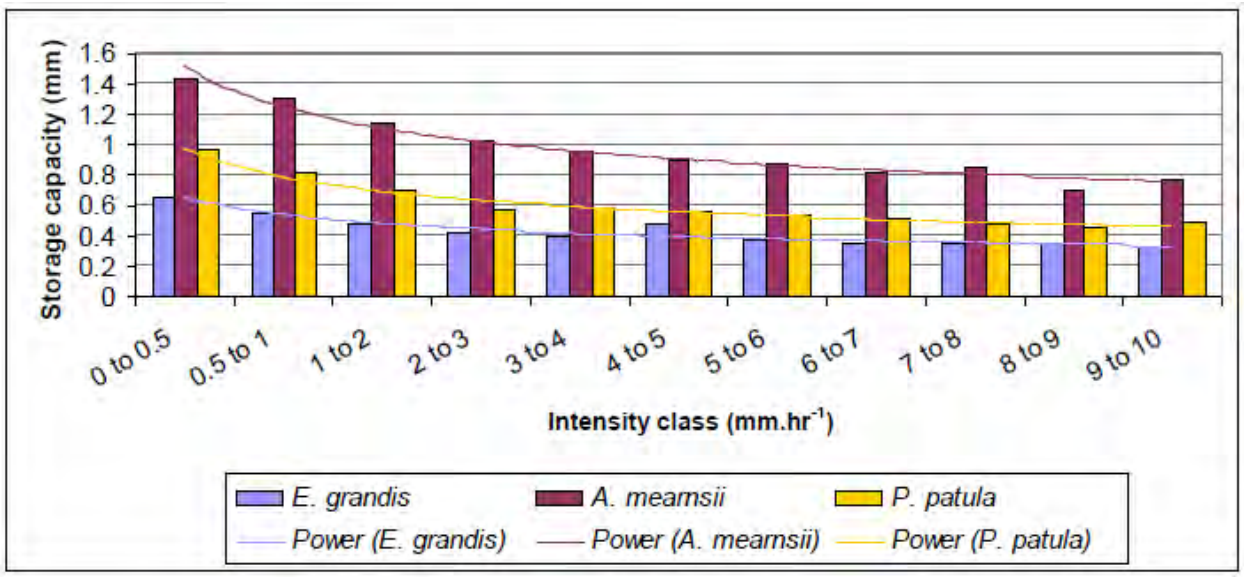

Figure 4.12: Canopy storage capacity for *E. grandis*, *A. mearnsii* and *P. patula* at different rainfall intensities.

The canopy properties such as "wettability" and leaf angle also affect the water retention and therefore canopy storage capacity. Although, the *E. grandis* had the largest LAI, it has the lowest storage capacity. The rainfall amount, duration, frequency and intensity also play an important role in determining the canopy interception as shown in Table 4.4.

Table 4.4: Observed canopy interception by *E. grandis*, *A. mearnsii* and *P. patula* for the two contrasting periods of February 2009 and 2010.

Time Period	Gross Precipitation (mm)	*E. grandis*		*A. mearnsii*		*P. patula*		No. of events
		(mm)	(%)	(mm)	(%)	(mm)	(%)	
Feb 2009	216.4	21.5	9.9	39.4	18.2	31.2	14.4	21
Feb 2010	43.0	9.1	21.2	13.5	31.4	11.1	25.8	17

The results of the interception study in the Two Streams catchment has provided very important information towards a better understanding of the water-balance and highlighted the significance of rainfall interception. It is therefore recommended that further research into canopy and litter interception be undertaken in other bioclimatic regions where rainfall patterns differ.

4.2.3 Stemflow

4.2.3.1 Analysis of Stemflow Data during the Winter Period

For the duration of the 2013 winter period, stemflow and rainfall data were summed to a daily level. Figures 4.13 to 4.16 show periods in which stemflow coincided with rainfall and also illustrate periods for when data was not attained due to instrument or logger faults.

Figure 4.13: Graph illustrating daily rainfall and stemflow values for the Upper Thinner stem

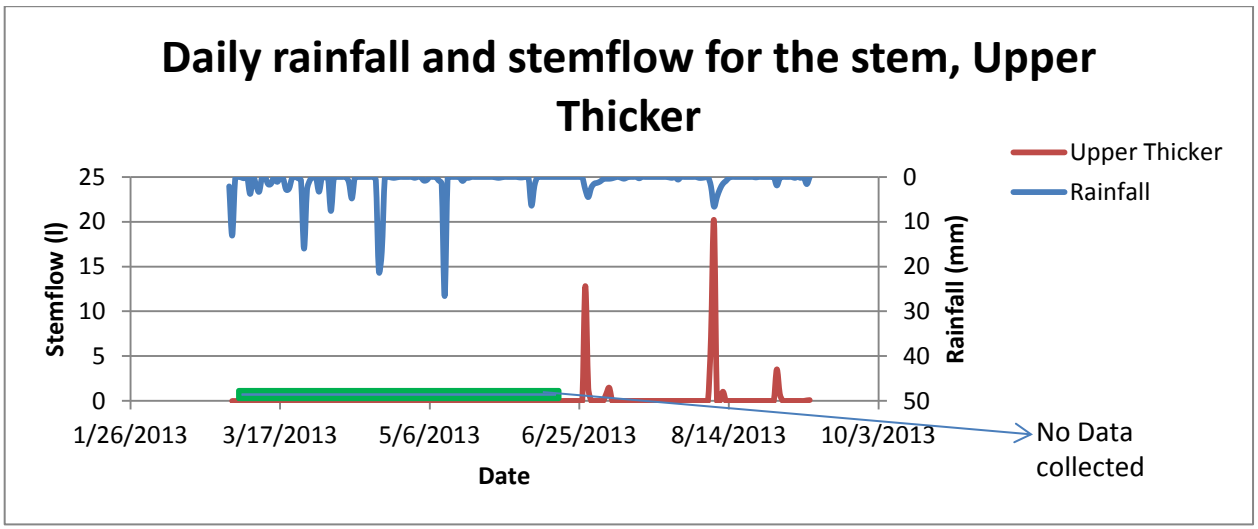

Figure 4.14: Graph illustrating daily rainfall and stemflow values for the Upper Thicker stem

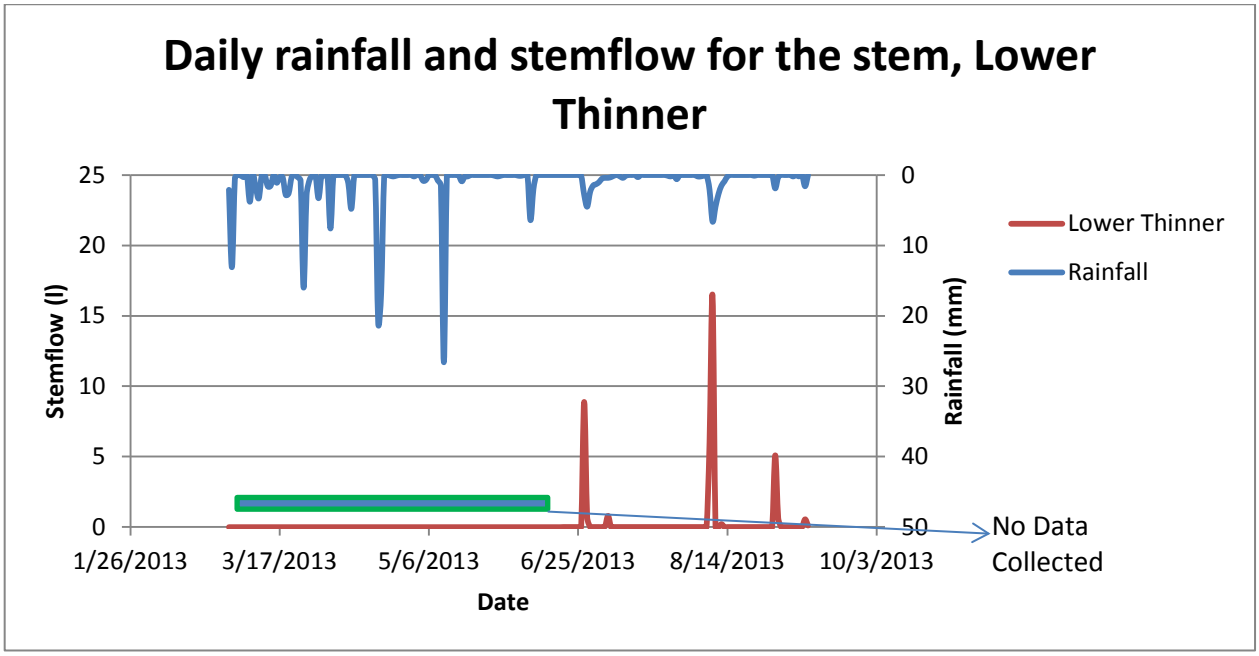

Figure 4.15: Graph illustrating daily rainfall and stemflow values for the Lower Thinner stem

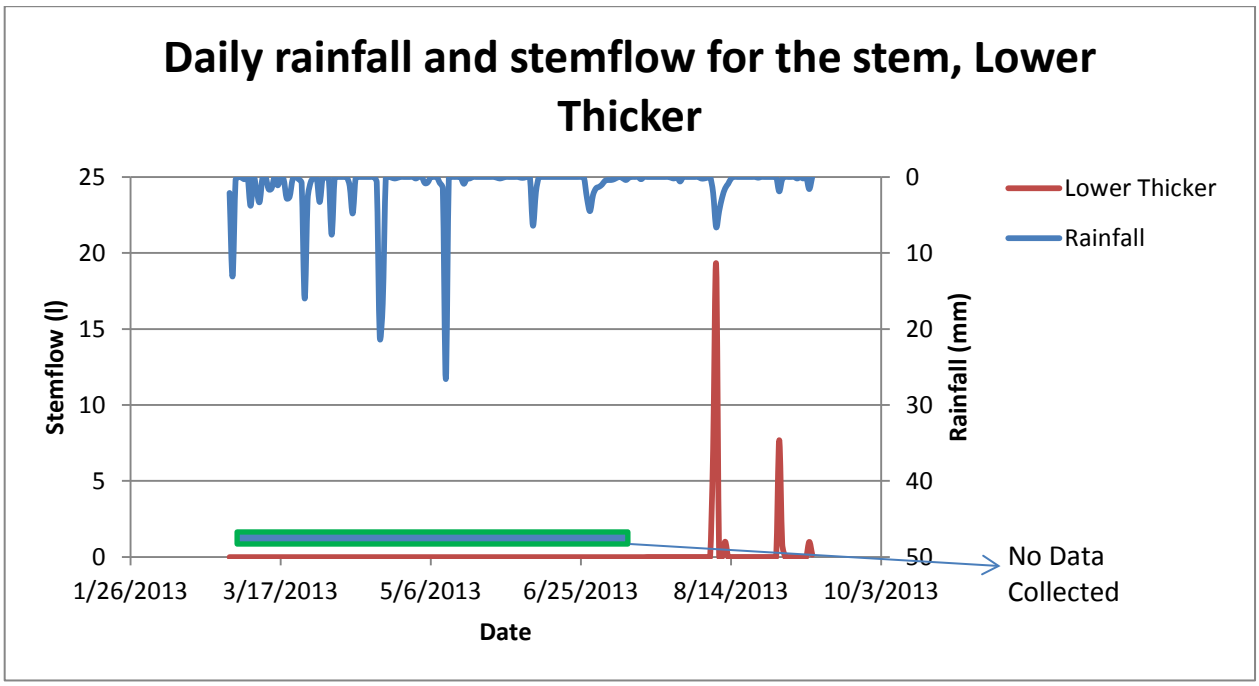

Figure 4.16: Graph illustrating daily rainfall and stemflow values for the Lower Thicker stem

There are a wide variety of methods that can be used to calculate stemflow for a stand area, based on easily measured tree characteristics (Crockford and Richardson, 1987). The methods used are discussed below together with the results obtained.

4.2.3.1.1 Stemflow Calculation Based on Crown Projected Area

The stemflow volume for each event was expressed by its Crown Projection Area (CPA). This method was adapted from Aboal *et al*. (1999). In order to calculate the CPA of each stem, a laser was placed on a level stand beneath the canopy and a beam was shown to the edge of the canopy. This was then marked on the ground surface, and measurements where made from the tree stem to the marked point. Measurements were taken in all directions about the tree stem. Small branches that protruded were not considered. The area was calculated using computer aided drawing software (Diagram 1). Due to high canopy overlap at the lower site, it was difficult to attain a CPA, therefore this was only calculated for the Upper Thinner and Upper Thicker stems.

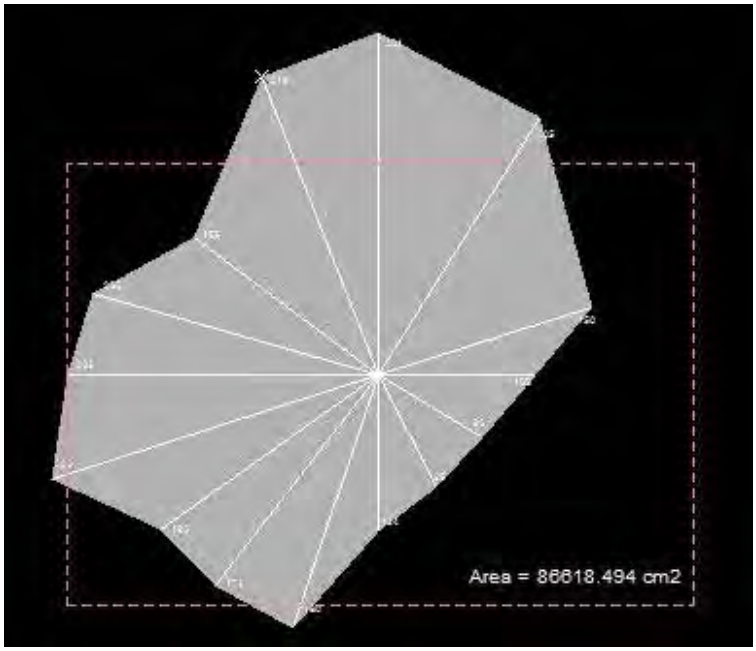

Diagram 1: Calculation of the Canopy Projected Area was performed using computer aided drawing software.

Two rainfall with stemflow events where selected for analysis during the winter period, as these events provided data for both stems (Table 4.5 and 4.6). Use of the CPA method does not account for the density of the foliage. This method also considers CPA as if it was the real stand area (Aboal *et al*., 1999). As a result, the total area is far greater, when compared to that of a stand basal area (described below). This can result in percentage values of rainfall converted to stemflow being of great significance for events with greater precipitation. The percentage conversion also changes between stems of different diameter. The individual trees converted between 1.3 and 28.1% of rainfall to stemflow, however the CPA for only two trees over two events were considered and further research is required.

Table 4.5: Stemflow as a unit depth (mm) and a percentage of rainfall for events dated for the Upper Thinner stem

	Upper Thinner						
Date	**Precipi-tation (mm)**	**CPA (m^2)**	**Stemflow Volume (l)**	**Stemflow Volume (m^3)**	**Unit depth (m)**	**Unit depth (mm)**	**% Rainfall converted to stemflow**
08/30/2013 - 08/31/2013	2.2	8.66	2.088	0.002088	0.00024	0.24	10.9
9/9/2013 - 9/10/2013	1.6	8.66	0.696	0.000696	0.00008	0.08	5.0

Table 4.6: Stemflow as a unit depth (mm) and a percentage of rainfall for events dated for the Upper Thicker stem

Upper Thicker							
Date	Precipitation (mm)	CPA (m^2)	Stemflow Volume (l)	Stemflow volume (m^3)	Unit depth (m)	Unit depth (mm)	% Rainfall converted to stemflow
08/30/2013 - 08/31/2013	2.2	6.978	4.305	0.004305	0.00061	0.61	28.1
9/9/2013 - 9/10/2013	1.6	6.978	0.148	0.000148	0.00002	0.02	1.3

4.2.3.1.2 Stemflow Calculations Based on the Basal Area (BA) of stem

Basal Area (BA) is a common term used in forestry to describe the cross-sectional area of a stem measured at breast height, which is usually 1.4 m above the ground. BA is easy to measure, and also useful in determining the area occupied by stems in a plantation. In order to measure the BA of a stem, the circumference of the stem is first measured. Since the stem is circular in shape, the circumference is then used to calculate a stem diameter, which is the Diameter at Breast Height (DBH). Hence the BA is expressed as m^2/tree (Table 4.7).

Table 4.7: Basal Area at Breast Height of the trees monitored at Two Streams.

Tree Name	Stem Circumference (cm)	Stem diameter (cm)	Basal Area (m^2/tree)
Upper Thinner	35.1	11.18	0.0098
Upper Thicker	44.5	14.17	0.0158
Lower Thinner	43.2	13.76	0.0149
Lower Thicker	49	15.61	0.0191

In order to attain stemflow as a unit depth (mm) for the entire stand plot, the method used by Baloutsos *et al*. (2010) was applied (4.8). Using this method, the percentage rainfall converted to stemflow is 26.1% and 4.6% for events 1 and 2 respectively. These values are comparable yet generally higher than the previous values using the CPA method, in which, for event 1 the percentage rainfall converted to stemflow was 10.9 and 28.1% for the Thicker Tree and for event 2, 5.0 and 1.3% for the Thinner Tree.

Table 4.8: Stemflow expressed as a unit depth for the entire stand for two events

	Rainfall (mm)	Total volume (l)	Total BA of selected stems	BA for entire stand	Ratio of stand BA to selected stems BA	Plot area (m^2)	Stemflow depth (mm)
Event 1	2.2	20.698	0.060	489.699	8223.309	296068.735	0.575
Event 2	1.6	2.640	0.060	489.699	8223.309	296068.735	0.073

4.2.3.1.3 Funneling Ratio

Funneling ratio is a meaningful method of comparing stemflow volumes between trees (Steinbuck, 2002). According to Herwitz (1986), the equation for determining the funnelling ratio is:

$$F.R. = \frac{V}{(B \times G)} \quad (4.1)$$

Where, V is the stemflow volume (ml) for a specific tree, B is the basal area of the tree (cm^2), and G is the rainfall depth (cm). The term (BxG) relates to the volume of rainwater that would have been collected in a rain gauge that occupies the same area as the trunk BA. The funnelling ratio is used as a means to determine if there is any contribution from the branches on stemflow volumes (Steinbuck, 2002). A ratio of greater than one indicates a stemflow contribution from the branches, whereas a ratio of one indicates no contribution (Steinbuck, 2002). The funnelling ratios for each selected stem is illustrated in Table 4.9 below for two events, the first occurring on the 30th of August 2013 and the second occurring on the 9th September 2013. The reason for selecting the above mentioned events is that data was collected across all four stems hence analysis between stems can be made.

Table 4.9: Funnelling ratio for each event

Stem ID	Stemflow Volume (ml)	Basal Area (cm^2)	Rainfall (cm)	Funnelling Ratio
Funnelling Ratio (30th August 2013)				
Upper Thinner	2088	98	0.22	96.8
Upper Thicker	4305.6	158	0.22	123.8
Lower Thinner	5745.6	149	0.22	175.2
Lower Thicker	8558.4	191	0.22	203.6
Funnelling Ratio (9th September 2013)				
Upper Thinner	696	98	0.16	44.3
Upper Thicker	148.8	158	0.16	5.8
Lower Thinner	652.8	149	0.16	27.3
Lower Thicker	1142.4	191	0.16	37.4

As can be seen from the above table, the funnelling ratio is greater for the thicker stems at each location. This indicates that, for thicker stems, the branches contribute greater quantities of stemflow compared to thinner stems. With regards to the event on the 9th of September 2013, the Upper Thicker funnelling ratio is lower when compared to the Upper Thinner stem. This is as a result of the stemflow volume generated from the event being lower compared to the thinner stem. This does not follow the general trend where, thicker stems generate greater stemflow volumes.

4.2.3.1.4 Stemflow Timing Analysis

In order to attain a stemflow timing analysis, rainfall data, together with stemflow data were analysed at a 10-minute interval. Two rainfall events were considered in order to determine lags between rainfall and stemflow (Figure 4.17 and 4.18).

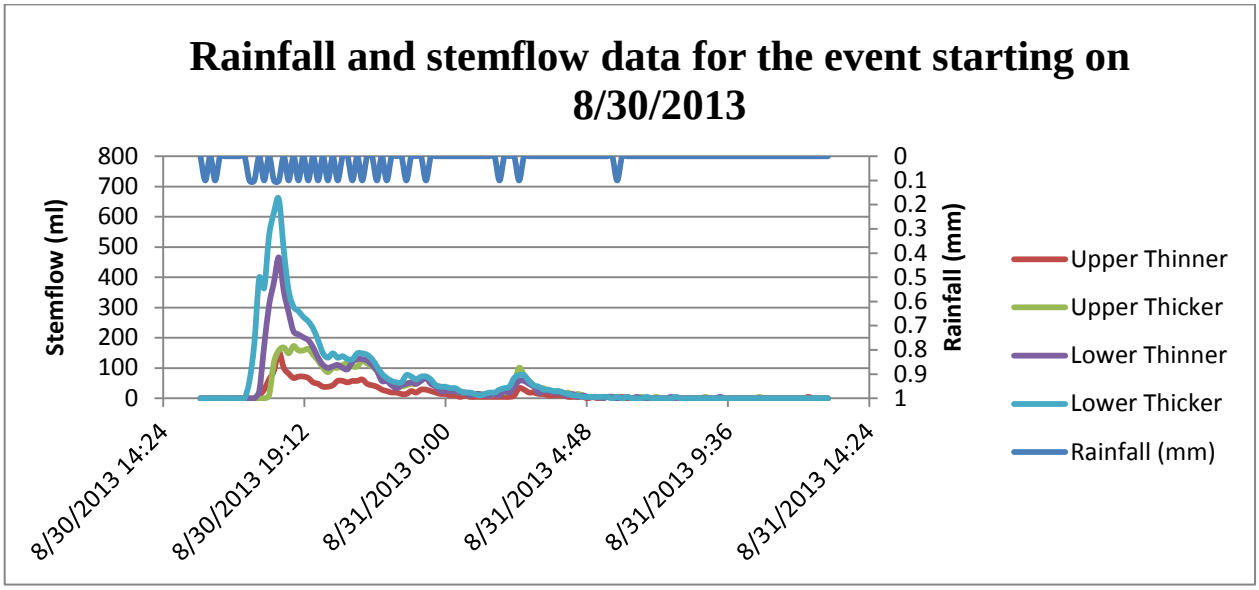

Figure 4.17: The 10-minute Rainfall and stemflow data for the event starting on the 8/30/2013

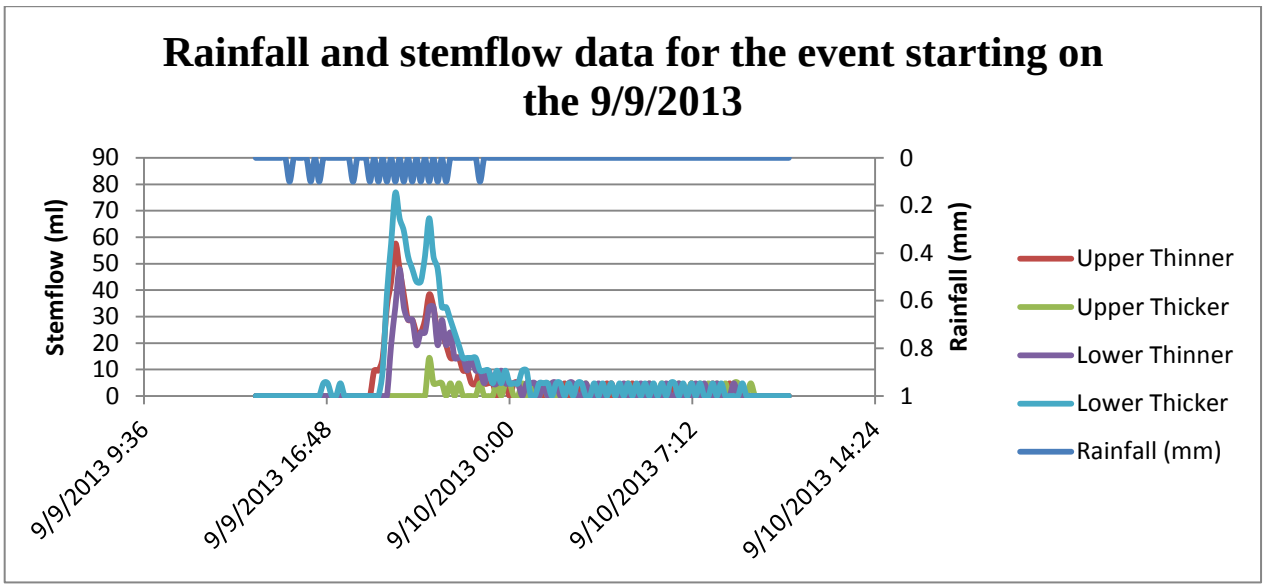

Figure 4.18: The 10-minute Rainfall and stemflow data for the event occurring on the 9/9/2013

In the case of the above events, between 0.2 and 0.8 mm of rainfall occurred prior to any stemflow being generated. Once the canopy had been "saturated" stemflow increased rapidly.

4.2.3.1.5 Volume of Stemflow Generated for the Different Stems

In order to attain a comparison between the volume of stemflow generated, two rainfall events were used, as data across all four stems were available for these two events, making for a useful comparative analysis between the four selected stems (Table 4.10 and 4.11) below.

Table 4.10: Total stemflow volumes for the event occurring on the 08/30/2013

Total Volumes (event 1)	
Stand ID	**Stemflow Volume (ml)**
Upper Thinner	2088
Upper Thicker	4305
Lower Thinner	5745
Lower Thicker	8558
Rainfall total (mm)	2.2

Table 4.11: Total stemflow volumes for the event occurring on the 09/09/2013

Total Volumes (event 2)	
Stand ID	**Stemflow Volume (ml)**
Upper Thinner	696
Upper Thicker	149
Lower Thinner	653
Lower Thicker	1142
Rainfall total (mm)	1.6

For event 1, the stemflow volume from the thicker stems is more than that of the thinner stem at the upper and lower sites. For event 2, the lower site shows a similar trend with the thicker stem having a higher stemflow. However, at the upper site the trend is significantly different as the thinner stem has a higher stemflow than the thicker stem.

The difference in stemflow volumes between thicker and thinner diameters varies with rainfall (Tables 4.10 and 4.11). For event 1, the difference between stemflow volumes amongst trees at the same location was between 49% and 104% for the upper and lower sites respectively. For event 2, which was a lower rainfall event, the differences between the stemflows at the lower site were 75%. The difference between the stemflow at the upper site during this event was a high proportion (>400%) and may be due to instrument failure.

The trees at the edge (lower site) of the plantation generated greater stemflow volumes compared to those at the centre (upper site) of the plantation for both events. Rainfall at the edge of the plantation is not obstructed by other tree canopies hence, it call fall directly on the stem along its entire length, depending on wind direction. This can increase the volume of stemflow generated and could be a reason for the difference in stemflow volumes between the stems at the centre and those at the edge of the stand.

4.2.3.2 Analysis of Stemflow Data during the Spring Period

Between 11 September and 18 October 2013, seven rainfall events occurred during which stemflow was monitored on three trees (Figure 4.19). The rainfall events varied between 0.8 mm in a day to 20.2 mm in three days and thus a range of conditions were captured. The stemflow was converted to depth (mm) according to the representative area method and scaled according to the tree density as in the winter period measurements. The percentage of rainfall converted to stemflow was modelled by least squares linear regression (Figure 4.20). The coefficient of determination for the three trees was >0.95 indicating the rainfall depth describes at least 95% of the variability in stemflow despite other factors such as duration of the rainfall event. The gradient of the trend line in Figure 4.20 indicates that the percentage rainfall converted to stemflow is 40%, 39% and 50% for the Upper Thicker and Lower Thinner and Lower Thicker stems.

Preliminary stemflow yields of a small sample of wattle trees have quantified and compared for a few rainfall events in both summer and winter in 2013. Yields of the individual trees are compared and have shown that stemflow yields are variable, but potentially an important variable for quantifying the effective rainfall. Further studies on the tree morphology and rainfall characteristics (event size, type, and season) responsible for the yield differences are required to properly quantify this component of the interception process.

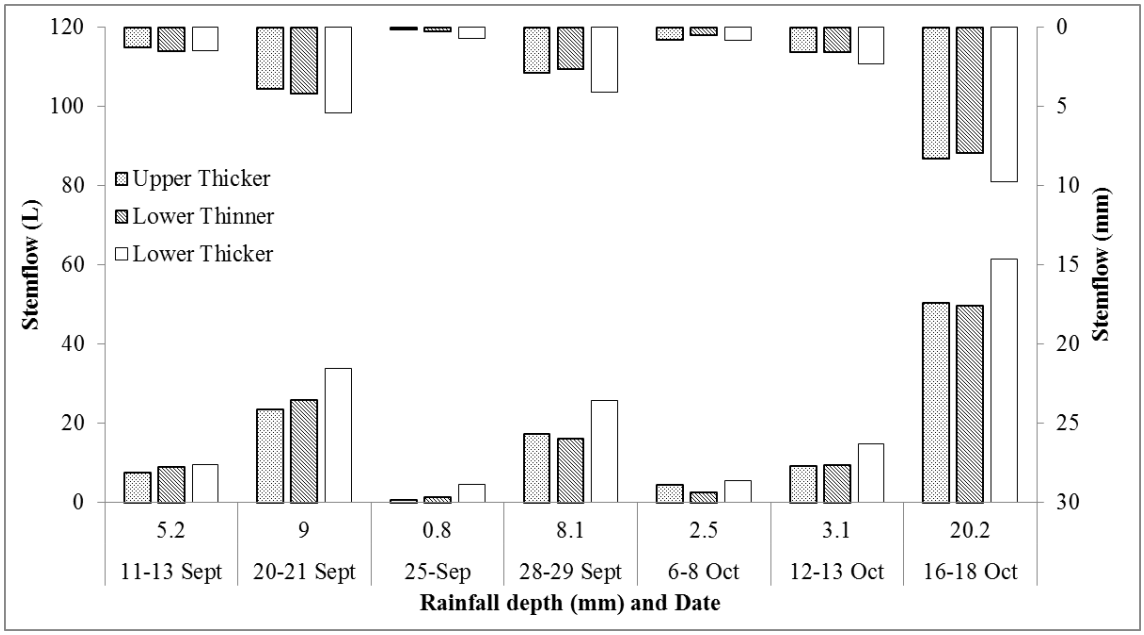

Figure 4.19: Stemflow (L) for three trees is shown on the lower x-axis for seven rainfall events of various depths. The Stemflow converted to mm is shown on the upper x-axis.

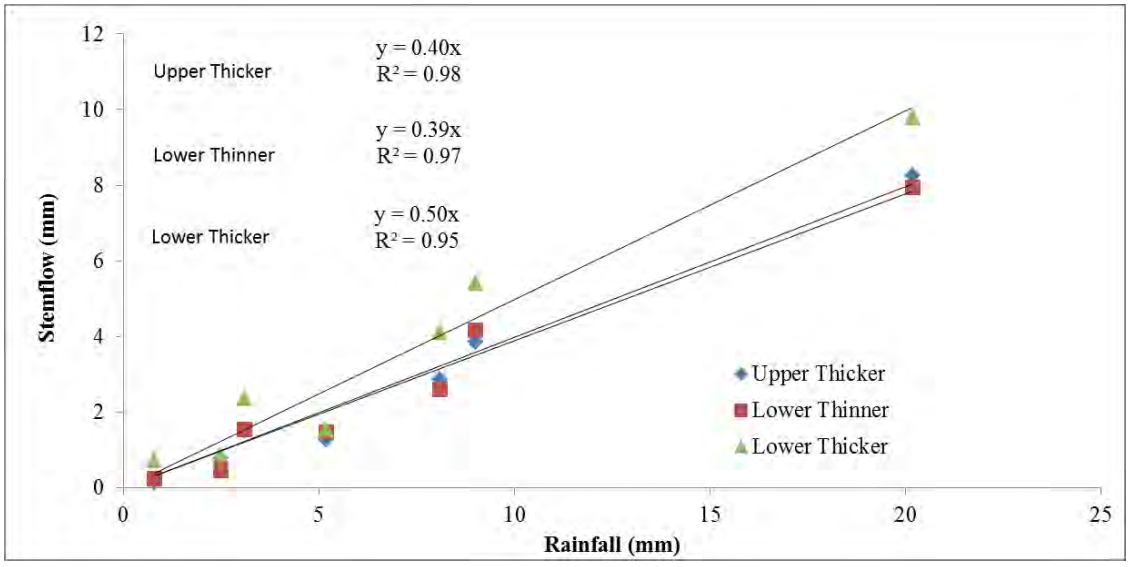

Figure 4.20: Least squares linear regression showing the relationship between rainfall and stemflow across three trees over seven events in the spring of 2013.

4.3 Water-use of Black Wattle

4.3.1 Surface renewal and eddy covariance estimates of total evaporation-October 2011 to July 2013

The net radiation followed a seasonal pattern, peaking in summer at approximately 1000 W m^{-2} (Figure 4.21). In winter the net radiation was more consistent as it was less affected by cloud peaks, but, decreased by 57% to approximately 430 W m^{-2}. The soil heat flux (Figure 4.22) follows a similar seasonal pattern to the net radiation, however, the peaks in summer (130 W m^{-2}) and winter (15 W m^{-2}) indicate a reduction of 89%. This is due to the low sun angles in winter resulting in more shading of the soil surface by the tree leaves and branches. In winter the soil heat flux is slightly more negative (up to -110 W m^{-2}) whereas in summer it is closer to -80 W m^{-2}.

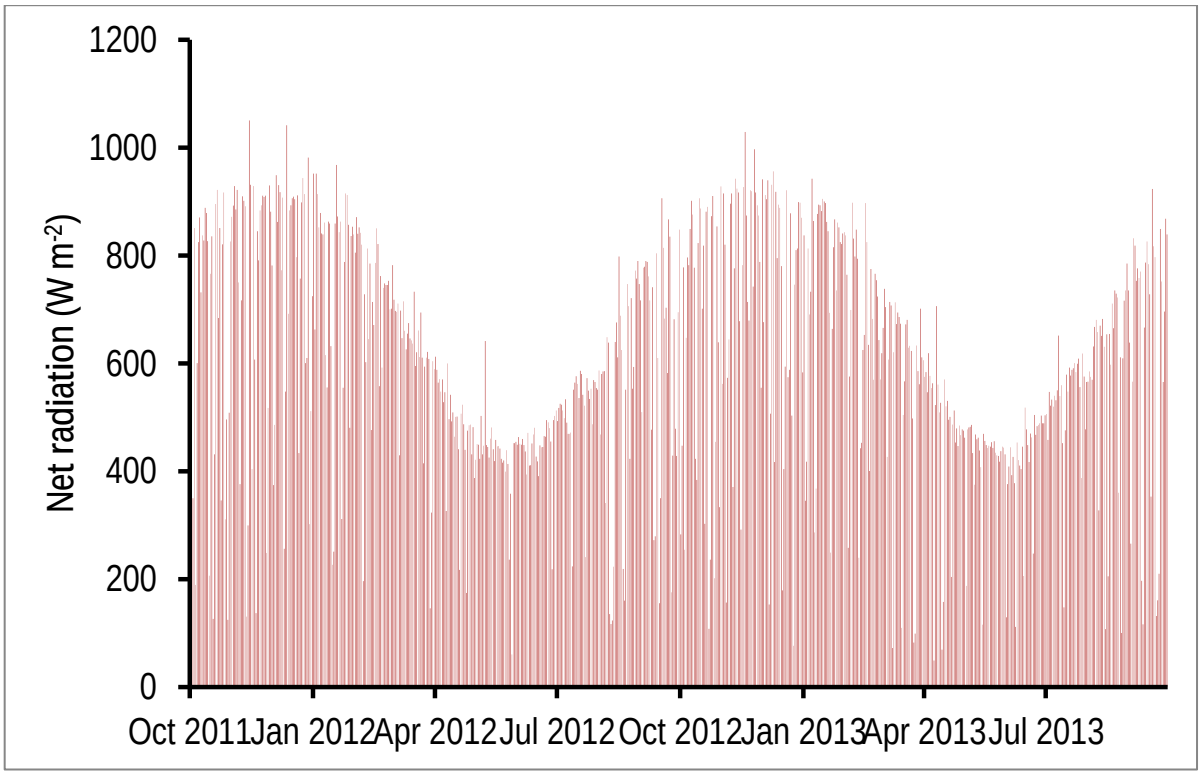

Figure 4.21: Net radiation (30 minute averages) above the Wattle stand at Two Streams from October 2011 to November 2013.

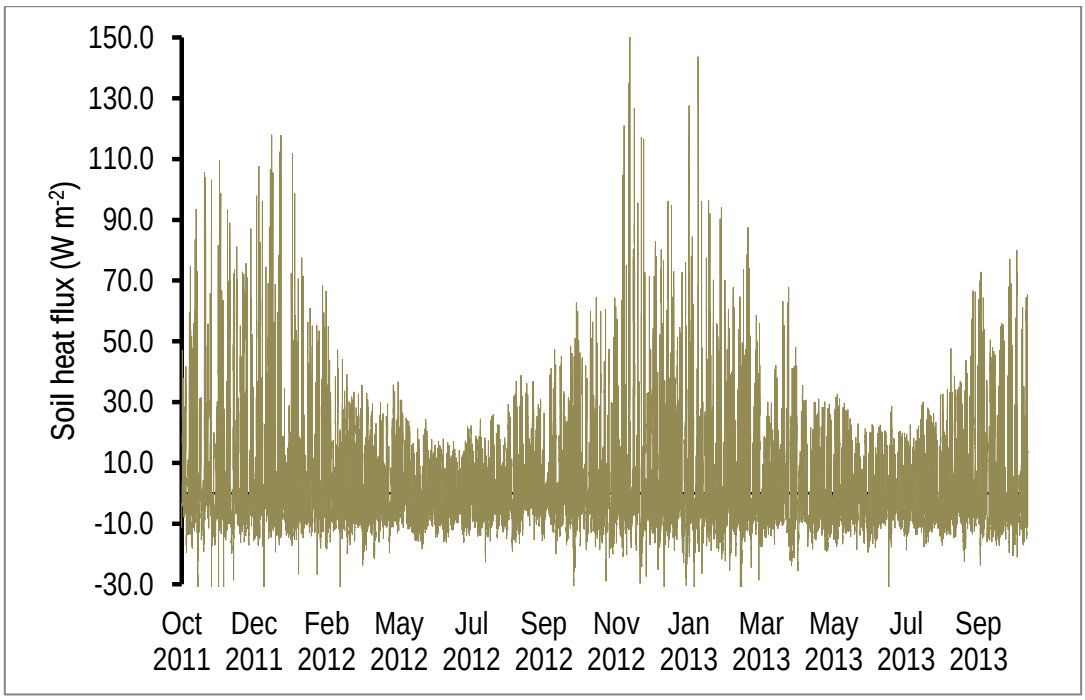

Figure 4.22: Soil heat flux (30 minute averages) at the Wattle stand at Two Streams from October 2011 to November 2013.

The energy balance was dominated by latent energy in summer (Figure 4.23) and winter (Figure 4.24). However, during summer the Bowen ratio was approximately 0.5 and in winter 0.4 indicating an increase in the dominance of latent heat energy over sensible heat energy in winter.

The surface renewal was calibrated using an "Sx" style Applied Technologies, Inc. sonic anemometer (Longmont, Colorado, USA) during intermittent periods totalling approximately nine months of measurement. An α weighting factor of was derived for both upper (21 m and later 22 m above the ground) and lower (19 m and later 20 m above the ground) thermocouples from a comparison of the 30 min sonic sensible heat flux with that estimated from the surface renewal system (Figure 4.25). There was almost no change in the alpha calibration when the height of the thermocouples was changed.

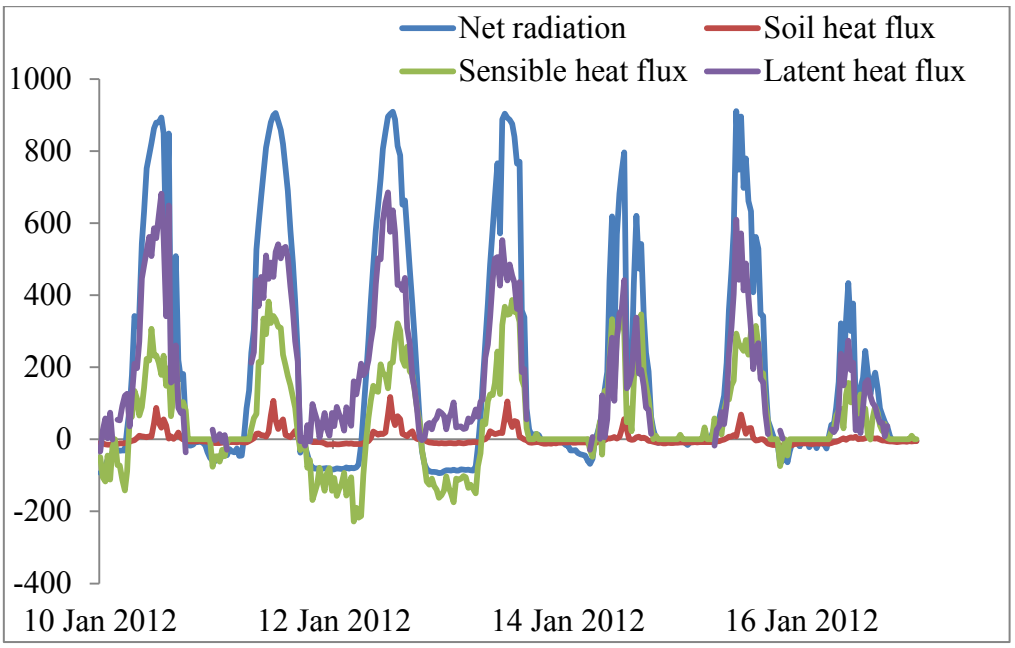

Figure 4.23: A week of energy balance data during summer (January 2012) at the lattice mast site with sensible heat flux measured using a sonic anemometer.

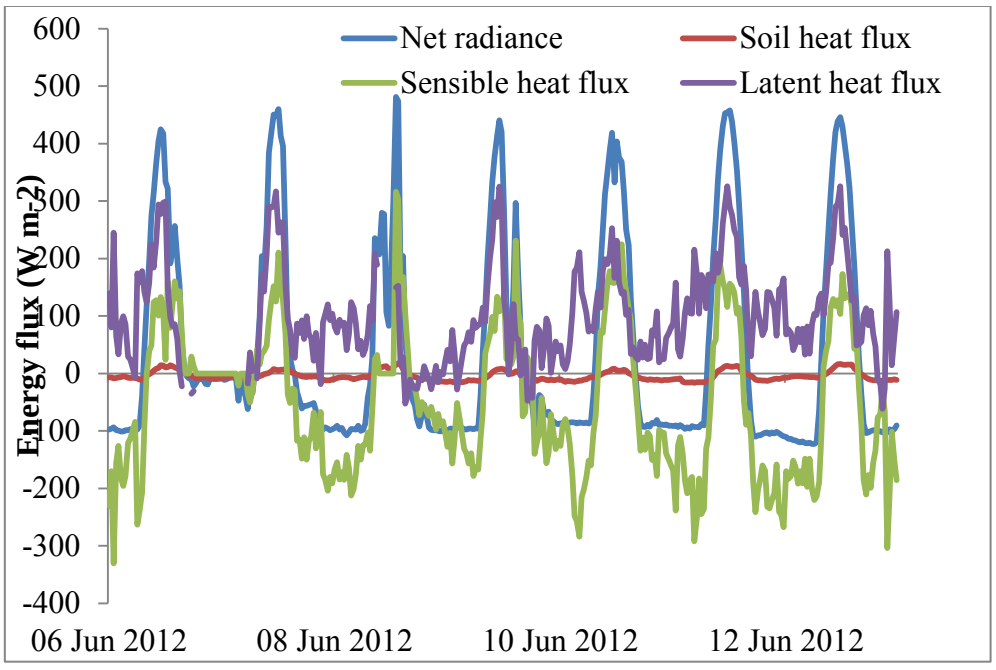

Figure 4.24: A week of energy balance data during winter (July 2012) at the lattice mast site with sensible heat flux measured using a sonic anemometer.

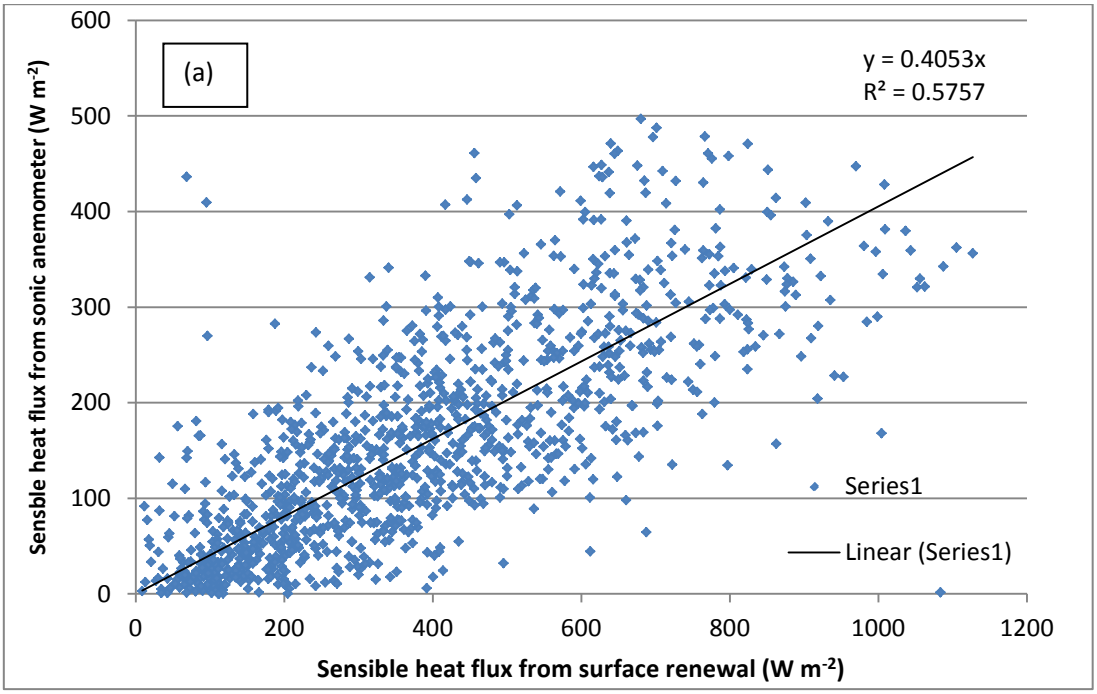
(a)
y = 0.4053x
R² = 0.5757
Series1
Linear (Series1)
Sensble heat flux from sonic anemometer (W m-2)
Sensible heat flux from surface renewal (W m-2)
0
100
200
300
400
500
600
0
200
400
600
800
1000
1200

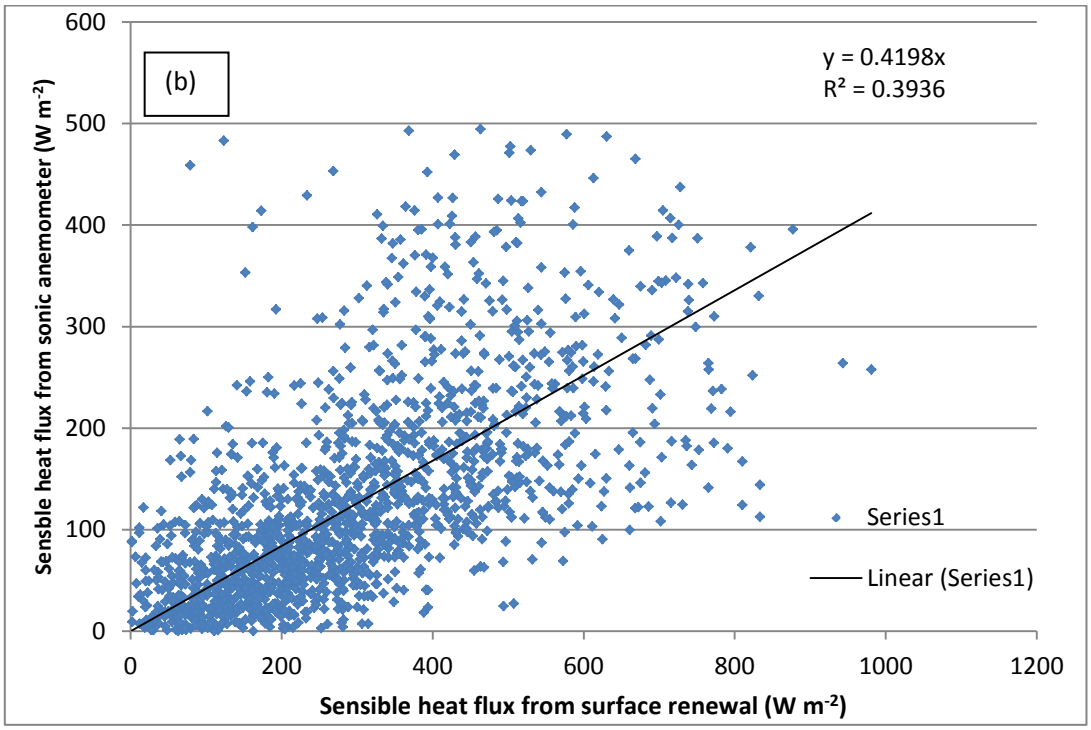
(b)
y = 0.4198x
R² = 0.3936
Series1
Linear (Series1)
Sensble heat flux from sonic anemometer (W m-2)
Sensible heat flux from surface renewal (W m-2)
0
100
200
300
400
500
600
0
200
400
600
800
1000
1200

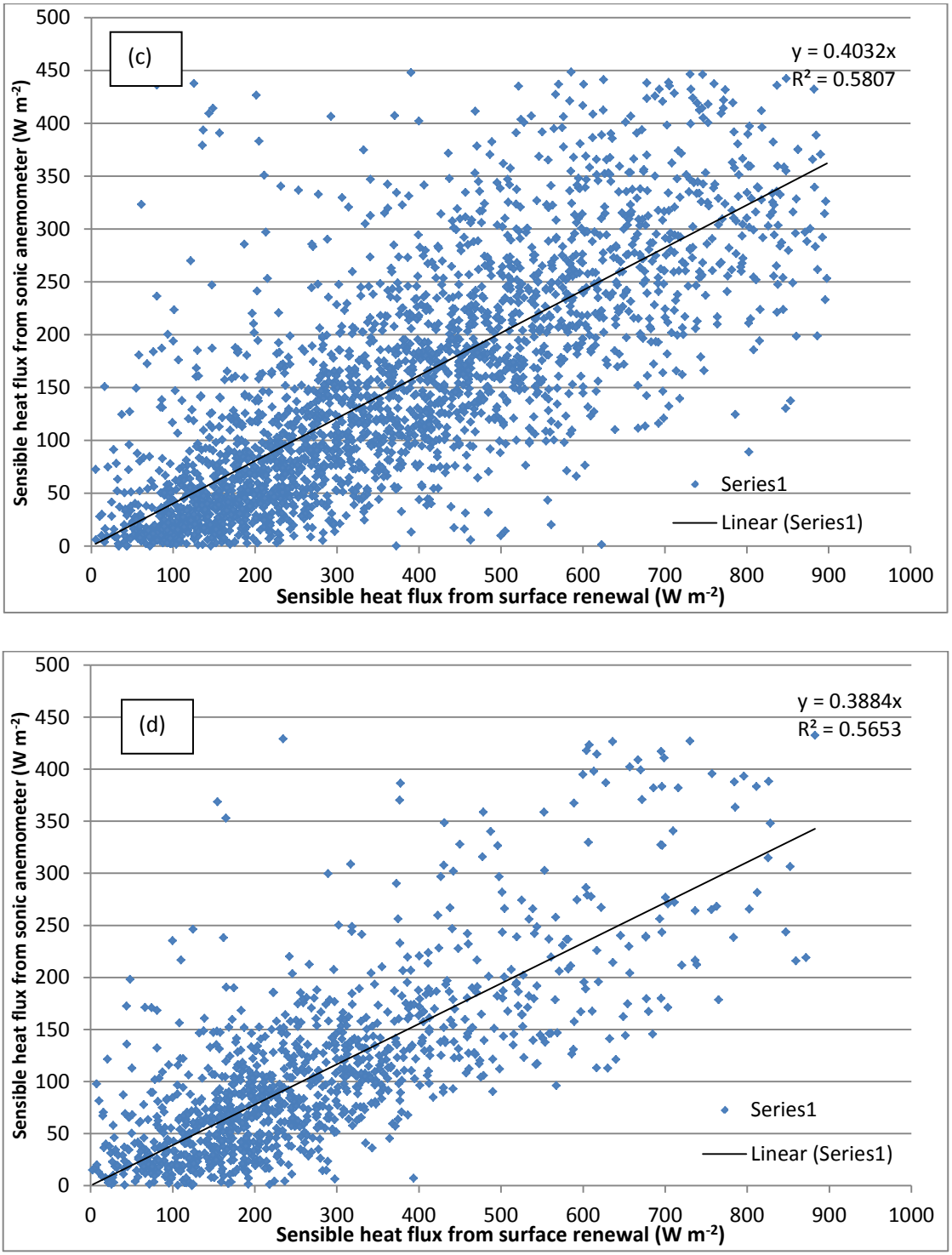

Figure 4.25: A weighting factor (α) for (a) Tc1 at 19 m (α =0.41), (b) Tc1 at 20 m (α =0.42), (c) Tc2 at 21 m (α =0.40) and (d) Tc2 at 22 m (α =0.39) were determined at 30 min intervals.

Total evaporation measurements from the *A. mearnsii* stand at the lattice mast were initiated on 27 October 2011 and are ongoing (Figure 4.26). The daily *ET* ranged from less than 1 mm on cool cloudy days to a maximum of 8.1 mm on clear days in summer. On these cool days the radiant flux density was below 4 mm of energy equivalent units (1 mm *ET* = 2.43 MJ). On clear summer days the *ET* was generally greater than 5 mm day^{-1} with a concomitant increase in the energy equivalent radiation to 9.0 mm day^{-1}.

Previous results from this stand of trees, measured with a large aperture scintillometer (Figure 4.27), indicated peak rates of 6.5 mm, 7.5 mm and 8.5 mm in the summer periods of 2006/2007, 2007/2008 and 2008/2009 respectively as the trees grew. The most recent set of data indicated that the upward trend in *ET* with tree size has halted. In 2011/2012 and 2012/2013 the peak rates of daily ET in the summer periods were 7.7 mm and 6.6 mm respectively. This highlights the importance of long-term monitoring for understanding the impacts of long crop rotations.

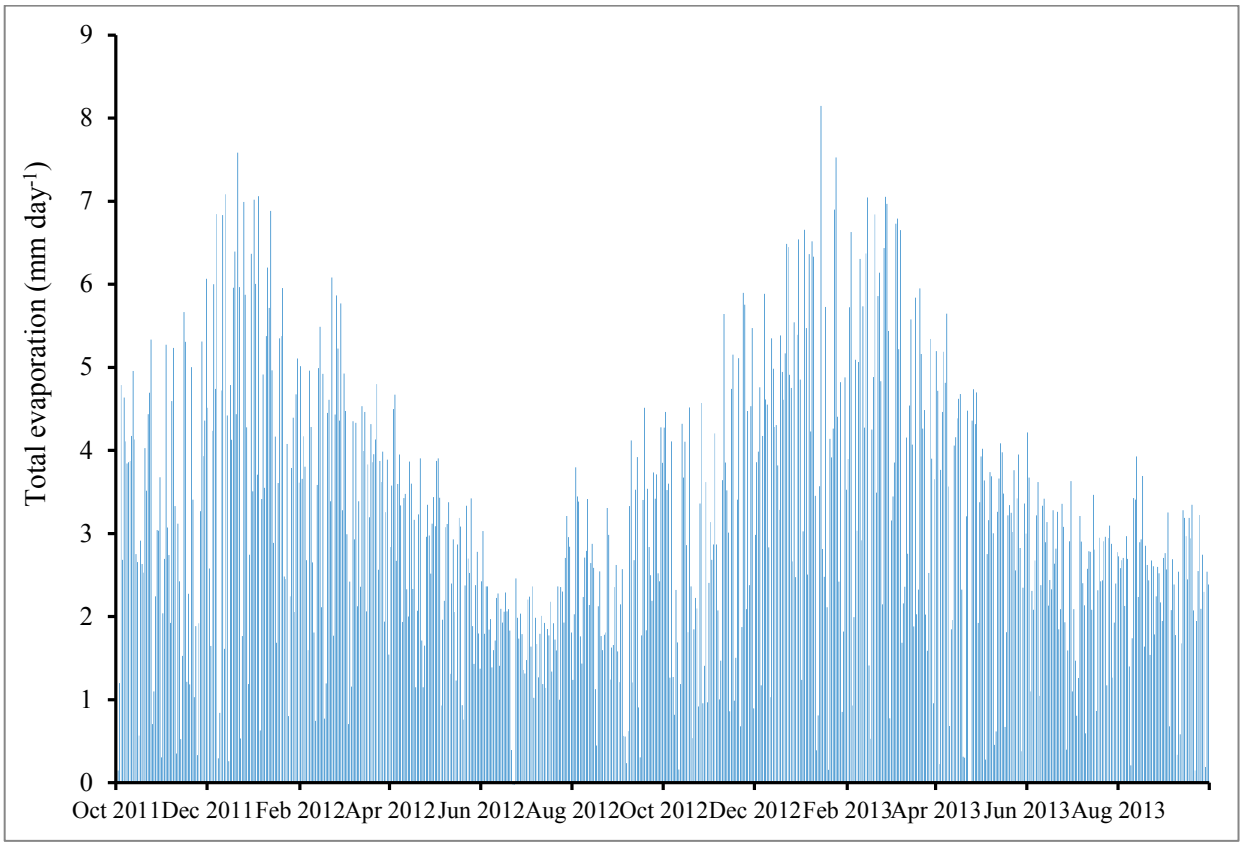

Figure 4.26: Daily total evaporation above the Wattle stand at Two Streams from October 2011 to September 2013 measured using eddy covariance and surface renewal to derive the sensible heat flux.

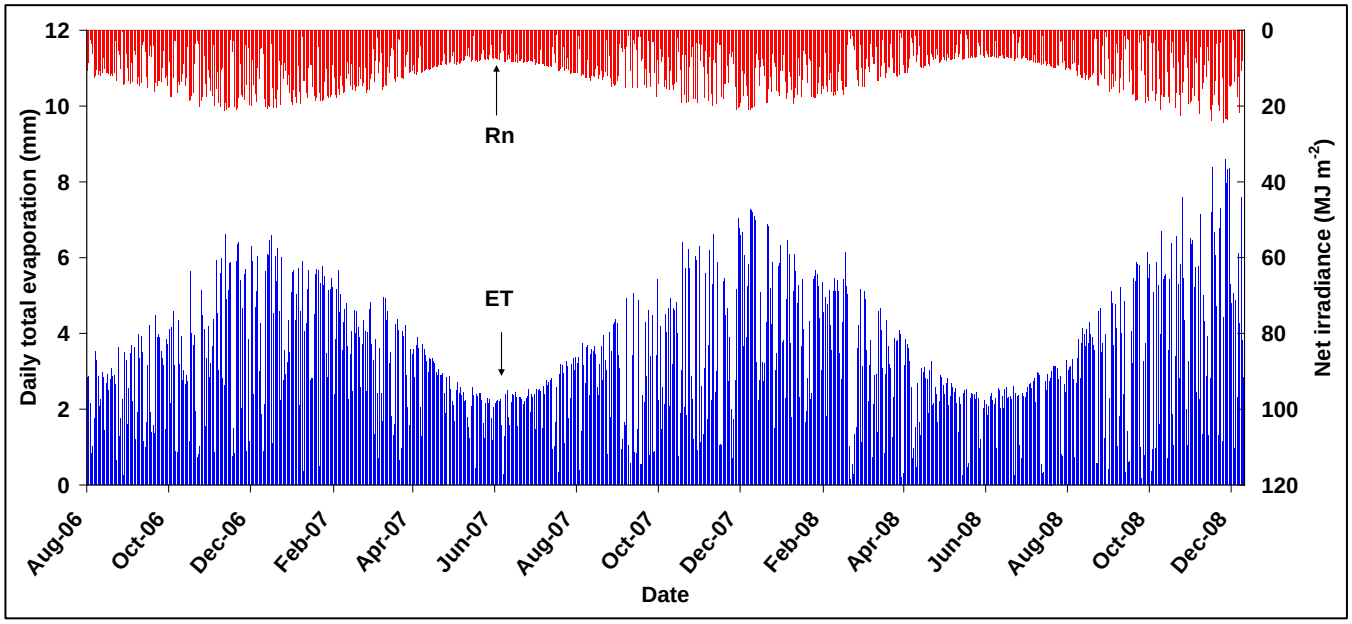

Figure 4.27: Daily total evaporation above the Wattle stand at Two Streams from planting in August 2006 to December 2008.

4.3.2 Sapflow and Transpiration

4.3.2.1 South Facing slope

A lower, south facing sapflow site, near the riparian area, was initially used to evaluate three different sapflow techniques to identify the most suitable method to compare tree water-use in different slope positions. This lower site was instrumented in August 2011. Subsequently, once the heat ratio method was identified as the most suitable technique, an up-slope site was instrumented near the lattice mast on the south-facing slope in January 2012. The northern aspect was later instrumented in early 2013 in a similar manner to include both riparian and upslope areas.

The daily sapflow of the south-facing sites was seasonal with the lowest sapflows in winter and the higher sapflows in summer (Figures 4.28 and 4.29). Sapflow started to increase in September 2012 at both the upper and lower sites, reaching peak water-use values of 20 L day^{-1} and 40 L day^{-1} at the upper and lower sites respectively.

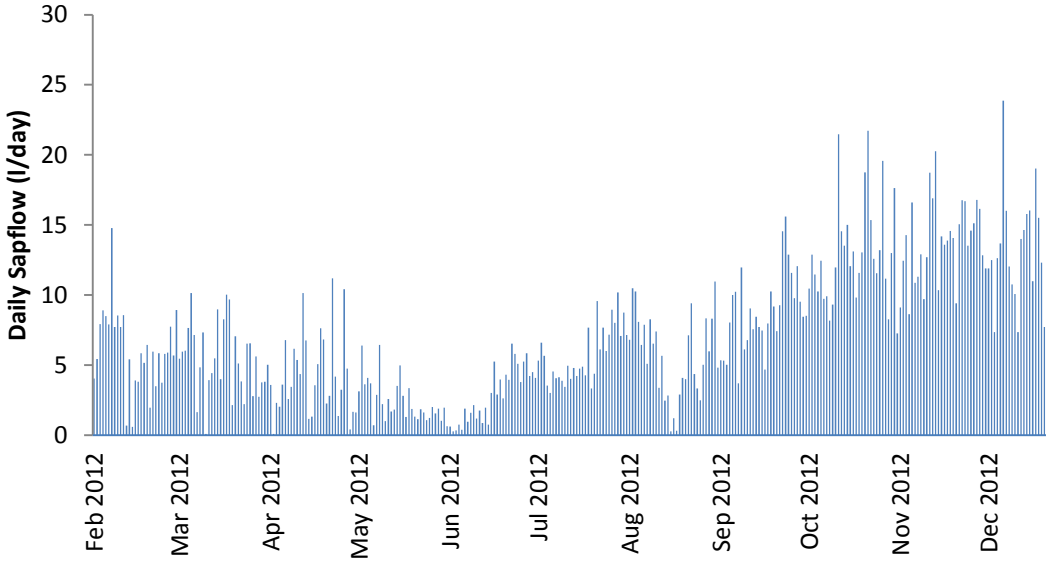

Figure 4.28: An example of daily sapflow from an *Acacia mearnsii* tree at the upper site from February 2012 to Jan 2013.

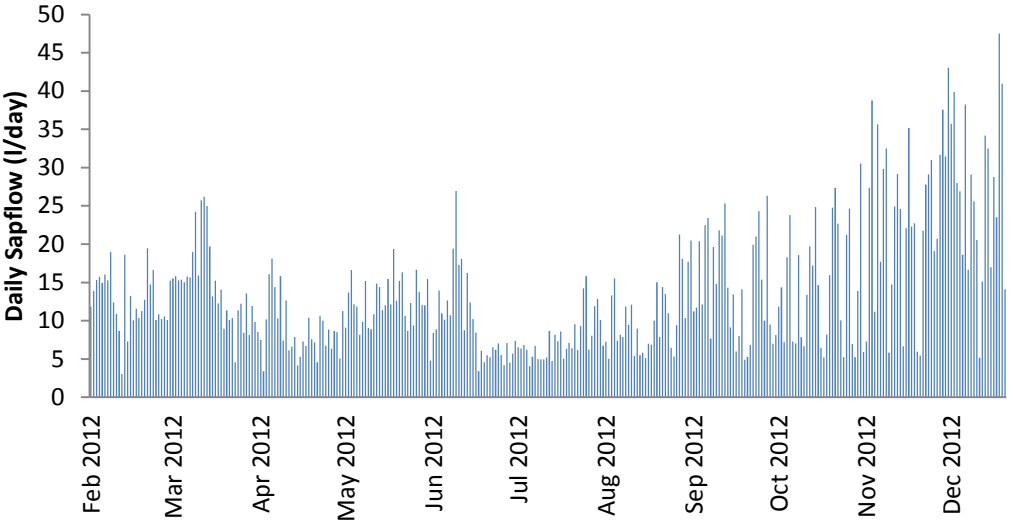

Figure 4.29: An example of daily sapflow from an *Acacia mearnsii* tree at the lower site from February 2012 to Jan 2013 after the sapwood area has been scaled-up for comparison with the larger trees of the upper site.

The diurnal trends in the hourly sap flow in winter showed typical bell-shaped curves associated with clear winter skies, with the sapflow closely following the net radiation (Figure 4.30). Maximum midday values were low and generally between 1.0 and 1.4 l hr^{-1} while the net radiation varied between only 400 and 500 W m^{-2}. During summer net radiation on clear days peaked at over 900 W m^{-2} and corresponded with sap flow maxima of approximately 5 l hr^{-1} (Figure 4.31). The impact of cloudy and rainy conditions on reducing both the net radiation and hourly sap flow was evident on the 1st (rainy); the 2nd and 5th of January (cloudy conditions) when the hourly sap flow was < 2l hr^{-1} (Figure 4.31). These data indicated that sap flow in the *A. mearnsii* trees at Two Streams was principally governed by radiation.

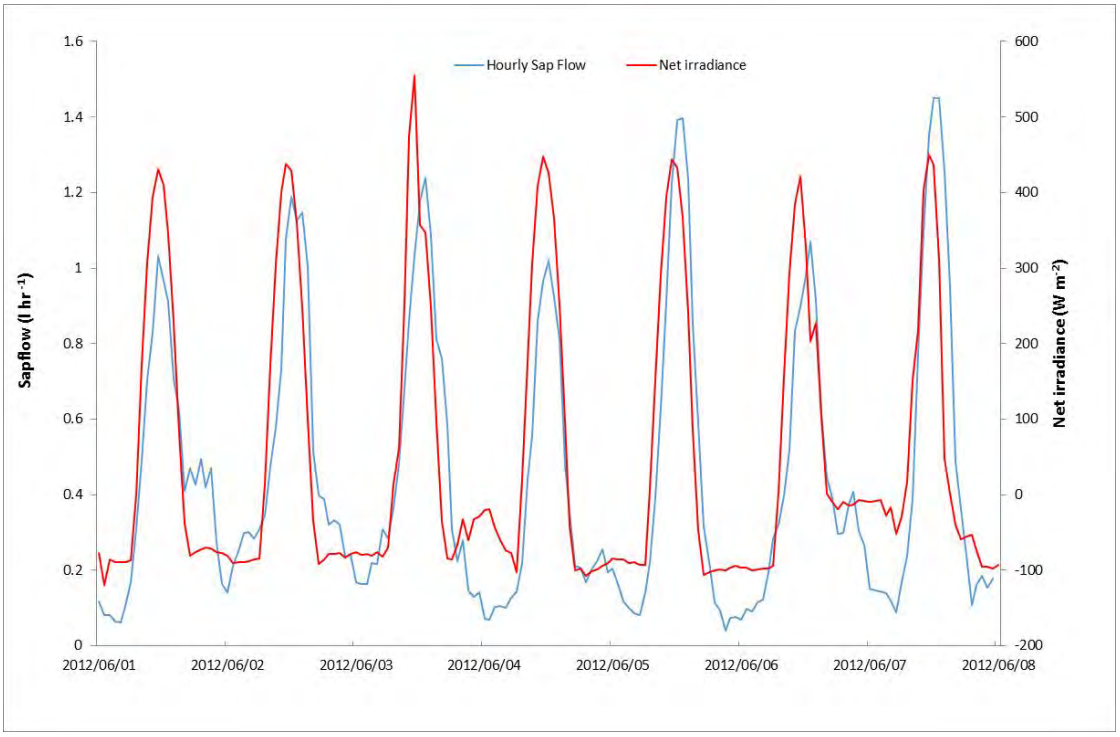

Figure 4.30: Diurnal trends of the hourly sapflow and net irradiance at the upper site in winter for a period of one week In June 2012.

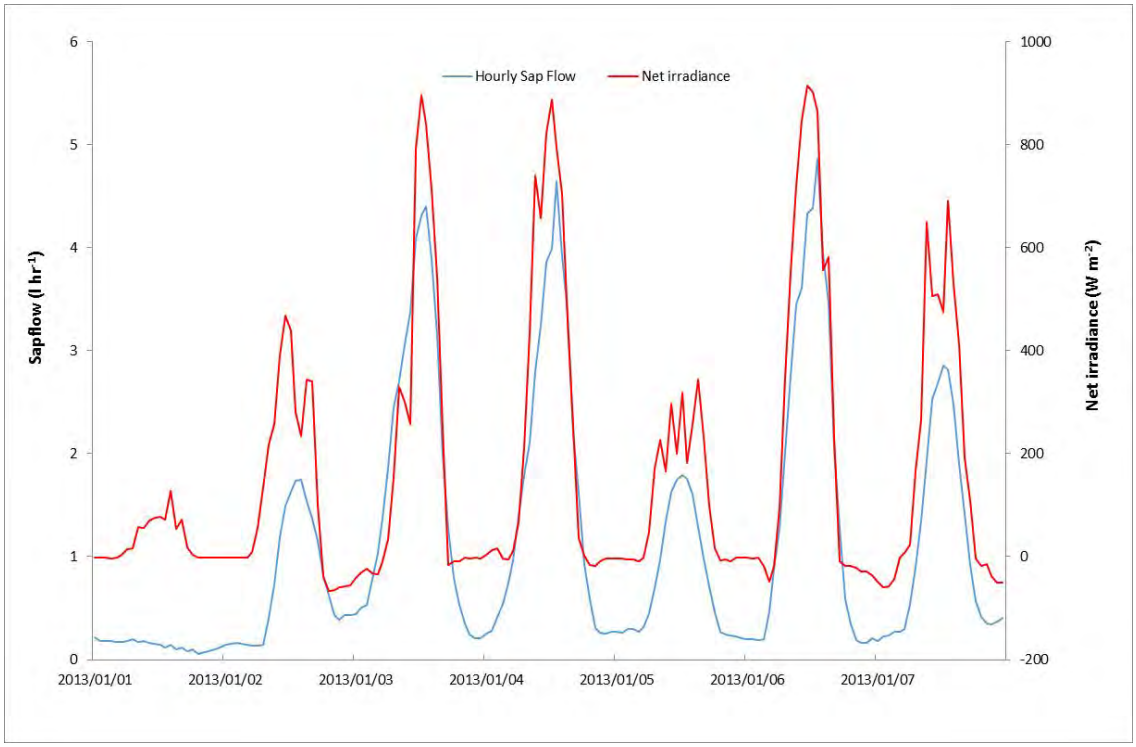

Figure 4.31: Diurnal trends of the hourly sapflow and net irradiance at the upper site in summer for a period of one week in January 2013.

The accumulated transpiration (mm) of the upper and lower trees over the 22 month period from 22 February 2012 to 9 December 2013 showed that the trees on the lower slope were transpiring at higher rates than trees on the upper slope. Using the hydrological year from 1 October 2012 to 30 September 2013 for comparative purposes, the total transpiration at the upper and lower sites was 1076 and 1171 mm respectively. This represents an annual difference of 95 mm (9%) (Figure 4.32). Since the trees were on the same transect with similar slope angles, it appears that trees in the riparian fringe had better access to soil water and the ground water table associated with the low slope hillslope position. Accelerated water-use during summer and reduced water-use during winter was clear from the s-shaped curves of the accumulated daily transpiration (Figure 4.32). There was a large difference in the accumulated water-use between the south-facing and upper-slopes with the latter trees using 9% less water than the lower-slope trees.

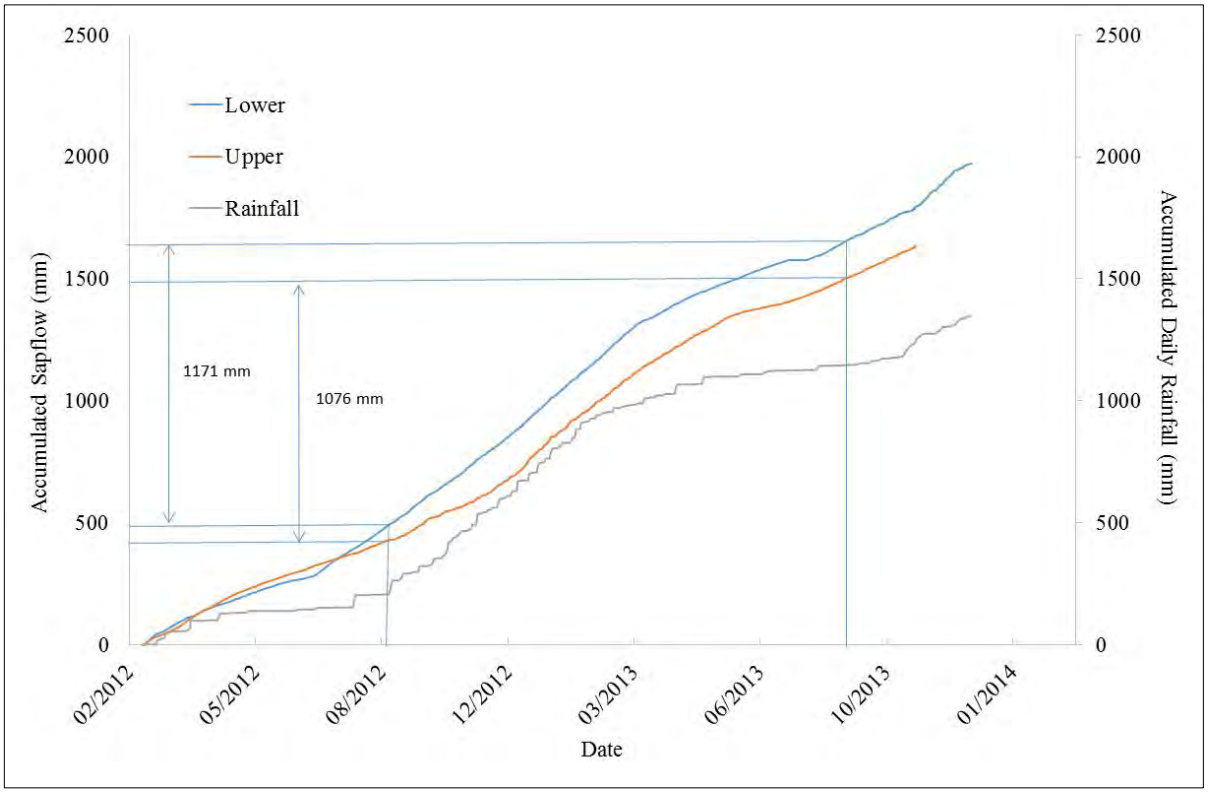

Figure 4.32: A comparison of the accumulated sapflows at the upper and lower South facing slope with the accumulated rainfall from 22 February 2012 to 9 December 2013.

4.3.2.2 North-facing slope

A comparison of the upper and lower slope sites on the North facing aspect over the 9 month period from 5 April 2013 to 9 December 2013 showed that during the winter period there were little differences between sites (Figure 4.33). However, as the summer progressed, the lower riparian fringe site (1097 mm) increased relative to the upper site (941 mm), a difference of 156 mm in only 110 days of measurement (Figure 4.33). Therefore, despite the radiation differences between the north and south aspects, the riparian fringe vegetation clearly had advantages to plants growing on the mid-slope positions.

The tree transpiration was much higher on the high radiation (hot) North-facing slope than on the cooler south aspect. Over the nine months of measurement where corresponding data were available, the accumulated North-facing transpiration at the upper site was 941 mm and at the lower site, 1097 mm. Over the same period at the south facing slope the transpiration was 463 mm and 617 mm at the upper and lower slopes respectively.

Over the 2012-2013 hydrological year, a comparison of the ET_{ec} and tree transpiration at the upper south site where the eddy covariance mast was situated, revealed differences of 1157 mm

and 1076 mm respectively. The 81 mm increase in the total evaporation compared to the tree transpiration is attributed to soil and litter evaporation not measured by the heat pulse methodology. Soil and litter evaporation therefore represented about 8% of the total evaporation in the wattle plantation.

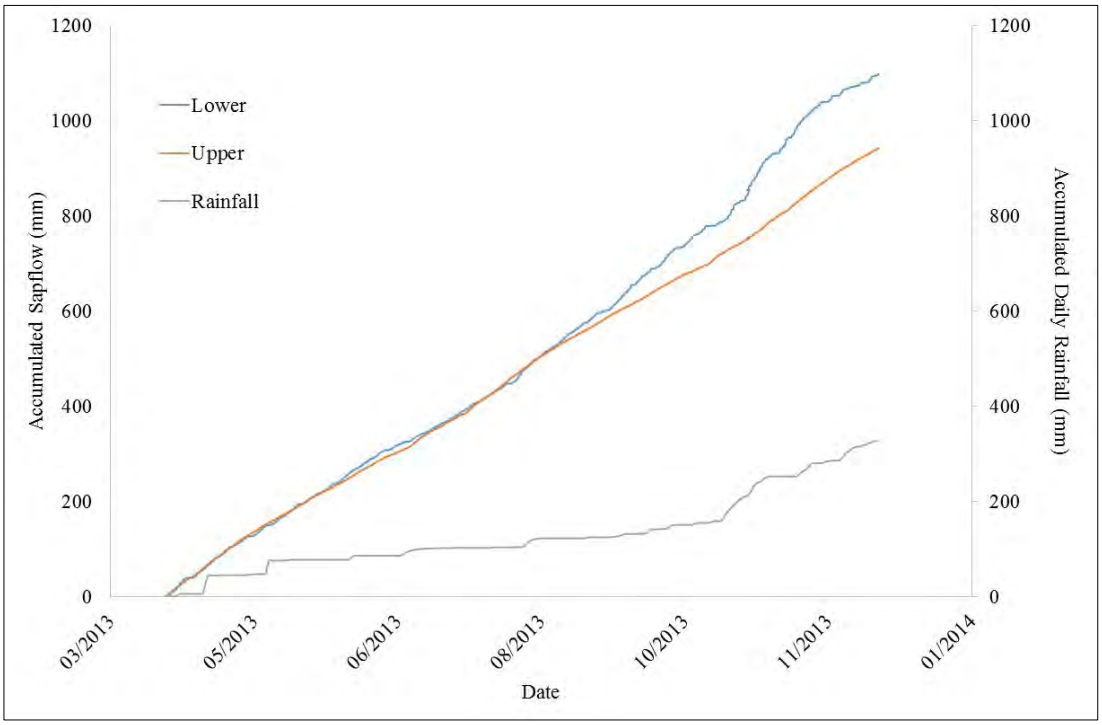

Figure 4.33: A comparison of the accumulated transpiration at the upper and lower North-facing slope with the accumulated rainfall from 5 April 2013 to 9 December 2013 (nine months).

4.4 Streamflow Gauging

Daily (Figure 4.34) and monthly (Figure 4.35) streamflow totals from January 2000 to December 2013, together with corresponding rainfall data clearly indicate the annual rainfall and streamflow patterns. As expected, the summer rainfall and streamflow were higher in the summer rainy season than the dry winter period. Despite the low rainfall in winter the streamflow has continued for 13 subsequent dry seasons, including droughts in 2003 and 2007, as a result of the riparian clearing in January 2000. Prior to the clearing, the stream was dry with no flow. The flows are calculated in terms of an equivalent depth of water over the entire catchment, enabling a comparison with rainfall. Note that the streamflow totals were plotted on a log scale in order to accentuate the lower flows.

A runoff:rainfall relationship of 0.03, 0.04, 0.01 and 0.02 for 2001 to 2004 was found for the afforested catchment with the riparian areas cleared (Figure 4.36). The complete clearing of the catchment took place in 2004 and corresponded to a significant increase in streamflow in

subsequent years. New runoff:rainfall relationships were established of 0.08, 0.07, 0.08 and 0.08 from 2005 to 2008.

The replanting of the catchment at the end of 2006 is evident from the runoff:rainfall relationship since 2009 which decreased to 0.06. It further decreased to 0.04 and 0.02 in 2010 and 2011 respectively with a slight increase to 0.03 in 2012 and an additional increase to 0.05 in 2013. Rainfall was consistently in the region of 850 mm per year over these three years, so the relative increase in streamflow compared to rainfall over this period is attributed to the mature trees requiring less water.

Peak flows of 10 mm were recorded in January 2005 which coincided with the clear-felling of the catchment. Due to the exposed soil surface and impact of heavy machinery on the soil structure, vast quantities of topsoil were washed into the river and weir at this time. Based on the damage caused during these events, it is strongly recommended that tree harvesting in wet seasons in areas susceptible to erosion be evaluated with further research.

The clearing of the riparian area of trees in 2000 and clear felling of the catchment in 2004 impacted the relationship between accumulated streamflow and accumulated rainfall (Figure 4.37). An initial calibration period was established from January to April 2000 using a breakpoint analysis which has been documented in Everson *et al.* (2007) and shown to be statistically significant using an analysis of variance with a goodness of fit (R^2) of 0.995. Based on this relationship, the impact of clearing the riparian vegetation followed by clear-felling the catchment in 2004, resulted in a total gain in streamflow of 259 mm by Jan 2013.

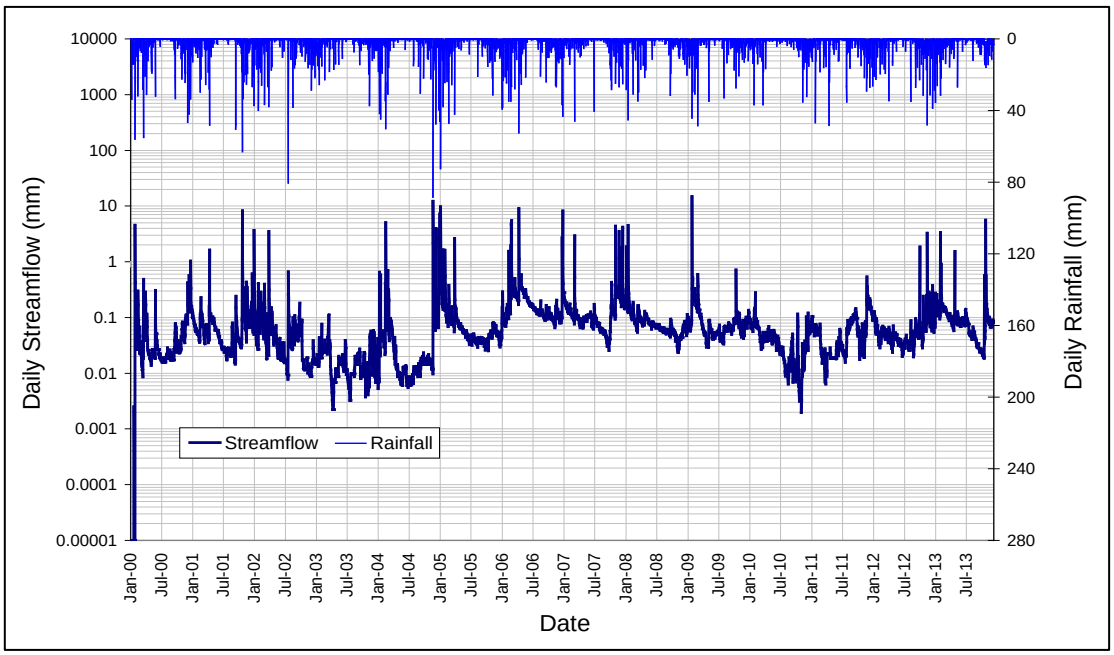

Figure 4.34: Daily streamflow totals (mm) with corresponding daily rainfall data (mm) for the treated catchment from January 2000 to December 2013.

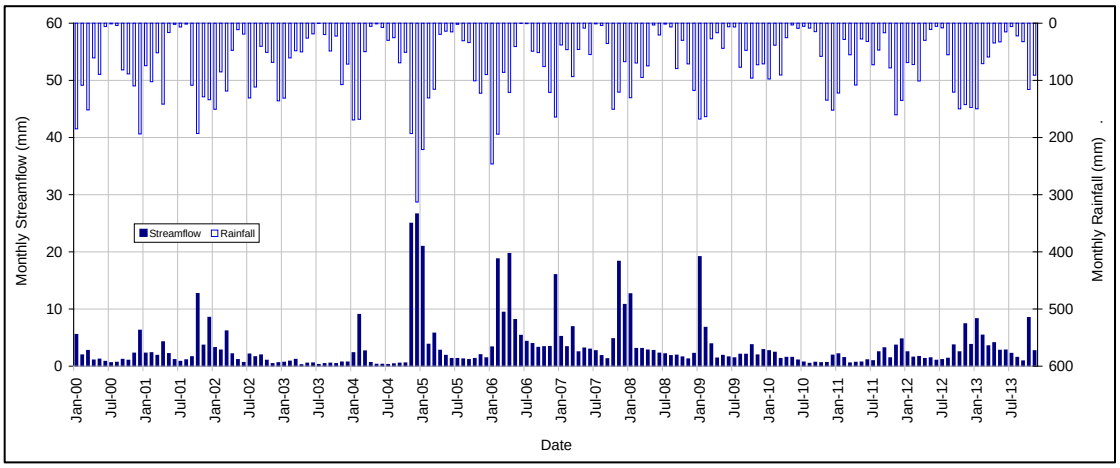

Figure 4.35: Monthly streamflow totals (mm) with corresponding monthly rainfall data (mm) for the treated catchment from January 2000 to November 2013.

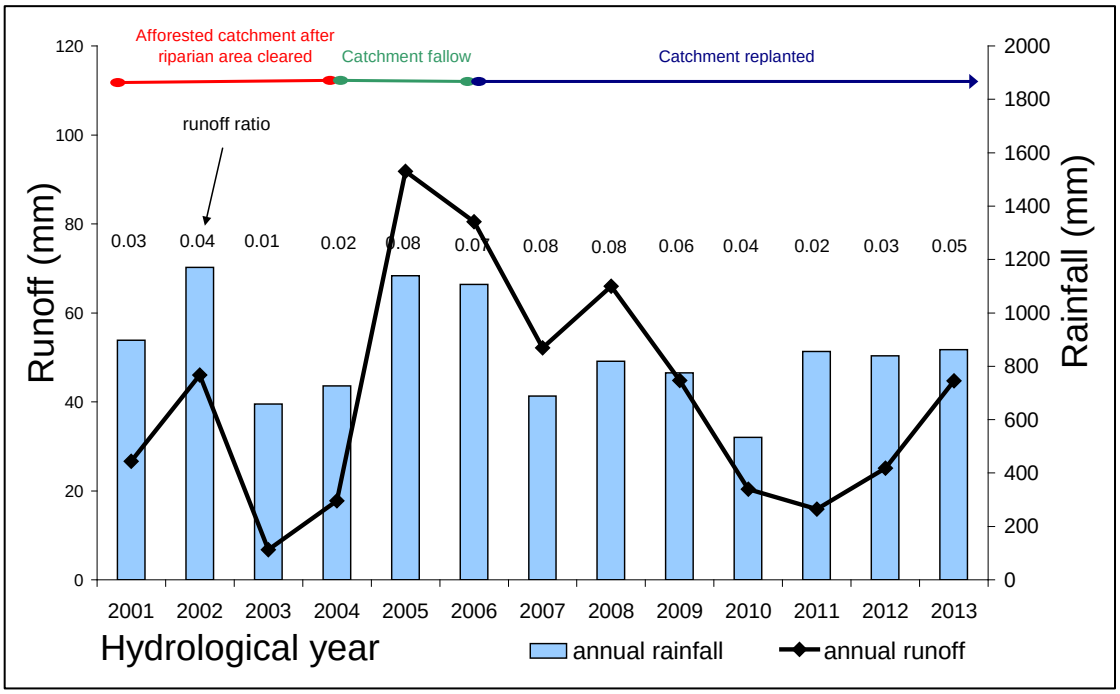

Figure 4.36: The annual rainfall and runoff measured in the Two Streams catchment also showing in text the ratio of annual runoff to annual rainfall with the different land-use in the catchment.

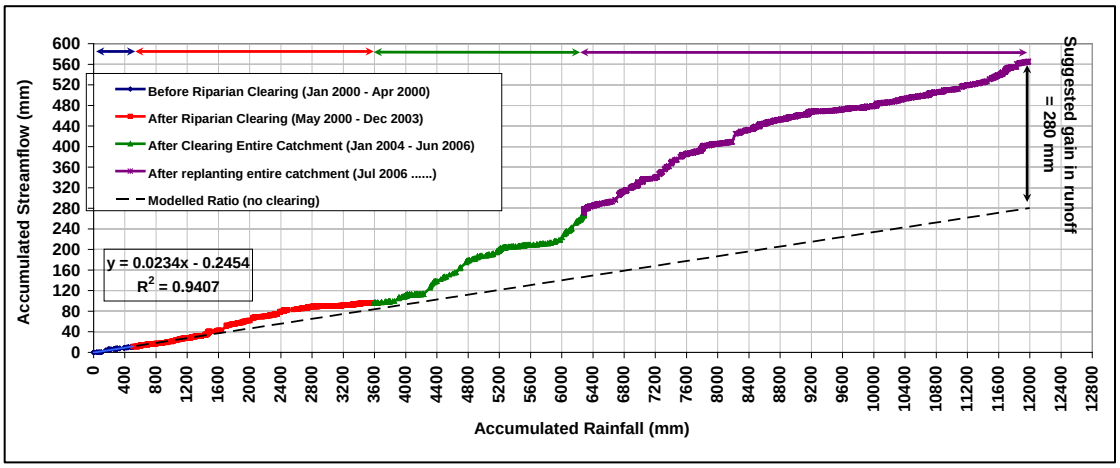

Figure 4.37: The relationship between accumulated rainfall and streamflow for the Two Streams weir for the period November 1999 to January 2013.

4.5 Ground Water

4.5.1 Water table depth

The water table levels were measured manually at monthly intervals until August 2011 (Figure 4.38). Ott loggers, installed in August 2011, measured water levels at hourly intervals in the central, northern and southern boreholes (Figure 4.39). Despite the relatively close proximity of the boreholes to each (Northern and Western boreholes are furthest apart at 500 m) they responded differently. The ground water level measured in the western borehole changed the least. It is located on the edge of the wattle stand, bordered to the west by sugarcane. It shows minor recharge (0.5 m) from the end of November 2011 to July 2012 when the sensor failed. The northern borehole is on the northern edge of the wattle stand and showed increased recharge (6.0 m) from the end of November 2011 to May 2012. The central borehole recharge (8.0 m) was, however, delayed until February 2012 and continued until May 2012. During the period between June to August 2012 the water level in the central borehole dropped 7 m from 19 m below the surface to 26 m below the surface.

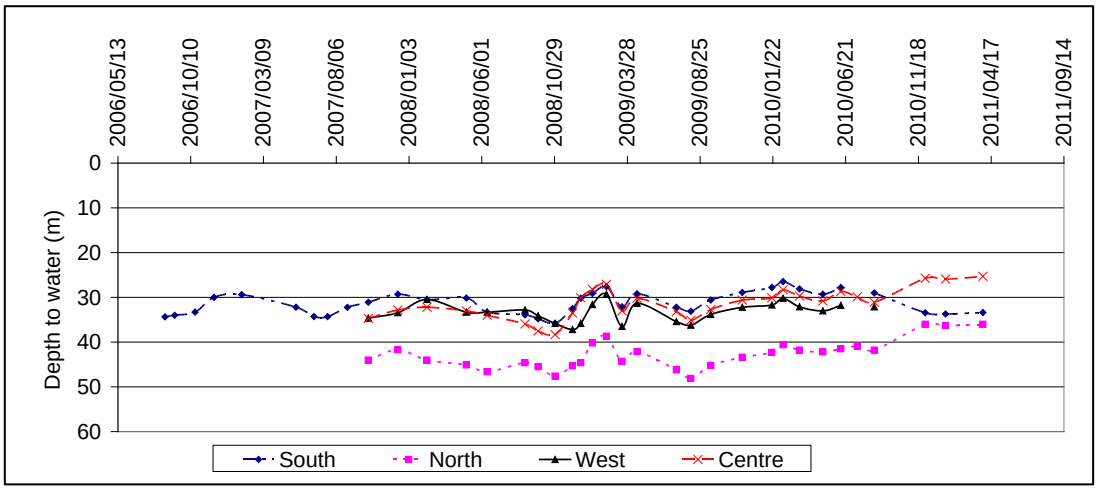

Figure 4.38: Water levels measured manually in boreholes in and around the Wattle stand at Two Streams from May 2006 to March 2011.

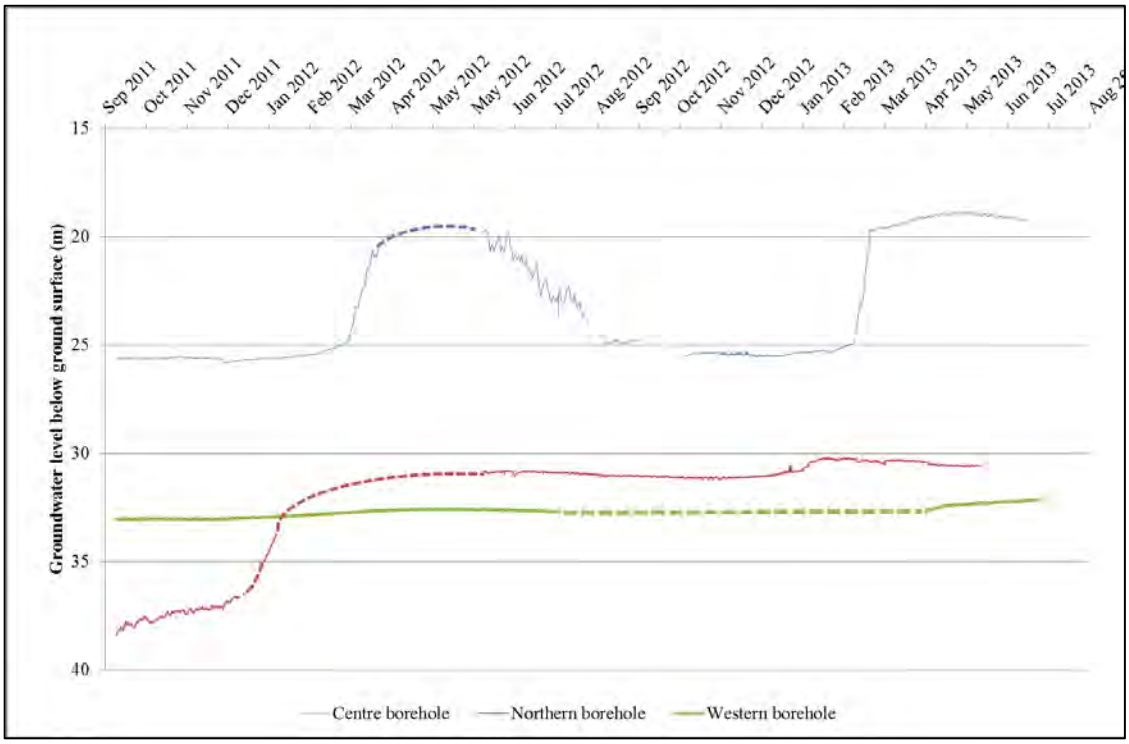

Figure 4.39: Hourly water levels recorded in boreholes in and around the Wattle stand at Two Streams from September 2011 to July 2013.

4.5.2 Groundwater electrical conductivity

In general, the electrical conductivity increased with water level depth (Figures 3 and 4). The EC ranged between 550-650 mS/m for the centre borehole (2STBH1) and 250-350 mS/m for the north borehole (2STBH3) (Figure 4.40). The similar pattern is observed in the Upper South borehole (2STBH4) and Lower South borehole (2STBH5), which ranged between 210 to 270 mS/m and 300 to 560 mS/m respectively (Figure 4.41).

The evidence from the conductivity profiles is that the EC increases with contact with the granite formation and increases with depth into the basement granite. This suggests that since the groundwater movement is very slow, time allows the salts in the granite composition (potassium, etc.) to ionise, increasing the electrical conductivity.

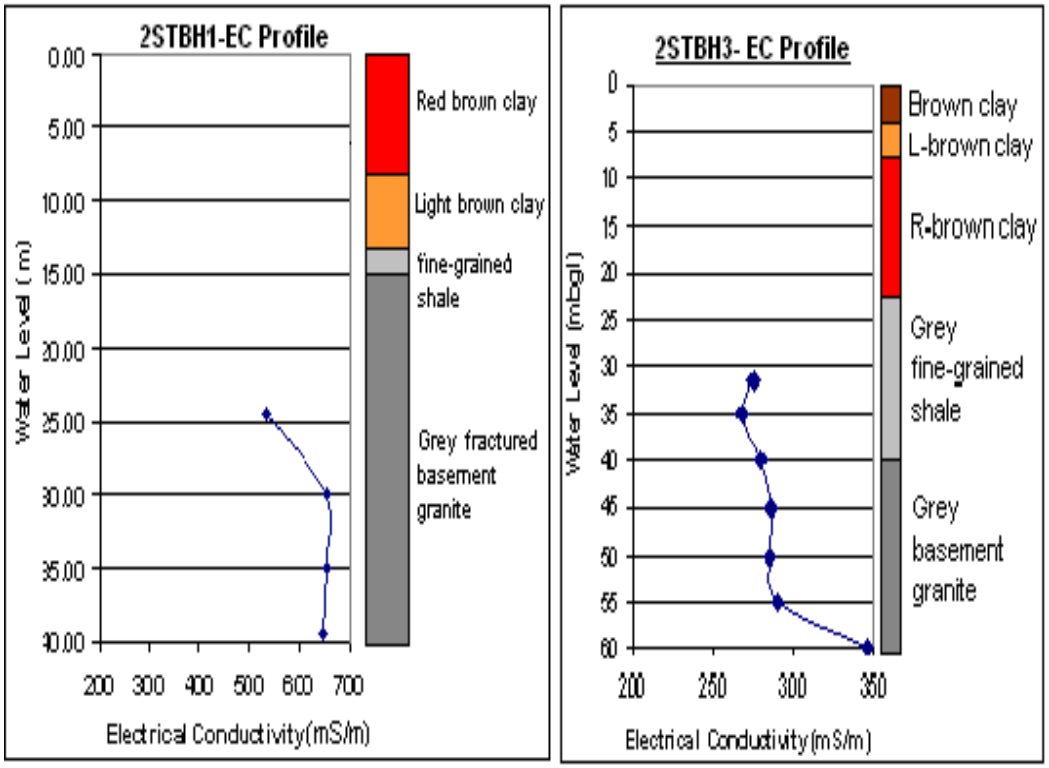

Figure 4.40: Electrical conductivity profiling for boreholes 2STBH1 and 2STBH3.

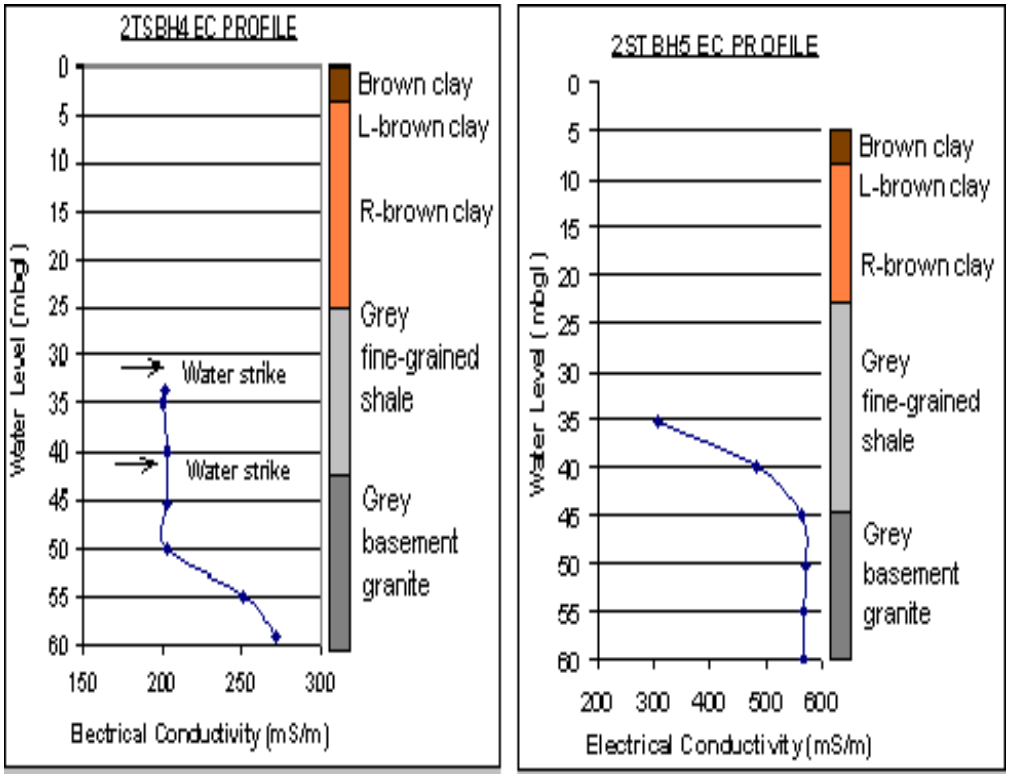

Figure 4.41: Electrical conductivity profiling for boreholes 2STBH4 (Upper South) and 2STBH5 (Lower South).

4.5.3 Groundwater temperature

The temperature in all four borehole profiles (Figure 4.42) was fairly constant ranging between 17.9 and 18.5, except for one spike of 19.9°C in borehole 1 at 35 m below ground level (mbgl). This is because the seasonal fluctuations in groundwater temperature generally occur at depths of 10 to 25 m and the water levels at the Two Streams boreholes are between 20 and 40 mbgl.

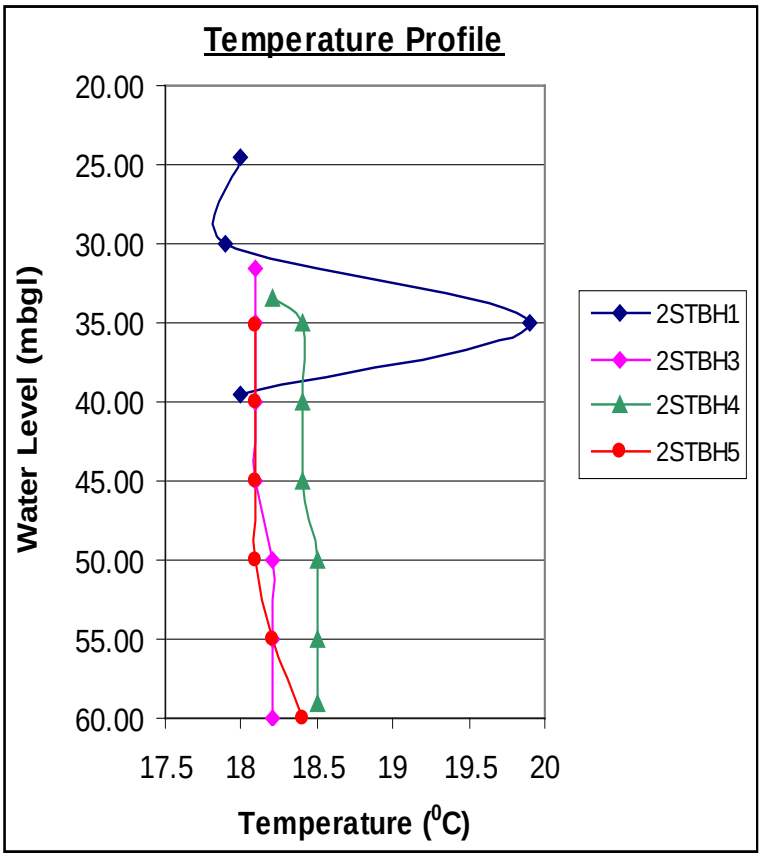

Figure 4.42: Temperature profile for groundwater at the Two-Streams Catchment

4.5.4 Total Alkalinity, Bicarbonate and pH

The bicarbonate (HCO_3) concentration is high in both surface and groundwater, ranging between 400 and 500 mg/l (Figure 4.43). The hydroxide (OH^-) disappears below pH 10.3, carbonate below 8.3 and bicarbonate below 4.3. (McDonald, 2006). The pH of all water samples ranged between 6.2 and 8.2 indicating that the majority of the alkalinity in water is due to the presence of bicarbonate, as the carbon ion is converted to bicarbonate at pH below 8.3.

The total alkalinity of water at Two-streams is low, ranging between 65 and 82 mg/l for both surface and groundwater as shown in Figure 4.43. The low alkalinity concentrations are predominantly associated with water flowing through the felsic igneous rock (granite). The magmatic and volcanic rocks are relatively insignificant sources of carbonate (McDonald, 2006). The primary source of alkalinity in water is carbonate containing rocks, which can come from natural erosion of carbonate containing limestone, such as calcium carbonate or dolomite and runoff from agricultural land where lime has been applied.

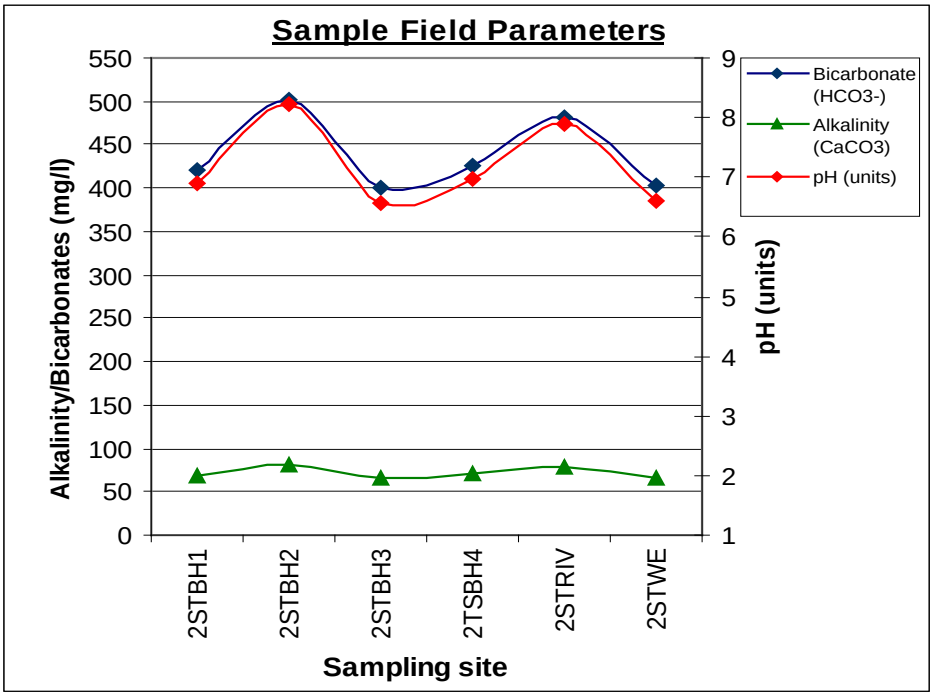

Figure 4.43: Graphical representation showing bicarbonate, total alkalinity and pH, of water samples taken at Two-Streams catchment.

There is no health standard set for alkalinity in the South African Water Quality Guidelines (DWAF, 1996). The pH value is used to determine the alkalinity or acidity of water. The average pH for all the water samples is 7.2 suggesting that the water at Two-streams is slightly alkaline and a lot of acid will be required to drop the pH to unacceptable limits. Based on the values of pH and alkalinity, it can be concluded that both the stream and the aquifer have the good buffering capacity.

4.5.5 Electrical Conductivity, Total Dissolved Solids and Temperature

The electrical conductivity (EC) for both surface and groundwater samples at Two-streams ranged between 15.8 mS/m and 25.8 mS/m at the standardised temperature of 25^{o}C. The spike of 51.8 mS/m in electrical conductivity is observed in borehole 2STBH1 (Figure 4.44). The Total Dissolved Solids (TDS) ranged between 92 mg/l and 144 mg/l with the spike of 258 mg/l in the same borehole. The temperature ranged between 17^{o}C at the weir and 21.5^{o}C at the stream and artesian borehole at the bottom of the catchment. This is an indication of the interrelationship between surface and groundwater at Two-Streams.

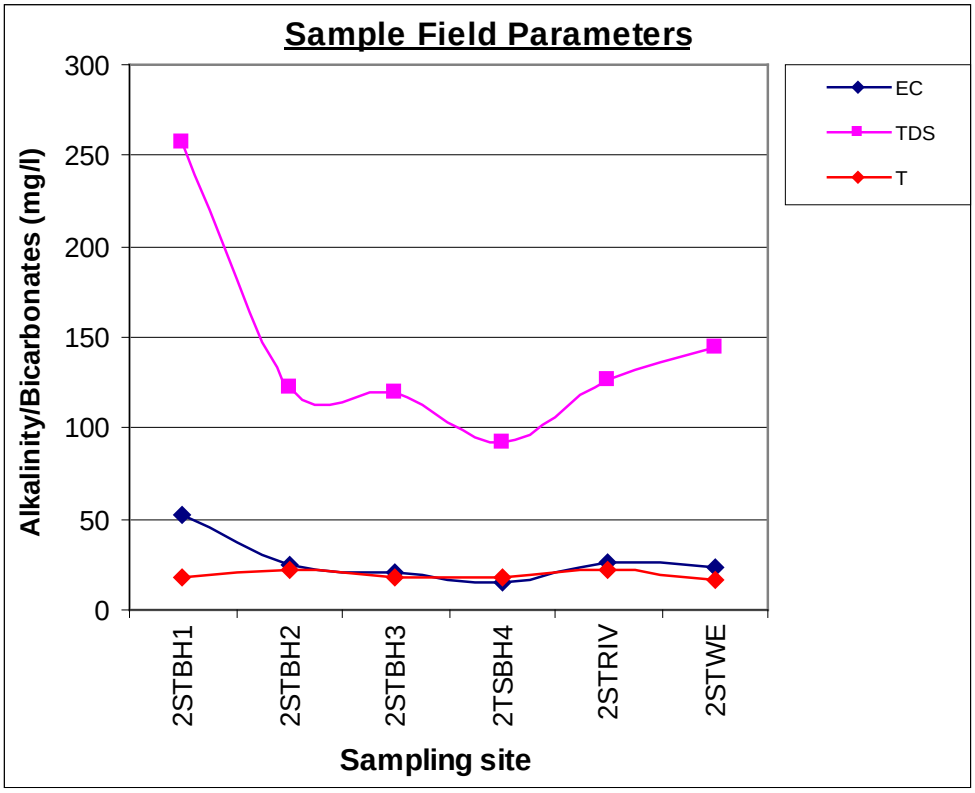

Figure 4.44: Graphical representation showing EC, TDS and temperature of water samples taken at the Two-Streams catchment.

According to the South African Water Quality Guidelines (DWAF, 1996), the electrical conductivity (EC) less than 70 mS/m and total dissolved solids (TDS) concentration less than 450 mg/l is good quality water with no health effects associated with it for all uses. The low EC and TDS concentrations are associated with the granite bedrock.

The water flowing through the granite bedrock tends to have low EC and consequently low TDS, because the granite is composed of more inert materials that do not ionize when washed into the water. On the other hand, streams that run through areas with clay soils tend to have higher conductivity because of the presence of materials that ionize when washed onto the water (APHA. 1992).

4.5.6 Redox Potential (Eh), Oxidation Reduction Potential (ORP) and Dissolved Oxygen (DO)

The Eh values in all the samples ranged between -64.8 mV and 14.5 mV, with only the north corner borehole (2STBH3) having a positive Eh value (14.5 mV) as shown in Figure 4.45 below. The negative Eh values reflect anaerobic (reducing) conditions and unpolluted water (Dimkic et al., 2008), suggesting that electron acceptors present yield less energy in redox reactions than the electron acceptors present at high values.

The dissolved oxygen values ranged between 0.11 mg/l in the centre borehole (2STBH1) to 0.50 mg/l in the South corner borehole (2STBH4). The DO for water samples taken at the stream at the bottom of the catchment is 0.2 mg/l and 0.40 mg/l for water samples taken at weir. It would be expected that DO concentration would be high on surface water samples than groundwater. However, this is not the case suggesting a close interrelationship between surface and groundwater in the catchment.

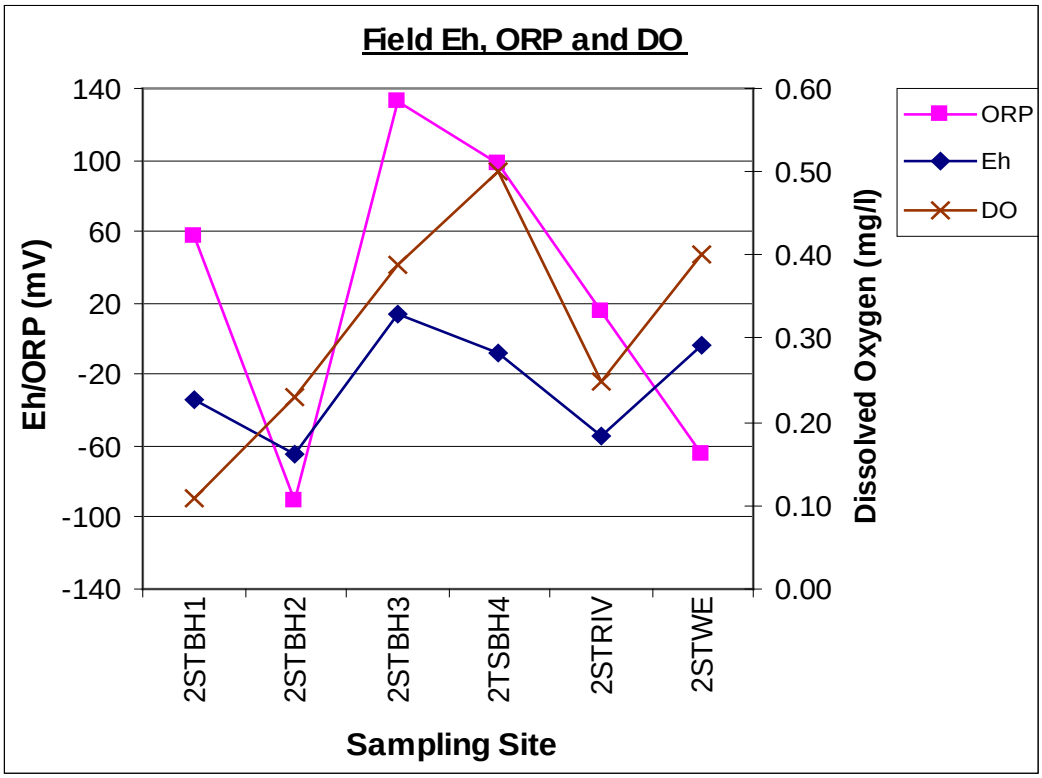

Figure 4.45: Graphical representation showing Eh, ORP and DO of water samples taken at the Two-Streams catchment.

4.6 Soil Water

Two pits (upper site and lower site) with CS616 sensors produced error-free data (despite being difficult to install) to a depth of 2.4 m. At the upper site (Figure 4.46), the surface probes at 0.4 and 0.8 m showed a higher variability in fractional volumetric soil water content than the deeper probes in response to dry and wet periods (0.12 to 0.25). Beyond 1.6 m the results were higher but less variable (0.26 to 0.33) until January 2013 when there was a distinct increase in the fractional water content from 0.28 to 0.33 (at a depth of 2.4 m). In general, volumetric soil water content increased with increasing depth. These results will provide useful verification of the new TDR_{UKZN} probes.

From April to August 2012 at the lower site (Figure 4.47), the fractional soil water content showed a decreasing trend associated with the lower rainfall of winter. The probe at 0.4 m responded to rainfall of 5 and 3.2 mm on consecutive days and increased by 3%. The soil water content at 0.8 and 2.0 m was consistently less than the soil water content at 0.4 m while the 1.2, 1.6 and 2.4 m the soil water content was highest. Following the rainfall on the 8 August 2012 of 40 mm there has been an increasing trend (linked to rainfall events) in fractional soil water content close to the riparian area.

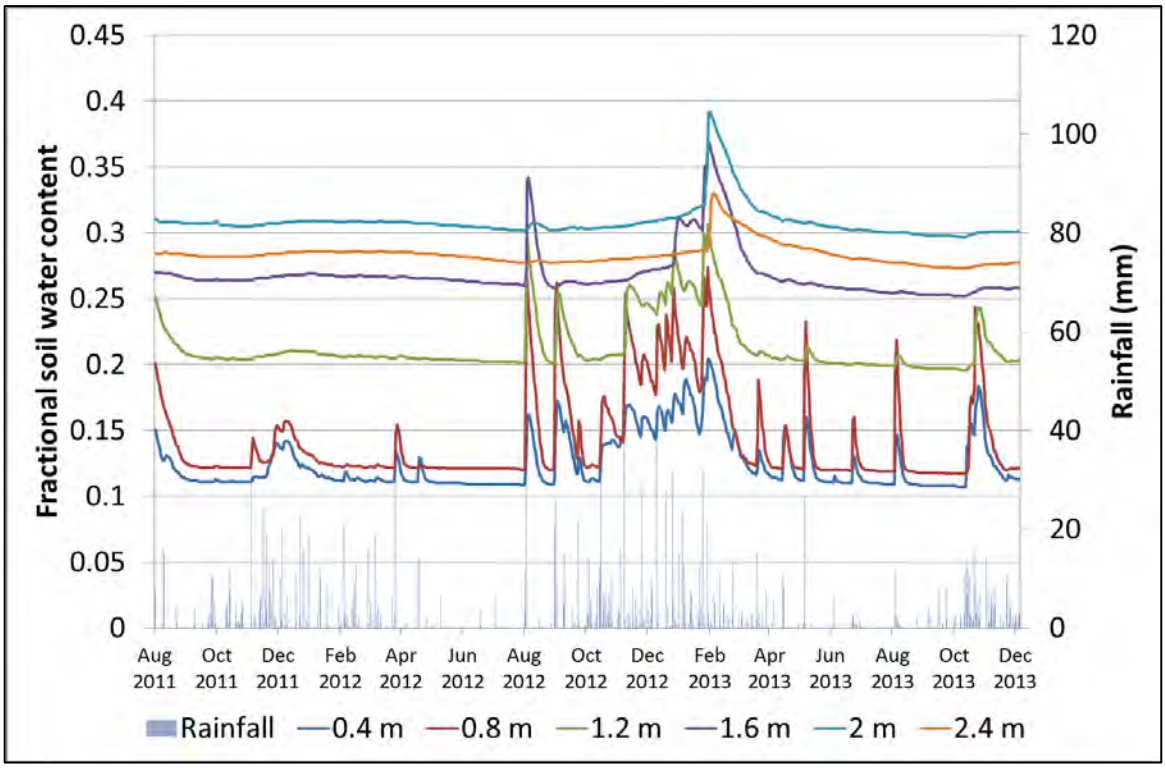

Figure 4.46: Fractional soil water measured with CS616 probes to a depth of 2.4 m from August 2011 to Dec 2013 at the South-facing mid-slope (near the lattice mast) site in the Two Streams catchment.

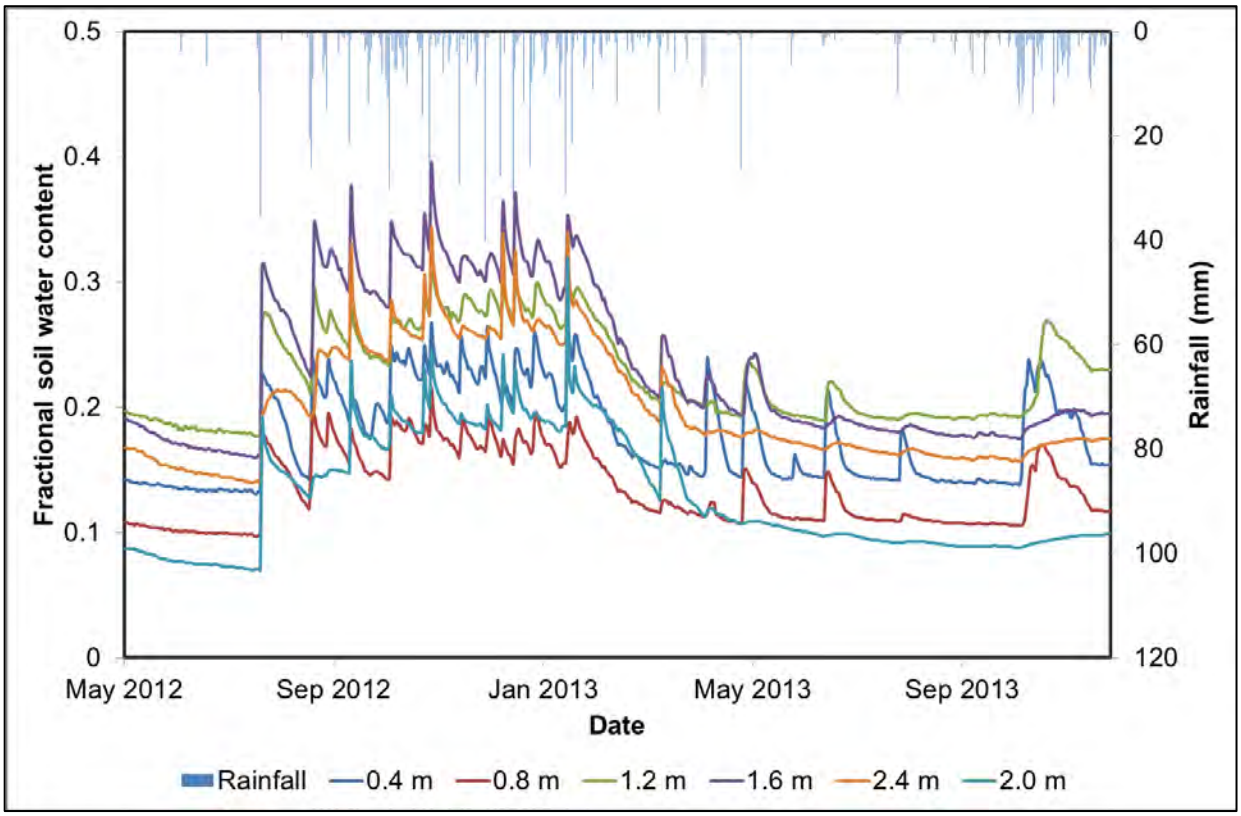

Figure 4.47: Fractional soil water measured with CS616 probes to a depth- of 2.4 m from April 2012 to December 2013 at the South-facing lower (riparian) sapflow site in the Two Streams catchment.

The average soil profile water content (Figure 4.48) at the riparian site at the end of winter was lower (13%) than at the upper site (19%). Following rainfall in August the soil profile at both sites was recharged but the recharge at the riparian site (10%) was more than at the upper site (7%). The average soil profile water content at both sites has increased during the course of the summer period, however, there is more recharge at the lower site (following rainfall), possibly due to subsurface flow accumulation from the catchment slope above the site.

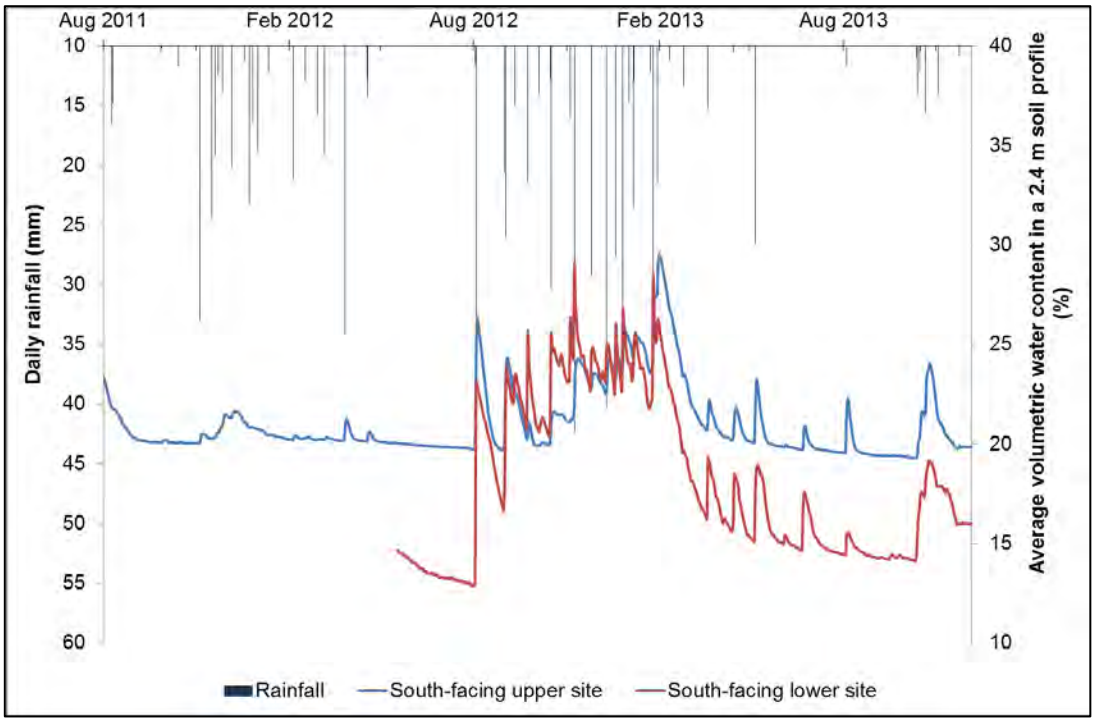

Figure 4.48: A comparison of the average soil profile water content from the South-facing upper site and the South-facing lower site.

The volumetric water content of the cylindrical TDR_{CSIR} probes at 1.6 and 4.8 m and a CS605 probe at 0.4 m showed that although the probes designed in the previous Two Streams work followed the overall trends in soil water, there was a high degree of noise associated with the new probes with a 0.075 m probe length (Figure 4.49). Thus although showing potential the probe required further investigation and development to improve performance.

In 2012 a new set of 15 TDR_{UKZN} cylindrical probes were manufactured to test the hypothesis that the noise was caused by the short probe length selected as appropriate in the first design stage. The probes (3 reps of each) covered the following range of probe lengths: 0.075, 0.10, 0.125, 0.15, 0.175 and 0.2 m.

The probes were initially installed vertically into the ground and later horizontally by excavating a shallow pit to try and avoid local soil water variation. The system consisted of a TDR 100, 3 SDMX50 multiplexers, the 15 cylindrical probes (5 probe lengths) and two CS605 probes to act as a control.

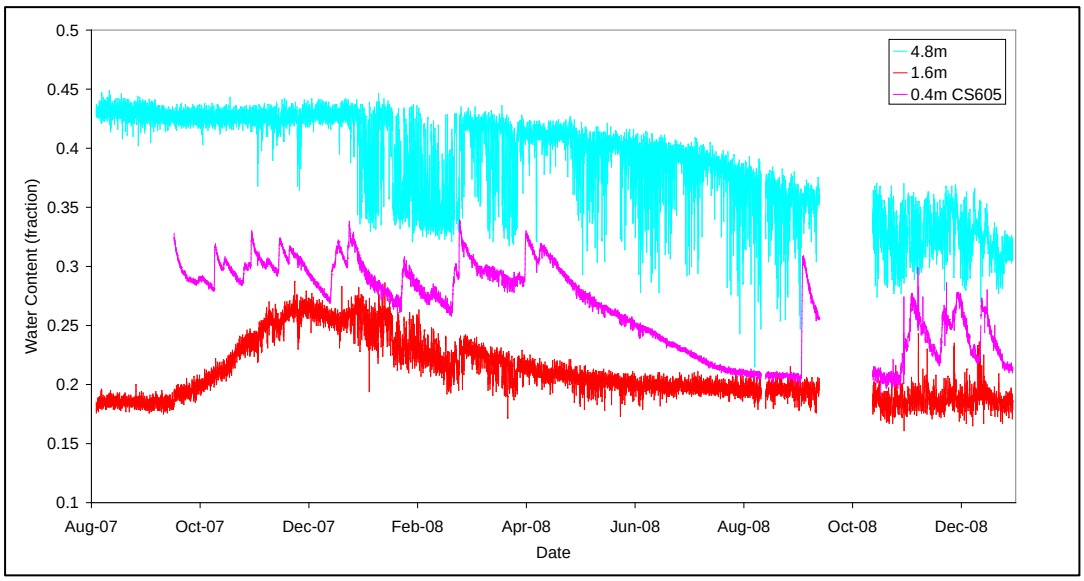

Figure 4.49: The fractional soil water content measured with cylindrical TDR_{CSIR} probes to a depth of 4.8 m from August 2007 to December 2008.

The vertically orientated probes exhibited a wide variation in θ, varying from 0.30 to 0.52 (Figure 4.50). The 0.075 probe showed the highest deviation from the CS605 probes (control). Interestingly, all the probes followed the same trend and it was felt that the vertical orientation might explain some of this high variation and the probes were installed horizontally on the 25/11/2011 (Figure 4.50). This reduced the variability but the high range in θ recorded was not considered acceptable. In the manufacture of all the probes (including the CS605 probe) the amount of probe embedded in the resin matrix was kept constant at 8.5 cm and the offset (0.085) recommended by Campbell Scientific was assumed. In order to investigate the effect of the system components (multiplexer, common cable and individual probes) on the variation in θ in the experimental test system and the probe offset, it was decided to determine the probe calibration individually for each probe using a procedure described by Campbell Scientific.

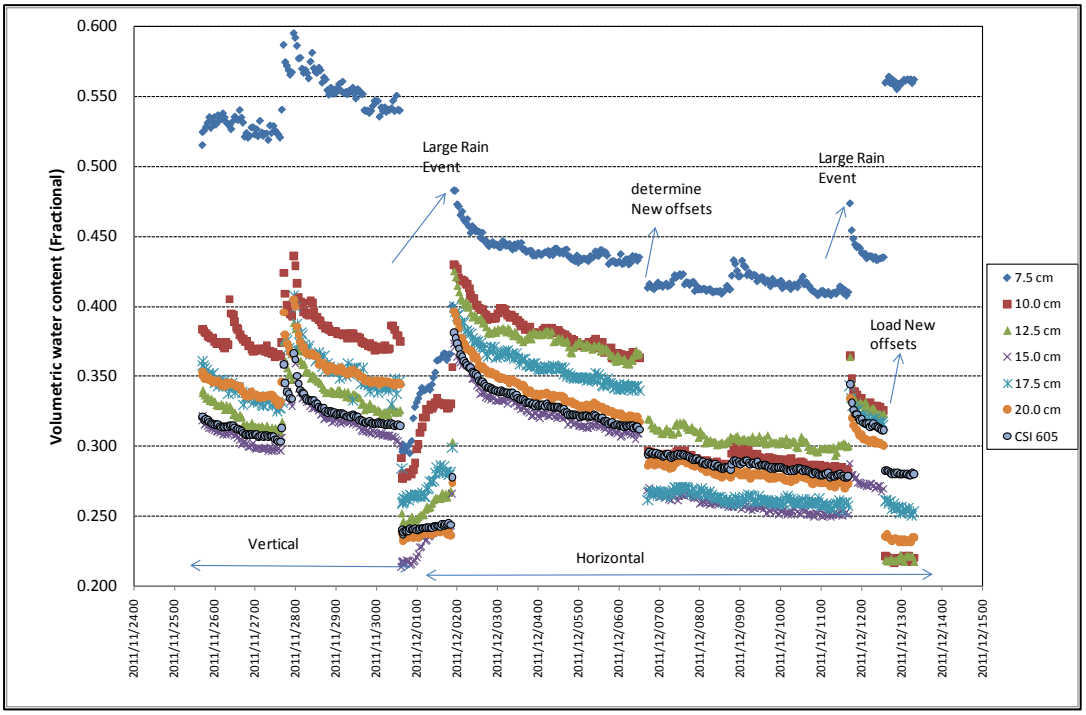

Figure 4.50: Volumetric water content collected using TDR probes with varying rod lengths.

4.6.1 Theory and procedure used for individual probe calibration

The location of the beginning of the probes that is calculated in the TDR100 software is the point along the cable where the transition from the RG58 cable and stainless steel cables begin. This is embedded in the head of the probe and needs to be accounted for (Figure 4.3 of Deliverable 2 shows a probe without a probe head and the transition from the black RG58 co-axial cable to the copper connecting the stainless steel is clearly visible). The distance of the wave guides in the resin matrix is a constant 8.5 cm and needs to be accounted for.

The Campbell system uses the following equation to calculate the apparent rod length to actual length, La/L and is equal to the square root of the dielectric permittivity, $\sqrt{\varepsilon}$ and can be expressed in terms of apparent to actual length (equation 4.1).

$$\frac{La}{L} = \frac{\frac{end - start}{Vp} - \mathrm{Pr}obeOffset}{L} \qquad (4.2)$$

Where *La* = apparent length, *L* actual length, *Vp* relative propagation velocity, *start* is distance for beginning of rod and *end* distance to end of rod in the TDR trace.

Letting Vp = 1 and solving for probe offset in equation 1 gives:

ProbeOffset = end – start –La

Using the TDR100 terminal emulation program it was possible to determine all the variables to calculate the Probe Offset, since $La = L * \sqrt{\varepsilon(T)}$ where L is actual rod length protruding from the matrix. The dielectric permittivity was calculated from tables provided by Campbell Scientific using actual temperature of the water measured during the calibration procedure. In this way the TDR100 software using terminal emulation returned La/L and the start and end values based on the following settings: Vp 1, Average 4 and Points 251.

A graphical plot of a CS605 probe in the experiment (Figure 4.51) showed that the probe offset for our system should be 0.199 and not the 0.086 as normally used and recommended in the Campbell manual for systems with short cable lengths. This confirmed the decision to individually calibrate each probe in the system.

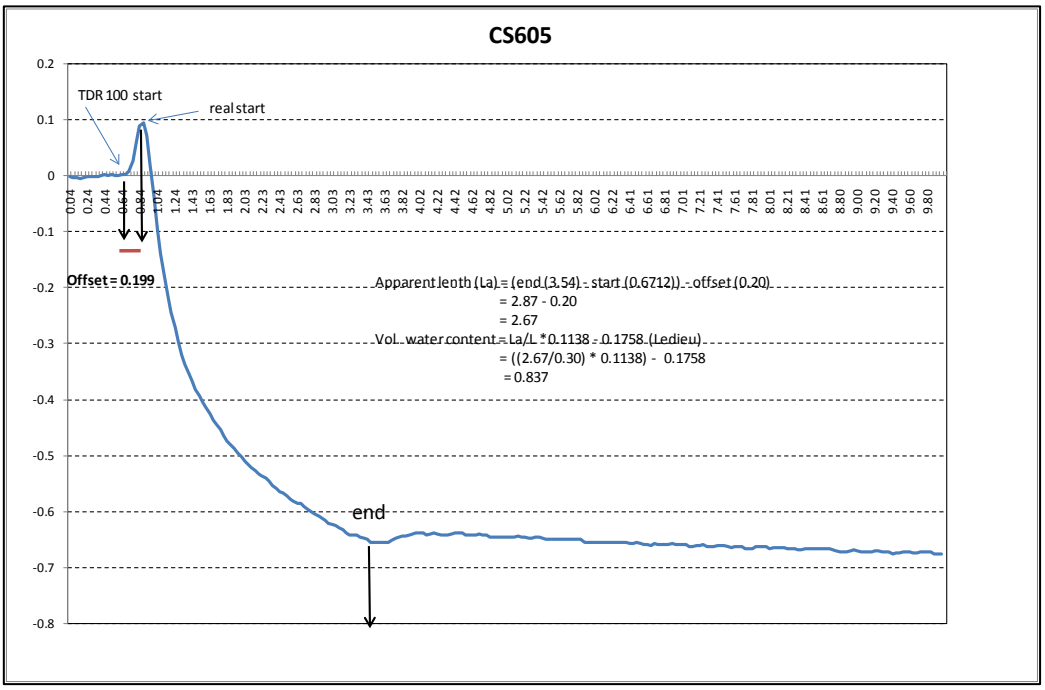

Figure 4.51: A TDR trace from a CS605 probe used in the calibration experiment.

The sensitivity of the apparent length measurement (La) is directly related to probe offset. Thus in our experiment the probe offset error of 0.093 (0.199-0.086) for the CS605 probe changed La by –0.093. In the above example this would result in a 4% change in θ from 84 to 80% or a significant 0.05% underestimation error in θ.

Probe offsets for all 22 probes in the experiment were determined using the above procedure and are presented in Tables 4.12 to 4.17. For each probe the procedure was repeated three times to obtain the best average.

Probe #	Length	Rep	La	GMO (La/L)	Start_index	START_dist	End_index	END_dist	Dielectric Perm @ 28C	Window	Data pts	Vp	Probe offset
1	0.075	1	0.65936	11.3200	28.3384	0.2834	113.2415	1.1324	77.29	2.5	251	1	0.1897
	0.075	2	0.65936	11.2351	28.9902	0.2899	113.2534	1.1325	77.29	2.5	251	1	0.1833
	0.075	3	0.65936	11.3171	27.8386	0.2784	112.7166	1.1272	77.29	2.5	251	1	0.1894
	0.075	Average	0.65936	11.2907	28.3891	0.2839	113.0705	1.1307	77.29	2.5	251	1	0.1875
2	0.075	1	0.65936	11.2909	137.4093	1.3741	222.6033	2.2260	77.29	2.5	251	1	0.1926
	0.075	2	0.65936	11.4010	137.3452	1.3735	222.3956	2.2240	77.29	2.5	251	1	0.1911
	0.075	3	0.65936	11.3064	137.4381	1.3744	222.2357	2.2224	77.29	2.5	251	1	0.1886
	0.075	Average	0.65936	11.3328	137.3975	1.3740	222.4115	2.2241	77.29	2.5	251	1	0.1908
3	0.075	1	0.65936	11.2249	134.7882	1.3479	218.9752	2.1898	77.29	2.5	251	1	0.1825
	0.075	2	0.65936	11.2624	133.6314	1.3363	218.0997	2.1810	77.29	2.5	251	1	0.1853
	0.075	3	0.65936	11.2616	133.7856	1.3379	218.2474	2.1825	77.29	2.5	251	1	0.1853
	0.075	Average	0.65936	11.2496	134.0684	1.3407	218.4408	2.1844	77.29	2.5	251	1	0.1844
											Mean offset		**0.1876**

Table 4.12: Probe offsets determined for probes 1 to 3 (0.075 m).

Probe #	Length	Rep	La	GMO (La/L)	Start_index	START_dist	End_index	END_dist	Dielectric Perm @ 28C	Window	Data pts	Vp	Probe offset
4	0.1	1	0.879147	10.6304	42.6682	0.4267	148.9720	1.4897	77.29	2.5	251	1	0.1839
	0.1	2	0.879147	10.6690	42.5049	0.4250	149.1954	1.4920	77.29	2.5	251	1	0.1878
	0.1	3	0.879147	10.7282	42.3959	0.4240	149.6783	1.4968	77.29	2.5	251	1	0.1937
	0.1	Av	0.879147	10.6759	42.5230	0.4252	149.2819	1.4928	77.29	2.5	251	1	0.1884
5	0.1	1	0.879147	10.7712	45.0248	0.4502	152.7367	1.5274	77.29	2.5	251	1	0.1980
	0.1	2	0.879147	10.7380	44.6155	0.4462	151.9958	1.5200	77.29	2.5	251	1	0.1947
	0.1	3	0.879147	10.7767	44.4180	0.4442	152.1846	1.5218	77.29	2.5	251	1	0.1985
	0.1	Av	0.879147	10.7620	44.6861	0.4469	152.3057	1.5231	77.29	2.5	251	1	0.1970
6	0.1	1	0.879147	10.4788	39.3070	0.3931	144.0949	1.4409	77.29	2.5	251	1	0.1687
	0.1	2	0.879147	10.5145	39.0072	0.3901	144.0949	1.4409	77.29	2.5	251	1	0.1717
	0.1	3	0.879147	10.3977	39.4563	0.3946	143.4334	1.4343	77.29	2.5	251	1	0.1606
	0.1	Av	0.879147	10.4637	39.2568	0.3926	143.8744	1.4387	77.29	2.5	251	1	0.1670
											Mean offset		**0.1842**

Table 4.13: Probe offsets determined for probes 7 to 9 (0.125 m).

Probe #	Length	Rep	La	GMO (La/L)	Start_index	START_dist	End_index	END_dist	Dielectric Perm @ 28C	Window	Data pts	Vp	Probe offset
7	0.125	1	1.098934	8.6906	45.8753	0.9175	111.0547	2.2211	77.29	5	251	1	0.2047
	0.125	2	1.098934	8.6319	45.4512	0.9090	110.1906	2.2038	77.29	5	251	1	0.1959
	0.125	3	1.098934	8.7845	44.8979	0.8980	110.7814	2.2156	77.29	5	251	1	0.2187
	0.125	Av	1.098934	8.7023	45.4081	0.9082	110.6756	2.2135	77.29	5	251	1	0.2064
8	0.125	1	1.098934	10.3998	39.5562	0.7911	104.5548	2.0911	77.29	5	251	1	0.2010
	0.125	2	1.098934	10.3467	40.0929	0.8019	104.7595	2.0952	77.29	5	251	1	0.1944
	0.125	3	1.098934	10.2230	40.4806	0.8096	104.3743	2.0875	77.29	5	251	1	0.1789
	0.125	Av	1.098934	10.3232	40.0432	0.8009	104.5629	2.0913	77.29	5	251	1	0.1915
9	0.125	1	1.098934	10.3998	39.5562	0.7911	104.5548	2.0911	77.29	5	251	1	0.2010
	0.125	2	1.098934	10.3467	40.0929	0.8019	104.7595	2.0952	77.29	5	251	1	0.1944
	0.125	3	1.098934	10.2230	40.4806	0.8096	104.3743	2.0875	77.29	5	251	1	0.1789
	0.125	Av	1.098934	10.3232	40.0432	0.8009	104.5629	2.0913	77.29	5	251	1	0.1915
											Mean offset		**0.1964**

Table 4.14: Probe offsets determined for probes 7 to 9 (0.125 m).

Probe #	Length	Rep	La	GMO (La/L)	Start_index	START_dist	End_index	END_dist	Dielectric Perm @ 28C	Window	Data pts	Vp	Probe offset
13	0.175	1	1.538508	9.7758	46.4262	0.9285	131.9644	2.6393	77.29	5	251	1	0.1722562
	0.175	2	1.538508	9.8914	45.9253	0.9185	132.4750	2.6495	77.29	5	251	1	0.1924862
	0.175	3	1.538508	9.8205	46.3223	0.9264	132.2516	2.6450	77.29	5	251	1	0.1800782
	0.175	Av	1.538508	9.8292	46.2246	0.9245	132.2303	2.6446	77.29	5	251	1	0.18160687
14	0.175	1	1.538508	9.9883	45.2343	0.9047	132.6319	2.6526	77.29	5	251	1	0.2094442
	0.175	2	1.538508	9.9765	45.2874	0.9057	132.5819	2.6516	77.29	5	251	1	0.2073822
	0.175	3	1.538508	9.9728	45.1485	0.9030	132.4103	2.6482	77.29	5	251	1	0.2067282
	0.175	Av	1.538508	9.9792	45.2234	0.9045	132.5414	2.6508	77.29	5	251	1	0.20785153
15	0.175	1											
	0.175	2											
	0.175	3											
	0.175	Av											
											Mean offset		**0.1947**

Table 4.15: Probe offsets determined for probes 13 to 14 (0.175 m). Note probe 15 was faulty.

Probe #	Length	Rep	La	GMO (La/L)	Start_index	START_dist	End_index	END_dist	Dielectric Perm @ 28C	Window	Data pts	Vp	Probe offset
16	0.2	1	1.758295	9.9614	43.4841	0.8697	143.0983	2.8620	77.29	5	251	1	0.2340
	0.2	2	1.758295	9.9557	43.0012	0.8600	142.5578	2.8512	77.29	5	251	1	0.2328
	0.2	3	1.758295	9.9608	43.1271	0.8625	142.7354	2.8547	77.29	5	251	1	0.2339
	0.2	Av	1.758295	9.9593	43.2041	0.8641	142.7972	2.8559	77.29	5	251	1	0.2336
17	0.2	1	1.758295	9.9403	36.6364	0.7327	136.0393	2.7208	77.29	5	251	1	0.2298
	0.2	2	1.758295	9.9450	36.7942	0.7359	136.2438	2.7249	77.29	5	251	1	0.2307
	0.2	3	1.758295	9.9369	36.7942	0.7359	136.1632	2.7233	77.29	5	251	1	0.2291
	0.2	Av	1.758295	9.9407	36.7416	0.7348	136.1488	2.7230	77.29	5	251	1	0.2298
18	0.2	1	1.768389	9.9027	35.8253	0.7165	134.8519	2.6970	78.18	5	251	1	0.2121
	0.2	2	1.768389	9.9761	35.1641	0.7033	134.9252	2.6985	78.18	5	251	1	0.2268
	0.2	3	1.768389	9.9068	35.9604	0.7192	135.0281	2.7006	78.18	5	251	1	0.2130
	0.2	Av	1.768389	9.9285	35.6499	0.7130	134.9351	2.6987	78.18	5	251	1	0.2173
											Mean offset		**0.2269**

Table 4.16: Probe offsets determined for probes 16 to 18 (0.20 m).

Probe #	Length	Rep	La	GMO (La/L)	Start_index	START_dist	End_index	END_dist	Dielectric Perm @ 28C	Window	Data pts	Vp	Probe offset
19	0.3	1	2.6831	9.7118	23.0923	0.4618	168.7699	3.3754	79.99	5	251	1	0.2304
	0.3	2	2.6831	9.7491	23.2377	0.4648	169.4738	3.3895	79.99	5	251	1	0.2416
	0.3	3	2.6831	9.6074	23.2641	0.4653	167.3754	3.3475	79.99	5	251	1	0.1991
	0.3	Av	2.6831	9.6894	23.1980	0.4640	168.5397	3.3708	79.99	5	251	1	0.2237
20	0.3	1	2.6831	9.6785	23.0923	0.4618	168.7594	3.3752	79.99	5	251	1	0.2302
	0.3	2	2.6831	9.5882	23.2377	0.4648	167.2378	3.3448	79.99	5	251	1	0.1969
	0.3	3	2.6831	9.6309	23.2641	0.4653	168.1636	3.3633	79.99	5	251	1	0.2149
	0.3	Av	2.6831	9.6325	23.1980	0.4640	168.0536	3.3611	79.99	5	251	1	0.2140
21	0.3	1	2.6831	9.9065	23.9620	0.4792	172.5591	3.4512	79.99	5	251	1	0.2888
	0.3	2	2.6831	9.9020	24.0157	0.4803	172.5454	3.4509	79.99	5	251	1	0.2875
	0.3	3	2.6831	9.8712	23.9638	0.4793	172.0312	3.4406	79.99	5	251	1	0.2782
	0.3	Av	2.6831	9.8932	23.9805	0.4796	172.3786	3.4476	79.99	5	251	1	0.2848
22	0.3	1	2.6831	9.8412	24.5502	0.4910	172.1685	3.4434	79.99	5	251	1	0.2693
	0.3	2	2.6831	9.7732	24.5061	0.4901	171.1037	3.4221	79.99	5	251	1	0.2488
	0.3	3	2.6831	9.9326	24.5485	0.4910	173.5377	3.4708	79.99	5	251	1	0.2967
	0.3	Av	2.6831	9.8490	24.5349	0.4907	172.2700	3.4454	79.99	5	251	1	0.2716
											Mean offset		**0.2485**

Table 4.17: Probe offsets determined for probes 19 to 22 (0.30 m standard CS605).

The offsets determined above were entered into the CR1000 program for each probe. In addition the probes were placed into a sealed container with a well-mixed soil to reduce the soil water variability. Following this procedure the soil water content showed very little variation and θ values for all probes were within a range of 5 to 8% (Figure 4.52). These values were similar to gravimetric samples which showed the same range with a mean of 6.3% and standard error of ±1.6%. These data showed that all the probes could be successfully calibrated provided all the attenuation losses in the entire system are accounted for. Clearly all probes in the future need to be calibrated on site to account for the different probe offsets and losses. In addition, it is strongly recommended that a very high quality low loss co-axial cable be used in probe manufacture to reduce these losses and that cost is not the most important consideration in cable choice as previously thought.

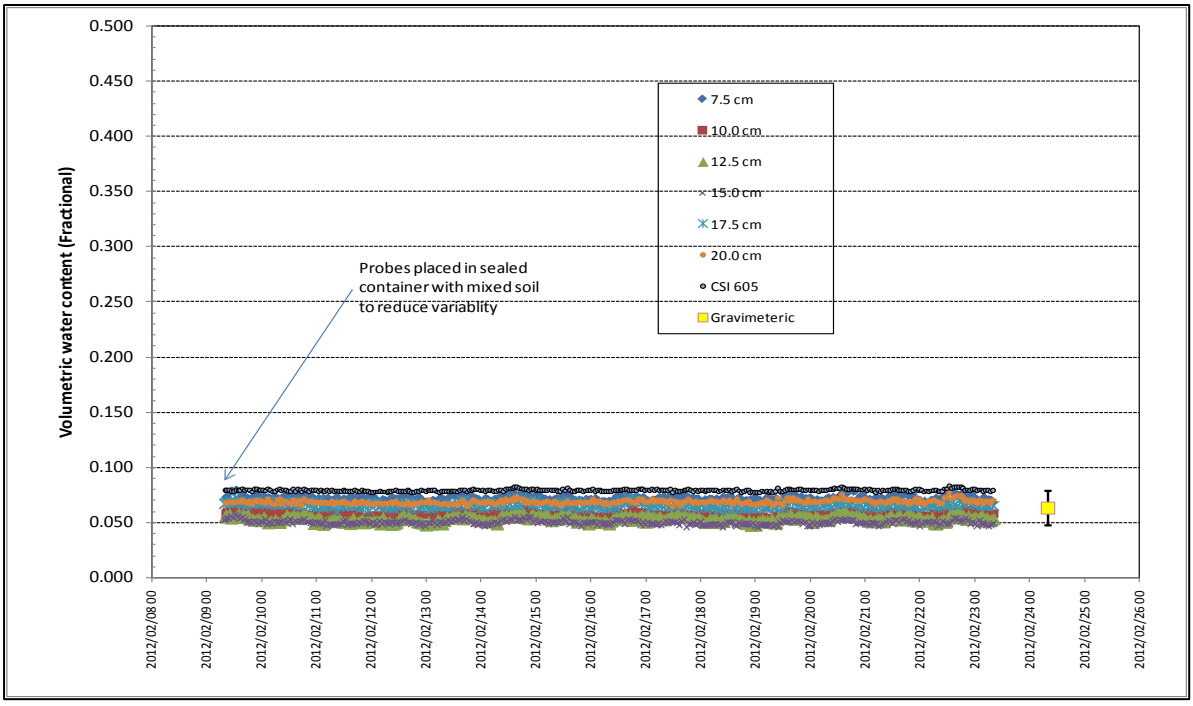

Figure 4.52: Volumetric water content measured with the calibrated probes. A single Gravimetric reference (3 reps) is included as a check on the validity of the TDR data.

This cable needs to be capable of being buried for long periods and therefore also needs to be moisture resistant. Probes with these design improvements were manufactured and installed at the Two Streams catchment. Although our data showed that all probes could be successfully calibrated and it is felt that the errors introduced by the 0.075 probe were clearly higher than the other configurations and therefore the minimum probe length should be 0.10 m.

4.6.2 Results from TDR_{UKZN} probes

The results from the TDR_{UKZN} probes (Figure 4.53) indicate that the longer waveguides (0.150 m instead of 0.075 m) have made a significant difference to the quality of the soil water data. The improved design of

the probe together with the rigorous calibration procedure now provides soil water content results to a depth of 4.8 m. The results indicate that the soil profile is wetter near the surface (26%) becoming progressively drier with depth (9% at 4.8 m). These results of deep soil water content were critical for understanding the isotope study results and determining the performance of the HYDRUS model.

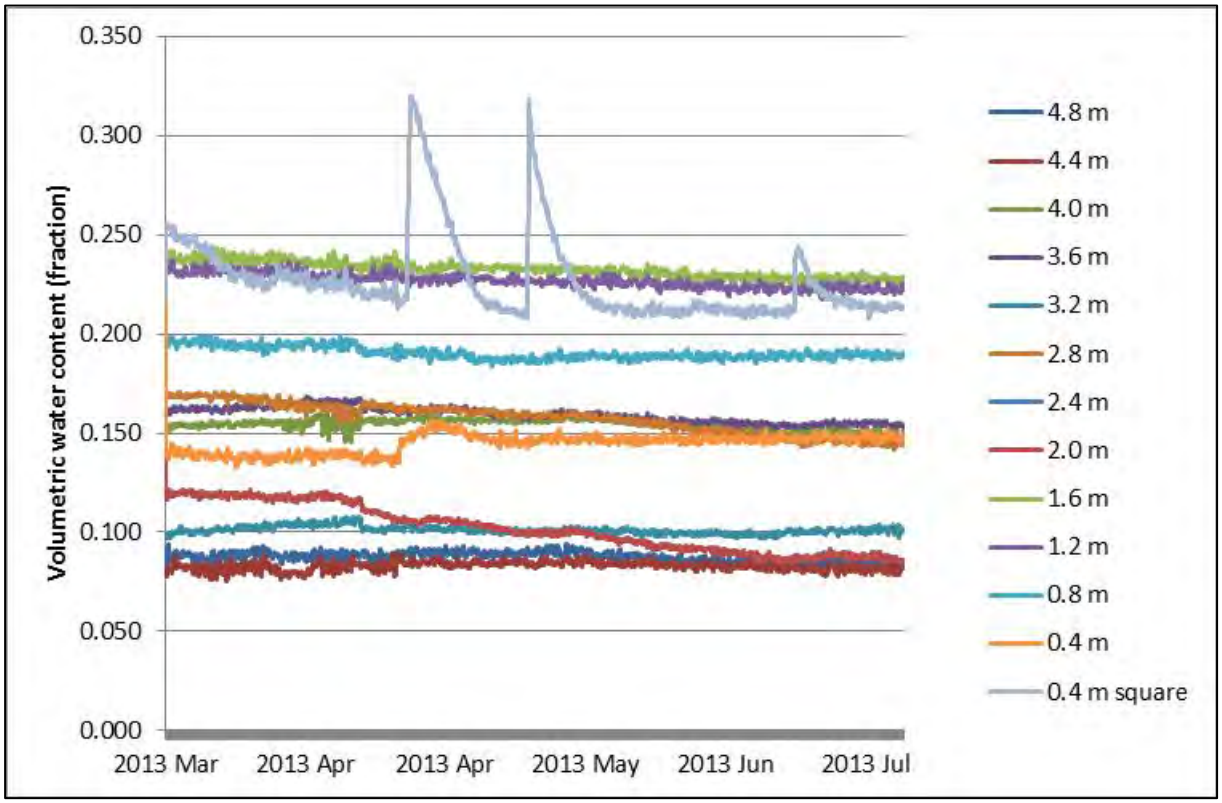

Figure 4.53: Fractional soil water content from the TDR_{UKZN} probes at 0.4 m intervals down to a depth of 4.8 m.

4.7 Catchment water balance

4.7.1 Monthly changes in the water balance

In the catchment water balance for Two Streams, rainfall was considered a positive gain into the catchment, while total evaporation (ET) and streamflow (Q) were considered losses (Figure 4.54). Changes in soil water storage (ΔS) were either losses or gains. Monthly totals of these four measured parameters from October 2011 to October 2013 showed that total evaporation was the most dominant variable, with monthly losses ranging from -52 mm in June 2012 to -136 mm in December 2012 (Figure 4.54). Although the rainfall inputs peaked at 160 mm in summer, there was little rain in the winter period when monthly values were generally < 10 mm in June and July. By contrast, the monthly streamflow was an order of magnitude smaller than the P and ET with a monthly average of only 3.1 mm. In the winter months, when rainfall was low and evaporation continued at potential rates, there was generally a deficit in the monthly

soil water balance this being particularly noticeable in 2013 when values were negative between February and August, varying between -3.8 mm (August 2013) and -164 mm (February 2013) (Figure 4.54). Not surprisingly recharge in the upper 2.4 m of the soil profile generally coincided with months of high rainfall as occurred between September 2012 and January 2013 (Figure 4.54).

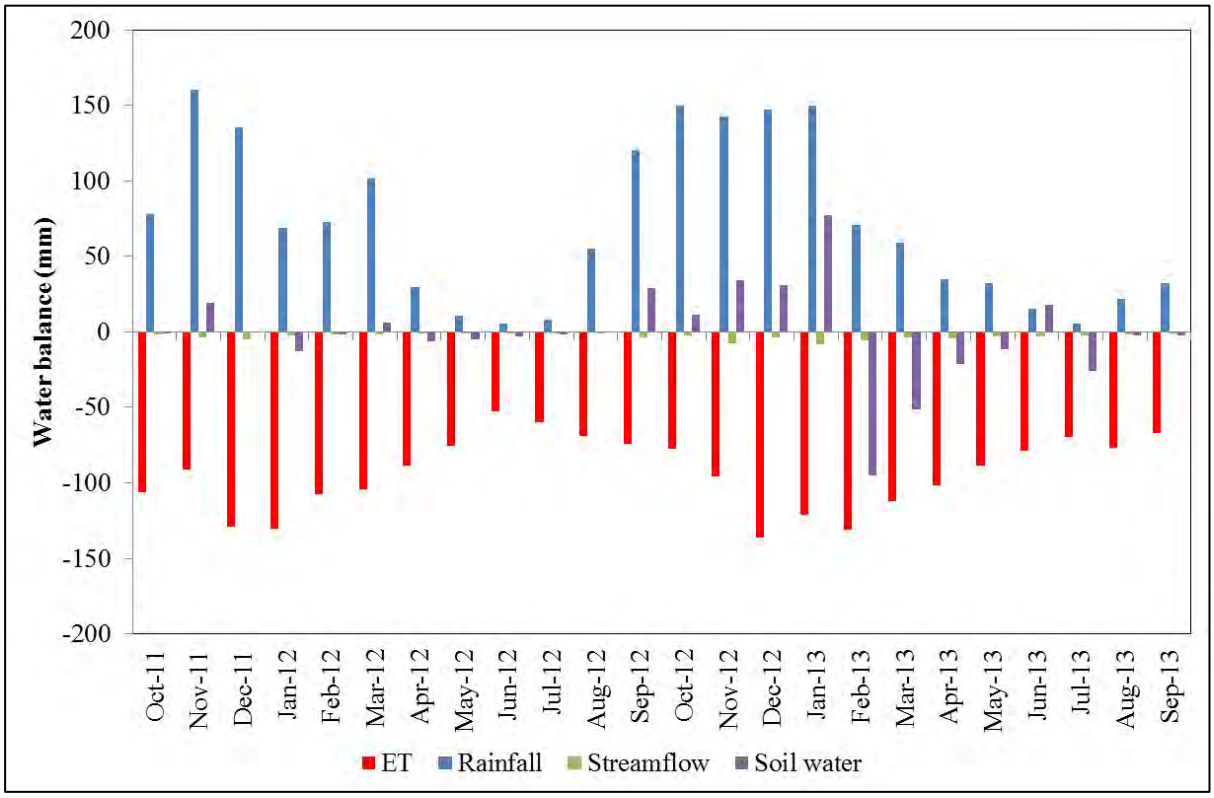

Figure 4.54: Monthly water balance showing rainfall and a positive change in soil water storage as additions (positive) and total evaporation, streamflow and soil water deficits as subtractions (negative) from the system.

Between October 2011 and October 2013 the accumulated values of rainfall and total evaporation using the actual total ET using eddy covariance and surface renewal systems were 1841 mm and 2245 mm respectively (Figure 4.55). Evaporation from the maturing wattle plantation (7 years stage) therefore exceeded the rainfall by 22%, showing a declining trend in P vs ET since the 2008-2009 period following planting, when the excess ET vs P was 32% (Figure 4.56). This corresponds with the slowing of the growth rate of the trees from the exponential to the stationary stage (Figure 4.3). It is interesting to note that between 2006 and 2008 this excess was 46% (Figure 4.57). The results have therefore continued to support the previous observations that ET in the wattle plantation exceeds the annual rainfall. It is also evident that this excess occurs in the dry periods between May and August when there is little rainfall but the trees still continue to freely transpire (Figures 4.57 and 4.58).

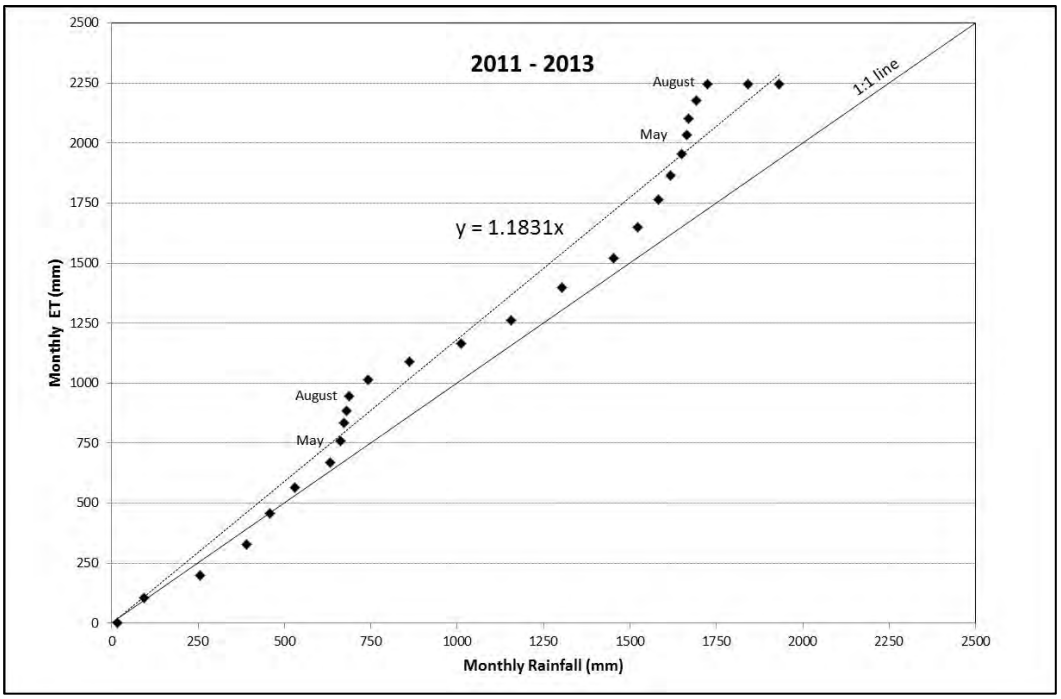

Figure 4.55: A comparison between monthly ET, and monthly rainfall from 2011 to 2013.

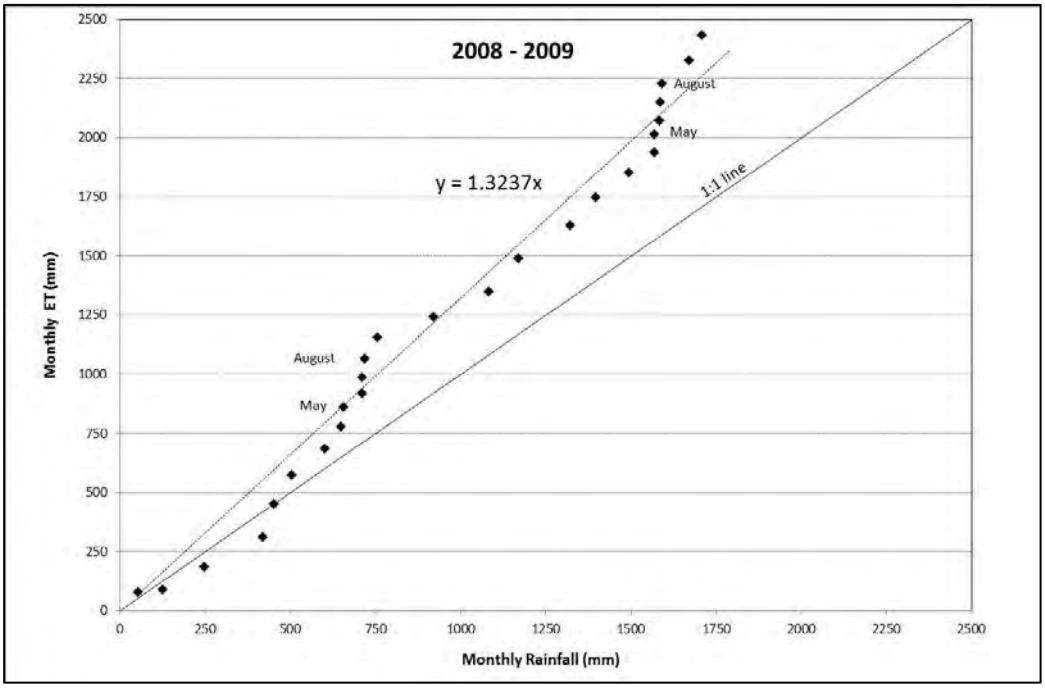

Figure 4.56: A comparison between monthly ET, and monthly rainfall from 2008 to 2009.

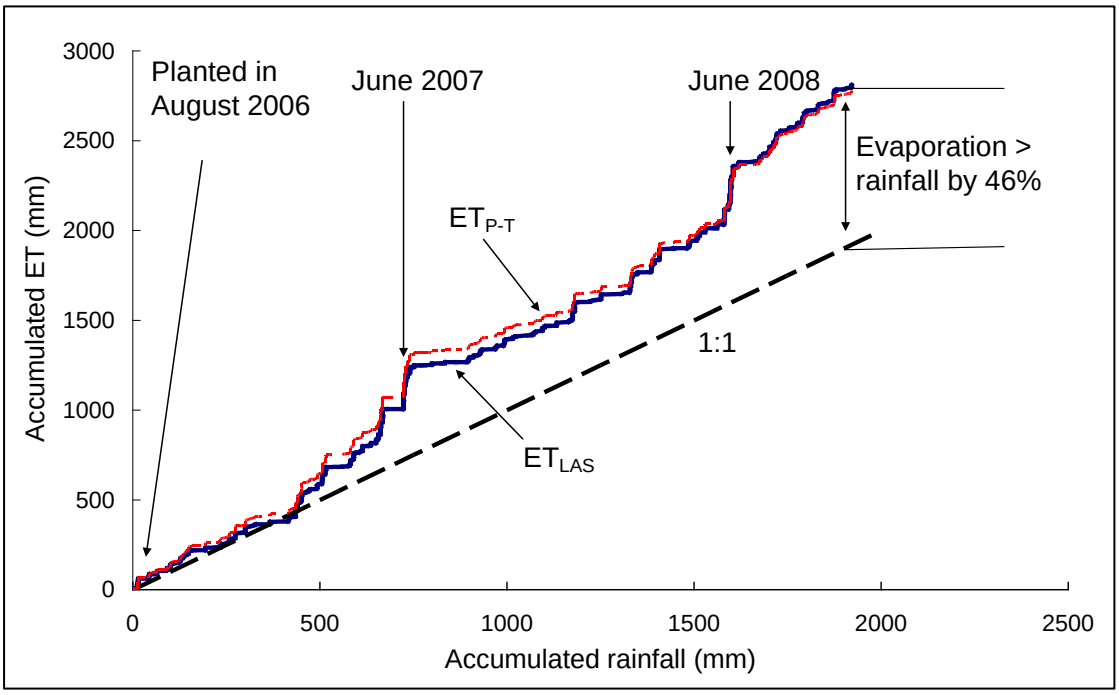

Figure 4.57: A comparison between ET_{LAS}, ET_{P-T} and rainfall from August 2006 to December 2008.

4.7.2 Annual changes in the water balance

Since the replanting of the wattle trees in 2006 all the components of the water balance equation were measured in the Two Streams catchment to the 2012/13 hydrological year (i.e. 7 hydrological years) (Table 4.18). If all these components balance then there is confidence that there are no unaccounted losses or gains in the catchment.

Table 4.18: Components of the water balance equation measured in Two Streams (2006/07 to 2012/14). P = Precipitation, ET = actual total evaporation; ΔS = change in soil storage (2.4 m profile); Q = streamflow calculated using the water balance equation; and Q_a = actual streamflow.

Hydrological Year	P	-ET	-ΔS	=	Q	Q_a	Unaccounted losses	% of P
2006/2007	869	-1242	58	=	-315	-52	-367	36
2007/2008	914	-1171	6	=	-251	-66	-317	34
2008/2009	765	-1173	-51	=	-459	-45	-504	65
2009/2010	587	-1132	-14	=	-559	-20	-579	98
1010/2011	856	-1143	-12	=	-299	-16	-315	37
2011/2012	846	-1088	-37	=	-279	-25	-304	36
2012/2013	862	-1157	-37	=	-331	-45	-376	43

In the wettest year in 2007/08 when rainfall was 914 mm the unaccounted losses were -317 mm or 34% or the rainfall. In the driest year (2009/10) when rainfall was only 587 mm the unaccounted loss was 579 mm or 98% of the rainfall. Rainfall was the most variable parameter (587 to 914 mm) while ET and Q_a remained in comparison relatively constant (e.g. ET only varied from 1088 to 1242 mm year^{-1}). Since the streamflow continuously flowed despite the large unaccounted losses, is evidence for the storage of large quantities of soil and ground water in the catchment below the 2.4 m profile depth. In Table 4.18, *P* was not adjusted for possible inputs from mist and stemflow or losses due canopy interception because of the uncertainty of these factors over this 7 year recording period. However, it is likely that the effective rainfall is lower than that presented in Table 4.18, considering the data presented from the interception studies.

Profile soil moisture data (top 2.4 m) in the catchment showed that from 2007 there was a steady annual decline in the water content in the catchment until 2013 from 617 mm to 466 mm respectively (a difference of 151 mm) (Figure 4.58). Although this is relevant it cannot explain the average annual unaccounted for losses of 395 mm year^{-1} over the 7 year measurement period. However that fact that the roots of the *Acacia* trees have been recorded at depths > 8 m suggests that the storage of water in the deep soils of the vadose zone is an unaccounted source of water in the catchment water balance at Two Streams. A schematic representation of all the measured and unaccounted components of the water balance for Two Streams is shown in Diagram 2.

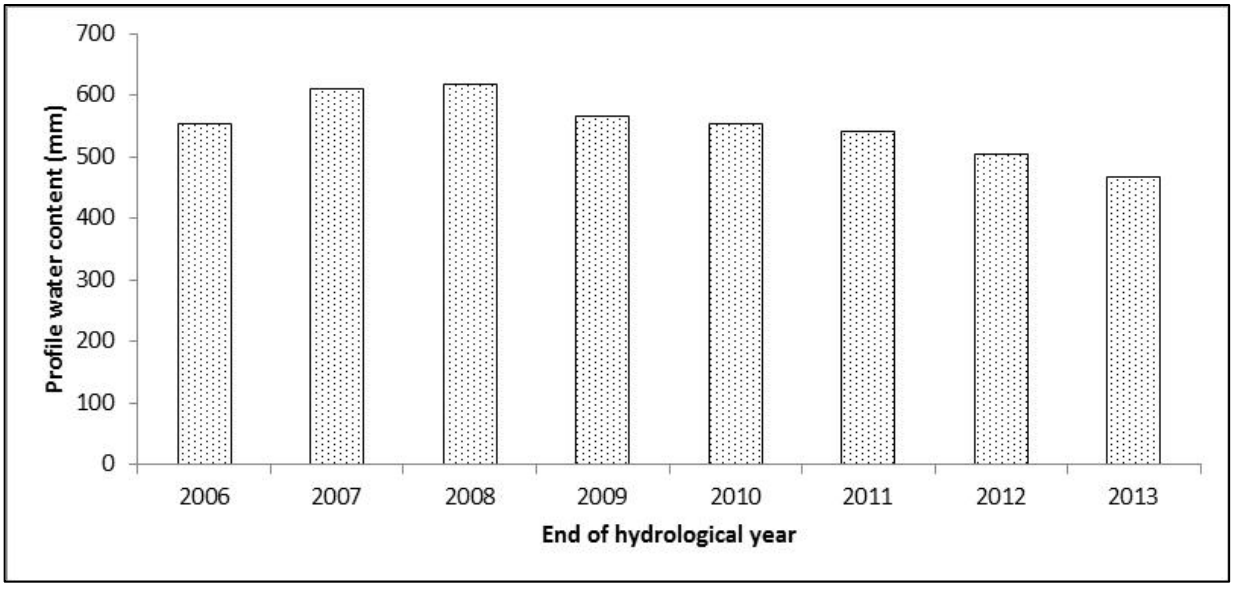

Figure 4.58: Trend in the total profile water content from 2006 to 2013 in the Two Streams catchment.

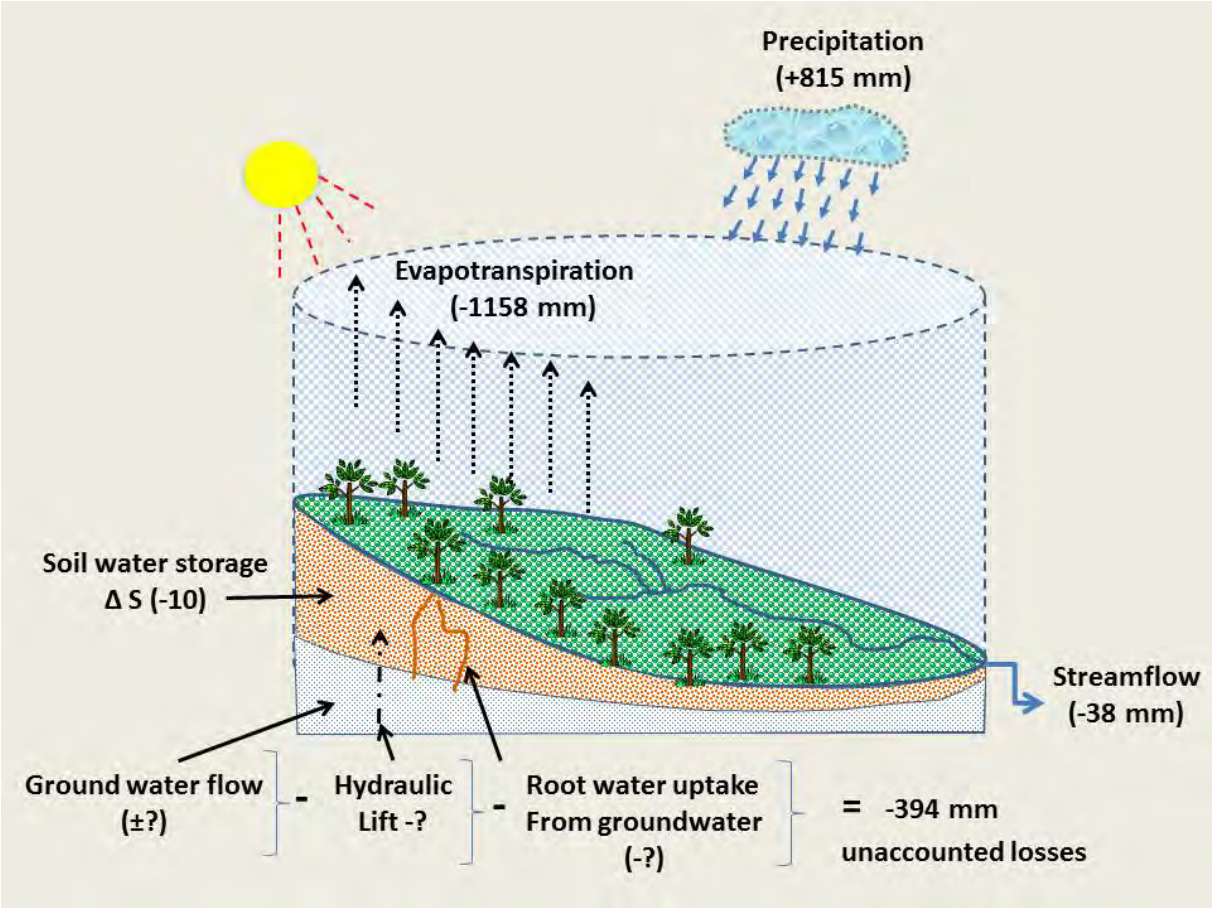

Diagram 2: Schematic representation of the average annual water balance components (7 year period) for the Two Streams catchment

4.8 Isotopes

4.8.1 Dry season

4.8.1.1 Rainfall signatures

In theory the isotopic composition of precipitation should follow the Rayleigh Equation for an open equilibrium system under ideal conditions, which is when condensation takes place without reaching super saturation and when rainfall falls as soon as droplets are formed. However in reality, the isotopic composition of precipitation follows the rules of a closed system, in that there is a depletion or enrichment of heavier isotopes as the liquid water content in the clouds increase or dissipates. The process is dominated by equilibrium fractionation (Gat, 2010).

Rainfall isotope signatures were collected using an automated sampler (ALCO). The rainfall isotopes are the incoming isotopic signature into the catchment. The rainfall signatures from the catchment were used to determine a Local Meteoric Water Line (LMWL) which was used to interpret samples collected at

different locations (Figure 12.1). The LMWL shows a slight deviation (y=8.2429x + 18.878) from the Global Meteoric Water Line (GMWL)(y=8x + 10) suggesting that samples from the catchment contain more δ^2H than international standards.

The local rainfall isotopic signature at Two Streams is similar to that of Lorentz *et al*. (2007) line b (Figure 4.59). The rainfall at Two Streams generally falls in the middle of the LMWL. According to Lorentz *et al*. (2007) rainfall that occurs at higher elevation, inland location and in cooler zones falls on the lower end of the LMWL, while rainfall that falls at low altitude, in warmer areas and near oceans usually falls at the higher end of the LMWL. Therefore one can presume that due to Two Streams being inland and having being at relativity high altitude (2800 m), the rainfall signatures should fall on the lower end of the LMWL.

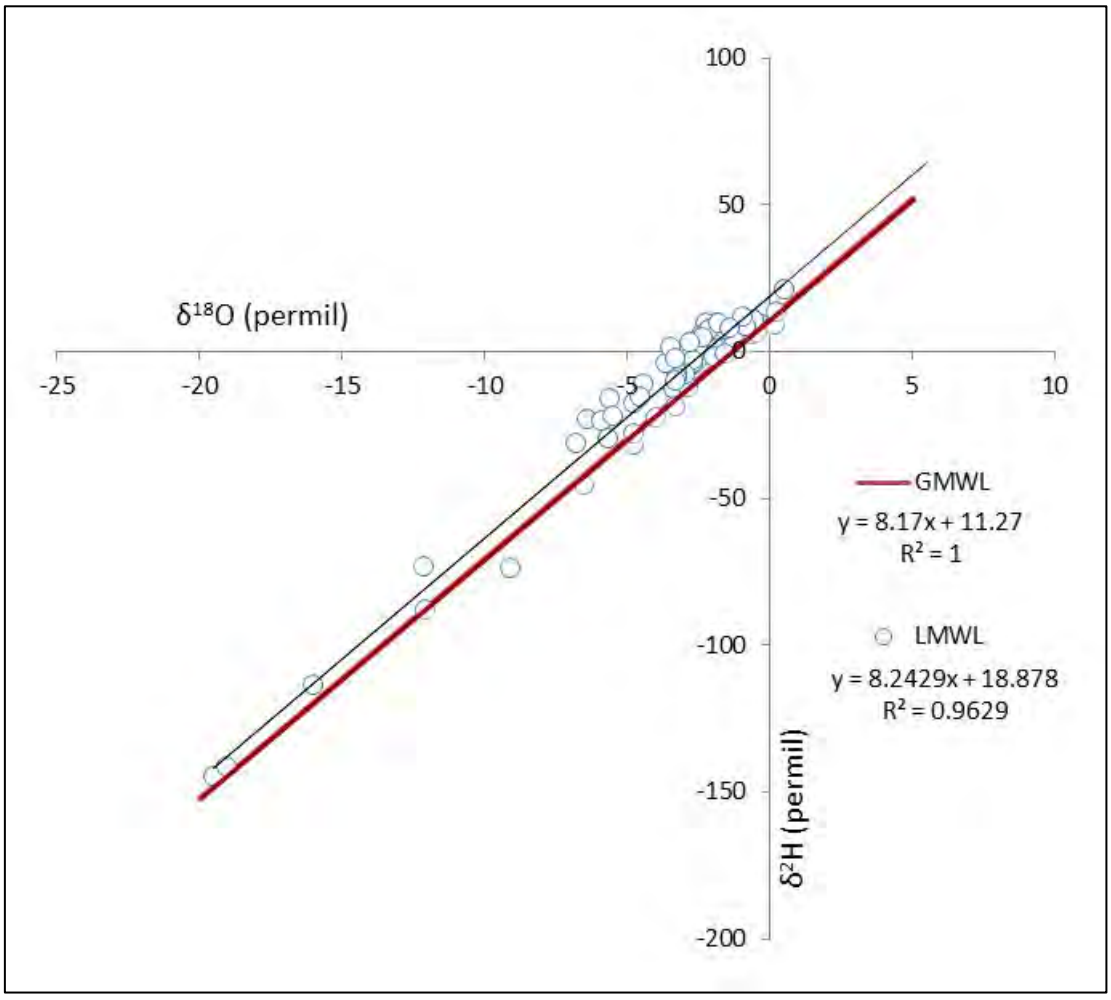

Figure 4.59: Establishment of Local Meteoric Water Line (LMWL)

Isotope fractionation occur when water evaporates and losses mass in its lighter isotope fractions. When rainfall falls water is subject to evaporation within the atmosphere. According to Dansgaard (1964) there are five factors that determine the composition of precipitation these are namely, altitude, climate (temperature), and the amount of precipitation, continentality and the source region of evaporation to form clouds. Due to the installation of an FAO-56 Automatic Weather Station that is position opposite the

automated rainfall sampler, it was possible to plot rainfall isotope signature with air temperature and amount of precipitation. There was no trend observed when plotting rainfall isotope signature with air temperature.

There was no evident trend when plotting rainfall isotope signature with rainfall volume, although it was noted that there was some relationship. Generally it would be expected that the larger events (greater than 1 mm) would yield a more negative signature as they are cold fronts and thus less evaporation occurs (Figure 4.60). On occasion, large events have a more negative signature, but in July during sampling of multiple events, it was evident that rainfall volume is not directly related to isotope signature (Figure 4.60).

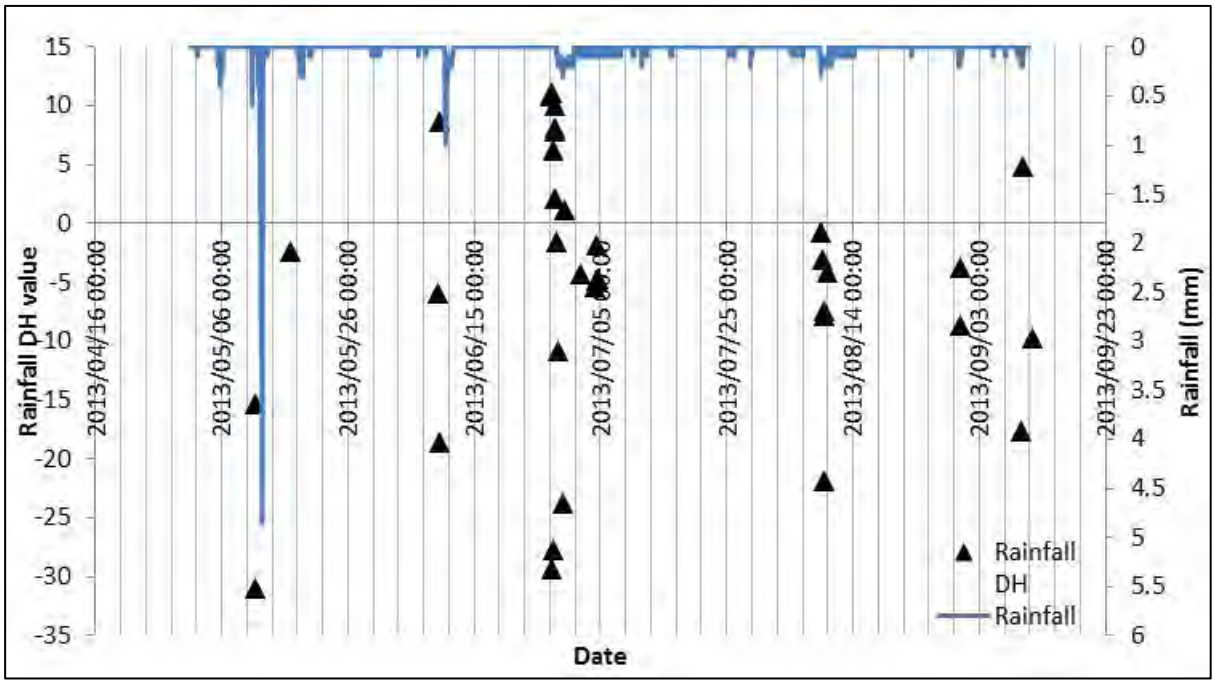

Figure 4.60: Relationship between rainfall volume and isotope signature

4.8.1.2 Streamflow and Groundwater

Shallow groundwater is not subject to high and low temperature and thus is similar to meteoric water. In regions where there are high temperatures, the isotopic composition of rainfall is different to that of precipitation due to the removal of lighter fractions during infiltration (Singh and Kumar, 2005). During tropical rainfall events rainfall is subject to high temperatures at Two Streams, thus there is a difference between rainfall composition and groundwater composition. At Two Streams the groundwater signature generally lies in-between the stream and the rainfall signature (Figure 4.61).

The δ^2H value of streamflow is generally between -5,-10‰, while the groundwater signature is generally between 5-12‰ (Figure 4.61). The main contributor to streamflow at the Two Streams Research

catchment is groundwater, on a few occasions the isotope signature of streamflow does not match (δ^2H value of -15, -20‰ and -25‰) that of groundwater and therefore the stream is fed by overland flow or direct rainfall (Although analysis of samples over the summer period have not yet been completed).

Streamflow samples were collected when there was a rise in streamflow of 5 mm and on specific days of the week. Slight variations in groundwater signature could be due to seasonal variation.

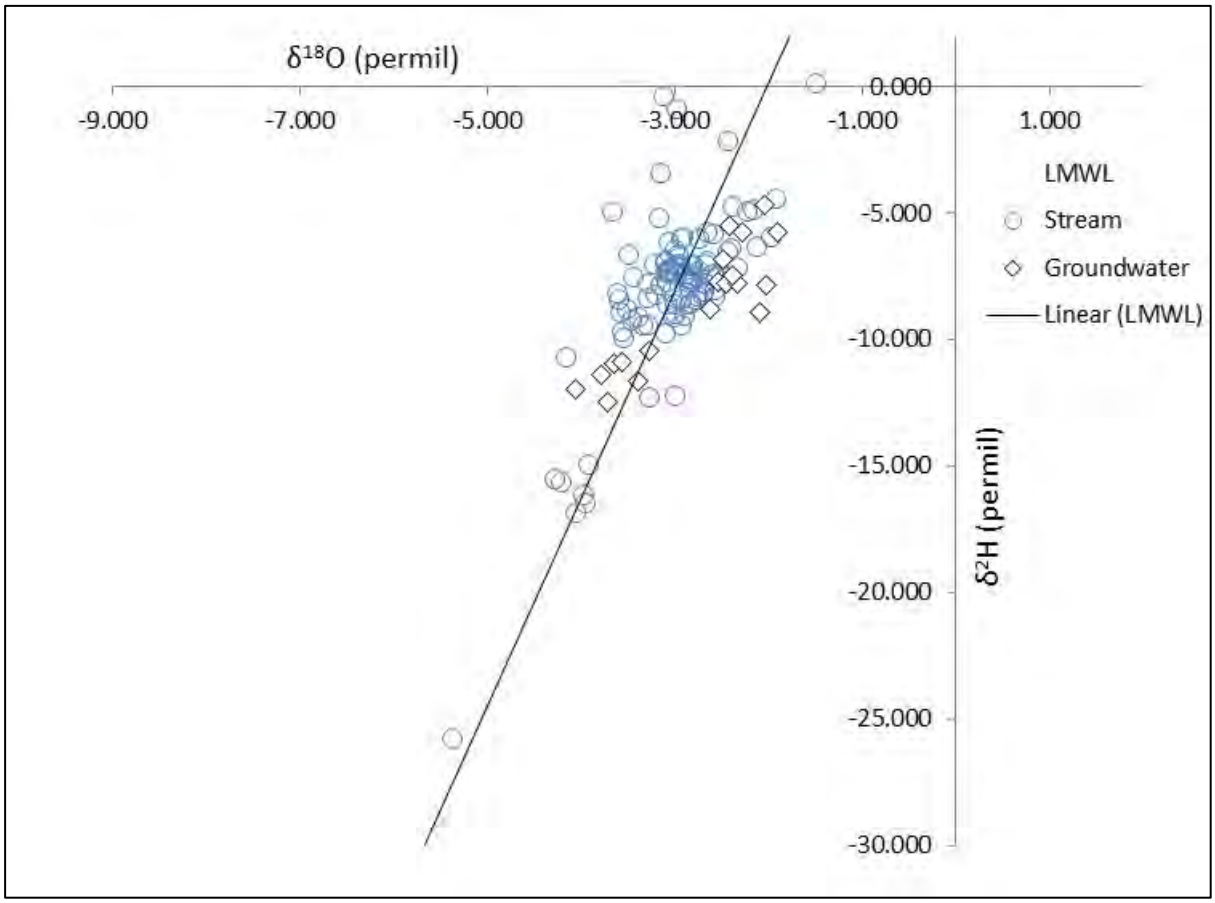

Figure 4.61: Stream signature with groundwater signature

Throughout the year there was a slight fluctuation in the groundwater isotope signature. This is due to seasonal fluctuations in the groundwater table and thus slight depletion of light isotopes towards the end of the dry season from -8‰ to -10‰ (Figure 4.62).

The isotope signature of rainfall varies significantly throughout the year. In South Africa there is a large variation in the rainfall isotope signature due to variations in the kind of rainfall events (cold front/tropical events). The groundwater isotope signature generally lies in the middle of the average rainfall signature and the stream water signature (Figure 4.63). The stream water signature varies throughout the year by main source leaving the catchment comes from groundwater.

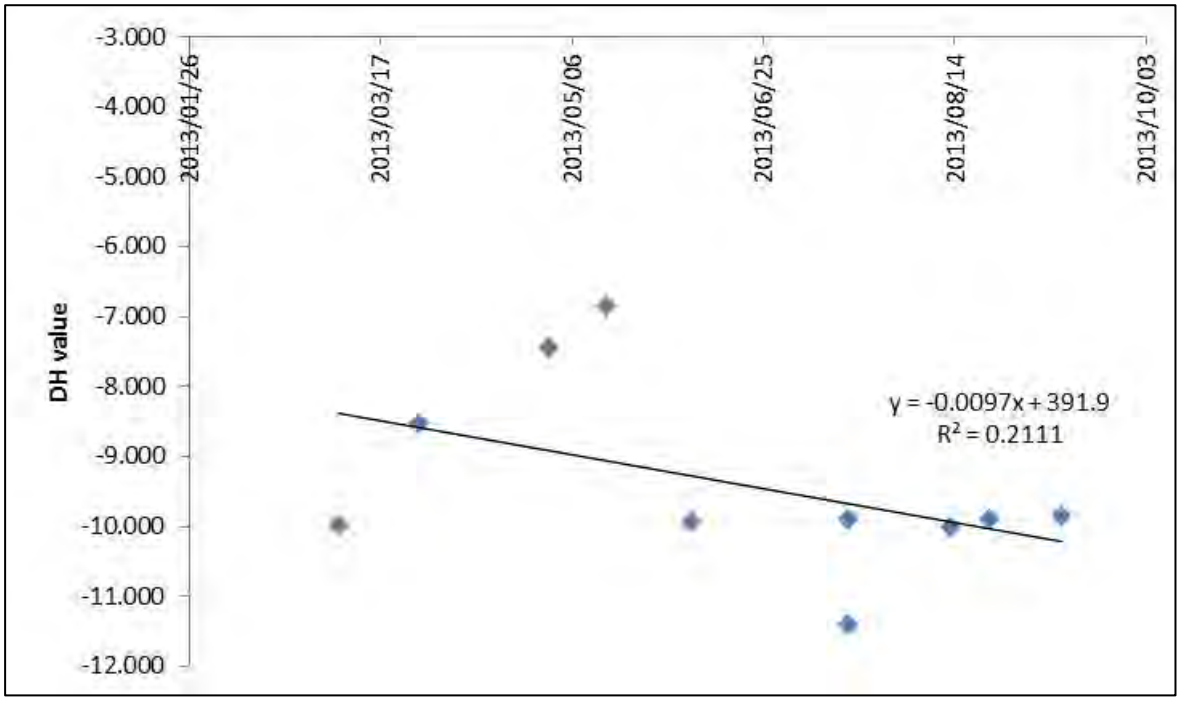

Figure 4.62: Changes in Groundwater DH throughout the year

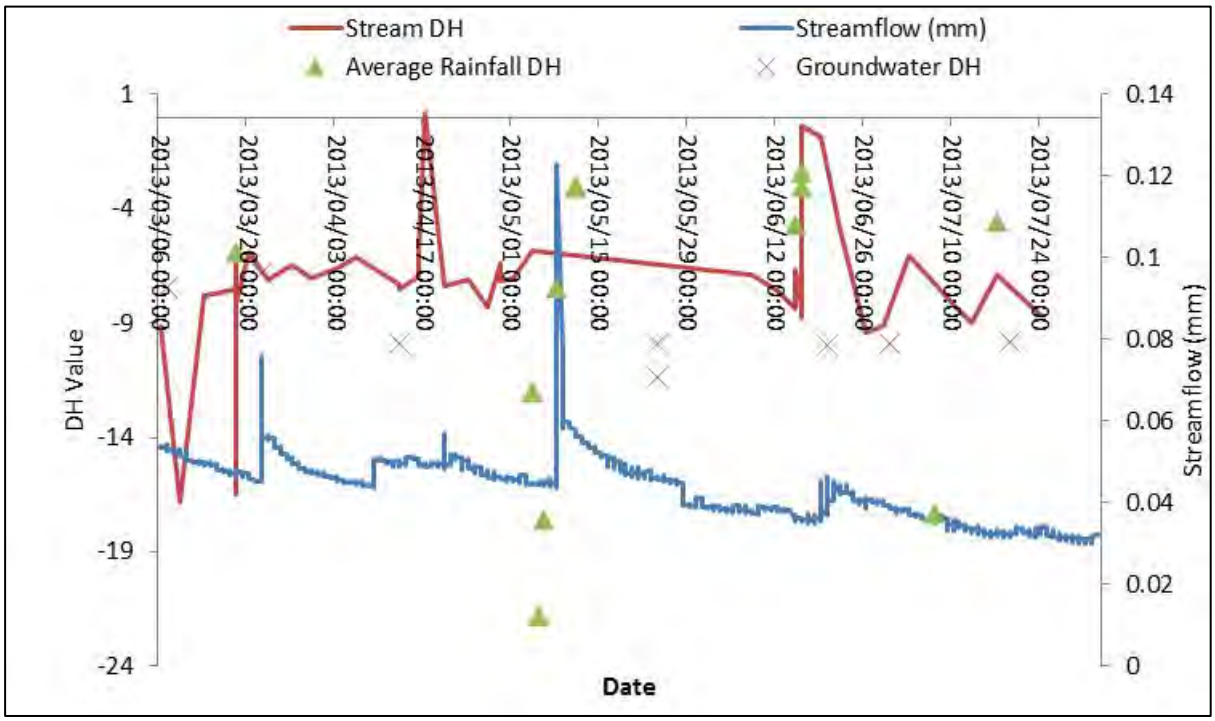

Figure 4.63: Isotope signatures of rain, groundwater and stream water with streamflow record

4.8.1.3 Soil Isotope signature

The isotopic composition of soil water varies with depth down the soil profile. It is generally accepted that the deeper down the soil horizon the more heavier isotopes. During the percolation of large rainfall events, soil water is subject to evaporation, therefore reducing the amount of light fractions. The Rainfall at Two Streams generally lies around the GMWL while groundwater lies lower down on the GMWL. The soil isotope signatures lie to the right of the GMWL suggesting there are more ^{18}O to ^{16}O and more ^{2}H to ^{1}H suggesting that evaporation has taken place (Figure 4.64). On two occasion 23/08/2013 and 13/07/2013 the 2, 2.4 and 1.6 meter soil horizon have the same isotope signature as groundwater (Figure 4.65), suggesting that hydraulic lift has moved groundwater from deeper horizons to this deep for root water uptake (see Figure 4.5 for root mass).

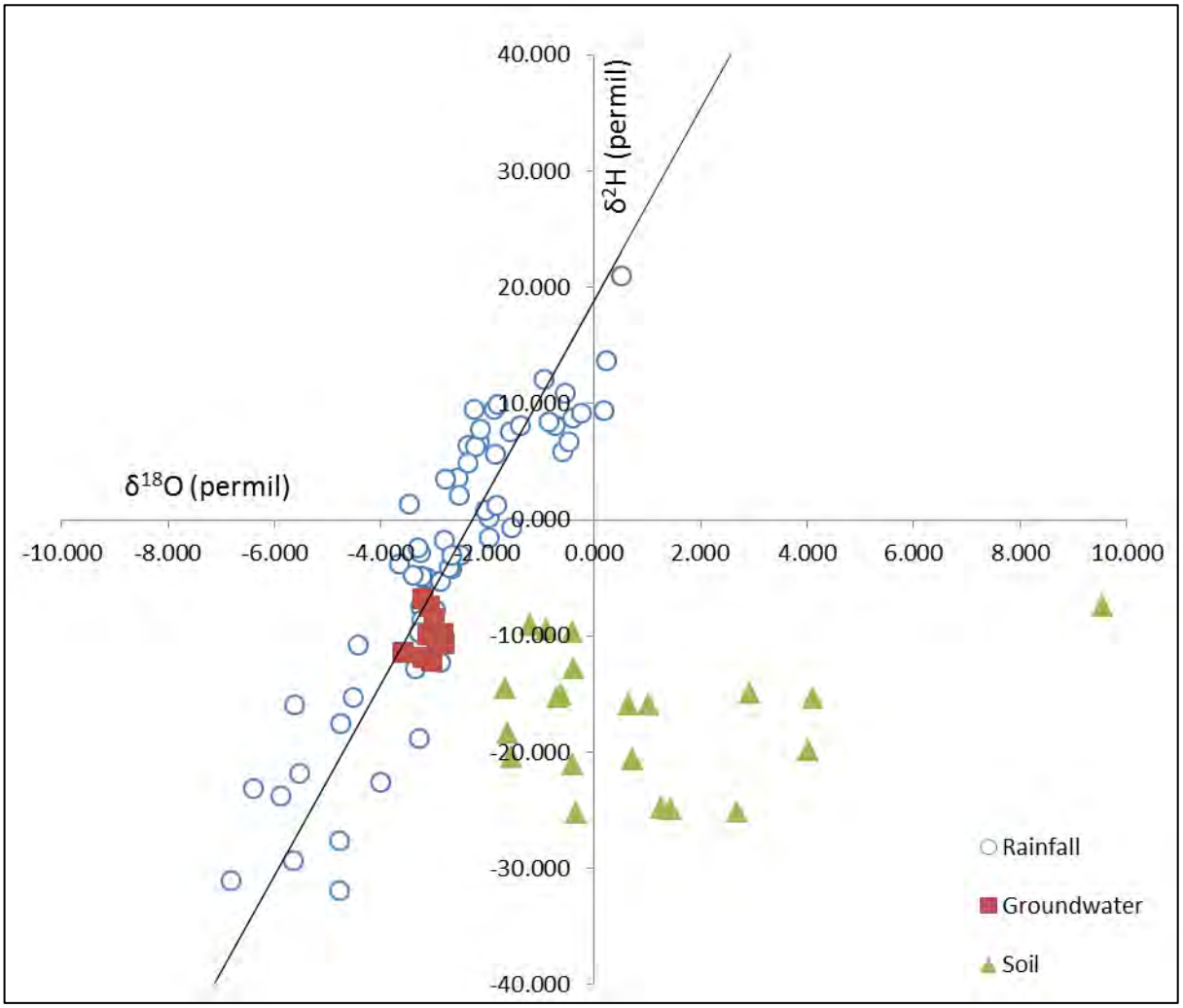

Figure 4.64: Combination of soil, rainfall and groundwater signatures

A possible reason to explain why hydraulic lift had moved groundwater to the 2, 2.4 and 1.6 meter horizons and that the isotope signature of deeper horizons' did not match that of groundwater, was that the existing soil isotope signature mixed with that of groundwater (Figure 4.65), therefore making it hard to identify the groundwater signature.

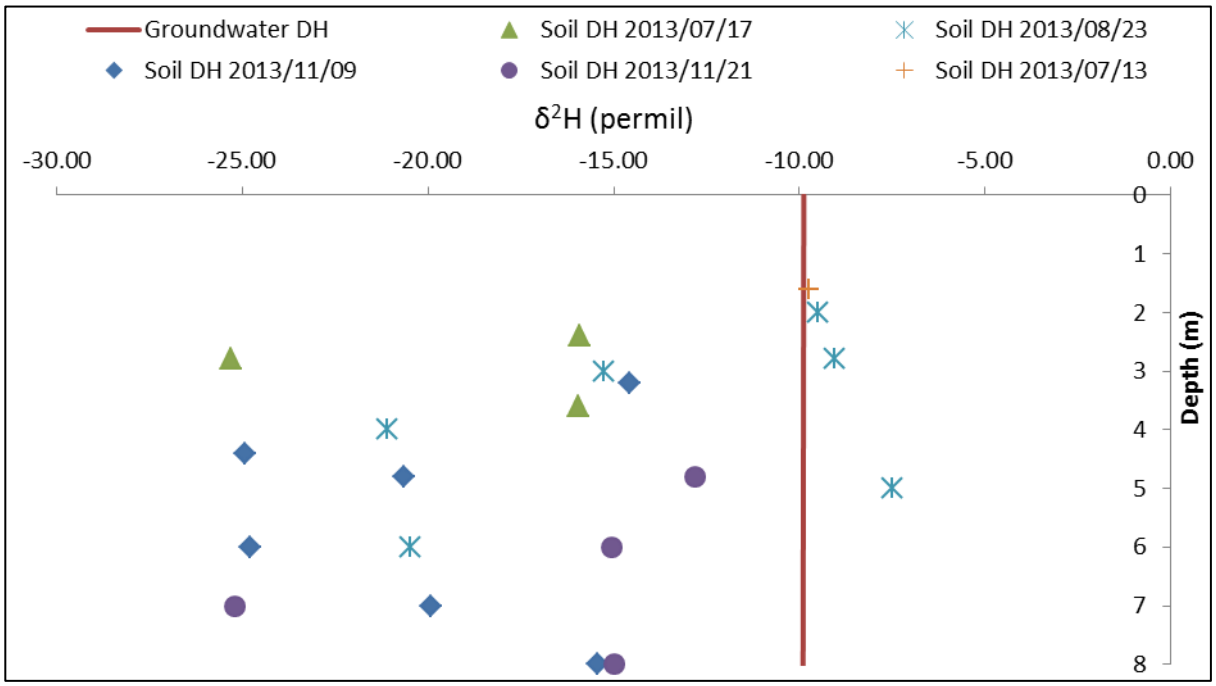

Figure 4.65: Combination of soil and groundwater signatures with depth.

4.9 HYDRUS

The HYDRUS model was run hourly and the outputs from the model are in different time steps to the input data, due to iteration criteria. A scale bar has been provided to indicate the month that the model is analysing.

Table 4.19: Time stamp for HYDRUS simulations

0	1000	2000	3000	4000
01-Jan-13	11-Feb-13	25-Mar-13	6-May-13	16-Jun-13

4.9.1 Infiltration

The output data from HYDRUS suggested that all rainfall that was input into the model infiltrated the soil surface, with there being no runoff. For a forestry catchment it is understandable that the majority of rainfall received is allowed to infiltrate due to the large amount of litter layer present below the canopy.

4.9.2 Root water uptake

HYDRUS was able to simulate actual root water uptake almost identically to input potential root water uptake. Therefore there was enough water in the soil for HYDRUS to simulate root water uptake to a depth of 5 m. Between January (0) and February (1000) there was higher potential and actual transpiration as there was more reference evaporation due to the availability of sunlight during summer times. From late February (1000) to July (4000) actual and potential evaporation are lower due to less reference evaporation as there is less sunlight (radiation) during winter (Figure 4.66 and 4.69).

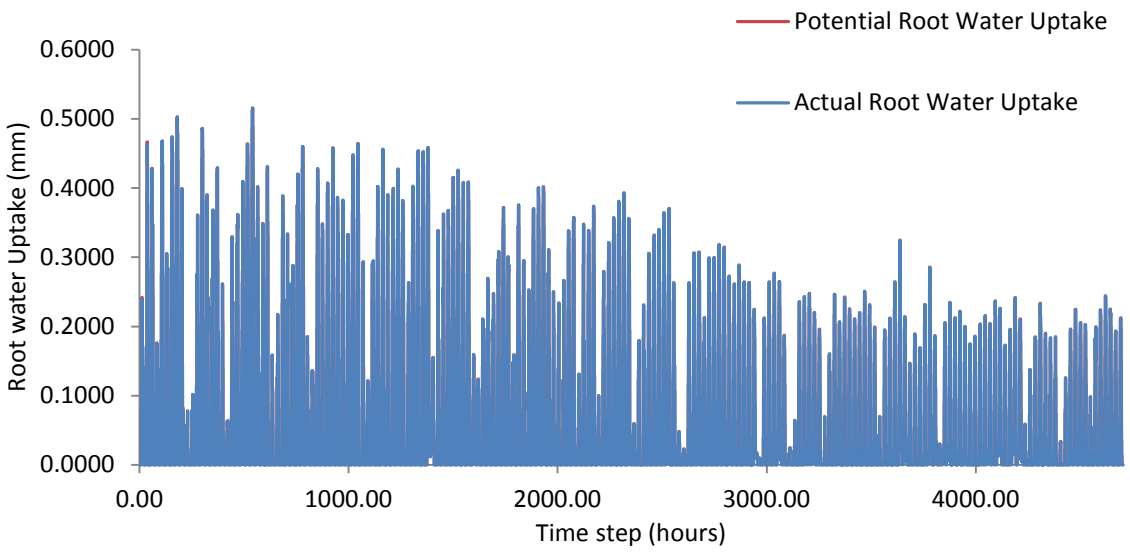

Figure 4.66: Potential and actual root water uptake to depth of 5 m

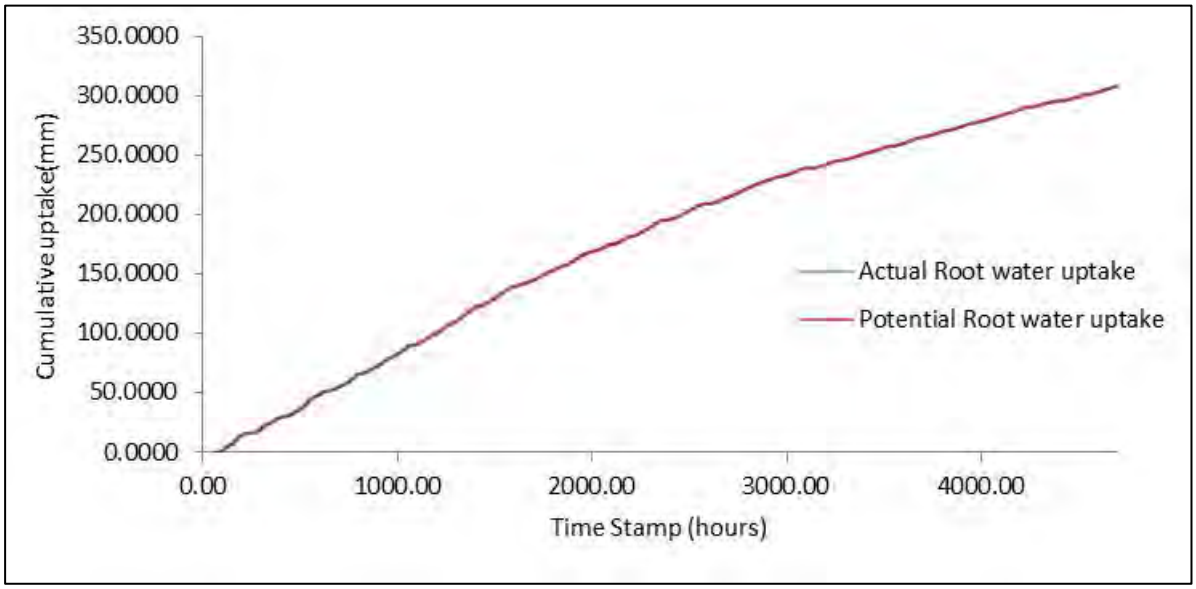

Figure 4.67: Difference between actual and potential root water uptake

The Actual and Potential Root water uptakes are equal to one another which suggest that there is enough water in the soil to allow for maximum uptake (Figure 4.67).

Root water uptake (308 mm) is greater than that of soil evaporation (185 mm). In forestry stands it is understandable that due to the large canopy cover which provides for shading of soil surface and litter there should be little soil evaporation. HYDRUS has simulated a Root water uptake as roughly double that of soil evaporation, which is considerable higher than expected. Potential soil evaporation and Potential Root water uptake was separated using LAI which should account for Evaporation Potential as groundcover is its driving factor. Root water uptake and soil evaporation amounts are similar during the first few days of January (0-100), but deviate considerably after that (Figure 4.68).

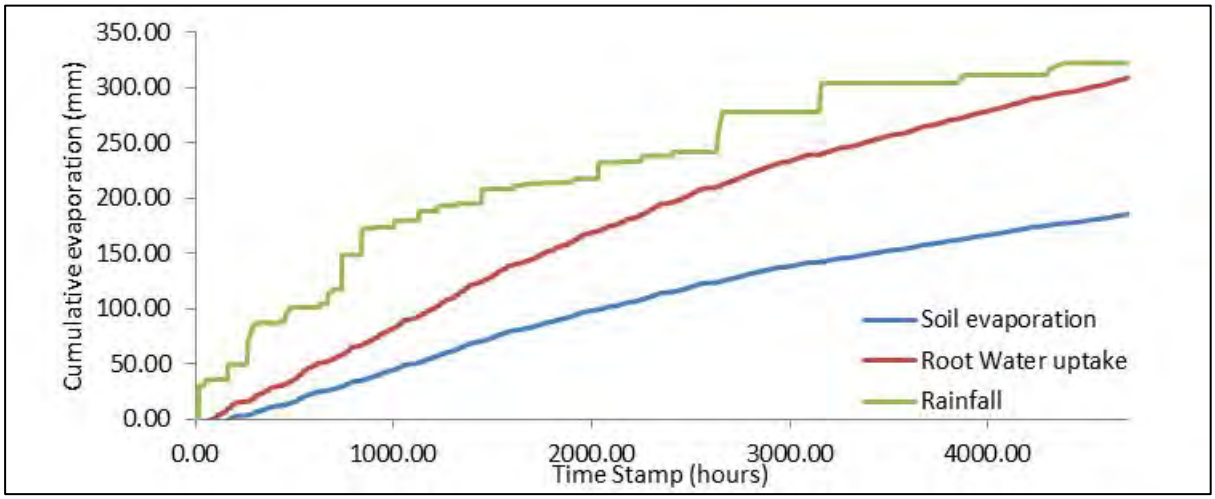

Figure 4.68: Cumulative evaporation with cumulative transpiration

4.9.3 Comparison between ET_{ec} and HYDRUS simulation

Total evaporation from HYDRUS was determined by adding soil evaporation and actual transpiration. There is a difference between measured Eddy co-variance total evaporation and simulated total evaporation from HYDRUS (Figure 13.4). Between January (0) to late February (1000), it was evident that actual total evaporation (Eddy co-variance) and simulated total evaporation (HYDRUS) were lower than that of the incoming rainfall. Simulated soil moisture content suggests that rainfall that is received is unable to contribute to soil moisture content deeper than 0.3 m. HYDRUS simulated no runoff, thus it is presumed that during late January 2013 to late February 2013, water was stored in the top soil horizons.

Actual total evaporation (665 mm) and simulated total evaporation (494 mm) were both greater than rainfall (321 mm). Simulated total evaporation and actual total evaporation measurements were in agreement with one another. A possible reason for HYDRUS simulating more evaporation than input rainfall might be due to the input soil moisture data (Figure 4.69).

Due to the Qr parameter, initial input soil moisture content could not be lower than 19%. The model was run from December 2013 to allow for a warming up of the model and to even out soil moisture contents. Measurements from TDR 100, from 0.4-4.4, do not exceed 30% and usually don't drop below 8%.

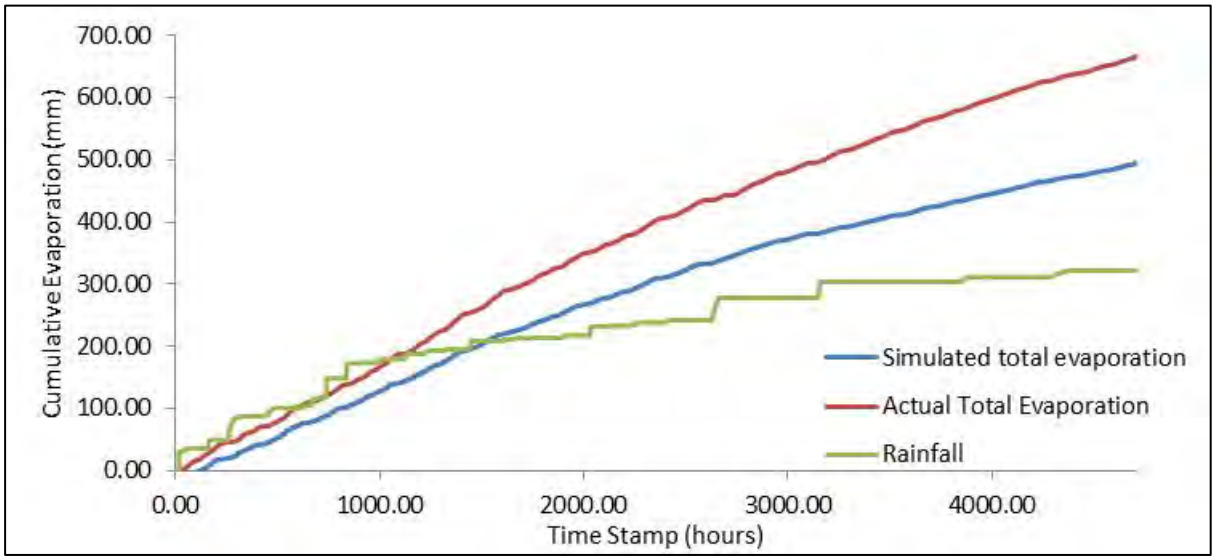

Figure 4.69: A comparison between Simulated Total Evaporation (HYDRUS) and Actual Total Evaporation (Eddy co-variance)

4.9.4 Validation

HYDRUS simulations were validated by comparing measured soil moisture from TDR 100 with those simulated by HYDRUS. The CS616 surface probe at 100 mm was used to compare with the surface observation node of HYDRUS. HYDRUS overestimated soil moisture content but was able to capture soil moisture content trends (Figure 4.70). HYDRUS responded similarly to that of observed CS616 probe but on average HYDRUS overestimated soil moisture content by 20%.

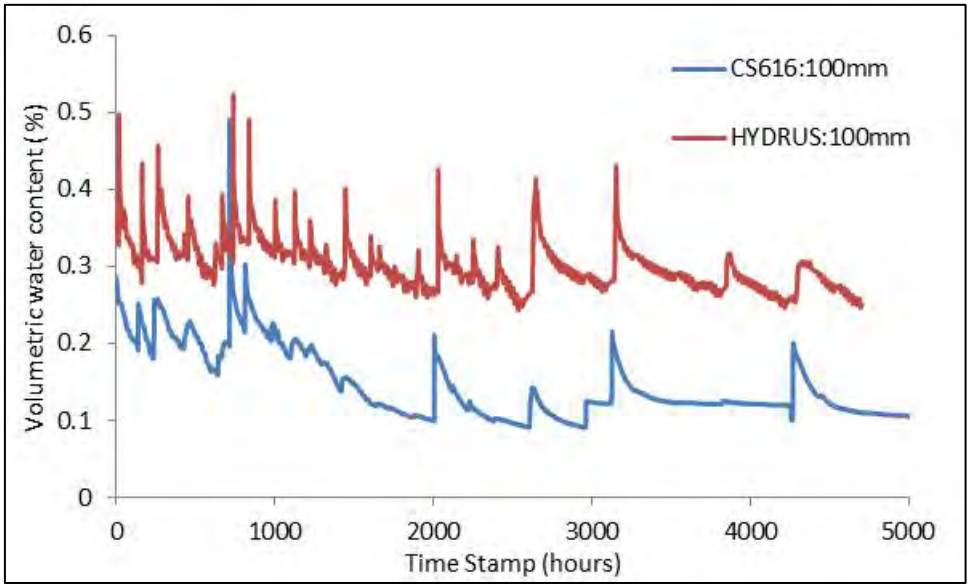

Figure 4.70: Comparison between CS616 surface probe 100 mm and HYDRUS simulation at surface

At a depth of 400 mm, HYDRUS simulated no change in soil moisture content (Figure 4.71). TDR 100 measurements are only available from late February. The initial soil moisture content of 0.19 was simulated for the entire period. Due to residual water content (Qr) (Van Genuchten curve) soil water content could not be lower than 0.19. TDR 100 at 400 mm suggested that there were slight fluctuations in soil moisture content, although there was little change in soil moisture content over the period of analysis (Figure 4.71). One would presume that rainfall would be able to replenish soil moisture stocks during the summer period.

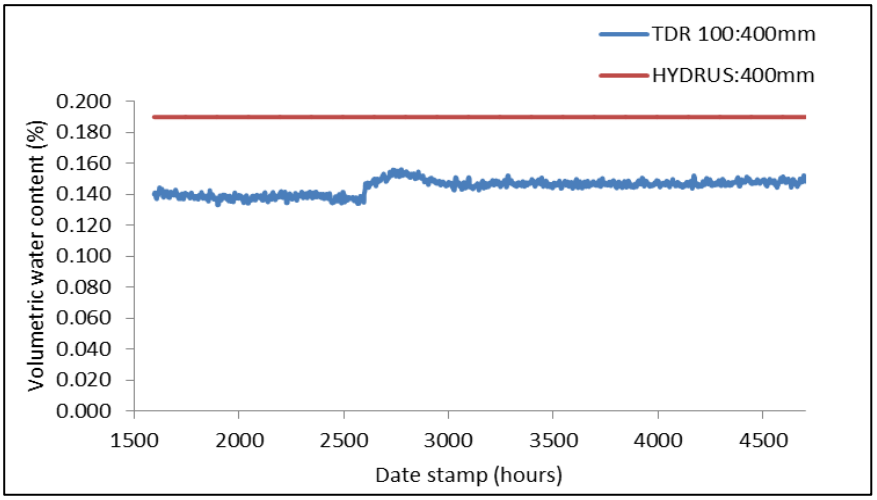

Figure 4.71: Simulated soil moisture content and observed soil moisture content

There were slight fluctuations that were simulated by HYDRUS for soil moisture in the 0.3 m soil horizon. Changes in soil moisture content were evident during the wet season between January (0) and February (1000) in 0.1 m horizon (Figure 4.72). There were slight changes in soil moisture content for 0.2 m and 0.3 m depth, but were time lagged from moisture received in the 0.1 m soil horizon. HYDRUS simulated that all three depths would have a plateau in soil moisture content from April-July 2013.

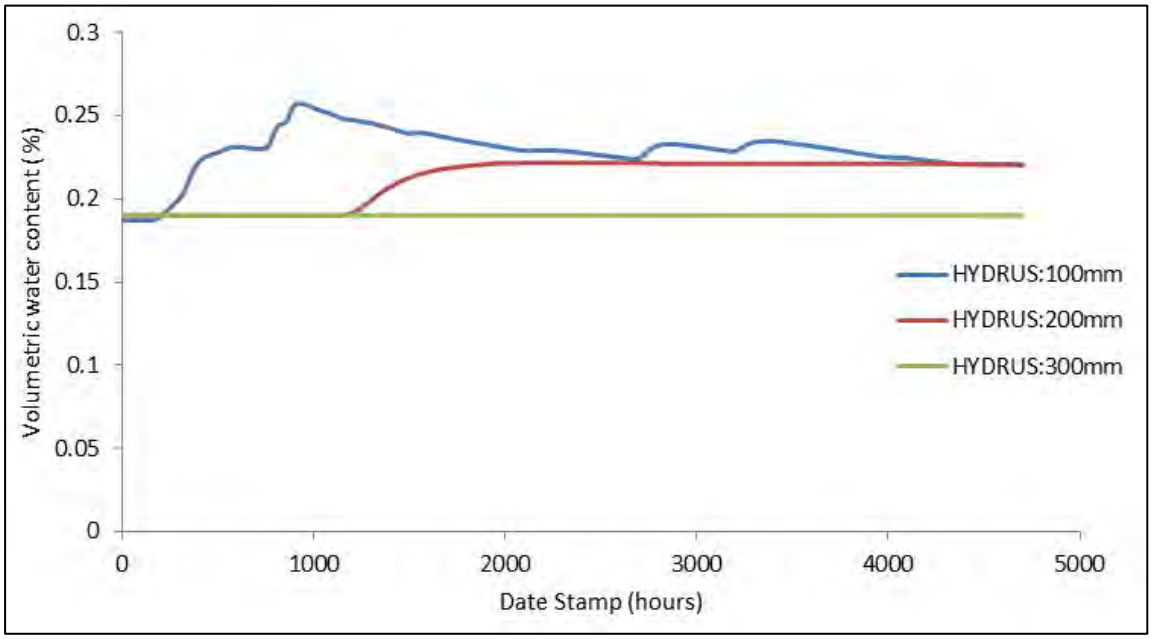

Figure 4.72: HYDRUS simulation of soil moisture content where no probes exist

Simulated soil moisture content was different to that of measured soil moisture content. HYDRUS was able to account for the fluctuation but was unable to get simulated values (0.5-0.3) close to that of observed CS616 values (0.3-0.15). Simulated soil moisture content at 100 mm was generally wetter than that of observed 100 mm CS616 values. Although measured CS616 soil moisture probes do not take into account spatial resolution.

Soil Samples at different depths were taken 5 metres away from the TDR 100 system and oven dried at 100 °C to determine the gravimetric soil moisture content and to not damage cables of the TDR 100 system. TDR 100 readings were on average lower than oven dry soil moisture contents. However, because the samples had to be taken away from TDR 100 system probes the variation observed is reasonable evidence to show the TDR probes were functioning correctly (Figure 4.73).

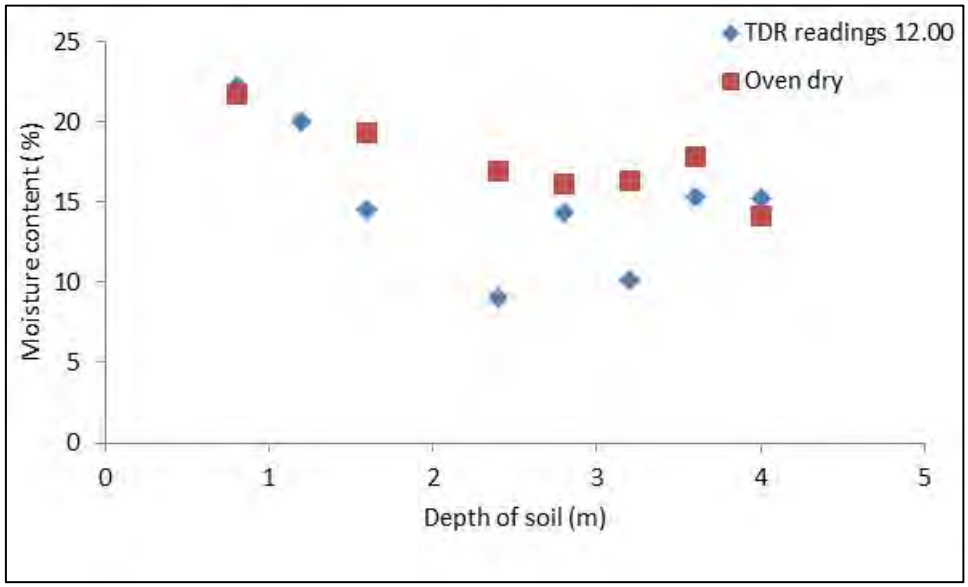

Figure 4.73: Comparison between TDR 100 and Oven dry method

4.10 Conclusion

The rainfall sampler able to differentiate between rainfall events and keep separate samples of different rainfall events was installed. This functioned well and separate samples from different rainfall events and even separate samples during extended rainfall events have been collected. In addition, a glass funnel with a U-tube trap has been inserted into the lids for the bottles to prevent evaporation which alters the isotope signature of the sample. This was particularly important for the rainfall samples which can often be small volumes. The innovation shown in sampling rainfall is likely to be beneficial to future isotope studies and were applied to an automatic streamflow sampling system which was also installed during 2013 at the weir so that samples were collected during events to understand the rapid response mechanisms of the catchment.

Majority of streamflow samples that were more positive than both baseflow samples and rainfall samples, suggesting that the samples were exposed to evaporation as they left the catchment. Although on occasion rainfall was the driving force in streamflow, majority of the water leaving the catchment came from baseflow.

Soil water was extracted successfully using water distillation and thoroughly tested as a technique and found to be more suitable. The soil water was extracted from samples down to 8 m covering the rooting depth of the trees and therefore provides the same isotopic signature as the sapflow. In 2013, the more reliable soil water samples did indicate the presence of groundwater at a depth of 2.0 m, 2.4 m on 23/08/2013 and 1.6 m on the 13/07/2013. Suggesting that the trees were using groundwater on these days for growth as there is a significant amount of rooting material at this depth. There was no other evidence that showed that the trees were using groundwater due to mixing of old rainfall and groundwater in the other soil horizons. The evidence showing that the trees were using groundwater on

the 23/08/2013 and on 13/07/2013 supports the theory by Kuenene (2013) who suggested that there was a large amount of water stored in deep saprolite and could supplement the growth of trees during the dry season.

HYDRUS 1D results showed that the Simulated Total Evaporation was less than that of Actual Total Evaporation (Eddy co-variance), suggesting that Potential evaporation was too low. HYDRUS results showed that using Potential Evaporation to simulate Total Evaporation yielded results less than that of Actual measured Total Evaporation. This was ascribed to the trees using an extra source of groundwater that had not been being accounted for in Potential Evaporation and roots being able to extract water from groundwater. The Simulated Total Evaporation measurement from HYDRUS provides for the amount of evaporation that can take place if rainfall is the only source. The portioning of root water uptake and soil evaporation was done using LAI, although it was assumed that soil evaporation was too high for a forested catchment. Therefore, soil evaporation and root water uptake needed to be partitioned using a different method. Due to the installation of instrumentation there was limitation to the conclusions that could be made from HYDRUS. On days such as 2527 the water content at 100 mm was 0.096, while at 400 mm it was 0.138, thus meaning the soil water tension was much higher at 100 mm than at 400 mm. Therefore fluxes are likely to be upward, but without deep soil water measurements the assumption of upward water movement of groundwater cannot be made.

HYDRUS was not able to simulate deep root water uptake due to the boundary conditions that were specified. The bottom boundary condition of free drainage is unable to allow for upward migration of water, which could very well be occurring. In future research it will be necessary to test a very deep profile to investigate how HYDRUS would simulate the deeper horizons. This would give an indication of the amount of water being drawn from the water table. Simulated Total Evaporation and Actual Evaporation were with agreement with one another throughout the simulations, thus changing the bottom boundary condition would not result in more transpiration due to reference evaporation being too low.

5. SUMMARY AND CONCLUSIONS

Internationally long term catchment studies including actual measurements of all the water balance components are scare, while locally this represents a unique study on the impact of an exotic tree plantation on catchment hydrological processes. The current study has enabled the data record and together with important landuse changes (riparian clearing, clear-felling, thinning, etc.) at Two Streams to be extended to 14 years. The only other long term data set to include actual measurements of *ET* was collected from the Cathedral Peak CVI in *Themeda triandra* dominated grassland in the KwaZulu-Natal Drakensberg (Everson et al., 1998). This study provided a baseline against which the impacts of commercial forestry and other landuses could be assessed. The daily total evaporation values for the *A. mearnsii* trees on cloudless summer days averaged 7 mm. On clear winter days the maximum total evaporation was approximately 2.4 mm day^{-1}. This contrasts with the *Themeda triandra* grassland evaporation rates measured in the Drakensberg of 7 mm in summer and < 1 mm in winter (Everson et al., 1998). It is therefore the difference in the winter *ET* between grasses and evergreen trees that will has the biggest impact on changing the catchment water balance. This will be particularly noticeable during the critical low flow (winter) periods.

During the reporting period, data records such as streamflow, rainfall and total evaporation have been extended and have proven the benefits of long-term monitoring. A 24 m lattice mast, funded by Mondi, was installed to measure above-canopy ET. The ET of the Wattle stand was measured using eddy covariance and surface renewal and found to follow a typical seasonal pattern with higher ET in summer and lower ET in winter. Most significantly, the increasing trend in maximum summer ET rates observed during the first three summer's over the wattle stand in a previous research project has halted, indicating that with maturity, the water-use of the trees has plateaued. The surface renewal system has rarely been used above trees and the calibration of the weighting factor, at a height of 19 m above the ground, is a useful result.

The previous report on the Two Streams catchment (Clulow *et al.,* 2011) showed that the *A. mearnsii* plants at Two Streams transpired at rates that were close to the Priestley-Taylor potential rate of evaporation (i.e. there was no evidence of reduced transpiration). The most plausible adaptation of the *A. mearnsii* trees to account for the high rates of ET was ascribed to the development of deep roots that can access alternative sources of water. In the previous study the annual *ET* of the actively growing *A. mearnsii* was 1156 mm and 1171 mm and the rainfall 689 mm and 819 mm for 2007 and 2008 respectively and there was obviously a negative imbalance between the rainfall and *ET*. The present study has continued to demonstrate the impact of the deep rooted trees on sourcing water from the deep soil profile and groundwater and shown that the average annual unaccounted losses estimated through the catchment water balance in the catchment are 395 mm yr^{-1} over the 7 year period from 2006 to 2013.

The long-term runoff:rainfall relationship has changed significantly each year from 2001 to 2013 with felling and planting cycles confirming that the commercial forestry at Two Streams has had an impact on streamflow. For example, the runoff:rainfall relationship (Rr) was 0.02 prior to clear-felling of the catchment in 2004. Following clear-felling the Rr increased to 0.08. This indicated increased runoff during the two year fallow period and the first two years of wattle tree development. The replanting of the

catchment at the end of 2006 is evident from the runoff:rainfall relationship since 2009 which decreased to 0.06. It further decreased to 0.04 and 0.02 in 2010 and 2011 respectively with a slight increase to 0.03 in 2012 and increased further to 0.05 in 2013 as the growth rate and water requirements of the trees slowed with maturity. Forest management practices therefore have significant impacts on catchment water yields. The impact of clearing the riparian vegetation followed by clear-felling the catchment in 2004, resulted in a total gain in streamflow of 235 mm by January 2009. At the end of 2013 the total gain was estimated as 290 mm.

The interception studies conducted at Two Streams showed that interception plays a very important role in the forest hydrological cycle, with only 65.7% of gross precipitation being available water that drains to the soil, after the losses due to canopy and litter interception under various commercial forestry species. Canopy interception by *A. mearnsii* accounted for losses of 27.7% of gross precipitation between April 2008 and March 2011. In addition, litter interception accounted for losses of 6.6%.

Due to the seasonal nature of the rainfall and mist in the Two Streams area, stemflow was monitored over a winter period (mist unlikely) and a spring period (mist highly likely). The rainfall during the winter period was unfortunately low and only two events of 2.1 and 1.6 mm occurred in which the percentage of stemflow converted to rainfall varied between 1.3% and 28.3%.The influence of stem thickness was evaluated and found that in most cases the trees with the thicker stem resulted in a higher stemflow depth.

During the spring period, seven separate rainfall events of varying length (one to three days) occurred between 11 September and 18 October 2013. The stemflow from three trees resulted in percentage rainfall to stemflow conversion of between 39% and 50%. At the lower site, the thicker stem (50%) was higher than the thinner stem (39%) which is in agreement with the results of the winter period. However, the percentage rainfall converted to stemflow was higher than in winter. This could be due to the prevalence of mist in this Midlands Mist-belt area. Mist, preceding rainfall, condensing on the leaves and stems of the trees, could fill the storage capacity of the leaves and stems, resulting in higher immediate rainfall to stemflow conversion at the onset of the rainfall event. Mist during rainfall events would add to the stemflow but is not measured by the standard raingauge used and therefore not accounted for in the water balance. The results have highlighted the importance of taking into account all the interception processes when attempting to account for losses and gains in effective rainfall.

Different sapflow techniques were evaluated and the heat ratio method determined to be most suitable for measuring tree transpiration in the Two Streams catchment. Four systems were installed in different slope positions. The tree transpiration was much higher on the high radiation (hot) North-facing slope than on the cooler South aspect. Over the nine months of measurement, the accumulated North-facing transpiration at the upper site was 941 mm and at the lower site, 1097 mm. Over the same period at the south facing slope the transpiration was 463 mm and 617 mm at the upper and lower slopes respectively. The results of tree transpiration measurements have shown that the *Acacia mearnsii* tree water use is highly variable with respect to both aspect and slope position and highlights the importance of accounting for this spatial variability in the catchment water balance and hydrological models.

Over the 2012-2013 hydrological year, a comparison of the ET_{ec} and tree transpiration at the upper south site where the eddy covariance mast was situated, revealed totals of 1157 mm and 1076 mm respectively. The 81 mm increase in the total evaporation compared to the tree transpiration is attributed to soil and litter evaporation not measured by the heat pulse velocity technique. Soil and litter evaporation therefore represented about 8% of the total evaporation in the wattle plantation.

The conceptual groundwater hydrological model has shown that the deeper soil represents the deep weathering of the bedrock surface and the fractured basement rock which are dominant factors governing the flow paths in the catchment. The water flow is likely to be horizontal, lateral and upward. The tree root systems may affect the groundwater by decreasing the recharge by extracting water from the unsaturated zone. The horizontal flow is minimal due to pathways formed by tree roots which favour the lateral flow. There are two aquifer systems in the catchment, shallow and deeper aquifer systems. The lateral flow is restricted at the bedrock and only occurs in fractures. Therefore, water ponds on the bedrock surface and leaks through granite fractures to recharge the deep aquifer. There is no evidence of tree roots extracting groundwater from the deep aquifer at this stage. There are artesian conditions in the borehole located at the bottom of the catchment, due to the fact that it intersects the water table that is trapped under pressure between impermeable layers (confining layers).

The electrical conductivity of the groundwater was fairly constant throughout the water column profiles of the boreholes. An increase was observed at the granite basement and increased with depth into the granite. This was because the chemical composition of granite consists of salts such as potassium. The slow groundwater movement has allowed the salts in the granite to ionise, increasing the electrical conductivity. The surface water EC was lower as there has been less time for inert materials to ionise.

The temperature profiles within the boreholes were fairly constant throughout the water column, though a slight increase of 1°C was observed from 50 mbgl in all the boreholes. A spike of 19°C was observed at 35 mbgl in the centre borehole (2STBH1).

The total alkalinity of all the samples taken from the boreholes ranged between 65 mg/l and 82 mg/l. The most important components of alkalinity are carbonates, bicarbonates and hydroxide of which the carbonate and hydroxide disappear at pH between 4.3 and 8.3. Since the pH in all samples ranged between 6.2 and 8.3, the bicarbonate is the only dominant compound contributing to the total alkalinity. The low alkalinity concentrations are associated with water flowing through felsic igneous rock, which are insignificant sources of carbonates. The water has an average pH of 7.2 suggesting that the water at Two-Streams is slightly alkaline, therefore a lot of acid will be required before the pH drops to unacceptable limits. Based on these results it can be concluded that the catchment has a good buffering capacity.

The electrical conductivity (EC) within the boreholes ranged from 15.8 mS/m to 25.8 mS/m, whereas the total dissolved solids (TDS) ranged from 92 mg/l to 144 mg/l. According to DWA (1996), water with EC less than 70 mS/m and TDS less than 450 mg/l is good quality water with no negative health effects associated.

The water samples showed low redox potential (Eh) in all the samples ranging between -64.8 mV and 14.5 mV. All values were negative except for the north corner borehole which showed a maximum value

of 14.5 mV. The negative Eh values reflect more educing conditions and thus anaerobic conditions and unpolluted water.

The TDR probes for measuring volumetric water content in the soil profile to depths of up to 4.8 m have been modified and improved. Long cable lengths combined with short waveguides (0.075 m) resulted in signal noise from the previous probes. The cable quality has been improved and the wave guides extended to 0.15 m.

Isotope samples provided information on the water pathways within the catchment. Exploratory sampling during the summer of 2012 (January to March) and winter of 2012 (August) brought to light some of the difficulties in sampling procedures particularly sap and soil water sampling. Extracting sap samples for isotope analysis proved to be a challenging component of the project. Hydrocarbons in the sap resulted in sample analysis difficulties and erroneous results at times. When the trees were water stressed in winter, a higher concentration of hydrocarbons were present in the sap samples collected due to the high pressures at which the samples were extracted. This resulted in analysis error caused by the presence of hydrocarbons and low injection volumes due to the high viscosity of the sap. When extracting xylem sap using the Scholander pressure bomb it was found that using the bomb at lower pressures resulted in a lower hydrocarbon content in the sample which improved results slightly. However, further research is required to improve sample extraction from tree sap.

During 2012, a basic rainfall sampler was used resulting in the mixing of rainwater from rainfall events. During 2013, an advanced rainfall sampler able to differentiate between rainfall events and keep separate samples of different rainfall events was installed. This functioned well and separate samples from different rainfall events and even separate samples during extended rainfall events have been collected. In addition, a glass funnel with a U-tube trap has been inserted into the lids for the bottles to prevent evaporation which alters the isotope signature of the sample. This was particularly important for the rainfall samples which can often be small volumes. The innovation shown in sampling rainfall is likely to be beneficial to future isotope studies and improvements to the system were subsequently applied to an automatic streamflow sampling system which was also installed during 2013 at the weir so that samples were collected during events to understand the rapid response mechanisms of the catchment.

In 2013, soil water extraction was used in place of tree sap to determine the link between tree water use and groundwater. Soil water was extracted successfully using water distillation and thoroughly tested as a technique and found to be more suitable than extracting tree sap due to the problems discussed above. The soil water was extracted from samples down to 8 m covering the rooting depth of the trees and therefore provides the same isotopic signature as the sapflow. However, the sap samples from the winter of 2012, although difficult to interpret due to the analysis problems, indicated that the sap was comprised of groundwater and rainwater.

The research site has been an integral part of the Hydrology courses offered at the University of KwaZulu-Natal. Undergraduate field excursions have offered practical exposure of field techniques to students and a number of postgraduate studies are based in the Two Streams catchment. In addition, it has encouraged collaboration with the University of the Free State who utilizes the research catchment for postgraduate studies.

In this study, the impact of *A. mearnsii* on soil hydrological processes was extended with additional detailed measurements of evaporation and soil water processes and expanded to include isotope, groundwater and rainfall interception studies to improve our understanding of processes such as low flows and deeper soil water dynamics. The ever-growing demand for water makes it imperative that water resource management procedures and policies be wisely implemented and improved. To do this we need to advance our understanding of the impact of different crops on the water balance of catchments. The Department of Water Affairs and Forestry is deeply concerned by the need to link afforestation schemes to low flows in streams and rivers, since the allocation of land use and re-allocation (changes in land use) depend on accurate estimates of tree water use impacts on low flows and ground water resources (Jewitt *et al.*, 2009). In addition, allocation of water to stream flow reduction activities must also take into account the difference in water use between forests and other crops and natural vegetation.

These long-term hydrological studies in the Two Steams catchment, which included detailed process measurements, need to be continued to quantify the effects of the continued growth of the *A. mearnsii* trees followed by the replanting of *Eucalyptus* species on the catchment water balance and to document the response to impending global climatic change. Finally, the measurements together with hydrological models, which were shown to need further improvement, should be used together with satellite observations to up-scale the information across much wider areas.

6. CAPACITY BUILDING AND COMPETENCY DEVELOPMENT

The Two Streams catchment is used as a field laboratory for numerous post-graduate students at the University of KwaZulu-Natal and Free State University. It provides an ideal research ground for students in the interdisciplinary fields of soil and hydrological processes studies. The research at Two Streams is an ideal showcase for forestry research in South Africa and is used for the third year Hydrology (UKZN) field trip for 35 students.

Name	Surname	Degree	Research field
Alistair	Clulow	Phd	Water and carbon fluxes over different vegetation types
Andrew	Watson	Honours/MSc.	The use of Environmental Isotopes to determine the source of water used by an *Acacia mearnsii* (Black Wattle) strand in KwaZulu-Natal
Bataung	Kuenene	Phd	Hydropedology of the hillslopes of the Two Streams catchment in the KwaZulu-Natal province
Caiphus	Ngubo	MSc	The impacts of *Acacia mearnsii* plantations on fractured rock aquifer systems, with reference to the Two Streams catchment, Seven Oaks, KwaZulu-Natal
Hartley	Bulcock	Phd/Post Doc	Canopy and litter interception in commercial forest plantations in the KwaZulu-Natal Midlands
Javed	Hoosen	Honours	A study of impacts of change in forest genus and climate change on water resources in the Two streams catchment
Matthew	Becker	Honours/MSc	Tree water-use in different topographic positions in the landscape
Michael	Mengistu	Post Doc	Surface renewal over tall plant canopies
Shaeden	Gokool	Honours	Modelling total evaporation in the Two Streams catchment using remote sensing
Zakariya	Nakhooda	Honours	The impact of stemflow on the water-balance of the Two Streams catchment
Siphiwe	Mfeka	Technical	Field Technician

7. CONFERENCE AND PAPER OUTPUTS

1. Becker M.G., Clulow A.D., Everson C.S., 2012. Tree Water-use in Different Topographic Positions in the Landscape. SANCIAHS 2012.

2. Bulcock, H.H. and Jewitt, G.P.W. 2012. Modelling canopy and litter interception in commercial forest plantations in South Africa. *Hydrology and Earth Systems Science* 16, 4693-4705, 8293-8333.

3. Bulcock, H.H. and Jewitt, G.P.W. 2012. Field data collection and analysis of canopy and litter interception in commercial forest plantations in the KwaZulu-Natal Midlands. *Hydrology and Earth Systems Science*, 16, 3717-3728.

4. Clulow, A. and Everson, C.S., Draft. The impact of deep rooted trees on the water balance of an *Acacia mearnsii* catchment. For submission to: Water SA

5. Everson, C.S., Clulow, A., Draft. The effect of riparian zone management on streamflow in an of *Acacia mearnsii* catchment in the KwaZulu-Natal midlands of South Africa. For submission to: WaterSA

6. Kuenene, B.T., le Roux, P.A.L. and Everson, C.S., 2012. Hydraulic Conductivity and Macroporosity of Diagnostic Horizons in the Two Streams catchment. SANCIAHS 2012.

7. Watson, A., 2012. The use of Environmental Isotopes to determine the source of water used by an *Acacia mearnsii* (Black Wattle) stand in KwaZulu-Natal during the wet-season. SANCIAHS 2012.

8. REFERENCES

Aboal, JR., Morales, D., Hernandez, M. and Jimenez, MS. 1999. Measurement and modelling of the variation of stemflow in a laurel forest in Tenerife, Canary Islands. *Journal of Hydrology*, 221: 161-175.

Allen, RG., Pereira, LS., Raes, D. and Smith, M. 1998. Crop Evapotranspiration (Guidelines for Computing Crop Water Requirements). *FAO Irrigation and Drainage Paper*, 56: FAO, Water Resources, Development and Management Service, Rome, Italy.

Allen, RG., Pereira, LS., Raes, D. and Smith, M. 1998. Crop Evapotranspiration (Guidelines for Computing Crop Water Requirements). *FAO Irrigation and Drainage Paper*, 56: FAO, Water Resources, Development and Management Service, Rome, Italy.

Allen, RG., Pruitt, WO., Wright, JL., Howell, TA., Ventura, F., Snyder, R., Itenfisu, D., Steduto, P., Berengena, J., Yrisarry, JB., Smith, M., Pereira, LS., Raes, D., Perrier, A., Alves, I., Walter, I. and Elliott, R. 2006. A recommendation on standardized surface resistance for hourly calculation of reference ET_o by the FAO56 Penman-Monteith method. *Agricultural Water Management*, 81: 1-22.

Allen, RG., Walter, IA., Elliott, R. and Howell, T, Itenfisu D, Jensen M(ed.), 2005. The ASCE standardized reference evapotranspiration equation. Environmental and Water Resources Institute of the American Society of Civil Engineers Task Committee Report.

Baloutsos, G., Bourletsikas, A. and Baltas. E, 2010. Interception, throughfall and stemflow of maquis vegetation in Greece. *WSEAS Transactions on Environment and Development,* 1(6): 21-32.

Benyon, RG. 1999. Nighttime water use in an irrigated *Eucalyptus grandis* plantation. *Tree Physiol.* 19:853-859.

Burgess, SO., Adams, MA., Turner, NC., Beverly, CR., Ong, CK., Khan, AAH. and Bleby, TM. 2001. An improved heat pulse method to measure low and reverse rates of sap flow in woody plants. *Tree Physiology* 21: 589-598.

Campbell Scientific, Inc. 2004. *TDR100 Instruction Manual*. 815 West 1800 North, Logan, Utah, USA, 84321-1784. pp. 48.

Clulow, A.D., Everson, C.S., and Gush, M.B. 2010. The long-term impact of *Acacia mearnsii* trees on evaporation, streamflow and ground water resources. Final Report to The Water Research Commission K5/1682.

Crockford, RH. and Richardson, DP. 1987. Factors affecting the stemflow yield of a dry sclerophyll eucalypt forest, a *Pinus radiata* plantation and individuals trees within a forest. Technical Memorandum 87/11 September 1987. CSIRO Institute of Natural Resources and Environment, Division of water resources research, Canberra.

Crockford, RH. and Richardson, DP. 2000. Partitioning of rainfall into throughfall, stemflow and interception: effect of forest type, ground cover and climate. *Hydrological Processes*, 14: 2903-2920.

Dansgaard, W. 1964. Stable isotopes in precipitation. *Tellus*. 16: 436-468.

Dimkic, M., Brauch, H-J. and Kavanaugh, M. 2008. Groundwater Management in Large River Basins. IWA Publishing, London.

DWAF, 2005. Department of Water Affairs and Forestry, South Africa. Groundwater Resource Assessment. Phase II. Methodology. Groundwater-Surface Water Interactions. Department of Water Affairs and Forestry, Pretoria.

Dye, P.J., Soko, S. and Poulter, AG. 1996. Evaluation of the heat pulse velocity method for measuring sap flow in *Pinus patula*. *J. Exp. Bot*. 47:975-981.

Dye, PJ. and Olbrich, BW. 1993. Estimating transpiration from 6-year-old *Eucalyptus grandis* trees: development of a canopy conductance model and comparison with independent sap flux measurements. *Plant, Cell & Environment*: 16, 45-53.

Ehleringer, J. and Osmond, C. 1989. Stable isotopes, In: Pearcy RW, Ehleringer JR., Mooney HA, Rundel PW (Eds.), Plant Physiology Ecology: Field Methods and instrumentation, Chapman and Hall Ltd., London, pp.281-300.

Everson, CS., Gush, M., Moodley, M., Jarmain, C., Govender, M. and Dye, P. 2007. Effective management of the riparian zone vegetation to significantly reduce the cost of catchment management and enable greater productivity of land resources. *Water Research Commission Report* No. 1284/1/07. Water Research Commission, Pretoria, RSA.

Everson, CS., Gush, MB., Moodley, M., Jarmain, C., Govender, M. and Dye. P. 2007. Effective management of the riparian zone vegetation to significantly reduce the cost of catchment management and enable greater productivity of land resources. Water Research Commission Report No. 1284/1/07, ISBN 978-1-77005-613-8, Pretoria, South Africa.

Everson, CS., Molefe, GL. and Everson, TM. 1998. Monitoring and modelling components of the water balance in a grassland catchment in the summer rainfall area of South Africa. Water Research Commission Report No. 493/1/98, Pretoria, South Africa.

Everson, T.M., Everson, C.S. and Zuma, KD. 2007. Community Based Research on the Influence of Rehabilitation Techniques on the Management of Degraded Catchments. *Water Research Commission Report* No. 1316/1/07. Water Research Commission, Pretoria, RSA.

Feddes, RA., Kowalik, PJ. and Zaradny, H. 1978. Simulation of field water use and crop yield. Centre for Agricultural Publishing and Documentation, Wageningen.

Gao, W., Shaw, RH. and Paw U, K T. 1989. 'Observation of Organized Structure in Turbulent Flow Within and Above a Forest Canopy'. *Boundary-Layer Meteorol*. 47,349-377.

Gat, J. 2010. Isotope Hydrology: A study of the Water cycle. Imperial College Press, Covent Garden, London.

Gerrits, AMJ. 2010. The role of interception in the hydrological cycle, VSSD, Delft, The Netherlands.

Gush, MB. 2008. Measurement of water-use by *Jatropha curcas L*. using the heat pulse velocity technique. *Water SA*, Vol. 34 (5): 579-583.

Hachmann, JW. 2011. In-situ measurements of saturated and unsaturated hydraulic conductivity in soils of granite hillslopes in the Kruger National Park, South Africa: a preliminary study. Thematic Research Project Ecohydrology, code 450135, 12 ECTS. South Africa.

Hanchi, A. and Rapp, M. 1997. Stemflow determination in forest stands. *Forest Ecology and Management,* 97: 231-235.

Helvey, JD. 1964. Rainfall interception by hardwood forest litter in the southern Appalachians, U.S. Forest Serv. Southeast. *Forest Expl. Sla. Res.Paper S*.

Hewirtz, ST. 1986. Infiltration-excess caused by stemflow in a cyclone-prone tropical rainforest. *Earth Surface Process Landforms*, 11: 401-412.

Kuenene, BT., Van Huyssteen, CW., Le Roux, PAL., Hensley, M. and Everson, CS. 2011. Facilitating interpretation of Cathedral Peak VI catchment hydrograph using soil drainage curves. *S. Afr. J. Geol.* 114:525-534. 114.3-4.525.

Levia, DF. and Frost, EF. 2002. A review and evaluation of stemflow literature in the hydrologic and biogeochemical cycles of forested and agricultural ecosystems. *Journal of Hydrology*, 274: 1-29.

Ling-hao, L. and Peng, L. 1998. Throughfall and nutrient depositions to soil in a subtropical evergreen broad-leaved forest in the Wuyi Mountains. *Journal of Environmental Sciences,* 10(4): 426-432.

Lorentz, SA., Bursey, K., Idowu, O., Pretorius, C. and Ngeleka, K. 2007. Definition and up-scaling of key hydrological processes for application in models. Report No. K5/1320. Water Research Commission, Pretoria, South Africa.

Lu, P., Urban, L. and Ping, Z. 2004. Granier's thermal dissipation probe (TDP) method for measuring sap flow in trees: Theory and practice. *Acta Botanica Sinica* 46(6) 631- 646.

Marshall, D.C. 1958. Measurement of sap flow in conifers by heat transport. Plant Physiology, 33:385-396.

Mengistu, MG. and Savage, MJ. 2010. Surface renewal method for estimating sensible heat flux *Water SA* Vol. 36 No. 1.

Mualem, Y. 1976. A new model for predicting the hydraulic conductivity of unsaturated porous media. *Water Resources Research*, 12(3): 513-522.

Mucina, L. and Rutherford, MC. 2006. The Vegetation of South Africa, Lesotho and Swaziland. *Strelitzia 19*, South African National Biodiversity Institute, Pretoria, South Africa.

Paw U, KT., Brunet, Y., Collineau, S., Shaw RH., Maitani, T., Qui, J. and Hipps, L. 1992. On coherent structure in turbulence within and above agricultural plant canopies. *Agric. For. Meteorol*. 61 55-68.

Paw U, KT., Qui, J., Su, HB., Watanabe, T. and Brunet, Y. 1995. Surface renewal analysis: a new method to obtain scalar fluxes. *Agric. For. Meteorol*. 74 119-137.

Paw U, KT., Snyder, RL., Spano, D. and Su, HB. 2005. Surface renewal estimates of scalar exchange. In: Hatfield JL and Baker JM (eds.) *Micrometeorology in Agricultural Systems. Agronomy Monograph*. No. 47. 455-483.

Pretorius, JJ. 2012. Isotope analysis report. School of Bioresources Engineering and Environmental Hydrology, University of KwaZulu-Natal. Pietermaritzburg, South Africa.

Priestley, CHB. and Taylor, RJ. 1972. On the assessment of surface heat flux and evaporation using large scale parameters. *Monthly Weather Review*, 100: 81-92.

Rassam, DW., Walker, G., and Knight, J. 2004. Applicability of the Unit Response Equation to assess salinity impacts of irrigation development in the Mallee region, *CSIRO Technical Report* 35/04

Raupach, MR., Finnigan, JJ. and Brunet, Y. 1996. coherent eddies and turbulence in vegetation canopies: the mixing-layer analogy. *CSIRO Centre for Environmental Mechanics*, GPO Box 821, Canberra, ACT 2601, Australia.

Savage, MJ. 2010. Surface renewal method for estimating sensible heat flux. Agrometeorology, Soil-Plant-Atmosphere-Continuum Research Unit. School of Environmental Sciences, Faculty of Science and Agriculture. University of KwaZulu-Natal, Pietermaritzburg, South Africa.

Scott, D., Prinsloo, F., Moses, G., Mehlomakulu, M. and Simmers, A. 2000. A re-analysis of South African catchment afforestation experiment. WRC Report No. 810/1/100. Water Research Commission, Pretoria, South Africa.

Scott, DF. and Le Maitre, DC. 1998. The Interaction Between Vegetation and Groundwater: Research Priorities for South Africa. WRC Report No. 730/1/98. Water Research Commission, Pretoria.

Šimůnek, J. and Sejna, M. 2011. Software Package for Simulating the Two-and Three-Dimensional Movement of Water, Heat and Multiple Solutes in Variably-Saturated Media. PC-Progress User Manual Version 2.

Šimůnek, J., Šejna, M., Saito, H., Sakai, M. and van Genuchten, TH. 2008. The HYDRUS-1D software package for simulating the one-dimensional movement of water, heat, and multiple solutes in variably-saturated media, Version 4.0, *Hydrus Series 3,* Department of Environmental Sciences, University of California Riverside, Riverside, CA, USA.

Šimůnek, J., van Genuchten, TH. and Sejna, M. 2011. HYDRUS: Model Use, Calibration and Validation. *American Society of Agricultural and Biological Engineers*. ISSN 2151-0032. 55 (4); 1261-1274

Singh, B. and Kumar, B. 2005. Isotopes in Hydrology, Hydrogeology and Water Resources. Narosa Publishing House, Delhi, India.

Snyder, RL., Spano, D., Paw U, UKT. 1996. Surface renewal analysis for sensible heat and latent heat flux density. *Boundry-Layer Meteorol*. 77, 249-266.

Spano, D., Duce, P., Snyder, RL. and Paw U, KT. 1997. Surface renewal estimates of evapotranspiration: tall canopies. *Acta Hort.* 449 63-68.

Spano, D., Snyder, RL., Duce, P. and Paw U, KT. 1997. Surface renewal analysis for sensible heat flux density using structure functions. *Agric. For. Meteorol.* 86 259-271.

Steinbuck, E. 2002. The influence of tree morphology on stemflow in a Redwood region second-growth forest. Unpublished MSc Geosciences, Faculty, California State University, Chicago, USA.

Sundaram, B., Feitz, A., de Caritat, P., Plazinska, A., Brodie, R., Coram, J. and Ransley, T. 2009. Groundwater sampling and analysis – A field Guide, Geoscience Australia, Record 2009/27: pp. 1-104.

Swanson, RH. and Whitfield, DWA. 1981. A numerical analysis of Heat Pulse Velocity theory and practice. *Journal of Experimental Biology*. 32(1): 221-239.

van Genuchten, MT. 1980. A closed-form equation for predicting the hydraulic conductivity of unsaturated soils. Soil Science Society of America Journal, 44: 892-898.

Weaver, J. and Talma, A. 2005. Cumulative rainfall collectors – A tool for assessing groundwater recharge. *Water SA,* 31(3): 283-290.

West, A., Goldsmith, G., Matimati, I. and Dawson, T. 2011. Spectral analysis software improves confidence in plant water stable isotope analysis performed by isotope ratio spectroscopy (IRIS). *Rapid Communications in Mass Spectrometry*, 25: 2268-2274.

Williams, BW. 2004. Investigating the contribution of stemflow to the hydrology of a forest catchment. Unpublished Thesis, University of Southampton, Southampton, England.

Wilson, K., Goldstein, A., Falge, E., Aubinet, M., Baldocchi, D., Berbigier, P., Bernhofer, C., Ceulemans, R., Dolman, H. and Field, C. 2002. Energy balance closure at Fluxnet sites. *Agric. For. Meteorol*. 113, 223-243.

Winograd, IJ. and Robertson, FN. 1982. Deep oxygenated ground water: anomaly or common occurrence?: *Science, v*. 216, p 1227-1230.